Early detection and rapid response to harmful algal blooms using hydrogen peroxide and cyanotoxin genes

Contract number: INV_007

Final report submitted on 8/12/2022 by:
PI: Hidetoshi Urakawa
Graduate students: Taylor L. Hancock, Elizabeth K. Dahedl, Michael A. Kratz
Co-PI: Barry H. Rosen
Florida Gulf Coast University
10501 FGCU Blvd S. Fort Myers, FL 33965-6565

This report was funded under the Innovative Technologies for Harmful Algal Blooms Program through a grant agreement from the Florida Department of Environmental Protection. The views, statements, findings, conclusions, and recommendations expressed herein are those of the author(s) and do not necessarily reflect the views of the State of Florida or any of its subagencies.

Cover page image: A hydrogen peroxide application monitoring day at W.P. Franklin South Recreation Area

Suggested citation:

Urakawa, H., T. L. Hancock, E. K. Dahedl, M. A. Kratz, B. H. Rosen. 2022. Early detection and rapid response to harmful algal blooms using hydrogen peroxide and cyanotoxin genes. Final report submitted to the Office of Water Policy and Ecosystem Restoration, Florida Department of Environmental Protection. pp.180.

Table of Contents

Chapter 1: Task 1 and Task 2 description and deliverables

Project research summary

The main goals of this project were to understand (1) the interaction between algal communities and natural hydrogen peroxide dynamics to examine if the natural hydrogen peroxide concentrations can be used to predict harmful algal blooms, and (2) evaluation of hydrogen peroxide as an effective algaecide. One year of biweekly monitoring was conducted at Franklin Lock and Dam in the Caloosahatchee River. We conducted two mesocosm experiments. In the first mesocosm experiment, we used a high concentration of hydrogen peroxide to examine the acute reaction of *Microcystis aeruginosa* to the algaecide. In the second mesocosm experiment, two algaecides, hydrogen peroxide, and L-lysine, were tested together. As the main part of this project, we applied hydrogen peroxide twice to river water. In the first application, we used a moderate concentration of hydrogen peroxide in the surface water of the Caloosahatchee River at Franklin Lock and Dam. The succession of the phytoplankton community and the change in water chemistry were monitored for two weeks. In the second field application, we partially worked with Blue Green Technology. Hydrogen peroxide products were applied three times and two-week monitoring was conducted. In the laboratory, we try to identify the mechanism of cyanobacterial sensitivity to hydrogen peroxide and L-lysine. We conducted a transcriptome study using pure cultures of *Microcystis aeruginosa* and found that their cellular response to reactive oxygen species differed in the strain level. As a part of this project, we attempted to develop a new on-site PCR detection system for cyanobacterial toxin genes. In the mesocosm experiments and field hydrogen peroxide applications, the succession of algal communities was examined using high-throughput amplicon sequencing and transcriptome analysis along with the monitoring of environmental parameters, microcystin concentrations, iron concentrations, and nutrients.

Highlights of our findings are shown below.

- We performed an in-depth field survey at Franklin Lock and Dam on the Caloosahatchee River for one year at twice monthly intervals from February 2021 through January 2022. We found that hydrogen peroxide consistently exist in the surface water, however, concentrations increased before and during *Microcystis* blooms. Hydrogen peroxide could be an effective early warning

system for HAB development given the cost efficiency and ease of measurement. The hydrogen peroxide concentration spanned greatly and ranged between 41 nM to 1582 nM. The baseline concentration was around 50 nM in this study. The average concentration was 390 nM and median was 273 nM. Based on this one-year monitoring, and two previous reports (Cory et al., 2016; Ndungu et al., 2019), we tentatively set a warning threshold value as 500 nM (17 μg/L) in the case of the Caloosahatchee River. For a better understanding of phytoplankton succession and bloom forming mechanisms, we introduced transcriptomic analysis for phytoplankton communities. We found that *Microcystis* encountered zinc deficit when they were in the process of establishing a spring bloom. Zinc is the most important trace metal to maintain numerous numbers of enzymes in cyanobacterial cells. Our data may suggest the zinc deficiency could be occur for freshwater algae under the bloom conditions due to the high requirement of zinc by phytoplankton to fix dissolved inorganic carbon. Right after the end of the spring *Microcystis* bloom, nitrogen fixation was strongly expressed at 68.1% of the transcriptome, corresponding with a sudden decrease of ammonia and nitrate/nitrite concentrations. We successfully demonstrated the usefulness of transcriptome analysis for a better understanding of phytoplankton succession and bloom forming mechanisms.

- In the first mesocosm experiment with high hydrogen peroxide concentration (374 mg/L), we observed a rapid (< 24 hour) *Microcystis* bloom collapse followed by a drastic change in microbial community composition with a nutrient anomaly. This resulted in an immediate release of toxins already present within cells, however, toxin levels did not increase after the treatment. Microcystin decreased over time in the control mesocosms, whereas the concentration in the treatment mesocosms remained elevated throughout the experiment. This lack of microcystin degradation most likely stemmed from impacts on the bacterial community.

- In the second mesocosm, hydrogen peroxide, L-lysine, and the combination of both chemicals were analyzed for algaecide treatment of cyanobacterial dominant microbial communities over a 7-day mesocosm experiment. Hydrogen peroxide was applied at a concentration of 33.3 mg/L, L-lysine at a concentration of 8 mg/L, and mixed mesocosms using both chemical concentrations. All treatment applications were found to be successful at reducing toxic cyanobacterial genera such as *Microcystis*, *Anabaena*, *Dolichospermum*, and *Cuspidothrix.* Succession by eukaryotic

algae varied in composition across treatments, with Eustigmatophyte becoming near solely dominant in hydrogen peroxide and mixed treatments, while L-lysine had a more diverse composition of Chlorophyta and picocyanobacteria. The combined treatments of L-lysine and hydrogen peroxide showed fast decomposition rates and effective removal of cyanobacteria, which warrants further use of this synergetic approach.

- In the first field application, we treated a 400 m^2 area using the 16.7 mg/L (0.0015%) of hydrogen peroxide concentration. The concentration of hydrogen peroxide decreased within the first hour and went back to the background level on the next day. Initially, no significant decrease in chlorophyll-a (Chl-a) concentration in the surface bloom was observed. However, we were able to detect the succession of the phytoplankton community after the treatment. A reduction of the relative abundance was observed in the populations of *Dolichospermum* and *Microcystis*. The major successor was picocyanobacteria. Our results indicated that hydrogen peroxide induced the succession of the phytoplankton community from HAB to non-harmful groups and could be used for the selective suppression of harmful cyanobacteria.

- In the second field application, we treated a 400 m^2 area using higher hydrogen peroxide concentration than in the first application (200.4 mg/L, 0.018%). After our treatment, BlueGreen Water Technologies applied Lake Guard Oxy twice. The surface hydrogen peroxide concentrations dropped to the natural level the next day. We confirmed that Lake Guard Oxy remained longer time and higher concentration on the surface than the regular liquid hydrogen peroxide. The chemical was considered effective because it helped hydrogen peroxide concentration higher near the surface. During the period of monitoring, we did not observe any fish kill or the corruption of the ecosystem. It suggests that our field application was correctly managed and no further harm to aquatic life was observed. In this application, *Microcystis* abundance decreased every time after the treatments but quickly bounced back every time. Despite the use of higher concentrations of hydrogen peroxide, the abundance of *Microcystis* remained constant after two weeks. It suggested that one-time dosing was not sufficient to manage the surface bloom. We concluded that a higher concentration of hydrogen peroxide is needed to immediately remove a surface HAB. We will need an additional study that can determine the appropriate concentration of hydrogen peroxide to effectively control HAB.

- Transcriptome RNA-seq methods were used to assess the modes of action of two algaecides, hydrogen peroxide and L-lysine, take in inhibiting the growth of *Microcystis aeruginosa,* where two toxic and two non-toxic strains were used to assess biological differences between these groups that may improve mitigation efforts and understanding of these organisms. We found that both hydrogen peroxide and L-lysine led to the downregulation of microcystin-toxin genes, further highlighting their use for safe application. The expression of photosynthetic genes was found to be diversely regulated between hydrogen peroxide and L-lysine treatments; however, overall abundance of these genes was also found to be downregulated. Differential antioxidant coping mechanisms were also discovered between toxic and non-toxic strains.

- In this study, qPCR assays were optimized and developed for quantifying commonly observed harmful cyanobacteria and toxin genes. The Biomeme assays amplified genetic material in two hours without the need of standard DNA extraction and purification methods.

Project overview

PROJECT LOCATION

This project was conducted at Franklin Lock and Dam (S-79), which is located at latitude 26° 43" 16', longitude 81° 41" 40', on the Caloosahatchee River about 33 miles (53 km) upstream of the Gulf Intracoastal Waterway. This is a property of the US Army Corps of Engineers and within W.P. Franklin South Recreation Area (https://www.recreation.gov/camping/campgrounds/261793). Laboratory-based activities occurred at the Florida Gulf Coast University (FGCU) campus (10501 FGCU Blvd, S. Fort Myers, Florida 33965) and the FGCU Emergent Technologies Institute (16301 Innovation Lane, Fort Myers, Florida 33913).

PROJECT BACKGROUND

South Florida endured exceptionally severe harmful algal blooms (HABs) during the 2016 and 2018 wet seasons, with multiple and lasting environmental and economic impacts. Major problems included massive harmful cyanobacterial blooms caused by *Microcystis aeruginosa* in freshwater and brackish water systems and massive red tide events caused by a toxic dinoflagellate, *Karenia brevis*, in saltwater systems. Innovative technology is proposed utilizing a hydrogen peroxide approach for early detection and rapid response to HAB in southwest Florida, with the anticipated large-scale application if blooms occur. If the use of hydrogen peroxide for HAB control in both mesocosm and field experiments can be proven effective, it will provide valuable scientific data for cost-effective water management purposes.

PROJECT DESCRIPTION

Recent HABs occurred in the Caloosahatchee River and Lake Okeechobee causing devastative damage to Florida waterways. Few methods exist for the rapid suppression of HABs. The development of prediction and prevention methods of HAB is a top priority issue in Florida. Preliminary research shows that through a hydrogen peroxide approach, HABs can be predicted and mitigated in a cost-effective manner. The Grantee proposes to combine the application of hydrogen peroxide and L-lysine to remediate natural algal blooms. This novel amino-acid based technology induces the selective death of specific cyanobacterial cells (e.g., *Microcystis aeruginosa*). The resulting data will be an excellent asset for local water managers to select effective and safe HAB management tools. Since hydrogen peroxide can be a selective and non-

invasive algal control method, it has the potential to provide sustainable mitigation programs nationwide. It has been used in Europe more often but not in the United States. Algal responses after hydrogen peroxide treatment should be different between Europe and southwest Florida, thus, a scientific assessment of phytoplankton dynamics must be conducted. Grantee's proposed combined application of hydrogen peroxide and the amino acid L-lysine is the first attempt in the world and requires to be examined more before use in natural waters. As the method proposed does not remove nutrients, it is important to determine the destination of the nutrients released by ruptured cyanobacteria, with the hypothesis that beneficial members of the phytoplankton community will take advantage of the released nutrients.

The Grantee will also develop a novel field-based molecular technique to monitor cyanobacteria for the presence of cyanotoxin genes. Early detection of toxin genes could be used in conjunction with control methods early before a bloom becomes too difficult to treat. This effort involves developing a targeted toxin gene technology that can be deployed in the field using a hand-held quantitative polymerase chain reaction (qPCR) machine. Early detection could be immediately followed up by a cyanobacteria-targeted treatment that should reduce the toxin producers long before bloom forms.

This 24-month project will reveal how hydrogen peroxide can suppress harmful algal growth and induce the succession of phytoplankton communities from harmful to non-harmful algal species. It must be determined in southwest Florida because the data from past studies in Europe is not applicable due to the difference in the climate. This project will also monitor the fate of microcystin after treatment. This project's data will help improve the State's ability to mitigate and clean up HAB. The Grantee's study and innovative technology application may pave the way for the next generation of harmful algae mitigation and water quality management in Florida.

TIMELINE

This study was funded during July 2020 to August 2022. We monitored Franklin Lock and Dam surface water for one year (Feb 2021 to Jan 2022) to examine how the measurement of natural hydrogen peroxide levels can be used to predict HAB. The mesocosm and field studies were conducted during April 2021 to June 2021.

GRANT AWARD AMOUNT

Total amount: $320,000

Subcontract amount: $26,000. The University of South Florida became a subcontractor in this project. The fund was used to support Taylor Hancock to conduct his research as a part of his dissertation project entitled “Algal ecology of extreme anthropogenic events in southwest Florida”. Dr. Mark Rains and the PI Dr. Hidetoshi Urakawa are the mentors of his dissertation work.

ANTICIPATED BENEFITS

Financial summary

A LIST OF INSTRUMENT COSTS THAT WERE NOT COVERED BY THIS GRANT (INV_007)

Items	Approximate cost	Funding source	Justification
Kayak	$179.99 x 2	US Army Corps of Engineers	The purchase of boats was not allowed in this Agreement. This item was used in the field application of hydrogen peroxide.
Aqua TROLL sonde (In-Situ, CO)	$3,898.71	The Water School, FGCU	The purchase of items that go over $1,000 was not allowed in this Agreement. This item was used in an annual monitoring of water quality at Franklin Lock and Dam. This sonde was also used in mesocosm experiments.
Aqua pen	$3,192.00	The Water School, FGCU	The purchase of items that go over $1,000 was not allowed in this Agreement. This instrument was used in mesocosm and laboratory experiments to examine the photosynthetic activity of algae.
Trilogy laboratory fluorometer	$6,220.00	The Water School, FGCU	The purchase of items that go over $1,000 was not allowed in this Agreement. This instrument was used in the measurement of colored dissolved organic matter.
Total cost	$13,670.69		

Here, we provide a financial summary of actual costs versus the budget. To conduct HAB study, not only this FDEP Agreement but also other funding agencies supported our research. We received funding from

U.S. National Science Foundation and U.S. Army Corps for Engineering. The later funding was through Nova Southeastern University as FGCU as a subcontractor.

PROJECT SCHEDULE

- The water quality and algal community monitoring of the project started in February 2021. This activity was performed according to the original plan.
- Our second field application was interfered with by the algaecide application of Blue Green Technologies. After the discussion, we decided to monitor the result of the algaecide demonstration.
- All field experiments were performed within the original project schedule.. However, laboratory analysis took much longer. We extended the project for two more months to complete laboratory analyses.

ACTIVITY SUMMARY

- One-year biweekly monitoring of water quality and algal communities at Franklin Lock and Dam was completed as planned. (PI, Dr. Urakawa)
- Two mesocosm experiments were completed as planned. (PI, Dr. Urakawa)
- Two field applications of hydrogen peroxide were performed. (PI, Dr. Urakawa)
- Gene expression pattern responses to hydrogen peroxide and L-lysine treatments in *M. aeruginosa* were examined using RNA-seq. (PI, Dr. Urakawa)
- Biome qPCR was used to detect cyanotoxin genes. (Co-PI, Dr. Rosen)

AMOUNT OF HYDROGEN PEROXIDE (HP) USED AND ITS COST

Experiment	Date	Application	Total (L)	Area	Cost
1st field HP application	4/14/2021	1 L x 2 bottles	2	400 m^2	$4
2nd field HP application	5/25/2021	1 L x 24 bottles	24	400 m^2	$48
1st mesocosm	5/11/2021	1 L x 4 bottles x 3 tubs	12	on land	$24
2nd mesocosm	6/21/2021	0.125 L x 6 tubs	0.75	on land	$2

A LIST OF SUPPORTED PERSONNEL

Name	Title and affiliation	Roles in this project	Other
Taylor Hancock	Ph. D. student at USF Joint Ph. D. program between FGCU and the University of South Florida (Geography & Environmental Science & Policy, School of Geosciences) OPS (Other Personal Services) at FGCU	Annual biweekly monitoring Primary researcher of the first mesocosm	Paid
Elizabeth Dahedl	M.S. Environmental Science student (FGCU)	Annual biweekly monitoring Primary researcher of the second mesocosm	Paid
Michael Kratz	M.S. Environmental Science student (FGCU)	Annual biweekly monitoring Mesocosm study Field study	Paid
Julia Davis	OPS (FGCU)	Annual biweekly monitoring Mesocosm study Field study	Paid
Colin McMullen	M.S. Environmental Science student (FGCU)	Field study Mesocosm study	Paid
Diana Diaz	Undergraduate (FGCU)	Laboratory experiments	Paid
Donald Pan	Post-doctoral fellow (FGCU)	Laboratory experiments Biomeme	Unpaid
Megan Feeney	Research assistant (FGCU)	Laboratory experiments Biomeme	Unpaid
Kacy Rodriguez	M.S. Environmental Science student (FGCU)	Laboratory experiments	Paid

		Biomeme	
Matthew Kirby	Undergraduate (FGCU)	Laboratory experiments Biomeme	Paid
Fednie Charles	Undergraduate (FGCU)	Laboratory experiments Biomeme	Paid

OUTPUT (PUBLICATIONS & PRESENTATIONS, MEDIA RELEASE)

Peer-reviewed journal

- Urakawa, H., Hancock, T.L., Steele, J.H., Dahedl, E.K., Urakawa, H.E., Ndungu, L.K., Krausfeldt, L.E., Rosen, B.H. & Lopez, J.V. (2020). Complete genome sequence of *Microcystis aeruginosa* FD4, isolated from a subtropical river in southwest Florida. Microbiology Resource Announcements, 9(38). 10.1128/MRA.00813-20

Oral presentations

- Hidetoshi Urakawa. Hydrogen peroxide in southwest Florida freshwater ecosystems and its application for cyanobacterial bloom control, South Florida Water Management District Brown Bag Seminar, Oct 29, 2021.
- Hidetoshi Urakawa. Hydrogen peroxide in subtropical aquatic systems and its application for cyanobacteria bloom control. The 32nd FLMS Annual Technical Symposium. Aug 31-Sep 3, Florida Keys, 2021.

Poster presentations

- Taylor L. Hancock, Elizabeth K. Dahedl, Julia N. Davis, Michael A. Kratz, Hidetoshi Haruka E. Urakawa, Haruka Hidetoshi Urakawa. Rapid response of *Microcystis aeruginosa* bloom microbiome to high concentration hydrogen peroxide. The 31st Annual Southwest Florida Water Resources Conference. Fort Myers, Florida Jan 25, 2022.
- Elizabeth K. Dahedl, Julia N. Davis, Taylor L. Hancock, Michael A. Kratz, Hidetoshi Haruka E. Urakawa, Haruka Hidetoshi Urakawa. *Microcystis* Growth Suppression- Laboratory Study of Three

Chemical Treatment Methods. The 31st Annual Southwest Florida Water Resources Conference. Fort Myers, Florida Jan 25, 2022.

- Diana Diaz, Taylor L. Hancock, Hidetoshi Urakawa. Identifying the microbial community in the phycosphere of *Microcystis aeruginosa*. The 31st Annual Southwest Florida Water Resources Conference. Fort Myers, Florida Jan 25, 2022.
- Diana Diaz., Taylor L. Hancock, Hidetoshi Urakawa. Identifying the microbial community in the phycosphere of *Microcystis aeruginosa*. STEM Undergraduate Research and Internship Symposium. Dec. 5, 2021.
- Julia N. Davis, Elizabeth K. Dahedl, Taylor L. Hancock, Michael A. Kratz, Haruka E. Urakawa, Emily E. Karwacki, Viviana Mazzei, Lauren E. Krausfeldt, Jose V. Lopez, Barry H. Rosen, Hidetoshi Urakawa. Taxonomic assessment and composition analysis of cyanobacteria present in Lake Okeechobee freshwater samples. The 32nd FLMS Annual Technical Symposium. Aug 31-Sep 3, Florida Keys, 2021.
- Taylor L. Hancock, Luka Ndungu, & Hidetoshi Urakawa. Fish predation of *Microcystis aeruginosa* bloom observed in the Caloosahatchee River, Florida. The 32nd FLMS Annual Symposium. Aug 31-Sep 3, Florida Keys, 2021.
- Elizabeth K. Dahedl, Julia N. Davis, Taylor L. Hancock, Michael A. Kratz, Hidetoshi Haruka E. Urakawa, Haruka Hidetoshi Urakawa. Exploration of three short-term suppression methods for the toxic cyanobacterium *Microcystis aeruginos*a. The 32nd FLMS Annual Symposium. Florida Keys, Florida. Aug 31-Sep 3, Florida Keys, 2021.

Media cover

- Fox 4 News (Florida) Researchers trying to find ways to kill blue-green algae as it begins to reappear. Apr 28, 2021.
- Wink News (Florida) FGCU students experimenting with hydrogen peroxide to kill blue-green algae. May 21, 2021.

Other activities

- Deposit of algal cultures: 25 cultures are in the process of depositing to the Algal Resources Collection (ARC) at the University of North Carolina at Wilmington (https://www.algalresourcescollection.com/).

PERMITTING

As Task 1, the Grantee was expected to obtain all necessary permits for the implementation of the project prior to applying any hydrogen peroxide and/or other chemicals to any natural water surface in a Florida waterbody. To conduct the proposed research, the Grantee obtained two permits. The first permit was obtained from the US Army Corps of Engineers to utilize the property for mesocosm settings (special activity permit number 2020-12). The second permit was obtained from the US Army Corps of Engineers Jacksonville office to use hydrogen peroxide in the Caloosahatchee River. In the second permit, FGCU is obligated to report the amount of annual use of hydrogen peroxide to the Jacksonville office (NPDES permit for discharge/herbicide application, # FLG510049).

QUALITY ASSURANCE PROJECT PLAN

As Task 2, the Grantee was expected to prepare, submit, and receive approval on a Quality Assurance Project Plan (QAPP) prior to commencement of any data collection associated with the project. The QAPP was prepared and submitted in December 2020 to the FDEP office. The QAPP was used to specify the sampling procedures, locations, instruments, frequency, and parameters to be sampled.

ANALYSIS METHODS

Water sampling

Water samples were collected by grab sampling at 30 cm water depth in two new 1 L amber bottles. Samples were transferred to the laboratory on ice in a cooler. The samples were processed within three hours of collection.

Sample preparation for nucleic acids extraction

Water samples (200 ml) were filtered with Sterivex filter (GP 0.22 um, SVGP01050, MilliporeSigma). The algal biomass samples on the filters were immediately frozen in the liquid nitrogen jar and transferred to the FGCU laboratory. At the laboratory, the samples were preserved at -80°C.

Water quality analysis

Physiochemical parameters of the river surface water were measured at a depth of 30 cm with a multiple parameter water quality sonde (Aqua TROLL 500, In-Situ Inc., CO, USA) outfitted with temperature/conductivity, pH/ORP, and RDO sensors. The sonde was quality checked according to FDEP SOPs prior to each sampling and calibrated as needed following the manufacturer's directions. The pH was calibrated with a two-point calibration method using 7 and 10 standards. Specific conductivity was calibrated with a one-point method using the 8,000 µS/cm standard. Dissolved oxygen was calibrated using a water-saturated air method by loosely enclosing the sonde in its restrictor with a saturated sponge for five minutes.

Nutrient analyses

We used Benchmark EnviroAnalytical as a certified NELAC lab (E84167) to analyze nutrients and chlorophyll *a*. Nutrients and chlorophyll *a* were quantified via autoanalyzer and spectrophotometer, respectively, using a NELAC-approved laboratory and methods (Benchmark EnviroAnalytical Inc., FL, USA) within 48 hours. Field samples were shipped out with ice in a styrofoam box on the day of sampling. Details of methods are shown below.

Parameter	Method used	Preparation	Holding time	Principle of the methods
Ammonia	U.S. EPA 350.1	1x1/2 pint plastic bottle, 1:4 H_2SO_4, pH <2	Within 2 days	Alkaline phenol and hypochlorite react with ammonia to form indophenol blue that is proportional to the ammonia concentration. The blue color formed is intensified with sodium nitroprusside. The measurement is performed by semi-automated colorimetry.
TKN	U.S. EPA 351.2	1x1/2 pint plastic bottle, 1:4 H_2SO_4, pH <2	Within 2 days	The sample is heated in the presence of sulfuric acid for 2.5 hours. The residue is cooled, diluted to 25 mL and analyzed for ammonia.
TP	TP 365.2	1x1/2 pint plastic bottle, 1:4 H_2SO_4, pH <2	Within 2 days	The sample is heated in the presence of sulfuric acid for 2.5 hours. The residue is cooled, diluted to 25 ml and analyzed for phosphorus.
TN	Calculated	1x1/2 pint plastic bottle, 1:4 H_2SO_4, pH <2	Within 2 days	Calculation. TN = TKN + (NO2+NO3)
NO2-NO3	Systea Easy	1x1/2 pint plastic bottle, 1:4	Within 2 days	The automated procedure for the determination of nitrate utilizes the reaction whereby nitrate is reduced by a proprietary Chemical R1. The reduced nitrate is then treated

		H_2SO_4, pH <2		with sulfanilamide and N-1-napthylethylenediamine dihydrochloride under acidic conditions to form a soluble dye which is measured colorimetrically at 546nm. (https://www.nemi.gov/methods/method_summary/10442/)
Ortho-phosphorus	U.S. EPA 365.3	1x1/2 pint plastic bottle	Within 2 days	Ammonium molybdate and antimony potassium tartrate react in an acid medium with dilute solutions of phosphorus to form an antimony-phospho-molybdate complex. This complex is reduced to an intensely blue-colored complex by ascorbic acid. The color is proportional to the phosphorus concentration.
Chlorophyll a	U.S. EPA 445.0 (corrected)	1 x 500 mL amber plastic bottle	Within 2 days	In Vitro Determination of chlorophyll a and pheophytin
TOC	SM5310B	1 x 40 mL, glass vial, 1:1 H_3PO_4	7 days. Analyze immediately, or refrigerate and add HCl, H3PO4, or H2SO4 to pH < 2	High-temperature combustion method

Microcystin analysis

Microcystin toxin samples were handled and analyzed via USEPA method 546 and manufacturer directions using an enzyme-linked immunosorbent assay (ELISA) microcystin tube kit (Beacon Analytic Systems Inc., ME, USA). Samples were stored in 20 ml glass scintillation vials at -80°C and underwent three freeze/thaw cycles with mixing for 20 sec with Vortex-Genie 2 Variable Speed Vortex Mixer (SI-0236) between each cycle prior to analysis. 0.5 ml of sample was used in 5 ml test tubes coated with anti-rabbit IgG containing 0.5 ml of microcystin-HRP enzyme conjugate. For each tube, 0.5 ml microcystin rabbit antibody solution was added, vortexed as detailed previously, and incubated at room temperature for 20 minutes. Tube contents were flooded completely with a wash solution and decanted four times. Tubes were tapped out upside down on absorbent paper to remove as much wash solution as possible, then 0.5 ml of the substrate was added followed by vortexing as detailed previously and a 20 min incubation period at room temperature. Immediately after incubation, 0.5 ml of 1N hydrochloric acid stop solution was added to each tube, stopping the reaction. All samples were quantified within 20 min of stopping the reaction using a Thermo Scientific GENESYS 20 visible spectrophotometer at 450 nm. Samples were measured in triplicate using either field or technical replicates, which were compared to a four-parameter fit curve of microcystin-LR standards (0.3, 0.8, 2, 5 µg/L microcystin-LR). A negative (0 µg/L microcystin-LR) and

positive (1 μg/L microcystin-LR) control were used to ensure the validity of the assay and parameter curve. A range of 0.80 – 1.30 μg/L was acceptable for the positive control, as per the manufacturer's directions.

Hydrogen peroxide measurements

Samples taken for hydrogen peroxide measurement were immediately filtered through 0.2 μm Sterivex filters and stored at -80°C until analyzed. Hydrogen peroxide was measured using a fast response amperometric 250 μm diameter tip hydrogen peroxide microelectrode with a built-in reference electrode (HP-250, Innovative Instruments) featuring a lower detection limit of 50 nM. The sensor was connected to an inNO-T meter operated by the inNO-T data acquisition system software (Innovation Instruments, Tampa, FL, USA). Hydrogen peroxide (3% w/v) was purchased from Sigma-Aldrich (St. Louis, MO, USA) and used in the preparation of a 400 μM hydrogen peroxide standard solution prepared by dissolving stock in 100 ml of high-performance liquid chromatography (HPLC) grade water (Fisher Scientific). A 0.22 μm filtered catalase solution (≈30,000 U/mL, ≈40,000 U/mg protein, Worthington Biochemical Corporation, Lakewood, NJ, USA) was also used. Before calibration, the condition of the sensor was monitored in HPLC water for at least 20 minutes before measurements to establish a stable background baseline. For standard addition measurement 4 ml of sample was used, 10 μl of 400 μM hydrogen peroxide standard was added after sensor stabilization (1 μM as final concentration), and then 10 μl of catalase (30 U/μl) was added for decomposition of hydrogen peroxide. Eight replicate readings were taken for each standard where the slope was calculated from sample baseline and hydrogen peroxide standard addition baseline and applied to the delta of standard addition baseline and post catabolic reaction baseline.

HOOH concentration (μM) = (original baseline – baseline after catalase addition)/(peak after standard addition – original baseline)

After the confirmation of the catalase reaction, the profile image data were stored as an iNO file. The calculation of the concentration of hydrogen peroxide was conducted using Microsoft Excel.

Fluorometric hydrogen peroxide measurements

Samples taken for hydrogen peroxide measurement were immediately filtered through 0.2 μm Sterivex filters and stored at -80°C until analyzed. A 0.5M phosphate buffer (PB) stock solution was used, combining 13.34 kg KH_2PO_4 and 21.58 g of Na_2HPO_4 dissolved in 500 ml ultrapure water. A 180 μM scopoletin stock solution was prepared using 0.03125 g scopoletin ($C_{10}H_8O_4$ Sigma-Aldrich, St. Louis, MO,

USA) dissolved in 500 ml pure water, for which 18 μl of the scopeletin stock solution and 1 ml of PB was prepared daily and used for measurements. A 20 p.u./ml horseradish peroxidase (HRP) stock solution was used, for which 1 mg HRP (Alfa Aesar, Thermo Fisher Scientific, Waltham, MA, USA) was dissolved in 1 ml ultrapure water, 100 μl of HRP stock solution and 900 μl PB solution was prepared daily for measurement. A 400 μM hydrogen peroxide (HP) standard solution was also prepared daily, combining 45 μl peroxide (3% w/v) (Sigma-Aldrich, St. Louis, MO, USA) and 100 ml ultrapure water. Hydrogen peroxide measurements were conducted in low light (semidarkness) room, using a Trilogy fluorometer with a Colored dissolved organic matter (CDOM)/UV module (Model 7200-041) at excitation of 365 nm and emission of 496 nm. Samples and ultrapure water standards were prepared in 2 ml triplicates for HP fluorescence measurement. 20 μl of PB was added to samples, shaken, and used for background measurement. 8 μl of scopoletin fresh daily solution was then added to samples, shaken, and used for 100% fluorescence measurement. Next, 12 μl of HRP fresh daily solution was added to samples, shaken, and allowed to sit for a minute before measurements. Samples were measured three times, or until fluorescence measurement began to increase, for which the lowest value was used for later calculation. Next, 5 μl of HP standard solution was added to samples, and shaken, before waiting two minutes for measurement. This procedure was repeated four times for standard addition calculation. Triplicate measurements for samples and standards were used to calculate mean sample hydrogen peroxide concentration, as well as to ensure the validity of the curve.

Total iron analysis

Total iron was determined by USEPA FerroVer Method Hach method 8008 (FerroVer® Iron Reagent Powder Pillows) using a Hach DR3300 spectrophotometer set in program 265 Iron (510 nm). For each sample, 10 ml was added to Hach sample cells followed by two five milliliter FerroVer Iron Reagent Powder Pillows. Sample cells were shaken thoroughly by hand until all visible powder was dissolved and then incubated at room temperature for three min before measurement. Samples were measured in triplicate using either field or technical replicates. A positive (1 mg standard) control was used to ensure the validity of the measurements.

Colored dissolved organic matter (CDOM)

Colored dissolved organic matter (CDOM) was fluorescently measured in the laboratory. Two milliliters of sample water were added to a disposable plastic cuvette and the concentration was determined using Trilogy fluorometer with a CDOM/NH4 module (Model 7200-041).

Algal colony counts

Algal colony abundance was quantified by filtering 50 ml of water through a binder-free borosilicate glass microfiber fiber (GF/F) filter with a 60 ml disposable plastic syringe and counting macroscopic algal colonies under a dissection microscope. Occasionally, the volume of filtered water was reduced or increased between 5 to 150 ml based on the density of colonies. Filters with algal colonies were placed on a plastic Petri dish with forceps. Only colonies with green coloration were subjects for counting. Three replicated filters were counted with an aid of a hand-held tally counter. The data were converted from colonies per ml to colonies per L and averaged for each sample.

Phytoplankton identification

For microscopic counting (abundance and species composition) of phytoplankton, 150 ml of water sample was used and fixed with 1% glutaraldehyde (final concentration) and stored at 4°C. Biomass was allowed to settle overnight and then concentrated to 10 ml before use. The sample was vortexed and then 1 ml was used for quantification using counting cells (Sedgewick-Rafter Cell S50, Graticutes Optics Limited, Kent, UK) and an inverted microscope (Olympus model CKX53SF, Tokyo, Japan). Total cell counts were completed for five replicates using 1 μl counting squares. Identification was done for picocyanobacterial and filamentous Cyanophyceae groups, Bacillariophyceae, Chlorophyceae, Euglenoidea, Chrysophyceae, Cryptophyceae, and unknown algal groupings. It should be noted that this method underestimates the numbers of picocyanobacteria due to their small size. To remediate this issue, fluorescence microscopy was used for counting picocyanobacteria.

Total bacterial and picocyanobacterial counts

Samples for cell enumeration were preserved with 2% formalin and stored at -80°C. Once the samples were thawed at room temperature, the sample tube was mixed for 20 sec with Vortex-Genie 2 Variable Speed Vortex Mixer (SI-0236). In general, one milliliter of the sample was used but was increased or decreased as needed if cell density was too little or too great for accurate counts; the resulting range was between 0.5 and 3 ml of sample. Cells were stained in a filtration unit with SYBR Green I (10x as a final

concentration) at room temperature for two minutes before filtering on a 0.2 µm pore-size black polycarbonate filter. Filtration was conducted with a hand-held pump. After filtration, the filter was washed twice with one-milliliter ultrapure water. The filter was transferred onto a glass slide and sealed with CitiFluor antifadent AF1 mounting solution (Electron Microscopy Sciences, Hatfield, PA, USA). Bacterial cells were determined by epifluorescence microscopy. FITC (fluorescein isothiocyanate) filter (excitation, 475 nm/emission, 530 nm) was used to count bacterial cells. Autofluorescent signals produced by chlorophyll pigments under a Texas Red filter (excitation, 559 nm/emission, 630 nm) were used to count picocyanobacteria. Enumeration was performed in a cross pattern, taking five subsamples total at each point and the intersection, of the filter. A minimum average of 40 cells per subsample was accepted to minimize counting errors.

High-throughput sequencing of bacteria and archaea

Microbial cells were collected by filtering 200 ml of water with a 0.22 µm cellulose nitrate filter. Genomic DNA was extracted from half cut filter samples using the DNeasy PowerSoil Pro Kit (Qiagen) following the manufacturer's instructions. High-throughput amplicon sequencing targeting bacteria was conducted via amplification of 16S rRNA gene using primer pair 515yF and 926pfR using the Illumina MiSeq system (MR DNA, Shallowater, TX, USA). For analysis, sequences are joined and those less than 150 bp were removed. Sequences with ambiguous base calls were also removed. The dereplicated or unique sequences were denoised; unique sequences identified with sequencing and/or PCR point errors were removed, followed by chimera removal, thereby providing a denoised sequence or Amplicon Single Variant (ASV). Final ASVs were taxonomically classified via representative ASVs through BLAST at NCBI.

Metatranscriptome

RNA samples for transcriptome sequencing were collected by filtering 200 ml of water using 0.2 µm Sterivex filters on-site which were promptly frozen in liquid nitrogen for transport to a -80°C freezer until further analysis. Total RNA was isolated from Sterivex filters using the RNeasy PowerMicrobiome Kit (Qiagen) following the manufacturer's instructions. For each filter sample, three extractions were performed. RNA was eluted in 100 µl RNase-free water and pooled. DNA contamination was removed using Baseline-ZERO™ DNase (Epicentre) following the manufacturer's instructions followed by purification using the RNA Clean & Concentrator columns (Zymo Research). DNA-free RNA samples were used for rRNA removal by using Ribo-Zero Plus rRNA Depletion Kit (Illumina). The rRNA depleted samples were used for library preparation via the KAPA mRNA HyperPrep Kits (Roche) by following the

manufacturer's instructions. The average library size was determined using the Agilent 2100 Bioanalyzer (Agilent Technologies) and the samples were then pooled in equimolar ratios of 0.6 nM, and sequenced with paired end for 300 cycles using the NovaSeq 6000 system (Illumina). After DNase treatment, whole transcriptome amplification (WTA) was performed on low RNA samples separately. The whole transcriptome amplified samples were used for library preparation using Illumina DNA Prep, (M) Tagmentation library preparation kit (Illumina) following the manufacturer's instruction.

Chapter 2: Franklin Lock and Dam monitoring

ABSTRACT

The largest freshwater aquatic system in the state of Florida is Lake Okeechobee and its downstream waterways with the Caloosahatchee River flowing west to the Gulf of Mexico. These warm, subtropical waters experience harmful algal blooms (HABs), with frequency and severity increasing in recent decades. The most common and pervasive freshwater HAB experienced in this system is a cyanobacterium, *Microcystis aeruginosa*. Mitigation of such blooms has become a greater focus for water managers of the region. Recent studies have highlighted the possibility of forecasting cyanobacterial HABs. Predicting HABs or detecting early accumulation of cyanobacterial biomass towards a bloom would allow water managers to rapidly respond with treatments to mitigate HAB impact at a more manageable stage. Hydrogen peroxide appears to be such a predictable factor but has not been examined yet in topical or subtropical areas like South Florida. To better understand cyanobacterial HAB ecology and associated hydrogen peroxide dynamics, we performed an in-depth field survey at Franklin Lock and Dam on the Caloosahatchee River for one year at twice monthly intervals from February 2021 through January 2022. We noted two distinct *Microcystis* HAB events which were associated with peaks of hydrogen peroxide. We also noted a pattern of *Microcystis* metatranscriptome expression around the time of these blooms. Our data yield a better understanding of cyanobacterial and HAB ecology in southwest Florida freshwater environments.

INTRODUCTION

The largest freshwater aquatic system in the state of Florida is Lake Okeechobee and its downstream waterways, the St. Lucie River to the East and the Caloosahatchee River to the West. These warm subtropical, nutrient-rich waters of this system provide the necessary environment for harmful algal blooms (HABs) (Burns et al., 2008). In recent decades, cyanobacterial HABs and their management and mitigation have become more of a concern due to an increase in frequency, severity, and duration of blooms.

By recognizing patterns in cyanobacterial succession and their relation to environmental parameters, factors that influence or forecast bloom formation can be identified. For example, there is well-documented succession from filamentous cyanobacteria (*Aphanizomenon* and *Dolichospermum*) to *Microcystis aeruginosa* with increases of nitrogen or phosphorous in shallow eutrophic lakes of China (Wu et al., 2016; Wan et al., 2019). Additionally, natural hydrogen peroxide levels appear promising as a HAB predictor, but little data exist on the subject thus far (Ndungu et al., 2019). Cory et al. (2016) documented that the hydrogen peroxide concentration of surface water in Lake Erie became the highest right before a large bloom was formed, however, it has not been tested yet in tropical and subtropical areas. The incorporation of such information into water resource management benefits the entire system by preventing or mitigating HAB extreme disturbance events.

Here we look to examine hydrogen peroxide trends as a predictor of *M. aeruginosa* HABs and establish year-long baseline data on environmental conditions and the cyanobacterial community for the Caloosahatchee River. To better manage cyanobacterial harmful algal blooms (HABs) in South Florida, a more thorough understanding of the region's cyanobacterial community ecology is needed. These data will be used to identify factors contributing to and forecasting bloom formation.

MATERIALS AND METHODS

The cyanobacteria community and environmental parameters of the Caloosahatchee River, Florida at Franklin Lock and Dam were monitored twice monthly from February 2021 through January 2022 (Fig. 2.1). Physiochemical parameters of the river surface water were measured at a depth of ~30 cm with an Aqua TROLL sonde (In-Situ, CO, USA). Two liters of surface water for additional analyses were collected in 1 L sterile amber bottles and stored on ice for transport and processed within a few hours. The presence or absence of algal blooms was visually monitored and recorded as digital pictures. The field log of each sampling is available as a supplemental file.

Water analytes

Nutrients and some analytes were measured by a NELAC-approved laboratory and methods (Benchmark EnviroAnalytical Inc., FL, USA) within 48 hours. These measurements included ammonia nitrogen, total Kjeldahl nitrogen (TKN), orthophosphate (OP), total phosphorus (TP), chlorophyll-a (Chl-a), total organic carbon (TOC), nitrate+nitrite (NOx), and total nitrogen (TN). Microcystin toxin samples were handled and analyzed via USEPA method 546 and manufacturer directions using an enzyme-linked immunosorbent

assay (ELISA) (Beacon Analytic Systems Inc., ME, USA). Total iron was determined by USEPA FerroVer Method Hach method 8008 (FerroVer® Iron Reagent Powder Pillows). These methods were documented in the QAPP. The samples were measured in triplicates. Colored dissolved organic matter (CDOM) was measured using a fluorometer with a CDOM/NH4 module (Model 7200-041). Samples for cell enumeration were preserved with 2% formalin on-site and stored at -80°C. Cells were viewed under UV excitation at 1,000x magnification using an Olympus BX-51 epifluorescence microscope. Bacterial cells were stained with SYBR Green I. Cyanobacterial cells were counted using autofluorescent signals under a Texas Red filter. The detailed methods are written in Chapter 1.

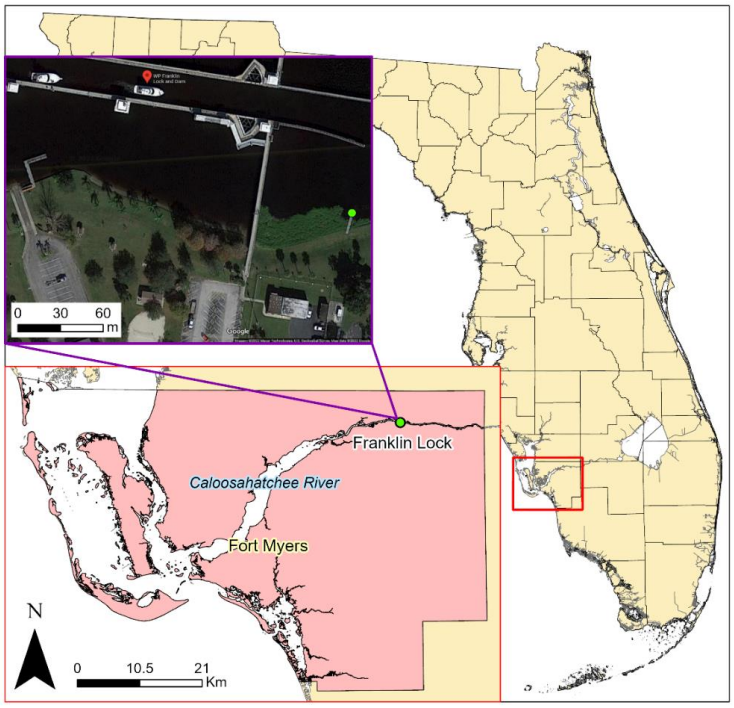

Figure 2.1. Map of monitoring site (green dot) at the end of a dock on the upstream side of Franklin Lock and Dam on the Caloosahatchee River in southwest Florida.

Algal colony counts

Algal colony abundance was quantified by filtering 50 ml of water with a GF/F filter and counting under a dissection microscope. Samples for microscopic counting (abundance and species composition) of phytoplankton were fixed with 1% glutaraldehyde as a final concentration and stored at 4°C until counting. The detailed methods are written in Chapter 1.

Hydrogen peroxide

Samples taken for hydrogen peroxide measurement were immediately filtered through 0.2 µm Sterivex filters and kept on ice and stored at -80°C until analyzed. Hydrogen peroxide was measured using a fast response amperometric 250 µm diameter tip hydrogen peroxide microelectrode with a built-in reference

electrode (HP-250, Innovative Instruments) featuring a lower detection limit of 50 nM. The detailed method is available in Chapter 1.

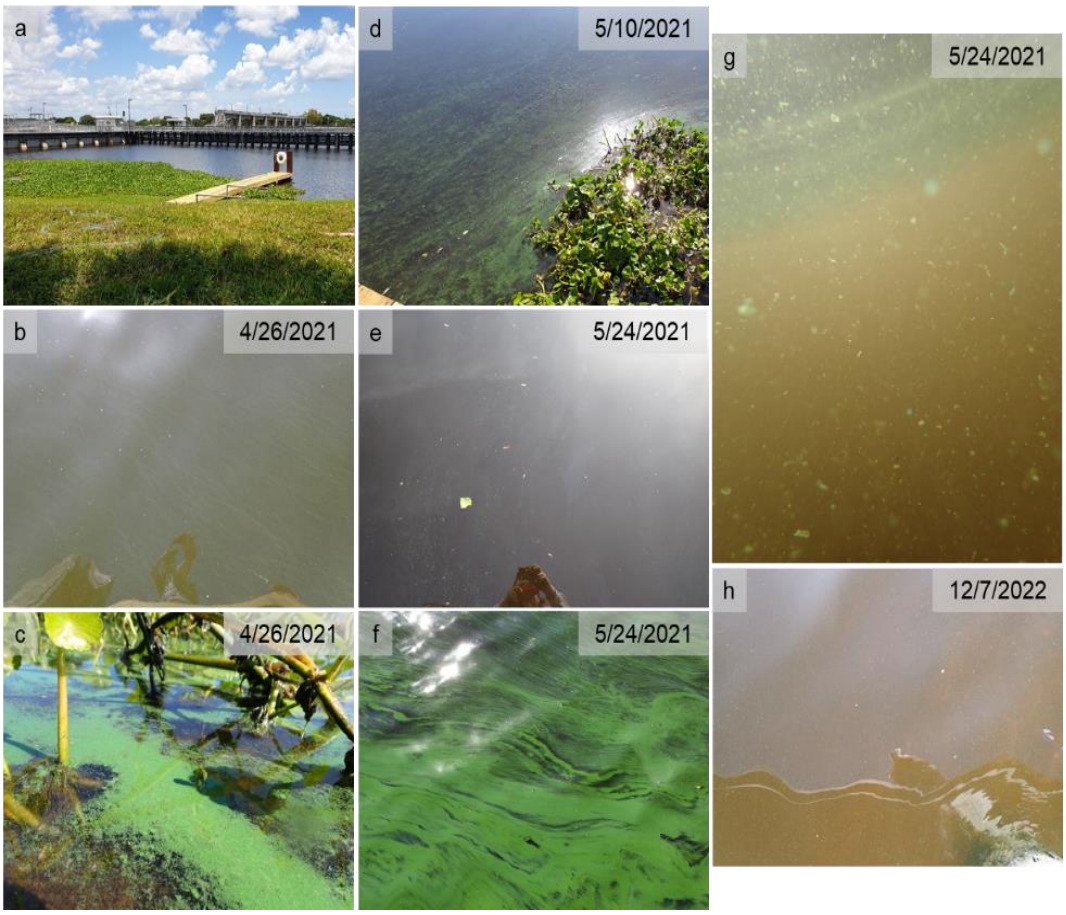

Figure 2.2. Field pictures. Photographs of algal bloom activity from year-long cyanobacteria monitoring site at Franklin Lock and Dam on the Caloosahatchee River. Dock used for sampling in reference to Franklin Lock (a); abundant cyanobacterial surface colonies present on April 26th, 2021, as seen from the dock, (b) with scum concentrated around nearby semiaquatic vegetation along the shoreline (c); the bloom persisted and increased in intensity through May 10th as seen from on top of the lock structure viewing upstream (d); the bloom peaked around May 24th with thick surface scum concentrated near the lock structure, as viewed from on top of it (f); large algal colonies existed throughout the surface water column (g); visible algal colonies returned for a short period on December 7th, as seen from the dock, but were not seen during the next or previous sampling (h).

DNA high-throughput sequencing

Microbial cells were collected by filtering 200 ml of water with a 0.22 µm cellulose nitrate filter. Genomic DNA was extracted from half cut filter samples using the DNeasy PowerSoil Pro Kit (Qiagen) following the manufacturer's instructions. High-throughput amplicon sequencing targeting bacteria was conducted via amplification of 16S rRNA gene using primer pair 515yF and 926pfR using the Illumina MiSeq system (MR DNA, Shallowater, TX, USA). For analysis, sequences were joined and those less than 150 bp were removed. Sequences with ambiguous base calls were also removed. The dereplicated or unique sequences were denoised; unique sequences identified with sequencing and/or PCR point errors and removed, followed by chimera removal, thereby providing a denoised sequence or Amplicon Single Variant (ASV). Final ASVs were taxonomically classified via representative ASVs through BLAST at NCBI.

Metatranscriptome

RNA Samples for transcriptome sequencing were collected by filtering 200 ml of water using 0.2 µm Sterivex filters on-site which were promptly frozen in liquid nitrogen for transport to a -80°C freezer until further analysis. Total RNA was isolated from Sterivex filters using the RNeasy PowerMicrobiome Kit (Qiagen) following the manufacturer's instructions. For each filter sample, three extractions were performed. RNA was eluted in 100 µl RNase-free water and pooled. DNA contamination was removed using Baseline-ZERO™ DNase (Epicentre) following the manufacturer's instructions followed by purification using the RNA Clean & Concentrator columns (Zymo Research). Whole transcriptome amplification (WTA) was performed, and samples were used for library preparation using Illumina DNA Prep, (M) Tagmentation library preparation kit (Illumina) following the manufacturer's user guide. Following library preparation, the average library size was determined using the Agilent 2100 Bioanalyzer (Agilent Technologies), and libraries were then pooled in equimolar ratios of 0.6 nM, and sequenced paired end for 300 cycles using the NovaSeq 6000 system (Illumina). Resulting data were processed and analyzed via the MG-RAST pipeline (Meyer et al., 2008) using SEED subsystems (Overbeek et al., 2014).

RESULTS

Water quality

We began a biweekly monitoring at Franklin Lock and Dam on February 1, 2021 and completed it on January 17, 2022. Water sampling was conducted 24 times. All water sampling activities were conducted by following the QAPP procedure. Minor algal blooms were seasonally observed. The largest activity was found between May and June and the second peak was found in December (Fig. 2.2). Physicochemical

water quality parameters (water temperature, salinity, dissolved oxygen, conductivity, total dissolved solids, and pH) were measured as triplicates using a calibrated Aqua TROLL 500 multi-parameter sensor (Table 2.1). Nutrients and a few additional parameters were also measured (Table 2.2). The data were

Table 2.1. Water physiochemistry

Date	Temp. °C	Sal. ppt	DO %	DO mg/L	Cond. µS/cm	TDS mg/L	pH	Depth cm
2/1/2021	20	0.20	82.32	7.50	416.00	0.3	7.83	29.14
2/15/2021	24	0.19	93.75	8.06	392.62	0.3	7.90	29.23
3/15/2021	23	0.10	90.41	7.85	226.15	0.1	7.87	26.47
3/29/2021	27	0.19	100.92	8.42	402.11	0.3	8.18	26.53
4/12/2021	25	0.19	80.70	6.73	398.44	0.3	8.02	29.78
4/26/2021	27	0.21	68.27	5.51	427.54	0.3	7.61	22.25
5/10/2021	29	0.20	64.08	5.04	416.23	0.3	7.58	35.58
5/24/2021	28	0.20	104.97	8.44	422.56	0.3	8.29	27.65
6/7/2021	30	0.20	98.56	7.70	410.84	0.3	8.22	28.72
6/21/2021	31	0.13	92.07	7.00	265.77	0.2	8.18	23.74
7/8/2021	29	0.24	47.26	3.74	494.71	0.3	7.42	16.68
7/19/2021	28	0.29	53.14	4.09	589.14	0.4	7.39	29.40
8/2/2021	30	0.27	59.16	4.57	555.23	0.4	7.44	19.25
8/17/2021	29	0.27	40.71	3.19	549.01	0.4	7.35	24.00
9/13/2021	30	0.26	47.54	3.70	530.34	0.4	7.19	19.35
9/27/2021	28	0.16	40.53	3.25	330.86	0.2	7.09	25.97
10/11/2021	28	0.18	36.29	2.90	368.79	0.2	7.22	25.38
10/25/2021	27	0.17	38.52	3.13	343.45	0.2	7.32	28.24
11/8/2021	23	0.22	60.83	5.27	452.50	0.3	7.53	28.33
11/22/2021	23	0.26	61.29	5.29	538.74	0.4	7.94	29.10
12/6/2021	22	0.21	74.30	6.71	437.20	0.3	8.04	29.49
12/20/2021	24	0.18	52.30	4.49	372.06	0.2	7.81	29.32
1/3/2022	23	0.19	70.69	6.20	390.97	0.3	7.94	29.51
1/17/2022	20	0.19	70.07	6.41	392.31	0.3	7.95	28.56

recorded as mean, median, and standard deviation, and descriptive statistics were listed in Table 2.3 and Table 2.4. A Pearson correlation matrix was prepared from annual water quality data (Fig. 2.3). The mean water discharge from S-79 was 2203 ft^2/sec and ranged between 944 to 6613 ft^2/sec. The water discharge was kept low in June and July 2021. The water discharge positively correlated to TP, OP, total iron, and CDOM (<0.01), and negatively correlated to DO and pH ($p < 0.01$). The average and standard deviation of TN and TP were 1.37 ± 0.46 mg-N/L and 0.13 ± 0.04 mg-P/L, respectively. The mean and standard deviation of the natural concentration of hydrogen peroxide was 390.3 ± 445.2 nM and ranged between 40.9 to 1582.1 nM. The lowest level of hydrogen peroxide was stable and distinguishable from the time algae associated with hydrogen peroxide. The background mean and standard deviation was 52.7 nM ± 11 nM (n = 8). The range was between 40.9 nM and 73.8 nM. In total 16 samples were identified as the samples that were higher than the background. The mean and standard deviation were 559.2 ± 461.2 nM. The range was between 103 nM and 1582 nM. Based on this one-year monitoring, and two previous reports (Cory et al., 2016; Ndungu et al., 2019), we tentatively set a warning threshold value as 500 nM (17 µg/L) in the case of the Caloosahatchee River. When Chl-a concentrations were low and algal colony counts

were low, hydrogen peroxide concentrations were low and constant (mean ± SD = 52.7 ± 10.9 nM). Peaks of elevated hydrogen peroxide concentration coincided or preceded cyanobacterial activity. Hydrogen peroxide significantly correlated with microscopic algal colony counts, chlorophyll-a, and microcystin (Fig. 3). We found OP and total iron dynamics were similar (Fig. 2.4a), with a strong positive correlation (R^2 =

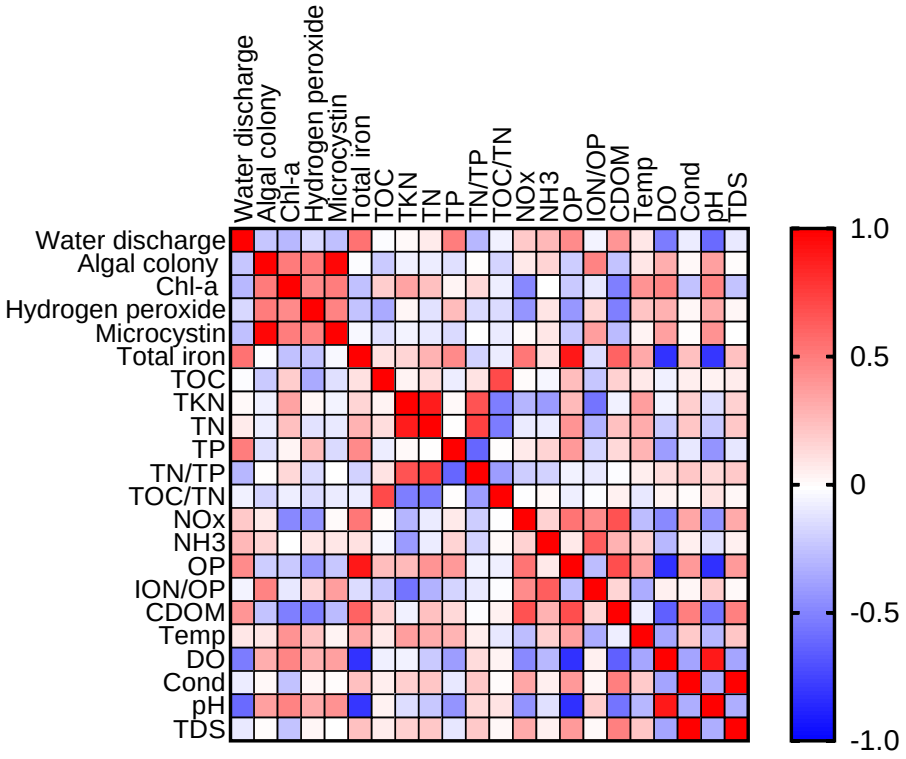

Figure 2.3. A Pearson correlation matrix was prepared from annual water quality data collected at Franklin Lock and Dam (*n* = 24). Hydrogen peroxide significantly correlated with microscopic algal colony counts, chlorophyll-a, and microcystin. Particularly, microscopic algal colony counts and microcystin showed a strong correlation (*r* = 0.54, *p* < 0.001). Colored dissolved organic matter (CDOM) and orthophosphate (OP) strongly correlated (*r* = 0.867, p < 0.001). CDOM was also highly correlated to total iron (*r* = 0.796, p < 0.001).

0.82, p < 0.001) and weaker correlations between total iron and CDOM (R^2 = 0.37) and OP and CDOM (R^2 = 0.48) (Fig. 2.5). Both OP and total iron were negatively correlated with dissolved oxygen (DO) (Fig. 2.3). We suggest the source of OP and total iron was potentially sediment and the drop of oxygen may induce the release of OP and total iron. The source of OP and total iron also could be groundwater. The mean and standard deviation of DO were 5.6 ± 1.8 mg/L and ranged between 2.9 and 8.4 mg/L. Chl-a was correlated with DO and pH, suggesting that the photosynthesis activity of algae produced DO and increased pH due to the consumption of CO_2. The relationship between NOx and Chl-a indicated that

nitrate fuels the algal community at the Franklin Lock and Dam in the Caloosahatchee River (Fig. 2.6a). A similar relationship was also found between Chl-a and ammonium (Fig. 2.6b). Microcystin ranged between 0 to 3.8 µg/L (mean 0.24 µg/L) and was negligible in many water samples but became high (0.12 to 3.8 µg/L) in May and June when a *M. aeruginosa* bloom appeared on the surface of the water. The mean algal colony count from S-79 was 2,374 colonies/L and ranged between 44 to 35,080 colonies/L (Table 2.2). They positively correlated to Chl-a, hydrogen peroxide, DO, pH, and microcystin ($p < 0.05$) (Fig. 2.3). Algae growth followed the dynamics of inorganic nitrogen and it was likely that algal blooms at the Franklin Lock and Dam in the Caloosahatchee River could be predicted based on the availability of nitrate and ammonia.

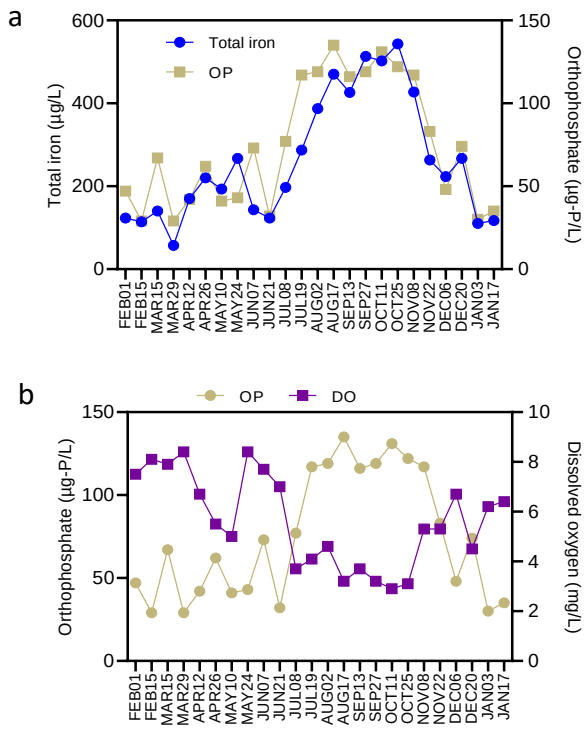

Figure 2.4. Seasonal dynamics of total iron and OP (a) and DO and OP (b) at Franklin Lock and Dam.

High throughput amplicon sequencing of microbial communities

In total, 925,737 bacterial sequences were determined in this study and the mean number of analyzed sequence reads after removal of non-target sequences (3,316 ± 343; mean ± standard error) was 35,256 ± 1867 (*n* = 24). After removal of non-target sequences, samples underwent normalization (scaled to 10,000 reads) before further analysis. The same was done for separately sequenced cyanobacteria, with 1,596,650 reads sequenced. The mean number of analyzed reads after removal of non-target sequences (1,148 ± 178) was 43,568 ± 5,470 (*n* = 24).

Microbial community shifts

Throughout our year-long monitoring, we observed four distinct shifts in the microbial community (Fig. 2.8). Early in 2021 from the beginning of February through mid-April, the community was dominated by Actinobacteria (29.8 ± 1.9%, *n* = *5*) followed by Proteobacteria (21.9 ± 2.9%), of which Betaproteobacteria was most abundant (10.1 ± 2.0%). Then from late April through mid-September, Cyanobacteria dominated (45.5 ± 5.1%, *n* = 10) followed by Proteobacteria (20.6 ± 4.0%) and Actinobacteria (17.6 ± 5.1%). Within Proteobacteria, Betaproteobacteria continued to dominate (12.3 ± 2.7%). From late September through the remainder of 2021, Proteobacteria replaced Cyanobacteria as the dominant phyla (48.4 ± 5.4%, *n* = 7) followed by Actinobacteria (22.9 ± 4.7%). The most abundant Proteobacteria continued to be Betaproteobacteria (33.4 ± 4.7%). However, there was a distinct trend of decreasing relative abundance of Proteobacteria and increase of Actinobacteria. This trend culminated in the January 2022 community returning to a similar composition as the early months of 2021 with a mean Bray-Curtis dissimilarity index of 0.19 ± 0.02 (*n* = 4) accounting for both samples for each respective month. Interestingly, Planctomycetes, a phylum noted to uptake nutrients from dead and decaying algal blooms exhibited a notable increase in abundance after the collapse of the cyanobacterial community and through the remainder of our sampling, with an average relative abundance of 4.4 ± 0.4% before and during the time period of cyanobacteria dominance (February through mid-September) and 7.9 ± 1.5% afterwards.

Cyanobacterial community shifts

Cyanobacterium generally dominated the cyanobacterial community throughout the year (52.2 ± 2.9%, *n* = 24) followed by *Synechococcus* (16.0 ± 1.4%) with the exception of three dates: April 26, May 24, and December 6 of 2021 (Fig. 2.8). During these dates, *Microcystis* dominated at 41.1, 28.2, and 57.2% whereas *Cyanobacterium* made up 40.9, 22.5, and 22.3% of the community, respectively. During these dates, *Microcystis* dominated at 41.1, 28.2, and 57.2% whereas *Cyanobacterium* made up 40.9, 22.5, and 22.3% of the community, respectively. These dates mark two bloom events at our study site, one occurring during late April through May and another in November through early December, with a gradual build up to *Microcystis* dominance in early and late November, 25.2 and 34.6%, respectively. Despite a larger presence within the cyanobacterial community, the December bloom was milder than the earlier bloom event, evidenced by a seasonal contraction of the cyanobacterial community, down to 27.7% of the microbial community from 63.8% during the previous bloom (Fig. 2.2). This was corroborated by Chl-a data, down to 3.63 µg/L from 11.3 µg/L on April 26 and 77.7 µg/L on May 24 (Table 2.2).

Table 2.2. Water quality parameters obtained at Franklin Lock and Dam during bimonthly monitoring

Date	Colony count	Chl-a	HP*	Microcystin	Total iron	TOC	TKN	TN	TP	NOx	NH3	OP	CDOM	Water discharge	PICO**	BAC†
	per L	µg/L	nM	µg/L	µg/L	mg/L	µg-N/L	µg-N/L	µg-P/L	µg-N/L	µg-N/L	µg-P/L	µg/L	cfs	cells/mL	cells/mL
2/1/2021	70	7.61	73.8	**0.01‡**	123	14.8	1050	1210	92	158	8	47	204.41	987	1520.8	6984.5
2/15/2021	108	20.0	407.9	**0**	114	16.4	910	961	108	51	10	29	204.95	1974	1621.0	5995.7
3/15/2021	228	46.1	138.8	**0.01**	140	16.3	1220	1280	169	57	8	67	202.00	2059	2052.8	6909.4
3/29/2021	312	18.6	359.4	**0.01**	57	15.7	1320	1320	82	6	37	29	181.65	1577	2209.3	6734.2
4/12/2021	1424	49.4	1287.1	**0.03**	170	15.0	1440	1460	144	20	108	42	191.23	1958	3880.3	21103.8
4/26/2021	1672	11.3	797.2	**0.02**	220	12.9	1100	1190	100	93	8	62	186.57	1835	4118.1	15996.8
5/10/2021	1828	23.0	1582.1	**0.04**	193	13.9	716	733	244	17	110	41	177.22	3021	3479.7	27712.8
5/24/2021	35080	77.7	1402.2	3.77	267	13.1	1100	1250	107	155	108	43	172.60	1121	4881.7	12166.6
6/7/2021	1084	79.3	385.2	0.37	143	42.6	1510	1510	116	8	21	73	164.35	944	4118.1	23657.3
6/21/2021	1313	50.6	277.2	**0.12**	123	13.7	1460	1470	129	8	54	32	163.75	1503	5651.5	24633.6
7/8/2021	1233	13.3	328.2	**0.06**	197	15.0	1220	1350	103	134	138	77	194.72	1675	3342.1	17686.6
7/19/2021	2678	22.2	60.1	**0**	287	17.3	1340	1540	142	200	113	117	288.70	2186	4881.7	12016.4
8/2/2021	93	37.1	505.1	**0**	387	19.4	3210	3250	138	38	28	119	284.19	2134	1595.9	6884.4
8/17/2021	150	7.66	405.1	**0**	470	20.1	1220	1370	133	151	13	135	306.09	2430	1251.7	6158.4
9/13/2021	116	11.0	45.5	**0.03**	426	20.3	723	882	133	159	96	116	298.37	2263	1068.1	4906.7
9/27/2021	44	16.8	48.4	**0**	513	20.7	1470	1580	166	108	132	119	261.17	6613	1783.7	6421.3
10/11/2021	1620	27.4	55.2	**0.04**	502	20.2	1590	1750	153	159	19.1	131	274.45	2913	1764.9	5726.6
10/25/2021	160	1.03	40.9	**0**	543	20.9	1130	1340	163	211	8	122	219.52	1678	1322.6	6008.2
11/8/2021	80	2.43	212.6	**0**	427	19.6	981	1300	180	320	64	117	300.94	3665	1164.1	6221.0
11/22/2021	1747	4.32	42.3	**0.17**	263	21.9	1080	1350	129	272	43	83	336.99	2303	1967.7	11903.7
12/6/2021	3347	3.63	486.4	1.04	223	19.6	1030	1050	122	22	8	48	212.65	1808	1817.5	10026.2
12/20/2021	1293	4.11	55.3	**0**	267	23.5	1080	1260	115	177	298	74	330.79	2304	1764.9	10026.2
1/3/2022	987	8.30	103.3	**0**	110	22.8	946	1050	73	103	8	30	225.08	1911	2515.9	13781.3
1/17/2022	300	5.70	269.0	**0.01**	117	18.6	1210	1330	90	124	8	35	213.63	2004	1890.1	5182.1

*HP: Hydrogen peroxide

**PICO: Picocyanobacteria cell density

†BAC: Bacteria cell density

‡Values in bold are below microcystin detection limit (0.3 µg/L)

Table 2.3. Descriptive statistics of water quality parameters obtained at Franklin Lock and Dam during bimonthly monitoring

	Water discharge	Temp	DO	Cond	pH	TDS	Algal colony	Chl-a	HP	MC	Total iron	TOC	CDOM
	cfs	°C	mg/L	µS/cm		mg/L	cells/L	µg/L	µg/L	µg/L	µg/L	mg/L	µg/L
Number of values	24	24	24	24	24	24	24	24	24	24	24	24	24
Minimum	944	20.13	2.9	226.2	7.1	0.14	43.9	1.0	1.40	0	57	12.9	163.8
25% Percentile	1676	23.30	3.8	376.8	7.4	0.2425	124.5	6.2	1.93	0	127.3	15	187.7
Median	1989	27.25	5.4	413.4	7.8	0.27	1036	15.1	9.25	0.01	221.5	19	213.1
75% Percentile	2304	28.95	7.4	484.2	8.0	0.3125	1659	34.7	15.9	0.055	416.3	20.6	287.6
Maximum	6613	30.50	8.4	589.1	8.3	0.38	35080	79.3	53.8	3.77	543	42.6	337
Range	5669	10.37	5.5	362.9	1.2	0.24	35036	78.3	52.4	3.77	486	29.7	173.2
Mean	2203	26.14	5.629	421.8	7.713	0.2729	2374	22.86	13.27	0.2388	261.8	18.93	233.2
Std. Deviation	1124	3.221	1.84	88.46	0.3579	0.05894	7025	22.64	15.15	0.7834	148.9	5.954	55.45
Std. Error of Mean	229.4	0.6574	0.3756	18.06	0.07306	0.01203	1434	4.621	3.093	0.1599	30.39	1.215	11.32
Lower 95% CI of mean	1728	24.78	4.852	384.5	7.561	0.248	-592.7	13.30	6.869	-0.09206	198.9	16.41	209.8
Upper 95% CI of mean	2677	27.5	6.406	459.2	7.864	0.2978	5340	32.42	19.66	0.5696	324.6	21.44	256.6
Coefficient of variation	51.03%	12.32%	32.69%	20.97%	4.641%	21.60%	296.0%	99.04%	114.2%	328.1%	56.87%	31.46%	23.78%
Skewness	2.796	-0.4054	0.03412	-0.03301	-0.074	-0.08402	4.769	1.397	1.698	4.373	0.6221	2.811	0.5287
Kurtosis	10.37	-1.045	-1.362	0.1563	-1.175	0.1817	23.1	1.225	2.103	19.94	-0.9457	10.92	-1.148

HP: Hydrogen peroxide

MC: Microcystin

After the spring *Microcystis* bloom event, *Cyanobium* and *Synechococcus* proportions of the microbial community increased, making up roughly half (49.5%) of the cyanobacterial community, which composed nearly half of the bacterial community (43.4%) until September 27 when cyanobacteria dropped to 1.2% of bacteria and *Microcystis* saw a slight increase (Fig. 2.8). This coincided with an increase of water discharge through our Franklin Lock and Dam study site, rising from 2,263 cfs on September 13 to 6,613 cfs on September 27.

When samples were plotted with a Principal Component Analysis (PCA) biplot using the relative abundance of cyanobacterial sequence reads at the genus level, taxonomic influencing factors appeared to group into three distinct clusters most strongly related to supplementary factors of discharge, nitrogen, and hydrogen peroxide, respectively (Fig. 2.9). This explained 40.0% of variation across samples. The taxonomic distribution across these clusters was varied, although the cluster associated with nitrogen mostly contained picocyanobacteria such as *Cyanobacterium*, *Cyanobium*, and *Synechococcus* that existed in high abundance throughout the year. *Microcystis* fell outside of these clusters and most strongly related to ammonia.

Table 2.4. Descriptive statistics of nutrients obtained at Franklin Lock and Dam during bimonthly monitoring

	TKN µg-N/L	TN	TP µg-P/L	TN/TP	TOC/TN	NOx µg-N/L	NH3 µg-N/L	OP µg-P/L	ION/OP
Number of values	24	24	24	24	24	24	24	24	24
Minimum	1.08	733	73	3	6	6	8	29	0.4
25% Percentile	993.3	1195	104	8.675	11.13	26	8	41.25	1.425
Median	1170	1325	129	10.9	13.55	116	32.5	70	2.15
75% Percentile	1415	1468	150.8	13.08	18.3	159	108	117	3.5
Maximum	3210	3250	244	23.6	28.2	320	298	135	6.4
Range	3209	2517	171	20.6	22.2	314	290	106	6
Mean	1207	1366	130.5	11.12	14.69	114.6	60.34	74.5	2.55
Std. Deviation	540	462	37.34	3.937	4.992	86.51	68.48	37.77	1.563
Std. Error of Mean	110.2	94.3	7.623	0.8036	1.019	17.66	13.98	7.71	0.319
Lower 95% CI of mean	979.4	1171	114.7	9.458	12.58	78.09	31.42	58.55	1.89
Upper 95% CI of mean	1435	1561	146.2	12.78	16.8	151.2	89.25	90.45	3.21
Coefficient of variation	44.73%	33.82%	28.62%	35.40%	33.98%	75.47%	113.5%	50.70%	61.28%
Skewness	1.84	3.008	1.121	1.077	0.9179	0.5501	1.975	0.3089	0.9217
Kurtosis	8.766	12.54	2.396	3.737	1.053	-0.1414	5.167	-1.53	0.8366

Metatranscriptome

In total across 24 samples, 5,999,144 sequences were determined. The mean number of cyanobacterial sequence reads was 1,399,642 ± 14,949 (*n* = 21), however, three samples (March 29, April 12, and December 20) did not contain any cyanobacterial sequences. As expected, photosynthesis, protein metabolism, and respiration were the three most abundant SEED subsystems for cyanobacteria throughout the year (Fig. 2.10). However, this was not true immediately following the Spring HAB, instead nitrogen fixation was strongly expressed at 68.1% of the transcriptome, corresponding with a sudden decrease of ammonia and nitrate/nitrite concentrations.

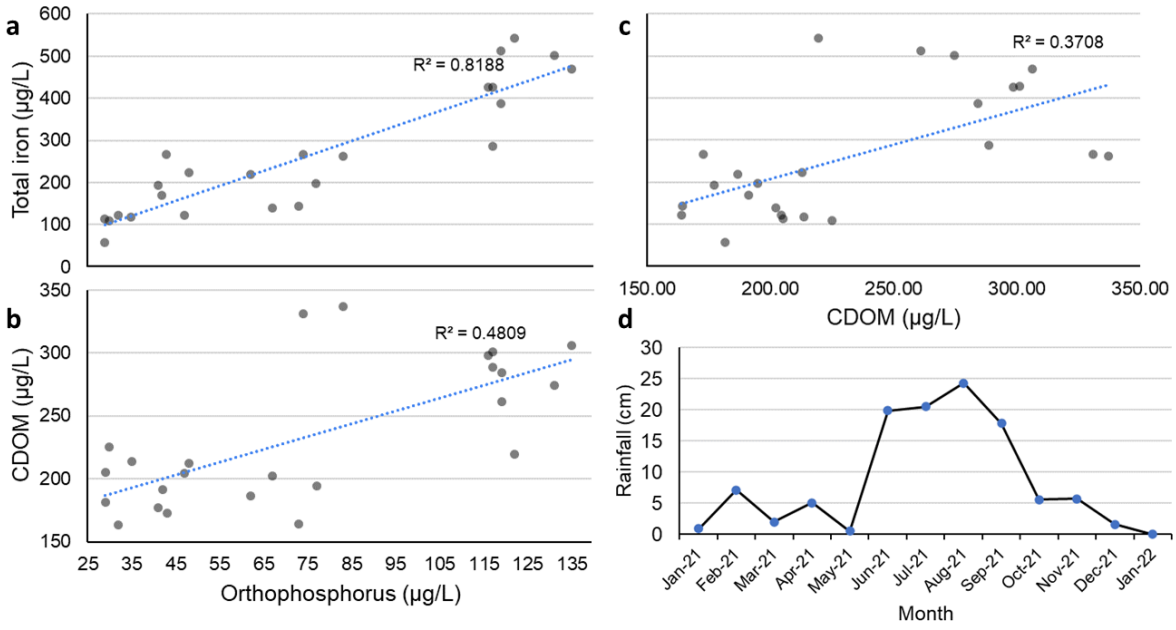

Figure 2.5. Relationships of total iron, CDOM, and rainfall. Plots with trendline of total iron by OP (R^2 = 0.82, *n* = 24) (A); CDOM by OP (R^2 = 0.48, *n* = 24) (B); total iron by CDOM (R^2 = 0.37, *n* = 24) (C); and monthly rainfall (D).

Microcystis sequence reads (103,050 ± 2,749, *n* = 21) mostly followed the trend of cyanobacteria, although distribution of subsystems was more sporadic likely due to the relatively low proportion of the transcriptome with a minimum of 57 sequence reads on January 17, 2022. Shortly before the apex of the spring bloom event on May 10, a protein relevant to the putative metallochaperone family COG0523 was sharply upregulated from 0 to 22.9% of identified transcripts. In freshwater cyanobacteria, this has been linked to zinc deficiency (Barnett et al., 2012). The authors mentioned that zinc is indispensable for the correct function of hundreds of enzymes and thousands of regulatory proteins and between 5 and 9% of

the predicted proteomes of most organisms correspond to zinc-requiring proteins (Barnett et al., 2012). Our data may suggest the zinc deficiency could be occur for freshwater algae under the bloom conditions due to the high requirement of zinc by phytoplankton to fix dissolved inorganic carbon. Additionally, pyridoxine, which is used in chlorophyll production, was upregulated at the same time (Parra et al., 2018). At the height of the bloom on May 24, protein metabolism transcripts increased greatly while photosynthesis reduced. The December bloom event provided a much lower resolution perspective of the *Microcystis* transcriptome leading up to the bloom, but the relative proportion of subsystems closely matched the beginning of the spring event on April 26. Their five most abundant SEED subsystems examined at level two overlapped except for one each. The fifth most abundant for May 26 was not very abundant on December 6, but the third most abundant for that date was sixth for May 26. With these five most abundant subsystems from the December bloom (protein binding, clustering (Null), CO_2 fixation, phages and prophages, and electron transport and photophosphorylation) made up 68.1% and 83.4% of total transcripts from May 26 and December 6, respectively. When these were examined for overlapping SEED functions, six were identified across all except the clustering (null) subsystem (protein binding: LSU ribosomal protein L3p (L3e), LSU ribosomal protein L4p (L1e); CO_2 fixation: ribulose bisphosphate carboxylase large chain (EC 4.1.1.39), possible RuBisCo chaperonin RbcX; electron transport: photosystem II protein D2 (PsbD), photosystem II protein D1 (PsbA); phages & prophages: r1t-like_streptococcal_phages (structural protein)), making up 40.7% and 42.9% of May 26 and December 6, respectively.

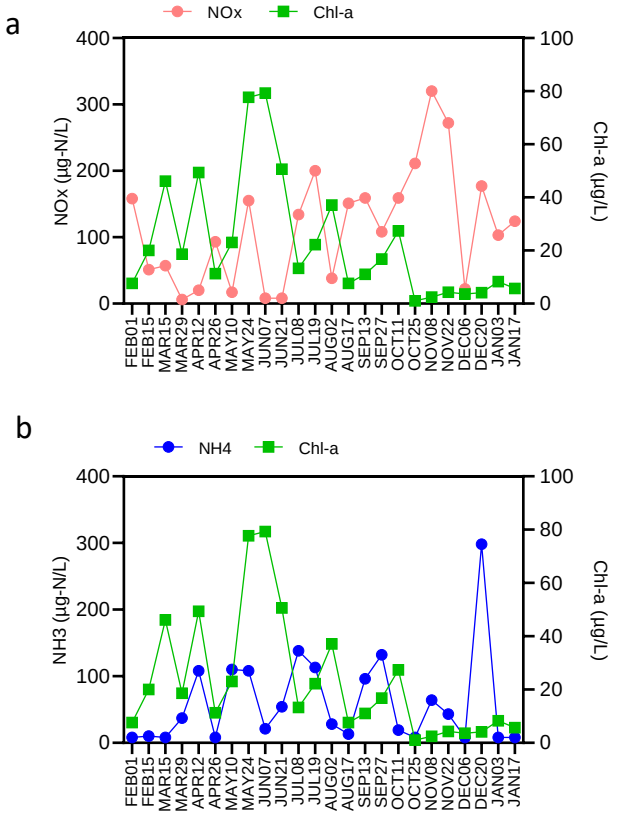

Figure 2.6. Seasonal dynamics of Chl-a and nitrate (a), and ammonia (b).

Harmful algal blooms

During our year-long monitoring, we observed two HAB events of varying intensity (Fig. 2.7). April 26 to May 24 marked a month-long *M. aeruginosa* bloom event which covered the water's surface at our sampling site in a corner where the Franklin Lock structure meets the shore (Fig. 2.2). Amongst semi-aquatic plants on the shoreline away from the lock, cyanobacterial scum existed. Away from the shore, colonies existed in large amounts at the surface and throughout the water column but did not completely cover the surface. On December 6, another *M. aeruginosa* bloom event occurred but was only captured by one day of our biweekly sampling, and colonies were not as abundant as during the spring event.

The end of these events marked the only sampling dates in which microcystin toxin was detectable (May 24: 3.77 µg/L, December 6: 1.04 µ/L). After the final sampling day of the spring event, microcystin persisted for two weeks later on June 7, which was slightly above the detection limit

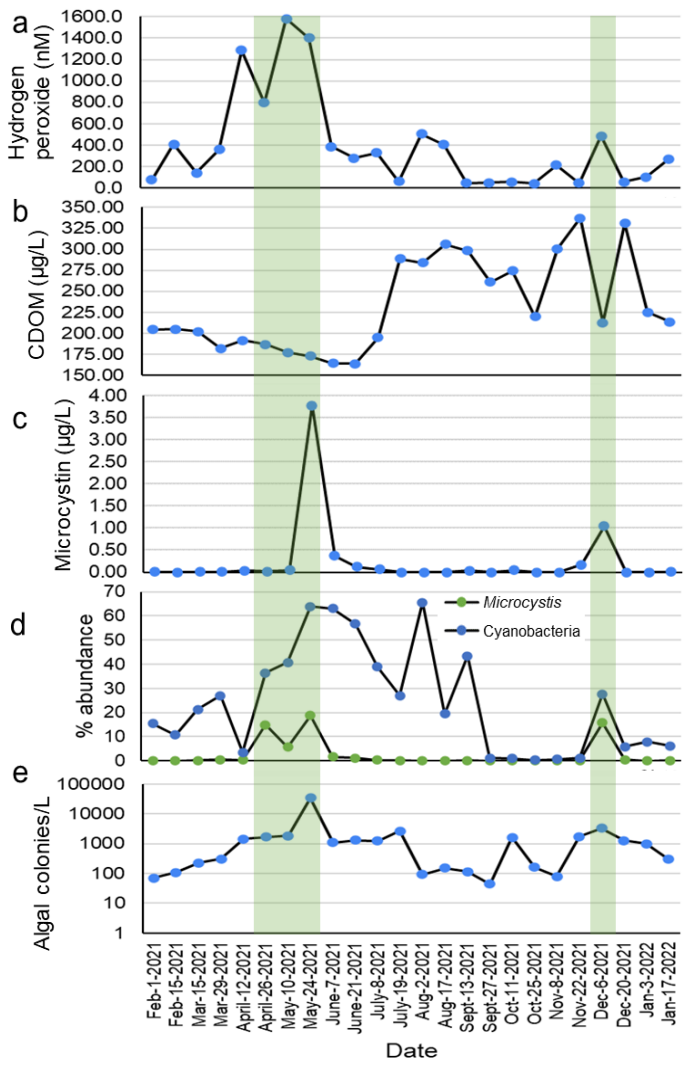

Figure 2.7. Algal bloom timeline. Hydrogen peroxide concentration sampled twice monthly over one year of monitoring with peaks coinciding with elevated activity of bloom-forming cyanobacteria (a). These periods were characterized by low CDOM (b), increased microcystin levels (c), Cyanobacteria and *Microcystis* high-throughput sequencing read abundance (d), and peaks of algal colony density (on a logarithmic scale) (e). The green line shade indicates Microcystis blooming periods.

(0.37 µg/L). Microcystin concentration strongly correlated to macroscopic algal colony density (R^2 = 0.94, *n* = 48).

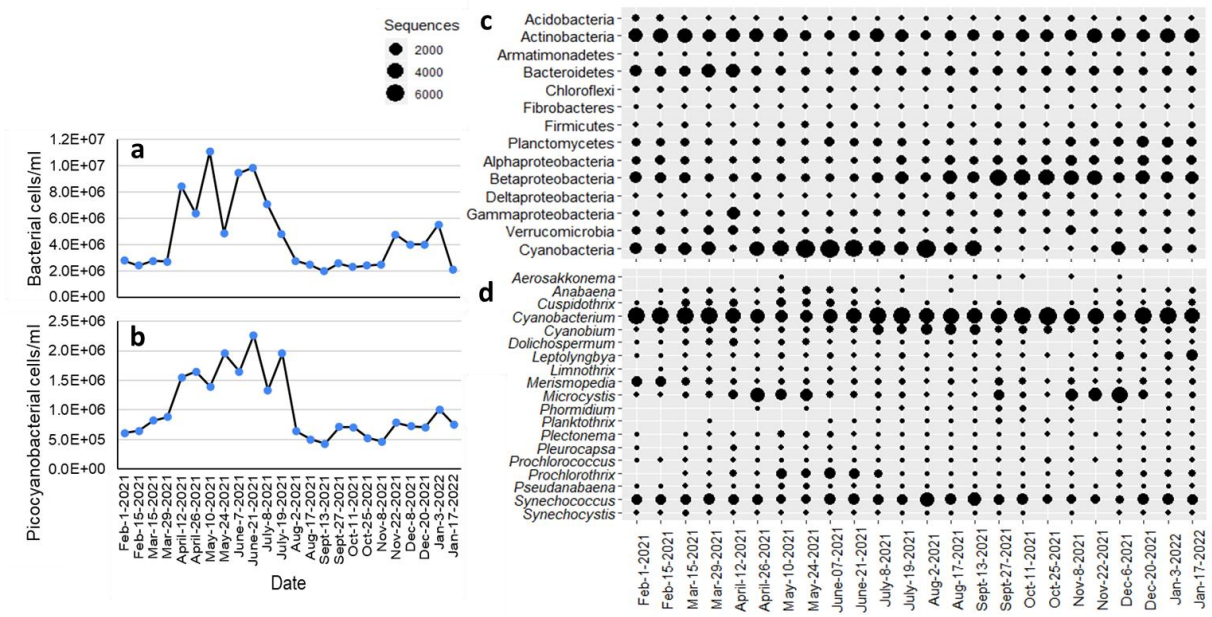

Figure 2.8. Bacterial and picocyanobacterial cell numbers and high-throughput sequencing analyses of bacterial taxa and cyanobacterial genera. Cell density of bacteria (a) and picocyanobacteria (b) over one year of biweekly monitoring. Bacteria (c) and cyanobacteria (d) sequence read abundance normalized to 10,000 reads showing major taxa (> 0.5%). Distinct succession patterns were evident throughout the year switching between periods of actinobacterial, proteobacterial, and cyanobacterial dominance of the microbial community. Within the cyanobacterial community, *Cyanobacterium* and *Synechococcus* dominated the majority of the year but were succeeded by *Microcystis* during two bloom events in April through May and in the beginning of December.

During the bloom events, dissolved oxygen (DO) increased as expected (Table 2.1), but the usual hypoxic aftermath of a HAB did not occur. This is most likely due to the smaller and more isolated impact of the blooms on our study site paired with the flowing nature of the system, flushing any stagnating and decaying bloom biomass before DO is consumed by decomposition processes (Paerl et al., 2001).

Hydrogen peroxide

Environmental hydrogen peroxide levels fluctuated throughout the year with a median value of 273.1 nM, a minimum of 40.9 nM on October 25, and a maximum of 1,582.1 nM on May 10 (Fig. 2.7). In total 54%

of samples showed higher concentrations than the average (coefficient of variation: 114%, skewness: 1.7). Peaks of elevated hydrogen peroxide concentration coincided or preceded cyanobacterial activity, specifically by *M. aeruginosa* during bloom events mentioned previously (May 10: 1,582.1 nM, December 6: 486.4 nM). Two peaks, relative to surrounding values, were unrelated to *M. aeruginosa* abundance on February 15 (407.9 nM) and August 2 (505.1 nM) through August 17 (405.1 nM) but associated with an increase in the cyanobacterial community dominated by *Cyanobacterium* and *Synechococcus*, respectively (Fig. 2.8).

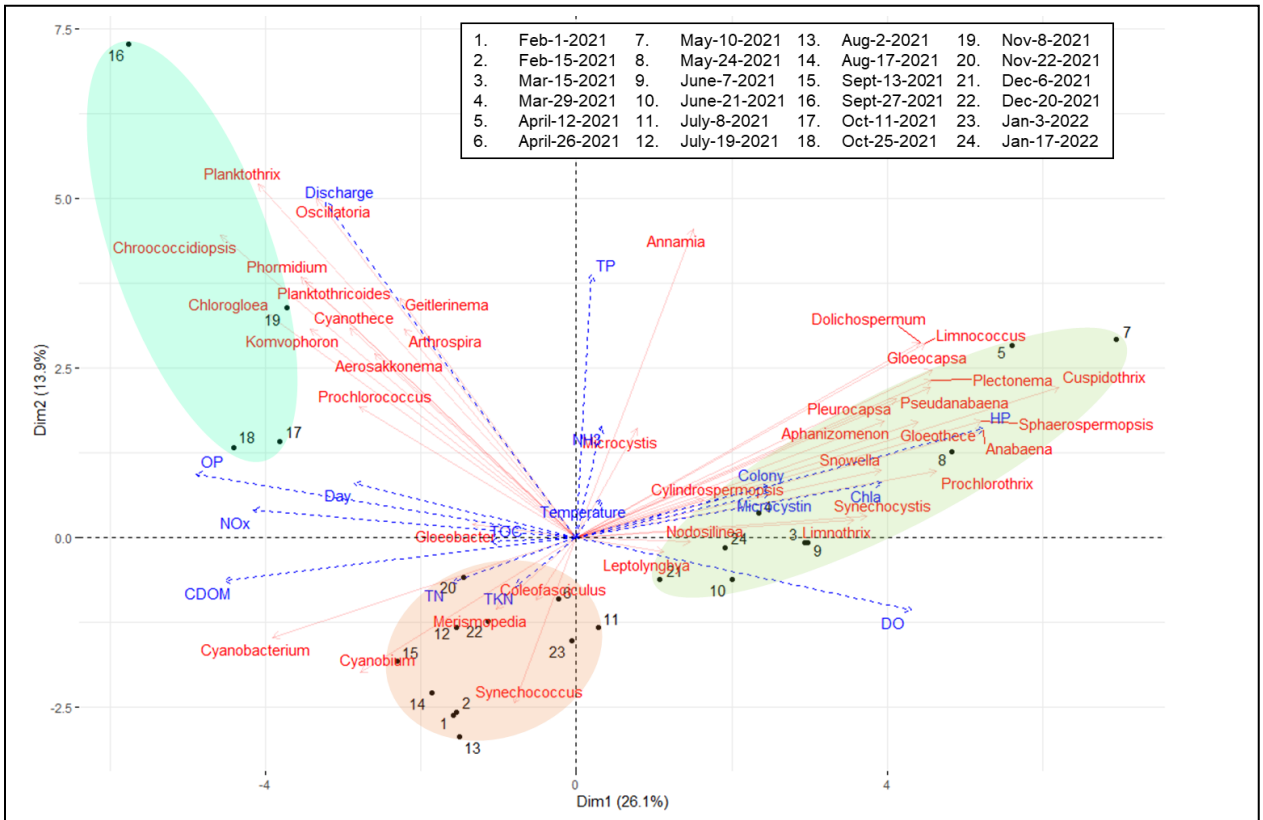

Figure 2.9. Cyanobacteria PCA. PCA of year-long sampling cyanobacterial high throughput sequencing reads (normalized to 10,000 reads). Ordination of sequencing reads identified at genus level in red, with supplemental ordination of relevant water quality parameters in blue. Samples and cyanobacterial genera ordination generally grouped into three distinct clusters (highlighted by circles). Cluster coincided with environmental supplementary ordination including, hydrogen peroxide (HP), Discharge, and total nitrogen (TN) and total Kjeldahl nitrogen (TKN).

DISCUSSION

In June and July, the water discharge was kept low and it could be a reason why major algal blooms were prevented this year. One major goal of this project was to reveal the interaction between hydrogen peroxide and algal dynamics. We hypothesized that hydrogen peroxide could be used to predict algal blooms.

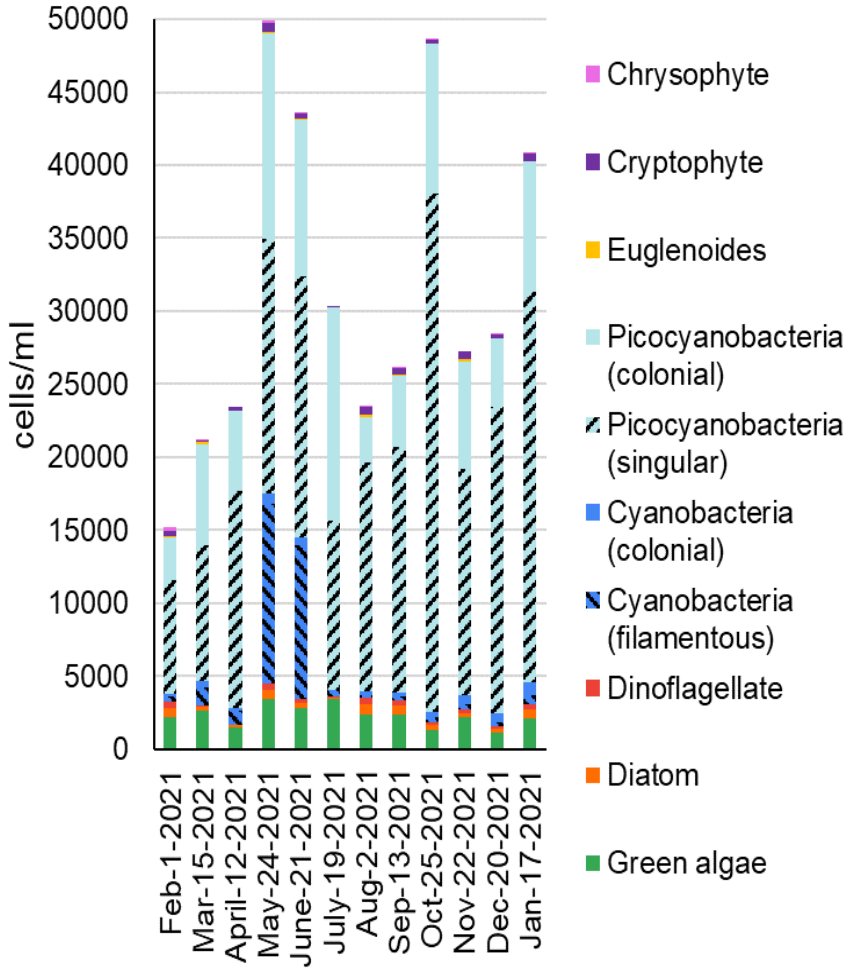

Figure 2.10. Bar graph of phytoplankton identification. Peaks of phytoplankton counts were seen in May, June, and October of 2021, and in January of 2022.

Our biweekly year-long monitoring at Franklin Lock and Dam on the Caloosahatchee River revealed a seasonal pattern of environmental conditions which appeared to be linked to seasonal rainfall and drought. A bimodal trend shared amongst various parameters existed in the data which corresponds to the wet/dry season and rainfall and river discharge. From July through the end of 2021, CDOM, iron, NOx, and OP saw elevated levels (Table 2.2). A strong positive correlation ($R^2 = 0.82$) existed between iron

and OP, and weaker correlations between iron and CDOM (R^2 = 0.37) and OP and CDOM (R^2 = 0.48) (Fig. 2.5). Conversely during this period, picocyanobacterial and bacterial counts, and Chl-a concentration saw decreased levels. This was most likely due to decreased visible light penetration, as indicated by CDOM,

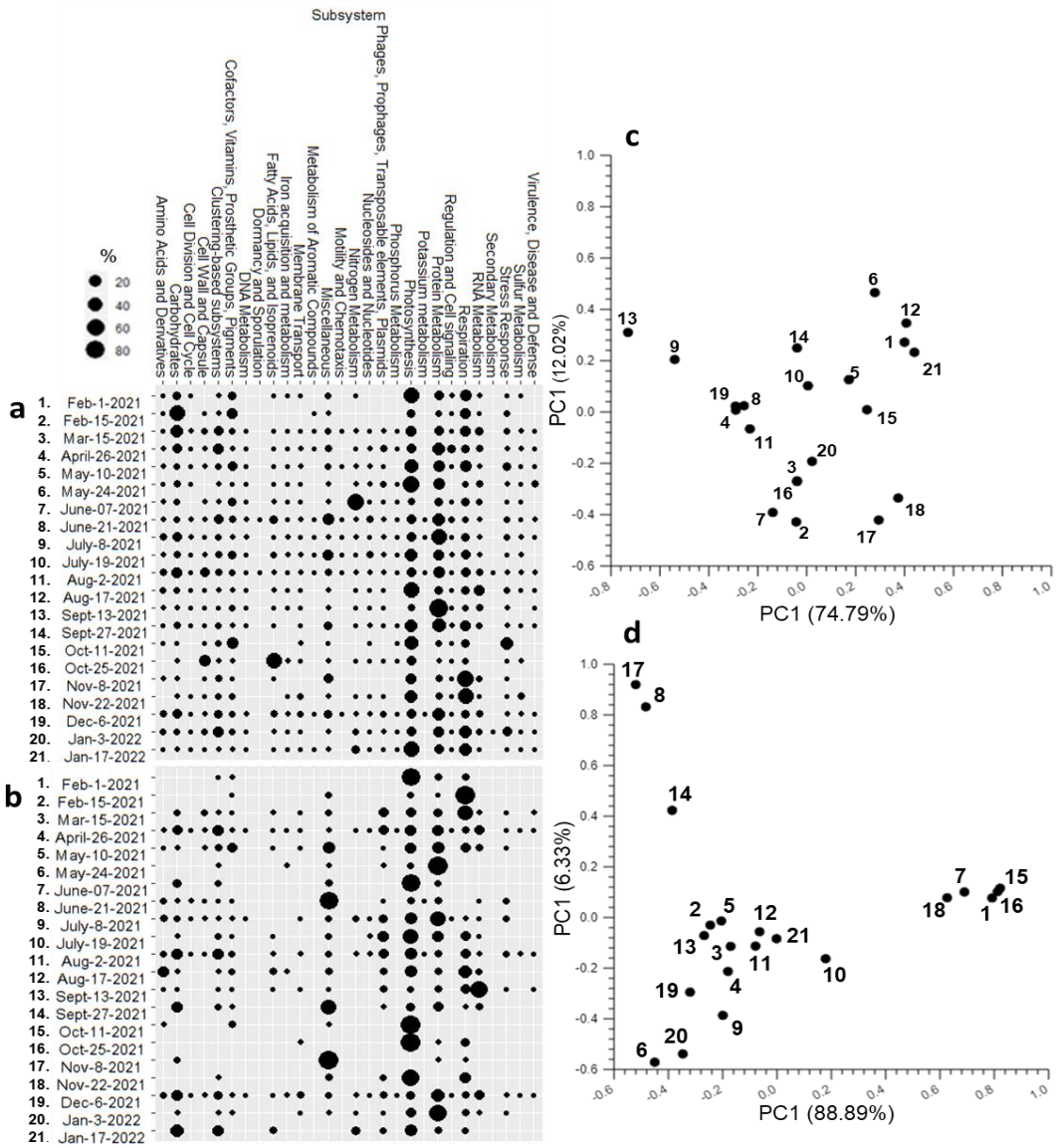

Figure 2.11. Cyanobacteria and *Microcystis* subsystem. Bubble chart and principal coordinate analysis of relative abundance of cyanobacterial (a, c) and *Microcystis* (b, d) SEED subsystems (level 1). Three dates analyzed did not contain any cyanobacterial transcripts and were removed from this analysis. PCoA of cyanobacterial transcripts in two dimensions explained 86.8% of variation of samples (*n* = 21), and PCoA of *Microcystis* transcripts in two dimensions explained 95.2% of variation of samples (*n* = 21).

leading to a reduction in primary productivity (Fig. 2.7). A lagged response of OP highly correlated to total iron indicates this nutrient influx is most likely derived from iron-rich groundwater discharge during seasonal rains (Hu et al., 2006; Charette et al., 2013). These environmental conditions influenced bacterial community succession with a steady increase of the Proteobacteria, specifically the Betaproteobacteria, to the dominance of the community. However, the only notable succession of the cyanobacteria community observed related to seasonal changes was an increase of *Cyanobium*, *Phormidium*, and *Synechococcus*. More impactful was a distinct increase of discharge through Franklin Lock on September 27, which drastically reduced the relative abundance of the cyanobacterial community within the bacterial community, with little impact on relative abundance within cyanobacteria. Interestingly, the relative abundance of *Microcystis*, *Phormidium*, *Planktrothrix*, and *Merismopedia* increased on this date before decreasing shortly after.

Hydrogen peroxide

Environmental hydrogen peroxide concentrations were comparable to previous measurements taken in the Caloosahatchee River, as were increased measurements around HAB events (Ndungu et al., 2019). During our biweekly monitoring, two weeks before the spring bloom, hydrogen peroxide increased greatly and was maintained until the bloom dissipated. During the brief December bloom, there was a smaller but noticeable increase. The lack of a hydrogen peroxide peak preceding this event may be due to the two-week gap between sampling dates, in which a preceding peak may have occurred. The workplan indicated a sampling frequency of 2-4 times per month. Future HAB studies would benefit from a sampling frequency at the upper end of that range.

Hydrogen peroxide peaked similarly to the December bloom during sampling on both February 15 and August sampling events but did not correspond to HAB events. These measurements fall in the high range of previously recorded measurements in the Caloosahatchee River outside of a bloom (Ndungu et al., 2019). The August peak occurred during a period of increased CDOM, which is known to contribute to hydrogen peroxide concentrations through photochemical processes. However, this does not fully explain these concentrations as all other peaks occurred during relatively low levels of CDOM and the lowest measurements of hydrogen peroxide taken were during a period of high CDOM. All hydrogen peroxide peaks aligned with increased relative cyanobacterial activity, specifically *Cyanobacterium* and *Synechococcus*. A recent three-year study in Lake Daecheong, Korea linked algal cell growth to hydrogen peroxide production (Yoon et al., 2021).

Both bloom events occurred during periods of relatively low CDOM, and the short December bloom event specifically occurred during a brief time frame when CDOM was reduced. CDOM influences light penetration of the water column and impacts the growth of algae (Buzzelli et al., 2014). This indicates relative peaks of hydrogen peroxide and relatively low levels of CDOM (< 250 µg/L) may be a useful predictive window for increased *M. aeruginosa* bloom activity. *Microcystis* is hypothesized to exhibit adaptations to defend from UV radiation, such as the formation of dense colonies and surrounding the cell membrane with a mucilaginous layer (Sommaruga et al., 2009). When CDOM is high, it reduces the risk of damage by UV radiation. In such environmental conditions, *M. aeruginosa* may not be able to compete with already dominant algal taxa. This may further explain a lack of noticeable preceding peak in our biweekly sampling structure. Cyanobacterial surface scum had not yet fully formed, indicating the bloom may have only begun to accumulate but was cut short by rising CDOM levels. However, the cyanobacterial community as a whole was reduced following the event, indicating conditions were likely disadvantageous to the entire cyanobacteria community, not just *Microcystis*.

Community succession

Previous studies have documented distinct succession patterns of cyanobacteria such as *Aphanizomenon* and *Dolichospermum* directly proceeding a *Microcystis* HAB (Wu et al., 2016; Wan et al., 2019), however, we did not observe such clear trends. *Aphanizomenon*, *Anabaena*, *Dolichospermum*, and *Pseudanabaena* increased in relative cyanobacterial abundance with *Microcystis*, but each represented less than 7% of the cyanobacterial community at most.

Unlike cyanobacterial succession, there were clear trends in bacterium succession. Prior to the height of the spring bloom, the gammaproteobacterium *Legionella* increased before quickly decreasing again. *Legionella* abundance during the accumulation of *Microcystis* blooms has been previously documented in Lake Taihu, China (Li et al., 2011), but the reason for this association is still unknown.

Metatranscriptome

Our metatranscriptome analysis found an expected distribution of SEED subsystems regarding cyanobacteria, with photosynthesis, protein metabolism, and respiration. However, *Microcystis* deviated from this around HAB events. Notably in the accumulation phase, a COG0523 protein is linked to zinc deficiency to maintain homeostasis. Bacteria have relatively minuscule zinc requirements, but it is still needed for many enzymes in cyanobacteria to function, such as alkaline phosphatase and DNA ligase. In

cyanobacteria, alkaline phosphatase contributes to survival during phosphate deficiency (Barnett et al., 2012). This coincided with a yearly peak of total phosphorous but a decrease in OP.

Additionally, the metatranscriptome of the singular December bloom sampling date and the beginning of the spring bloom event were highly similar despite different environmental conditions, highlighting a connection to *Microcystis* HAB accumulation, especially as many of the functional subsystems identified are associated with growth. If these transcripts are consistent beyond this one year of monitoring, they may be useful for rapid transcriptional profiling via real-time quantitative PCR to obtain gene-copy numbers of these specific transcripts in comparison to others not associated with this bloom accumulation fingerprint (Sharma et al., 2022).

Conclusion

We monitored a single site at the downstream end of the non-tidally influenced portion of the Caloosahatchee River known to experience isolated cyanobacterial HABs for a full year at twice monthly intervals from February 2021 through January 2022. This focused water monitoring program allowed us to perform in-depth analyses of the cyanobacterial community and witness two distinct HAB events during the second and last quarters of the year. Our findings indicate the accumulation phase of *Microcystis* HABs in the Caloosahatchee River appears to exhibit a distinct metatranscriptome profile and may be useful as a HAB forecasting method. While both are able to yield data on the same day as collection, hydrogen peroxide appears more promising as an effective early warning system for HAB development given the cost efficiency and ease of measurement. Our data exhibit that environmental hydrogen peroxide in the subtropical waters of the Caloosahatchee River greatly increases before and during increases in bloom-forming *Microcystis* biomass.

Chapter 3: Mesocosm experiment #1

ABSTRACT

Hydrogen peroxide has recently gained popularity as an environmentally friendly treatment for cyanobacterial harmful algal blooms (HABs) when used at low concentrations. However, the general populace desires rapid removal of HABs. High concentration treatments can achieve this but may introduce an increased risk to the environment. Most susceptible is the microbial community, with hydrogen peroxide noted to have temporary but recoverable impacts at low concentrations. This is concerning as the importance of HAB-associated microorganisms has been highlighted recently, shown to directly impact HAB succession and nutrient modulation. Over the course of four days, we monitored *Microcystis* bloom biomass retrieved from Lake Okeechobee in six mesocosms filled with 300 L of sieved river water on the bank of the Caloosahatchee River. Three mesocosms received a hydrogen peroxide spray treatment of 92x the lethal dose for *Microcystis* (theoretical concentration of 13 mM). This treatment achieved rapid (< 24 hour) bloom collapse followed by drastic change in microbial community composition. The treatment group also saw large increases of ammonia (13.9x higher) and nitrate/nitrite (14.5x higher). Our study identified hydrogen peroxide resilient microbial components of a South Florida *Microcystis* HAB, specifically Planctomycetes (0.58% to 46.85%) and Gammaproteobacteria (0.81% to 17.38%) which steadily increased in relative abundance post-treatment. Theses taxa are different from previously reported hydrogen peroxide resilient bacteria and even show opposite trends in studies from other geographic regions. This further highlights the importance of understanding local systems and populations with respect to water resources and HAB management.

INTRODUCTION

Hydrogen peroxide has recently gained popularity as an environmentally friendly treatment for cyanobacterial harmful algal blooms (HABs), with the first application used in the Netherlands (60 µM hydrogen peroxide concentration throughout the water column) by Matthijs and colleagues (Matthijs et al., 2012). Low concentration applications in lentic systems have proven effective with desirable outcomes as the treatment degrades into water and oxygen and does not harm non-target aquatic life such as zooplankton, insects, or fish (Drábková et al., 2007). Additionally, it takes advantage of cyanobacterial sensitivity to hydrogen peroxide. For example, a dosage of 0.12 mM is the lethal threshold for *Microcystis*

aeruginosa (Sukenik and Kaplan, 2021), a cosmopolitan toxic bloom-forming cyanobacterium, with only temporary yet recoverable impacts to the rest of the microbial community (Piel et al., 2021).

While these low concentration treatments are an effective treatment and regarded as environmentally friendly (Piel et al., 2021), they can be relatively slow to achieve visible results over the span of weeks or longer, sometimes requiring successive treatments. Higher hydrogen peroxide concentration can be used to attain a more rapid HAB removal that may appear desirable, especially for the general populace. However, this may introduce an increased risk to the environment as higher concentrations go beyond the selected sensitivity of cyanobacteria. Of specific concern is the microbial community, due to its sensitivity to environmental change (Urakawa and Bernhard, 2017), but also in regard to the recently highlighted importance of associated microorganisms to HABs. Previous studies have demonstrated direct impacts to HAB development, succession, and nutrient modulation (Wang et al., 2021; Zhang et al., 2021). More specific to hydrogen peroxide application, the microbial community also impacts degradation of cyanotoxin and hydrogen peroxide (Giannuzzi et al., 2021).

We currently have a poor understanding of the environmental impacts of high concentration hydrogen peroxide treatments for cyanobacterial HABs, especially to the associated microbial community. Previously, limited small-scale laboratory studies have examined the effects of high concentration (1.5 mM) hydrogen peroxide on phytoplankton, further highlighting the impact to cyanobacteria with a resulting succession of eukaryotes (Weenink et al., 2015). However, impacts to non-target bacteria and nutrient modulation were not measured. The current gap in our knowledge between laboratory experimentation and real-world field studies must be bridged with a mesocosm study due to its ability to simulate the environment on a larger scale without any potential for environmental harm.

In this study we sought to gain a better understanding of how a high concentration hydrogen peroxide treatment of *M. aeruginosa* HAB impacts succession and gene regulation of the associated microbial community and the resulting effects on nutrient modulation and toxin degradation. To achieve this, we applied a high concentration hydrogen peroxide treatment (theoretical concentration of 13 mM) to *M. aeruginosa* HAB biomass collected from Lake Okeechobee, Florida, USA within a 300 L mesocosm and examined them for four days. We hypothesized the treated microbial community abundance and succession will differ from the control and will result in disrupted nutrient modulation and cyanotoxin degradation.

MATERIALS AND METHODS

M. aeruginosa surface scum biomass from a toxic algal bloom in Lake Okeechobee was collected, concentrated, and acclimated for three days before being distributed evenly (~0.75 L) across six mesocosms. Treatment and control mesocosms were established in triplicate by filling 415 L black oval tubs with 300 L of Caloosahatchee River water sieved through a 70 µm phytoplankton net to remove macrophytes. *M. aeruginosa* biomass was added the next day. Mesocosms fluctuated with ambient environmental conditions and were located ~35 m from the river and ~45 m upstream from the Franklin Lock structure (latitude, longitude: 26.720727, -81.692851) (Fig. 3.1). Light and UV levels were measured using an Extech light meter and SPER Scientific UVC light meter, respectively, and surface physiochemical parameters were measured using an Aqua Troll sonde (In-Situ, CO, USA) for each mesocosm. Mesocosms were sampled before and one hour after treatment, then once daily for a total of three days.

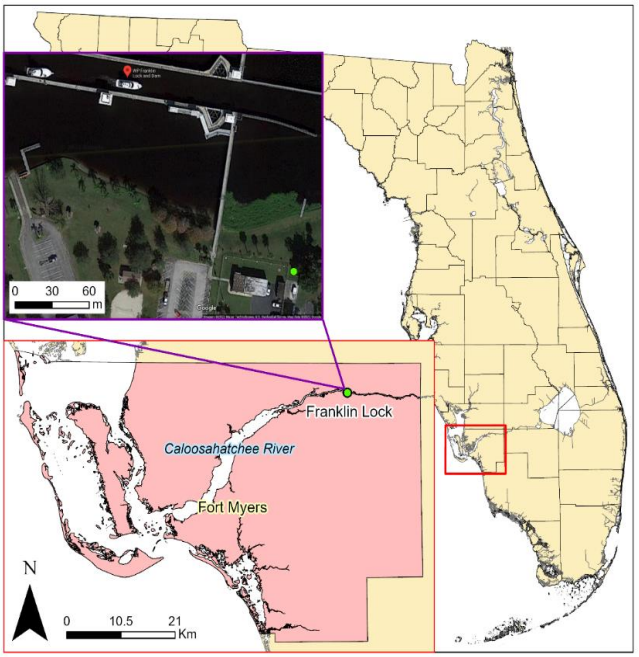

Figure 3.1. Location map. Mesocosms were placed on relatively flat ground close to the shoreline of the Caloosahatchee River on the upstream side of Franklin Lock and Dam in southwest Florida. There were placed in a secluded area to prevent disturbance.

For each treatment mesocosm, four liters of 3% hydrogen peroxide solution was directly applied to the surface biomass via a pump-up herbicide spray applicator over the course of seven minutes (Fig. 3.2). The force of the spray output effectively mixed the mesocosms, resulting in a theoretical diluted hydrogen peroxide concentration of 13 mM applied, which was supported by our measurements (15.7 mM). Hydrogen peroxide samples were collected before treatment, immediately after, one hour post-treatment, and once daily for the remainder of the experiment. Samples were immediately filtered through 0.2 µm Sterivex filters and kept on ice and stored at -80°C until analyzed. Hydrogen peroxide was measured using a fast response amperometric 250 µm diameter tip hydrogen peroxide microelectrode with a built-in reference electrode (HP-250, Innovative Instruments) featuring a lower detection limit of 50 nM (Ndungu et al., 2019).

High-throughput sequencing

Microbial cells were collected by filtering 200 ml of water with a 0.22 µm cellulose nitrate filter. Genomic DNA was extracted from half cut filter samples using the DNeasy PowerSoil Pro Kit (Qiagen) following the manufacturer's instructions. High-throughput amplicon sequencing targeting bacteria was conducted via amplification of 16S rRNA gene with a primer pair 515yF and 926pfR using the Illumina MiSeq system (MR DNA, Shallowater, TX, USA). For analysis, sequences are joined and those less than 150 bp were removed. Sequences with ambiguous base calls were also removed. The dereplicated or unique sequences were denoised; unique sequences identified with sequencing and/or PCR point errors were removed, followed by chimera removal, thereby providing a denoised sequence or Amplicon Single Variant (ASV). Final ASVs were taxonomically classified via representative ASVs through BLAST at NCBI.

Metatranscriptome

RNA Samples for transcriptome sequencing were collected by filtering 200 ml of water using 0.2 µm Sterivex filters on-site which were promptly frozen in liquid nitrogen for transport to a -80°C freezer until further analysis. Total RNA was isolated from Sterivex filters using the RNeasy PowerMicrobiome Kit (Qiagen) following the manufacturer's instructions. For each filter sample, three extractions were performed. RNA was eluted in 100 µl RNase-free water and pooled. DNA contamination was removed using Baseline-ZERO™ DNase (Epicentre) following the manufacturer's instructions followed by purification using the RNA Clean & Concentrator columns (Zymo Research). The RNA samples were used for rRNA removal by using Ribo-Zero Plus rRNA Depletion Kit (Illumina). rRNA depleted samples were used for library preparation via the KAPA mRNA HyperPrep Kits (Roche) by following the manufacturer's instructions. The average library size was determined using the Agilent 2100 Bioanalyzer (Agilent Technologies) and the sample was then pooled in equimolar ratios of 0.6nM, and sequenced paired-end for 300 cycles using the NovaSeq 6000 system (Illumina). After DNase treatment, two samples (HP051221H and HP051321H) showed too low RNA, therefore whole transcriptome amplification (WTA) was performed on them separately. The whole transcriptome amplified samples were used for library preparation using Illumina DNA Prep, (M) Tagmentation library preparation kit (Illumina) following the manufacturer's user guide.

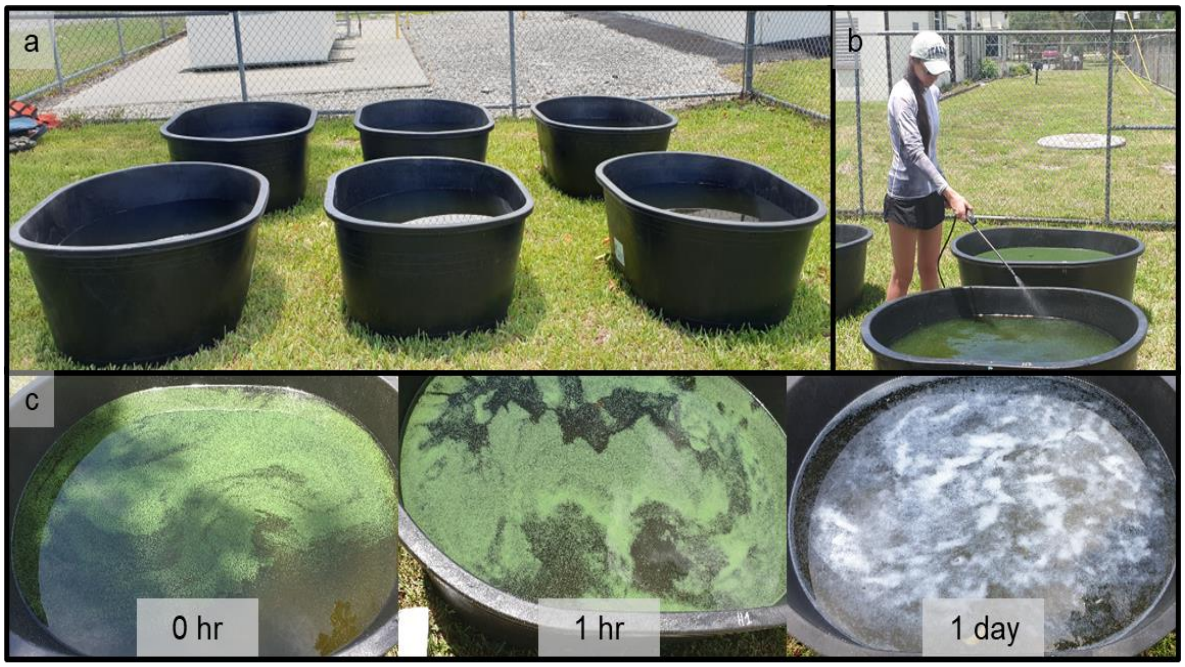

Figure 3.2. Mesocosm set-up (a), hydrogen peroxide spray application (b), and time series of a treatment mesocosm immediately after, 1 hour, and 1 day after treatment. Mesocosms were spaced evenly apart and spraying was conducted pointing away from control mesocosms to prevent overspray and cross contamination; wind was negligible in this respect. Bleaching of colonies in the treatment mesocosms was noticeable within one hour and were fully bleached within one day.

Log_2 fold change was analyzed by aligning metatranscriptome reads to the most abundant taxa expressed in the metatranscriptome after treatment in the KBase environment using HISAT2. This was gammaproteobacterium *Escherichia coli* (K-12; NC_000913) Transcripts were assembled using StringTie and a differential expression matrix was created using DESeq2. To achieve the necessary replication required by DESeq2, days 1 and 2 were assigned as replicates of one another within the control and treatment groups to represent the only distinct post-treatment expression changes within our metatranscriptome dataset.

RESULTS

Hydrogen peroxide

An hour after hydrogen peroxide application to mesocosms, a mean hydrogen peroxide concentration of 12.5 ± 0.6 mM (± SE) was measured (Fig. 3.3). Hydrogen peroxide did not readily degrade and levels

remained high throughout the experiment, with a concentration of 11.9 ± 2.5 mM measured on the final day (Table 3.1). We confirmed no cross-contamination to our control mesocosms occurred from overspray of hydrogen peroxide with levels measured at near zero throughout the experiment and the highest concentration of 0.002 ± 0.003 mM measured on the final day. The treatment mesocosms had higher dissolved oxygen (DO) levels throughout the experiment post-treatment with a range of 135.9 to 149.6 % DO in the treatment as opposed to 102.9% to 113.9% in the control (Fig. 3.3 and Table 3.2). This was presumably from oxygenation by the hydrogen peroxide as it reacted in the mesocosm.

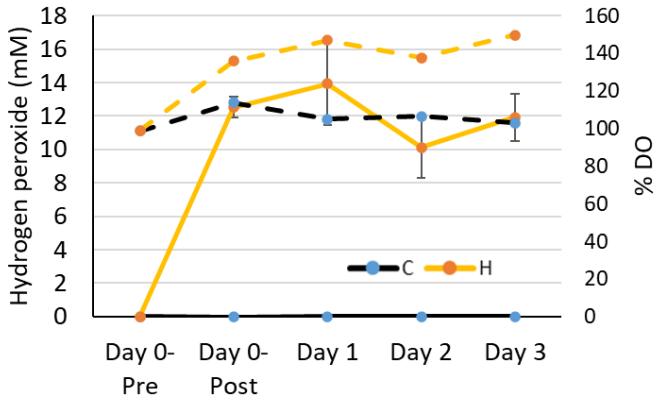

Figure 3.3. Change of average hydrogen peroxide concentrations. Average hydrogen peroxide concentration (solid) with corresponding dissolved oxygen (DO) levels (dashed) of control (C, black) and treatment (H, orange) mesocosms, with error bars representing standard deviation (SD), (*n* = 3). The control displayed minimal hydrogen peroxide levels throughout, whereas the treatment mesocosms maintained a high concentration throughout the experiment with only slight degradation. DO levels were elevated in the treatment mesocosms as a result of oxygenation from the

Microbial community high throughput sequencing

In total, 747,541 sequences were determined in this study and the mean number of analyzed reads after removal of non-target sequences (228 ± 59) was 24,001 ± 862 (*n* = 30). After removal of non-target sequences, samples underwent normalization (scaled to 10,000 reads) before further analysis.

Microbial community shifts induced by hydrogen peroxide treatment

The control and treatment mesocosms started the experiment with similar microbial communities when examined at the genus level, exhibiting a mean Bray-Curtis dissimilarity index of 0.09 ± 0.02 (*n* = 9), and a

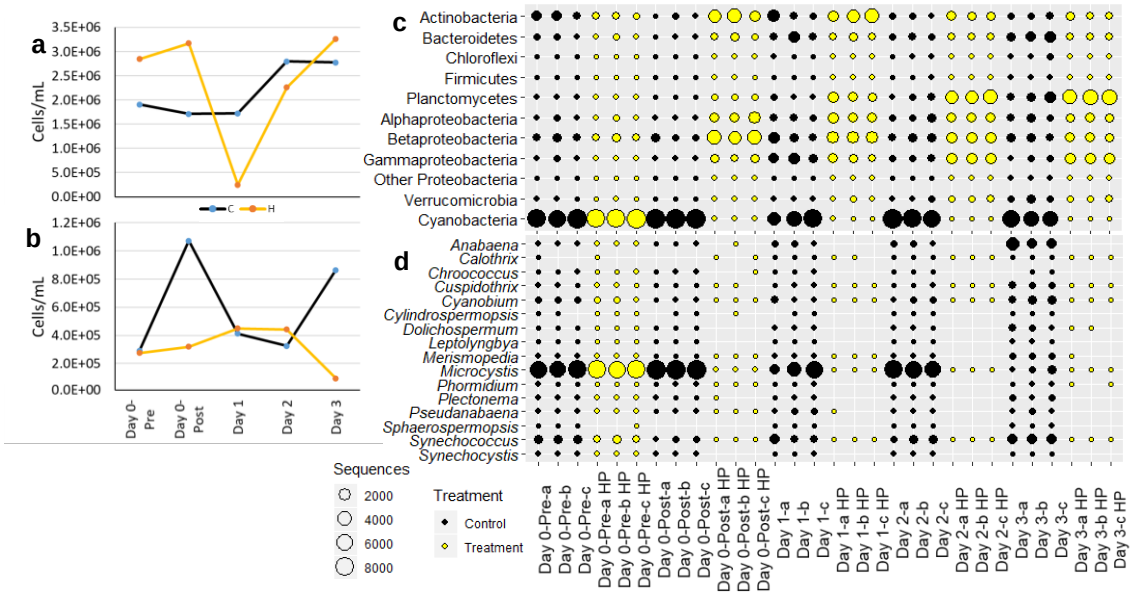

Figure 3.4. Average cell density of bacteria (a) and picocyanobacteria (b) in the control (C) and treatment (H) mesocosms as determined by microscopy cell counting. In the treatment, bacteria levels drastically declined after one day before recovering whereas the control did not see such drastic changes. Picocyanobacteria levels varied in the control over time whereas the treatment saw an overall decline. Bacterial (c) and cyanobacterial (d) sequence read abundance normalized to 10,000 reads showing major taxa (> 0.5%). The control mesocosms maintained cyanobacterial dominance of the microbial community throughout the experiment, primarily consisting of *Microcystis* until the final day when the community exhibited succession towards greater diversity of cyanobacteria. The treatment group exhibited a distinct reduction in cyanobacteria within an hour after hydrogen peroxide treatment. Throughout the experiment, distinct bacterial succession was observed in the treatment group, leading to a dominance of Planctomycetes. This succession directly related to the changes in bacterial cell density observed.

Table 3.1. Water analytes of mesocosms

Day	Treatment	Chl-a	HP*	MC‡	Extracellular MC‡	TOC	TKN	TN	TP	NOx	NH3	OP	CDOM	PICO**	BAC†
		µg/L	nM	µg/L	µg/L	mg/L	µg-N/L	µg-N/L	µg-P/L	µg-N/L	µg-N/L	µg-P/L	µg/L	cells/ml	cells/ml
0	C Pre	478.00	0.26	5.9	2.09	26.9	11400	11426	981	26	75	22	191.3	290,476.3	1903797
0	C Post	1536.00	0.11	4.2	2.12	54.6	14000	14034	1020	34	69	27	233.0	1072113	1711618
1	C	513.00	0.77	10.8	2.56	18.3	9210	9216	780	6	104	28	215.7	413301.4	1721432
2	C	58.30	1.34	4.3	0.61	24.5	2470	2477	122	7	56	15	178.6	325477.4	2796816
3	C	15.90	2.43	0.9	**0.04**	15.0	1060	1066	69	6	20	20	181.2	864396	2772282
0	HP Pre	878.00	0.09	6.7	0.93	22.2	15800	15831	1150	31	85	33	189.7	274161.5	2844247
0	HP Post	967.00	12520.77	7.5	4.95	43.4	16500	16520	1930	20	1250	2	174.5	319752.9	3168089
1	H	6.09	13936.76	9.7	9.13	41.1	6770	6776	951	6	1270	27	139.6	450393.6	246316
2	H	0.79	10129.64	3.0	2.96	24.1	4450	4930	819	478	1260	6	109.1	442692.8	2256262
3	H	0.25	11918.56	5.2	5.18	20.8	2490	2940	224	448	1180	14	154.6	95353.42	3261316

*HP: Hydrogen peroxide

‡MC: microcystin. Values in bold are below microcystin detection limit (0.3 µg/L)

**PICO: Picocyanobacteria cell density

†BAC: Bacteria cell density

Table 3.2. Water physicochemistry of mesocosms

Day	Treatment	Temp.	Sal.	DO	DO	Cond.	TDS	pH
		°C	ppt	%	mg/L	uS/cm	mg/L	
0	C Pre	26.0*	0.20	98.7	8.2	409.81	0.27	8.47
0	C Post	31.5	0.18	113.9	8.8	363.73	0.27	8.87
1	C	26.6	0.19	104.9	8.5	389.92	0.25	8.96
2	C	26.5	0.20	106.6	9.0	418.23	0.27	9.07
3	C	22.6	0.19	102.9	9.0	393.77	0.26	9.13
0	HP Pre	25.4*	0.20	99.0	8.3	413.92	0.27	8.50
0	HP Post	31.7	0.18	135.9	10.5	368.55	0.27	8.30
1	HP	26.6	0.19	147.0	12.1	388.4	0.25	7.94
2	HP	26.5	0.21	137.6	11.6	424.99	0.28	8.20
3	HP	22.6	0.20	149.6	11.0	405.62	0.26	8.16

*Temperature taken an hour prior to treatment

Throughout the experiment, the control mesocosms maintained a relatively stable microbial community for the first three days of the experiment (Bray-Curtis dissimilarity: 0.20 ± 0.02, *n* = 27) until diverging from the initial community condition on the final day (Bray-Curtis dissimilarity: 0.33 ± 0.02, *n* = 9) *M. aeruginosa* was primarily succeeded by *Anabaena* (18.2 ± 5.1%) and *Synechococcus* (12.3 ± 0.4%).

Within one hour of hydrogen peroxide application, the microbial community of the treatment mesocosm changed drastically, exhibiting a mean Bray-Curtis dissimilarity index of 0.84 ± 0.01 (*n* = 9) and a 99.0% decrease of the previously dominant cyanobacteria (Fig 3.5). While still abundant, *Microcystis* colonies began to disassociate, and cells were visibly bleached (Fig 3.6). In its place, Proteobacteria (59.0 ± 8.9%) and Actinobacteria (30.9 ± 10.8%) became the dominant phyla. Within Proteobacteria, Betaproteobacteria (17.8 ± 3.5%) and Alphaproteobacteria (15.7 ± 4.9%) were most abundant. Interestingly, Chl-a readings increased from 878 to 967 µg/L after one hour but were then reduced to 6.07 µg/L the next day (Table 3.1), indicating all photosynthetic organisms were heavily affected by the treatment. This is supported when examining the relative abundance non-target eukaryotic high-throughput sequence

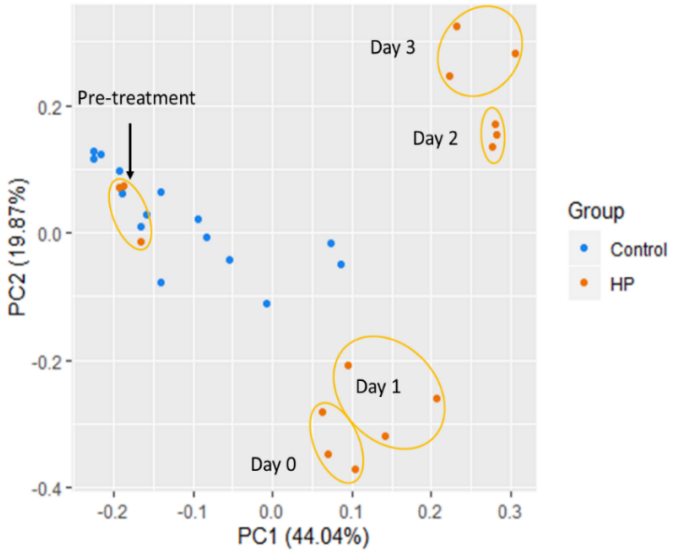

Figure 3.5. Principle component analysis of normalized bacterial community sequence reads at the phylum level. Hydrogen peroxide treatment (HP) mesocosms showed distinct clustering and change over time as opposed to the control. Additionally, as reflected in the bacterial cell count data, three general states are evident in the mesocosm: pre-treatment which mirrors the control, post-treatment which incorporates one hour and one day after treatment, and recovery which includes day two and three.

reads where the control mesocosms increased from 1.14 ± 0.11% to 4.01 ± 1.84% over the course of the experiment with an overall positive trend and conversely the treatment mesocosms decreased from 0.93 ± 0.19% to 0.01 ± 0.00%. One day after treatment, bacterial cell count decreased sharply from 3,168,089 cells/ml to 246,316 cells/ml but Proteobacteria (47.9 ± 3.6%) and Actinobacteria (14.8 ± 10.4%) maintained their relative dominance. During this time, Planctomycetes saw a notable increase from 2.8 ± 0.1% to 13.4 ± 3.5%. Planctomycetes continued to occur in abundance, replacing Actinobacteria as one of the most dominant taxa (33.0 ± 1.2%) 24 hours later alongside Proteobacteria (45.9 ± 1.7%). This shift in relative community abundance occurred as bacterial cell count increased drastically by over 8X to 2,256,262 cells/ml within 24 hours, indicating these sequence data reflect true succession and cell growth within the community. On the next and final day of the experiment, bacterial cell count increased further to 3,261,316 cell/ml as Planctomycetes became the dominant taxa at 46.9 ± 2.2%, followed by Proteobacteria at 38.1 ± 1.9%.

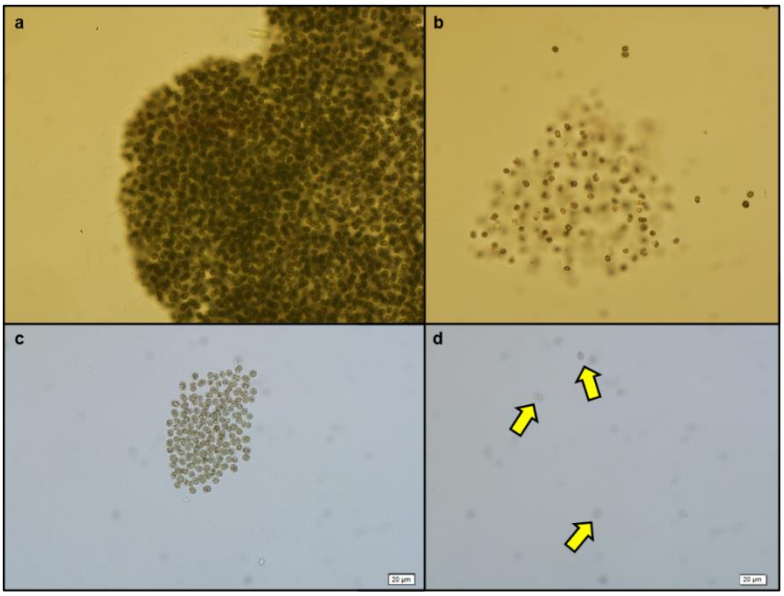

Figure 3.6. Microcystis colonies under 40X light microscope magnification after one hour in a control (a) and treatment (b) mesocosm. After an hour, colonies in the treatment began to visibly disassociate and break down with some cells already bleaching. Near the end of the experiment on day two, the control (c) still had visible healthy *Microcystis* colonies but had decreased in abundance. The treatment (d) had very few *Microcystis* cells (indicated by yellow arrows) remaining, all of which were bleached.

Cyanobacterial relative abundance in the treatment group steadily decreased throughout the experiment as well as species richness, from an average of 26 species to 8 at the end of the experiment. Across the three mesocosms, nine genera were still detectable albeit at minuscule proportions, including

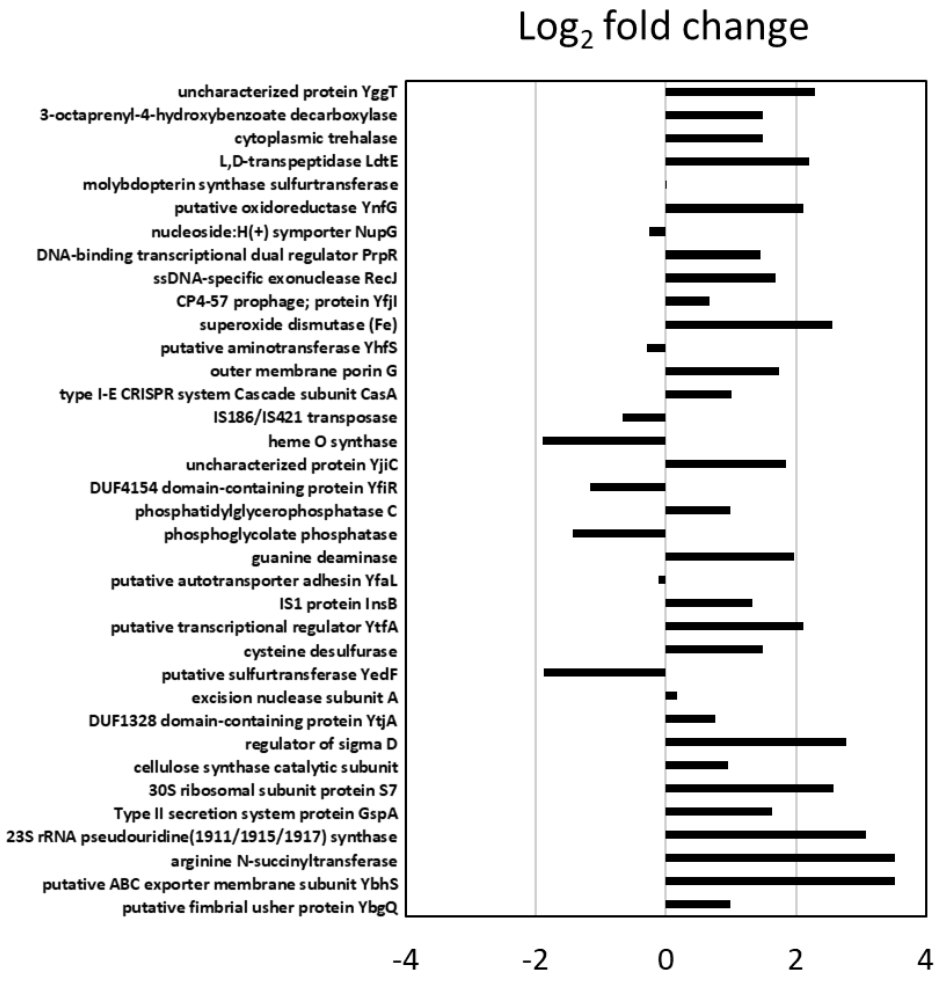

Figure 3.8. Mean $\log_2$ fold change (n=2) comparing expression changes in a hydrogen peroxide treatment (+ fold change) and control (-) mesocosm post treatment for genes exceeding 0.01% of the metatranscriptome. Sequence reads were aligned with the most abundantly taxa expressed (*E. coli*), and data from day one and two were pooled as replicates within each treatment group as the only samples exhibiting distinct transcriptional differences within and amongst treatments.

five filamentous: *Calothrix*, *Cuspidothrix*, *Prochlorothrix*, *Phormidium*, and *Dolichospermum*; three picocyanobacteria: *Cyanobium*, *Synechococcus*, and *Merismopedia*; and *Microcystis*. The most abundant genus was still *Microcystis* (0.06 ± 0.02%), followed by *Calothrix* (0.02 ± 0.01%) and *Cuspidothrix* (0.02 ± 0.01%). Although minor, *Calothrix* was the only cyanobacterium to increase in relative abundance from the beginning of the experiment where it was only detectable in one mesocosm at 0.004% of microbial community sequence reads, an increase of 500%.

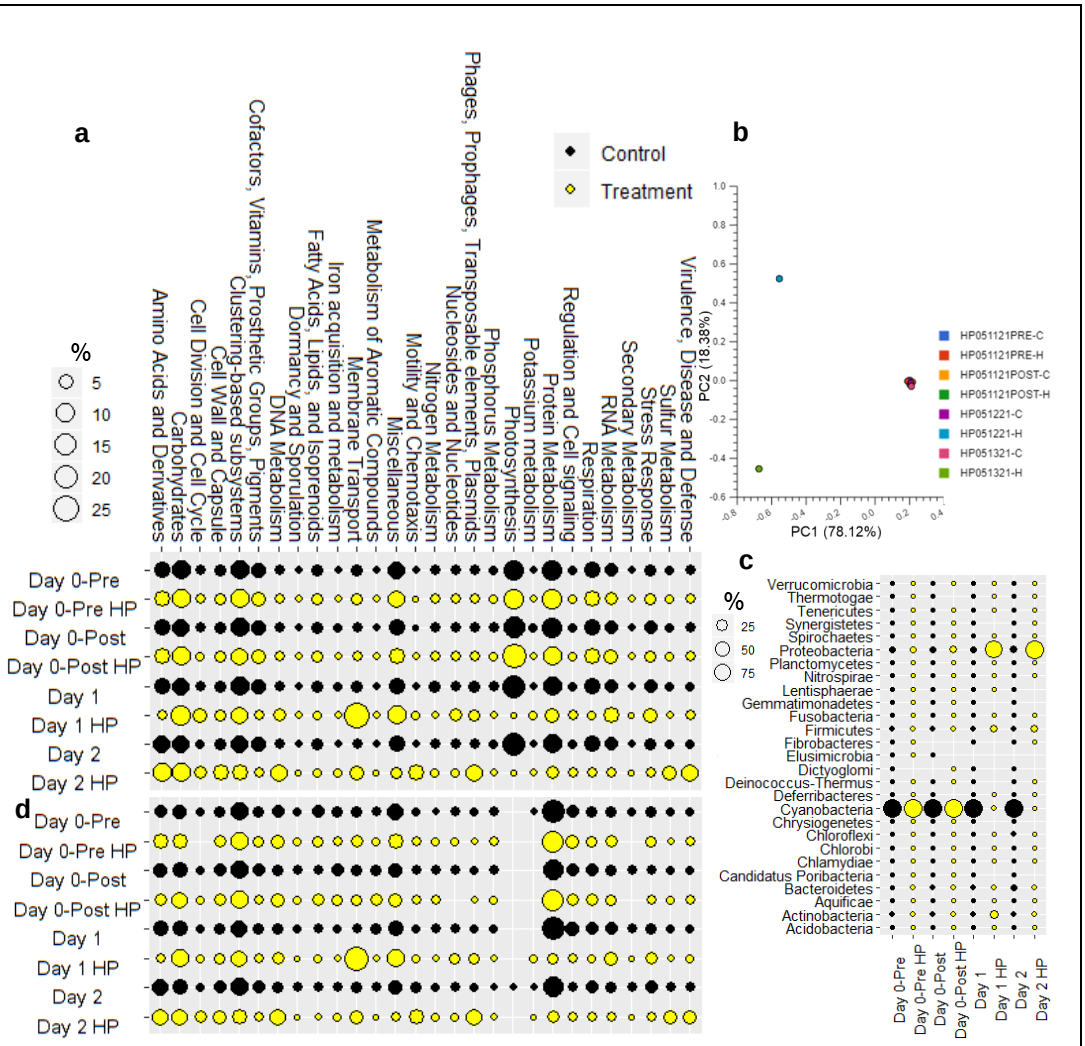

Figure 3.7. Bubble chart (a) and PCoA (b) of relative abundance of bacterial metatranscriptome SEED subsystems (level 1), taxonomic representation of bacterial metatranscriptome (c), and bubble chart of gammaproteobacterial SEED subsystems (d). Hydrogen peroxide treatment (HP) mesocosms showed distinct clustering and change over time as opposed to the control. Pre and post-treatment mirrored the control, but day one and two after treatment were different than the control and each other. This was primarily due to a change in taxonomic expression, with the Proteobacteria, particularly Gammaproteobacteria becoming dominant for days 1 and 2. However, even within Gammaproteobacteria, subsystems expressed changed on these days.

In the control mesocosms, cyanobacteria dominated throughout the experiment at 70.6 ± 5.7%. Within cyanobacteria, *Microcystis* remained highly abundant through day 2 at 81.0 ± 5.4% (Fig 3.6). On

day 3 the cyanobacterial community became more evenly distributed across six taxa; *Microcystis* abundance dropped to 6.6 ±4.4% and the most abundant genus was *Anabaena* (32.5 ± 8.0%) followed by *Synechococcus* (24.5 ± 3.6%).

Metatranscriptome

In total, 2,088,644 sequences were determined, and the mean number of bacterial reads was 248,959 ± 67,251 (*n* = 8). Samples underwent normalization (scaled to 10,000 reads) before further analysis. Upon plotting SEED subsystems (level 1) on a PCoA biplot, hydrogen peroxide treatment mesocosms showed distinct clustering and change over time as opposed to the control (Fig. 3.7b). Pre- and post-treatment mirrored the control, but day 1 and 2 after treatment were different than the control and each other (Fig. 3.7a). This was primarily due to a change in taxonomic expression, with the Proteobacteria class Gammaproteobacteria representing nearly the entire transcriptome at 80.7% and 92.8% for days 1 and 2, respectively. However, even within Gammaproteobacteria, subsystems expressed changed on these days (Fig. 3.7c). On day 1, membrane transport increased from 2.7% of the Gammaproteobacterial transcriptome to 30.8% before dropping back to 5.0% on the following day (Fig. 3.7d). 94.8% of the membrane transport subsystem on day 1 consisted of Colonization factor antigen I fimbriae (CFA/I), which is involved in the production of fimbriae, filamentous polymeric protein structures, that allow pathogenic bacteria to adhere to epithelial surfaces. On Day 2, the gammaproteobacterial transcriptome changed drastically with amino acids and derivatives being most abundant at 11.4%, followed closely by carbohydrates (11.0%) and DNA metabolism (10.1%).

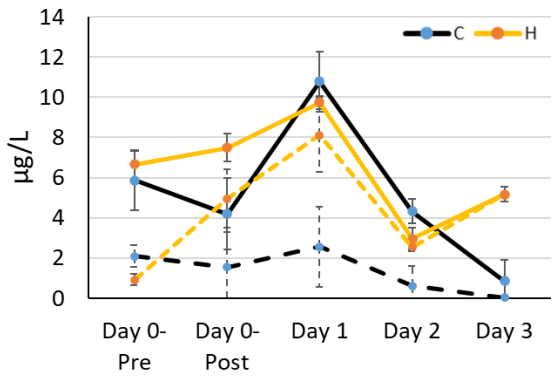

Figure 3.9. Average microcystin (solid) and extracellular microcystin (dashed), with errors bars in SD. Microcystin levels were similar between the control and treatment mesocosms, however released extracellular microcystin was elevated in treatment mesocosm until all microcystin present was extracellular.

Log_2 fold change was analyzed using DESeq2 with an input of metatranscriptome reads aligned to the most abundant taxa expressed in the metatranscriptome, gammaproteobacterium *E. coli*. To meet replication requirements of DESeq2, days 1 and 2 were assigned as replicates of one another within the control and treatment groups to represent the only distinct post-treatment expression changes within our metatranscriptome dataset. With a cut-off of 0.01% of the metatranscriptome, 36 genes were identified, of which 28 were upregulated for the hydrogen peroxide treatment group and eight were downregulated (Fig. 3.8). Of the 28 genes upregulated, many were involved with typical cellular processes such as DNA replication, but 10 were involved in membrane creation and transport, and seven were involved with stress responses and DNA repair. The eight downregulated genes exhibited various functionalities.

Microcystin

Microcystin levels between the control and treatment mesocosms were similar throughout the experiment, starting at an average of 5.9 and 6.7 µg/L, respectively. However, the treatment mesocosms ended the experiment with a higher concentration (5.2 µg/L) than the control (0.9 µg/L) (Fig. 3.9). Additionally, extracellular microcystin levels were much higher in the treatment due to cells lysing upon

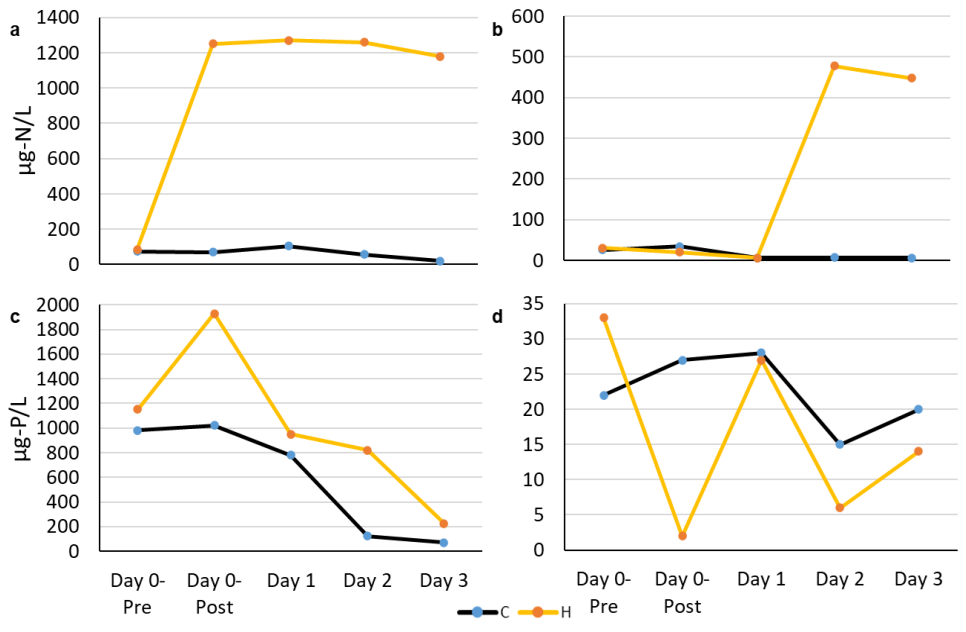

Figure 3.10. NH3 (a), NOx (b), TP (c), and OP (d) of a control (C) and treatment (H) mesocosm.

death and releasing toxins. For the treatment, extracellular microcystin accounted for 93.7% of total microcystin after one day and then 100% for the remainder of the experiment.

Nutrient modulation

After one hour, ammonia in the treatment mesocosm increased by 13.9x to 1,250 µg/L (Fig. 3.10a), and after one day nitrate and nitrite increased by 14.5x to 478 µg/L (Fig. 3.10b), whereas the control only experienced minor fluctuations around 65 and 16 µg/L, respectively. Total phosphorus nearly doubled from 1,150 to 1,930 µg/L one hour after treatment, but otherwise decreased in both the control and treatment mesocosms throughout the experiment (Fig. 3.10c). Orthophosphorus experienced fluctuations around 19 µg/L in both groups (Fig. 3.10d).

DISCUSSION

Hydrogen peroxide effectiveness

The high concentration treatment with 13 mM of hydrogen peroxide was highly effective at reducing the cyanobacterial community. Within one hour, cyanobacteria became a negligible portion of the microbial community as represented by our high-throughput sequencing data. It indicates that this level of hydrogen peroxide may cause the breakdown of cellular DNA. Microscopy observations generally support this with *Microcystis* cells beginning to visibly bleach as colonies dissociated after one hour. Albeit at a miniscule fraction, nine cyanobacteria genera persisted three days after treatment with the majority consisting of filamentous cyanobacteria and picocyanobacteria. However, the bacterial community exhibited a lagged response, substantially decreasing after one day before a rapid succession dominated by Proteobacteria and Planctomycetes. The cyanobacterial community showed no signs of recovery within the four-day timespan of the experiment. This further demonstrates the sensitivity of cyanobacteria and resiliency of the bacterial community to hydrogen peroxide (Matthijs et al., 2012; Sandrini et al., 2020; Piel et al., 2021). While not specifically evaluated in this experiment, eukaryotic algae appear to have been impacted by the treatment and did not show signs of recovering according to decreasing levels of Chl-a from one day post-treatment onwards.

Over the three-day duration of the experiment, hydrogen peroxide levels remained highly elevated and did not degrade much. This was supported by the increasing levels of dissolved oxygen measured, showing the reactive oxygen species was still present and oxygenating the water. This lack of

degradation was a result of the enclosed nature of the mesocosm and the extremely high concentration that substantially exceeded the natural hydrogen peroxide level.

Microcystin

Microcystin is a common cyanotoxin produced by several freshwater harmful algal groups that is lethal to humans and wildlife (Stevenson, 2014). This compound only enters the environment via cell lysis as cyanobacteria have no mechanism to transport it through their cell membrane. As such, these toxins are a major concern for water resource managers, especially with respect to the aftermath of HAB treatments which induce cell lysis. Due to this, it has been hypothesized that microcystin serves a purpose protecting cyanobacterial species against hydrogen peroxide (Cory et al., 2016). Past studies have demonstrated that hydrogen peroxide introduces selective pressure or stimuli resulting in upregulation of microcystin toxin production (Liu et al., 2017; Yoon, Kim and Kim, 2021). However, we did not see this in our treatment. We believe this is a result of the high concentration of hydrogen peroxide used; rapidly damaging and destroying cells before they have time to respond. This resulted in an immediate release of toxins already present within cells, explaining the increased proportion of extracellular microcystin in our treatment mesocosms. Microcystin decreased over time in the control mesocosms, whereas the concentration in the treatment mesocosms remained elevated throughout the experiment. This lack of microcystin degradation most likely stemmed from impacts on the bacterial community.

Planctomycetes importance

Planctomycetes is a phylum of cosmopolitan gram-negative bacteria capable of anammox (Van Teeseling et al., 2015) and nitrogen fixation (Delmont et al., 2018). They have also been known to associate with *Microcystis* blooms as the most dominant bacterial taxa, as witnessed in a study from Lake Taihu, China (Cai et al., 2013), and play a role in the degradation of algal biomass (Wiegand et al., 2018). Previous studies such as Lusty & Gobler's (Lusty and Gobler, 2020) used 0.12 mM hydrogen peroxide to assess impacts on cyanobacterial blooms and non-target microbial communities, and Santos et al. (Santos et al., 2021) used a 0.3 mM treatment to examine effects on phytoplankton and bacterioplankton in a drinking water reservoir, noted planctomycetes as being negatively impacted by hydrogen peroxide treatments. However, our results are contrary to this and align more with an industrial study where the phylum is noted to thrive in systems treated with a higher concentration of hydrogen peroxide (0.5 mM) (Pang et al., 2005; Wang et al., 2018). This is due to a unique cell structural organization that compartmentalizes cell components, effectively protecting them from oxidative stress (Lindsay et al., 2001). These results

indicate Planctomycetes cannot outcompete other more susceptible taxa recovering from lower concentration treatments but can take advantage of more extreme oxidative stress disturbances to achieve dominance.

Metatranscriptome

Our metatranscriptome data did not reflect the community succession seen in the high-throughput sequencing data. Whereas taxonomic succession occurred within one hour, the metatranscriptome exhibited a lagged response with changes in expression only evident after one day post-treatment. Additionally, Gammaproteobacteria was the most abundant taxa in the metatranscriptome on days 1 and 2 but was only fourth and fifth most abundant in the high-throughput sequencing data for days 1 and 2, respectively. Specifically, *E. coli* was the most abundant identified taxa expressed, but was not found in our high-throughput sequencing data. We believe this is due to a bias and lack of representation in available genetic databases. *E. coli* is an exceedingly popular research subject with 191,237 genomes present in the National Center for Biotechnology Institute (NCBI) GenBank database (as of June 22, 2022), whereas our most abundant high-throughput sequencing phylum, Planctomycetes, is only represented by 3,132 genomes, with our top three most abundant genera within the phylum, *Phycisphaera*, *Blastopirellula*, and *Algisphaera* only represented by 50 altogether.

Consistent with studies of other Gammaproteobacteria responses to hydrogen peroxide stress, genes relevant to DNA repair and membrane proteins were upregulated after exposure to hydrogen peroxide exposure (Palma et al., 2004; Small et al., 2007). Genes relevant to iron-sulfur clusters were also upregulated. These clusters are essential to crucial biological processes and are sensitive to reactive oxygen species such as hydrogen peroxide, however Damage to these clusters is sufficient to trigger upregulation for prompt replacement (Riboldi et al., 2014). Interestingly, we did not find any OxyR regulon genes in our analysis. OxyR is a transcription factor critical to transcriptional regulation of defensive systems for oxidative stress, which responds to hydrogen peroxide (Seo et al., 2015). The lack of any distinctive gammaproteobacterial OxyR genes in response to hydrogen peroxide may be further evidence of an incorrect taxonomic classification.

Water management implications

The High concentration hydrogen peroxide treatment used here was highly effective at rapidly destructing a cyanobacterial HAB in environmental conditions typical of southwest Florida's subtropical climate. We

found that the tested level of hydrogen peroxide induces microbial community shifts. We found no evidence that human and animal pathogens increase after hydrogen peroxide treatment. In an open system, non-target microbial impacts should be minimized because the replacement of microbial communities from the surrounding environment will quickly occur after treatment. During a severe HAB event, this treatment may be favorable as the microbial community is already disturbed and the oxygenation seen in our mesocosms could alleviate hypoxic conditions induced by the bloom (Paerl et al., 2001). While not tested in this mesocosm experiment, previous studies have documented the impacts of low dosage hydrogen peroxide treatments to non-target organisms are low (Matthijs et al., 2012). However, at high dosages larger non-target organisms are negatively impacted at different rates. In a study of Rainbow Trout (*Oncorhynchus mykiss*), Channel Catfish (*Ictalurus punctatus*), and Bluegill (*Lepomis macrochirus*), the lowest 24 hour LC_{50} (lethal concentration to for 50% mortality) of the three species was found to be 320 mM (Rach et al., 1997), which far surpasses the concentration used in this study (15.7 mM). Additionally, macroorganisms have the option to retreat from a treatment area to mitigate impact. Unfortunately, zooplankton are not capable of this and the 48 hour LC_{50} concentration for two representative zooplankton, *Daphnia* and *Moina*, has been quantified as 0.16 mM and 0.05 mM respectively (Reichwaldt et al., 2012). However, as the same reason with the case of bacteria exposure, non-target zooplankton impacts should be minimized in an open system because the replacement of zooplankton communities from the surrounding environment will quickly occur after treatment.

Conclusion

We conducted a mesocosm experiment treating a simulated *Microcystis* HAB with high concentration hydrogen peroxide which succeeded in rapidly destructing the bloom, allowing us to examine ensuing effects on the sensitive microbial community. Our finding indicated a distinct succession pattern favoring taxa resistant to hydrogen peroxide rather than those capable of decomposing it. Additionally, we identified 28 bacterial genes which were upregulated after exposure to hydrogen peroxide, further supporting a strong response for DNA repair from oxidative damage caused by hydrogen peroxide. The high concentration treatment used in our mesocosms did not cause a lethal response to the microbial community and it may be desirable to rapidly end extreme bloom conditions which have already negatively impacted the aquatic environment.

Chapter 4: Mesocosm experiment #2

ABSTRACT

Cyanobacteria harmful algal blooms (cyanoHABs) have been increasing globally, causing environmental and human health concerns. Many current algicidal chemical treatments are not fast acting or cause ecological harm directly to aquatic organisms or through accumulation of trace chemicals after application. Hydrogen peroxide, l-lysine, and the combination of both chemicals were analyzed for algicidal treatment of cyanobacterial dominant microbial communities over a 7-day mesocosm experiment. Hydrogen peroxide was applied at a concentration of 33.3 mg/L, L-lysine at a concentration of 8 mg/L, and mixed mesocosms using both chemical concentrations. All treatment applications were found to be successful at reducing toxic cyanobacteria genera such as *Microcystis*, *Anabaena*, *Dolichospermum*, and *Cuspidothrix*. Succession by eukaryotic algae varied in composition across treatments, with Eustigmatophytes becoming near solely dominant in hydrogen peroxide and mixed treatments, while L-lysine had a more diverse composition of Chlorophyta and picocyanobacteria. To our knowledge combined treatments of L-lysine and hydrogen peroxide have never been assessed before and given fast decomposition rates and effective removal of cyanobacteria we feel warrants further research in the water management of CyanoHABs.

INTRODUCTION

In recent decades rising temperatures and anthropogenic related eutrophication have allowed for the proliferation of cyanobacteria harmful algal blooms (CyanoHABs) in freshwater and brackish ecosystems worldwide (Paerl and Huisman, 2009). These blooms pose serious risk for wildlife, human health, and the economy. Dense surface blooms can result in reduced light penetration, suppressed growth of submerged aquatic vegetation, as well as oxygen depletion affecting wildlife and the ecosystem-services these freshwater systems provide (Wilson et al., 2006; Jeppesen et al., 2007). Toxin production by many of these organisms and potential exposure can be a significant human health concern and impairs the use of water resources for drinking water, recreation, and agricultural irrigation where mitigation costs can negatively impact on local economies (Huisman et al., 2005). Nutrient reduction is currently considered the best strategy to reduce CyanoHAB events. However, these strategies can take many years to show positive results and do not address the immediate risk to wildlife and residents (Kinley-Baird et al., 2021). Many short-term reduction methods have focused on chemical spraying methods, such as copper sulfate and

aluminum, but these chemicals can become concentrated in the environment, and often are non-selective in targeting cyanobacteria (Hanson and Stefan, 1984).

Hydrogen peroxide, a reactive oxygen species (ROS), has recently gained popularity as an environmentally friendly algaecide alternative for CyanoHAB mitigation. Unlike many other chemical treatments, hydrogen peroxide quickly degrades into water and oxygen after application, making it more environmentally friendly with diminished long-term impacts to the waterbody (Wang et al., 2019). The method is more ecologically friendly due to selective targeting of cyanobacteria over other eukaryotic algae caused by differential coping mechanisms between the two groups for dealing with high light exposure (Weenink et al., 2015). This selective targeting has shown in both laboratory and field trials (Weenick et al., 2015; Matthijs et al., 2012; Drabkova et al., 2007a).

The amino acid L-lysine is another ecological alternative which has also shown powerful algaecidal effects against growth of the widespread bloom-forming toxic cyanobacterium *Microcystis* (Takamura et al., 2004; Tian et al., 2019). Hehmann and colleagues (2002) found that concentrations of L-lysine at or below 5 mg/L were able to completely kill nine strains of *Microcystis* after 48 hours, while both Bacillariophyceae and Chlorophyceae along with other Cyanophycean were not sensitive up to concentrations of 10 mg/L. The mechanisms of L-lysine to inhibit the growth of *Microcystis* are still not well understood. Cell membrane damage after treatments has been documented (Yamamoto et al., 1998; Tian et al., 2019) and may be a result of oxidative stress causing lipid peroxidation (Tian et al., 2019). Another possibility is that growth inhibition and cell wall damage after exposure to L-lysine may be caused by feedback inhibition of biosynthetic enzymes (Zimba et al., 2001). Being a requirement for fish and other organisms, application of this amino-acid treatment can be seen as environmentally friendly due to fast metabolization rates in freshwater ecosystems (Takamura et al., 2004).

A continuous dilemma in CyanoHAB bloom mitigation is the need for re-application of algaecides to completely alleviate these blooms. For hydrogen peroxide, fast decomposition in waters with strong reductive powers can lead to short residence times, leading to the need for further application where higher concentrations can be harmful to other eukaryotic algae (Weenick et al., 2015; Wang et al., 2019). This phenomenon has also been seen with L-lysine, where field application led to immediate reduction in CyanoHAB abundances but eventual recovery was seen (Takamura et al., 2004). Effective methods for one-time application and elimination of noxious CyanoHABs are needed to reduce risk for residents and wildlife as well as to diminish remediation costs.

In this study, the effects of both the forementioned treatments were compared for the treatment of *Microcystis* in a mesocosm field study, as well as the novel effects of both used together. The potential

of targeting different growth suppression mechanisms by use of both treatments in tandem has, to our knowledge, never been explored and could lead to new insight for *Microcystis* bloom mitigation. Treatment impacts to the phytoplankton community and potential succession were also assessed along with changes in nutrient and physiochemical characteristics of the aquatic environment in mesocosms.

MATERIALS AND METHODS

Mesocosm experiments were done near the Franklin Lock and Dam (S-79) in Alva, FL (latitude, longitude: 26.720727, -81.692851), from 06/21/21 through 06/28/21. Mesocosms were located ~35 m from the bank of the Caloosahatchee River. For each mesocosm, 250 L of water from the freshwater portion of the Caloosahatchee River was pumped into 100-gallon black plastic tubs. Mesocosms were done in triplicate for the control, hydrogen peroxide, L-lysine, and mixed treatments (*n*=12). Mesocosms were set up in groups of 4 with covered awnings (10 ft x 10 ft) where one control, hydrogen peroxide, L-lysine and mixed treatment replicate mesocosm was placed under each to equally disperse any environmental impacts from placement (Fig. 4.1). Concentrated *Microcystis* biomass was collected from a surface bloom on the freshwater side of S-79 one-day prior to the start of the experiment. Concentrated biomass (10 ml) was then added to each mesocosm replicate on day 0 prior to treatment application.

Each respective treatment was prepared as follows: L-lysine monohydrochloride solution (50 g/L) was prepared and applied (40 ml) to each treatment mesocosm at a final concentration of 8 mg/L. A 3% hydrogen peroxide solution was applied via spray application (125 ml) for a final concentration of 33.3 mg/L to treatment mesocosms. For mixed treatments, the above concentrations of both chemicals were added. Nutrients were added for each mesocosm to maintain the phytoplankton population and bloom formation. A nitrate solution ($NaNO_3$, 6.07 g/L) was prepared and added to a final concentration of 200 μg-N/L (50 ml), and phosphate solution (KH_2PO_4, 4.4 g/L) was prepared and added to a final concentration of 28 μg-P/L (7 ml). After treatment and nutrient additions, mesocosms were manually mixed.

Surface physiochemical parameters of each mesocosm were measured using Aqua Troll Sonde 500 multi-parameter (In-Situ, CO, USA). A continuous reading setting was used, and sonde was circled around surface waters of individual mesocosms for 1 minute for which associated parameter measurements were measured every second. From these data, three randomized measurements were selected for replicate measurements and averaged. Surface water samples from treatment and control replicates were pooled for nutrient and Chl-a analysis and shipped for measurement using previously described methods.

Hydrogen peroxide measurements

Hydrogen peroxide samples were taken from control, hydrogen peroxide, and mixed mesocosm replicates on sampling days. Samples were filtered through 0.22 μm Sterivex filters and kept on ice and later stored at -80 °C until being analyzed later that day. Hydrogen peroxide was measured using a fast response amperometric 250 μm diameter tip hydrogen peroxide microelectrode with a built-in reference electrode (HP-250, Innovative Instruments) featuring a lower detection limit of 50 nM. The sensor was connected to an inNO-T meter operated by the inNO-T data acquisition system software (Innovation Instruments, Tampa, FL, USA). Hydrogen peroxide (3% w/v) was purchased from Sigma-Aldrich (St. Louis, MO, USA) and used in the preparation of a 400 μM hydrogen peroxide standard solution prepared by dissolving stock in 100 ml of high-performance liquid chromatography (HPLC) grade water (Fisher Scientific). A 0.22 μm filtered catalase solution (Worthington Biochemical Corporation, Lakewood, NJ, USA) was also used. Before calibration, the condition of the sensor was monitored in HPLC grade water for at least 20 min before measurements to establish a stable background baseline. For standard addition measurement 4 ml of sample was used, 10 μl of 400 μM hydrogen peroxide standard was added after sensor stabilization (1 μM as final concentration), and then 10 μl of catalase was added for decomposition of hydrogen peroxide. Eight replicate readings were taken for each standard where the slope was calculated from sample baseline and hydrogen peroxide standard addition baseline and applied to the delta of standard addition baseline and post catabolic reaction baseline.

Figure 4.1. Field. Experimental mesocosm set up at the Caloosahatchee River (S-79) Franklin Lock and Dam, Alva, FL.

L-lysine measurements

L-lysine samples were taken from control, L-lysine, and mixed treatment mesocosms on sampling days. Samples were filtered and stored using the same methods described for hydrogen peroxide. Samples

were measured using a fluorometric lysine assay kit (Biovision, Mipitas, CA, USA) to determine L-lysine concentration. Prior to measuring, samples were thawed in the dark and then centrifuged for 10 minutes. 20 μl of sample was added to three wells of black 96-well plate. For spiked and unspiked wells, a 40 μl of sample reaction mix was added containing lysine assay buffer, lysine enzyme mix, developer mix, and probe solution. For background wells, all the forementioned solutions were added except the enzyme mix. For spiked wells, an additional 4 μl of L-lysine standard was added. Plates were then incubated at 25 °C for 45 minutes in the dark. Fluorescence was detected using GENios Pro plate reader (Tecan Trading AG, Switzerland), with excitation of 535 nm and emission of 580 nm to determine L-lysine measurements.

High-throughput sequencing

Surface water samples were collected for all mesocosms on each sampling day and refrigerated until returned to the laboratory. Cells were collected by filtering 200 ml of water with a 0.22 μm cellulose nitrate filter. Genomic DNA was extracted from half cut filter samples using the DNeasy PowerSoil Pro Kit (Qiagen) following the manufacturer's instructions. High-throughput amplicon sequencing was done by amplification of 16S rRNA gene using primer pair 515yF and 926pfR for targeting of bacterioplankton (Parada et al., 2016) and cya359F and Dcya781R (Nubel et al., 1997) for targeting cyanobacteria and eukaryotic algal taxa via Illumina MiSeq system (MR DNA, Shallowater, TX, USA). Dereplicated or unique sequences were denoised; unique sequences identified with sequencing and/or PCR point errors and removed, followed by chimera removal, providing a denoised sequence. Final sequences were taxonomically classified via representative of denoised sequence through BLAST or NCBI. More detailed protocol is found in Chapter 1.

Metatranscriptome

RNA Samples for transcriptome sequencing were collected by filtering 200 ml of water using 0.2 μm Sterivex filters on-site which were promptly frozen in liquid nitrogen for transport to a -80°C freezer until further analysis. Total RNA was isolated from Sterivex filters using the RNeasy PowerMicrobiome Kit (Qiagen) following manufacturer's instructions. For each filter sample, three extractions were performed. RNA was eluted in 100 μL RNase-free water and pooled. DNA contamination was removed using Baseline-ZERO™ DNase (Epicentre) following the manufacturer's instructions followed by purification using the RNA Clean & Concentrator columns (Zymo Research). DNA free RNA samples were used for rRNA removal by using Ribo-Zero Plus rRNA Depletion Kit (Illumina). rRNA depleted samples were used for library preparation via the KAPA mRNA HyperPrep Kits (Roche) by following the manufacturer's instructions.

Whole transcriptome amplified samples were used for library preparation using Illumina DNA Prep, (M) Tagmentation library preparation kit (Illumina) following the manufacturer's user guide. Following library preparation, the average library size was determined using the Agilent 2100 Bioanalyzer (Agilent Technologies) and were then pooled in equimolar ratios of 0.6 nM, and sequenced paired end for 300 cycles using the NovaSeq 6000 system (Illumina).

RESULTS

Hydrogen peroxide application

Average hydrogen peroxide concentrations after application on day 0 were 309.15 ± 40.10 μM (9.1 ± 1.2 mg/L) for hydrogen peroxide treatment mesocosms and 245.98 ± 47.96 μM for mixed mesocosms. One day after application, concentrations in hydrogen peroxide treatment mesocosms had degraded to 33% (204.27 ± 107.79 μM) of the previous day values, and by day 3, values were found to be around control values (Fig. 4.2). For mixed mesocosms one day after application, hydrogen peroxide had degraded to 13% (212.59 ± 127.95 μM) of application day values and by day 3 hydrogen peroxide had also returned to similar concentrations of the control (Fig. 4.2).

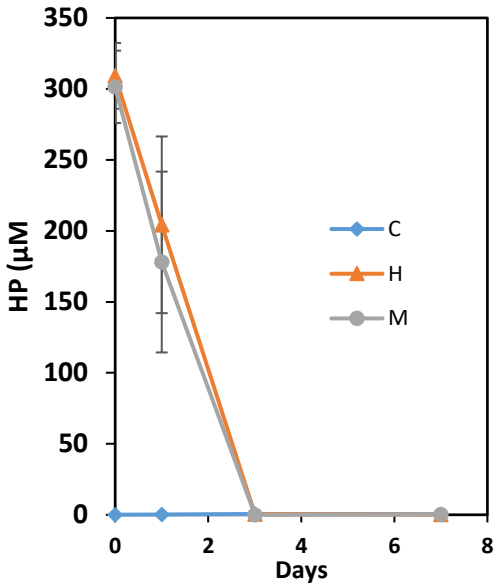

Figure 4.2. Hydrogen peroxide concentrations of control (C), HP (H), and mixed (M) replicate mesocosms (*n* = 3). Error bars in SD.

L-lysine application

Average L-lysine concentrations after application on day 0 were 45.88 μg/L in L-lysine mesocosms (Table 4.1). After 24 hours, lysine was found to have increased to 67.97 μg/L in lysine mesocosms and 55.53 μg/L in mixed mesocosms, which then returned to levels found in control mesocosms by day 3 (Table 4.1).

Table 4.1. Nutrient and other water parameters found in mesocosms throughout 7-day experiment.

Treatment	Day	Chl-a (µg/L)	TOC (mg/L)	TKN (µg-N/L)	TP (µg-P/L)	TN (µg-N/L)	OP (µg-P/L)	NOx (µg-N/L)	NH3 (µg-N/L)	TN / TP Plim>7.2	HP (nM)	MC (µg/L)	L-lysine (µg-N/L)	MC-filtered (µg/L)	CDOM (µg/L)
Control	0	60.7	16.0	1950	189	2086	53	136	13	11.0	0.07	1.05	0.54	0.02	181.94
	1	72.1	18.9	1380	173	1405	81	6	25	8.1	0.32	2.25	0.17	0.00	188.94
	3	121.0	17.9	1670	184	1676	67	6	25	9.1	0.59	0.18	0.99	0.07	178.44
	7	46.0	17.2	1430	164	1436	71	6	12	8.8	0.41	0.20	0.99	1.36	208.86
HP	0	78.0	15.3	1690	197	1758	54	68	55	8.9	309.15	1.09	nd	0.15	187.31
	1	36.9	20.7	1180	513	1298	446	118	53	2.5	204.27	0.92	nd	1.03	195.18
	3	19.6	16.6	1520	242	1639	139	119	151	6.8	0.36	0.56	nd.	0.76	193.50
	7	27.2	17.8	3050	249	3164	144	114	143	12.7	0.06	0.11	nd	0.19	213.08
L-lysine	0	74.1	17.1	2750	95	2872	66	122	40	30.2	nd	0.28	45.88	0.03	185.46
	1	55.2	18.3	2350	170	2358	98	8	53	13.9	nd	0.05	67.97	0.01	189.39
	3	58.7	15.8	2440	156	2446	142	6	741	15.7	nd	0.39	0.41	0.60	188.54
	7	34.0	17.0	1670	154	1721	55	51	376	11.2	nd	0.07	0.06	0.19	255.24
Mixed	0	55.1	17.5	2890	201	2954	57	64	56	14.7	245.99	0.47	nd	0.09	187.99
	1	37.1	21	2370	151	2473	136	103	70	16.4	212.59	0.73	55.53	0.71	199.02
	3	10.8	16.9	2620	249	2739	93	119	953	11	0.02	0.62	0.73	0.49	193.71
	7	26.9	17.0	2020	nd	2152	nd	132	641	2.7	0.16	0.32	nd	0.34	219.52

Physiochemical Parameters

Dissolved oxygen (DO) was similar across all mesocosms on day 0 (9.4 $\pm$ 0.1 mg/L, *n* = 12), 24 hours later hydrogen peroxide and mixed mesocosms appear to have been oxygenated by treatment application, with a 10-15% DO increase (Table 4.1.). Mixed (M) and L-lysine (L) treatments saw a decline in DO on day 3 (M: 3.82 $\pm$ 0.15, *n* = 3; L: 4.61 $\pm$ 0.45, *n* = 3), before recovering to similar values seen in other mesocosms on day 7 (Table 4.2). Total nitrogen (TN) generally decreased 24 hours after treatment application across all mesocosms (Fig. 4.3). By day 3, however, TN had increased across all mesocosms with significant increases in ammonia for L-lysine-containing treatment mesocosms (Fig. 4.3). This correlated to degradation of L-lysine found on this day (Table 4.1). OP increased rapidly in hydrogen peroxide

Table 4.2. Mean value of measured water parameters in mesocosm replicates during 7-day experiment (*n* = 9) (±SD).

Mesocosm	Day	Temp. (°C)	Sal. (ppt)	DO (%)	DO (mg/L)	Cond. (uS/cm)	TDS (mg/L)	pH
Control	0	28.77	0.22	118.63	9.43	452.17	0.29	8.80
	±SD	0.25	0.00	3.07	0.25	1.05	0.00	0.06
	1	26.21	0.22	106.04	8.84	452.06	0.29	8.76
	±SD	0.16	0.00	4.07	0.34	0.70	0.00	0.08
	3	24.68	0.22	97.19	8.32	448.00	0.29	8.87
	±SD	0.11	0.00	1.28	0.05	1.77	0.00	0.06
	7	25.66	0.23	79.21	6.64	473.43	0.31	8.46
	±SD	0.14	0.00	6.17	0.52	3.06	0.00	0.07
HP	0	28.72	0.22	117.34	9.32	451.73	0.29	8.78
	±SD	0.16	0.00	6.09	0.42	1.14	0.00	0.11
	1	26.25	0.22	129.45	10.80	452.13	0.29	8.73
	±SD	0.16	0.00	10.18	0.84	0.63	0.00	0.09
	3	24.70	0.22	84.32	7.22	460.65	0.30	8.27
	±SD	0.17	0.00	1.74	0.20	0.68	0.00	0.03
	7	25.75	0.23	82.18	6.90	474.30	0.31	8.35
	± SD	0.23	0.00	5.01	0.39	1.14	0.00	0.13
L-lysine	0	29.05	0.22	116.96	9.28	452.68	0.29	8.79
	±SD	0.44	0.00	3.67	0.35	1.79	0.00	0.06
	1	26.16	0.22	97.83	8.19	455.53	0.30	8.68
	±SD	0.06	0.00	2.03	0.17	1.07	0.00	0.04
	3	24.61	0.23	53.76	4.62	465.28	0.30	8.13
	±SD	0.19	0.00	5.33	0.45	1.90	0.00	0.06
	7	25.70	0.23	77.77	6.55	474.72	0.31	8.31
	SD	0.21	0.23	2.77	0.22	1.75	0.00	0.10
Mixed	0	28.68	0.22	119.13	9.49	450.43	0.29	8.83
	±SD	0.35	0.00	3.00	0.23	1.41	0.00	0.06
	1	26.24	0.22	125.61	10.49	456.03	0.30	8.75
	±SD	0.19	0.00	8.15	0.64	1.31	0.00	0.04
	3	24.55	0.23	44.50	3.83	468.98	0.31	7.81
	±SD	0.09	0.00	1.81	0.15	0.82	0.00	0.02
	7	25.64	0.23	82.65	6.97	479.40	0.31	8.30
	±SD	0.03	0.00	4.35	0.39	1.69	0.00	0.09

mesocosms 24 hours after treatment application, and to a lesser extent in mixed mesocosms. Afterward, OP returned to levels similar to starting values for the remainder of the experiment.

Phytoplankton shifts induced by algaecide treatments

To target cyanobacteria and other photosynthetic eukaryotic algae present in mesocosm phytoplankton communities a cya359F and Dcya781R primer pair was used. This primer pair has been shown to effectively target cyanobacteria as well as some Bacillariophytes (Nubel et al., 1997). Our findings show this primer pair identified more Cyanobacteria and eukaryotic algal taxa than the bacterial targeting primer pair 515yF and 926pfR pair (Table 4.3) and was used for phytoplankton analysis.

Compositional analysis was done at the genus level and underwent normalization (scaled to 10,000 reads), for which 71 phytoplankton taxa were identified.

Table 4.3. Comparison of ASVs between using the bacterial primer pair and the cyanobacteria specific primer pair, showing cyanobacteria specific primer accomplished more sequence read hits for cyanobacteria and was able to identify eukaryotic algal phyla.

Phytoplankton phyla	Bacteria primer	Cyanobacteria primer
Cyanobacteria	257311	814741
Chlorophyta	34564	88735
Euglenida	2661	172
Eukaryota	8742	11617
Bacillariophyta	17370	50019
Eustigmatophyceae	73010	483066
Rhodophyta	102	916
Haptista	X	17
TOTAL	393760	1449283

Water samples for sequence analysis were taken an hour after treatment application on Day 0. When examining algal communities at the genus-level, hydrogen peroxide and mixed treatments already showed signs of change compared to controls, exhibiting a mean Bray-Curtis dissimilarity index 0.31 $\pm$ 0.08 (n = 9) and 0.22 $\pm$ 0.06 (n = 9), respectively, while L-lysine was found to be similar (Bray-Curtis dissimilarity index: 0.06 $\pm$ 0.02, n = 9). All mesocosms had high cyanobacterial dominance (C: 95.1 $\pm$ 0.79%, n = 3; H: 92.2 $\pm$ 0.81%, n = 3; L: 94.9 $\pm$ 0.46%, n = 3; M: 92.2 $\pm$ 1.23%, n = 3), primarily consisting of the *Synechococcus, Cyanobium*, and *Microcystis* genera (Fig. 4.4). Control mesocosms continued throughout the experiment to exhibit cyanobacterial dominance with a mean relative abundance for the following three sampling days of 92.21 $\pm$ 1.24% (n = 9). Interestingly, the relative abundance of the toxin-producing *Microcystis* more than doubled within the first 24 hours of the experiment in control mesocosms, which also correlated to a spike in microcystin content (Fig. 4.4). Notable increases were also seen from the toxic cyanobacterial genera *Anabaena* and *Dolichospermum* on days 1 and 3 (Fig. 4.4). Chl-a concentrations had risen significantly by day 3 in control mesocosms along with an increase in Bacillariophytes and Cyanobacteria relative abundance (Fig. 4.5). By day 7 Chl-a concentrations had dropped along with Bacillariophyte relative abundance to below the starting values, while cyanobacteria remained dominant and Chlorophyta saw a relative abundance increase to 5.16 $\pm$ 1.60 % (n = 3) of the phytoplankton community (Fig. 4.5). Throughout the experiment algal communities in the control mesocosms remained relatively similar (Bray-Curtis mean dissimilarity index: 0.17 $\pm$ 0.06, n = 27) (Fig. 4.6).

Cyanobacterial growth inhibition occurred rapidly after 24 hours in hydrogen peroxide and mixed mesocosms. The relative abundance of phyla had dropped to 51.9 $\pm$ 2.21% (n = 3) in hydrogen peroxide and 73.3 $\pm$ 2.83% (n = 3) in mixed mesocosms, corresponding to a decline in Chl-a (Fig. 4.5). Eustigamtophytes replaced cyanobacterial dominance, with a relative abundance of 56.7 $\pm$ 2.83% in

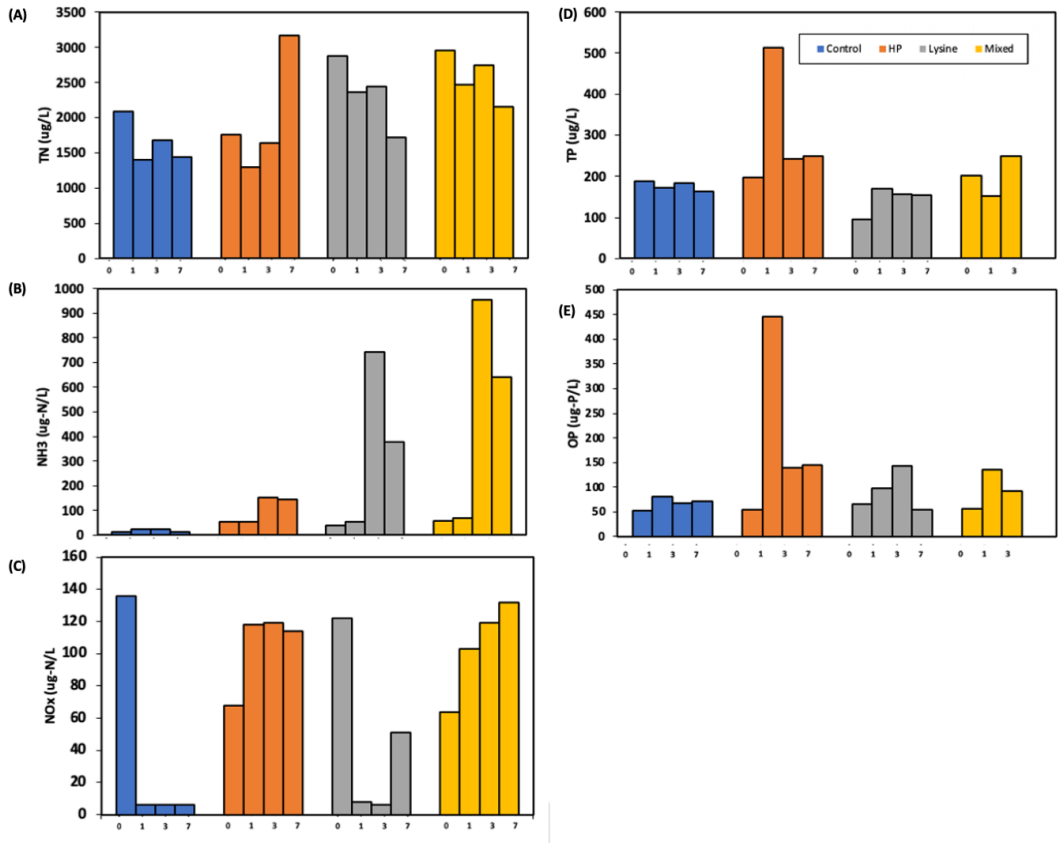

Figure 4.3. Nutrients. Pooled nutrient concentrations from control (*n* = 3), HP (*n* = 3), L-lysine (*n* = 3) and mixed (*n* = 3) treatment mesocosms on sampling days (0, 1, 3, 7). TN (A), NH3 (B), NOx (C), TP (D), and OP (E) of control, HP, L-lysine and mixed mesocosms.

hydrogen peroxide and 75.1 ± 2.51% in mixed mesocosms 24 hours after application and remaining as the dominant phytoplankton phyla till the end of the experiment. Their relative abundance reached 93.9 ± 2.04% in hydrogen peroxide and 93.9 ± 0.81% in mixed mesocosms by the last day (Fig. 4.5). All Eustigmatophyte were found to come from *Nannochloropsis* identified as 24 separate ASVs. Although present in control and L-lysine mesocosms at the end of the experiment (relative abundance: L: 5.41 ± 1.53%; C: 2.17 ± 0.53%), this succession by one genus for mixed and hydrogen peroxide mesocosms was quite unique and contributed to differentiation from the control (Bray-Curtis dissimilarity index: H: 0.96 ± 0.01, *n* = 9; M: 0.96 ± 0.01, *n* = 9) and L-lysine (Bray-Curtis dissimilarity index: H: 0.92 ± 0.02, *n* = 9; M: 0.93 ± 0.02, *n*=9) phytoplankton communities seen on the last day (Fig. 4.6). Less notable shifts were seen for the bacillariophyte relative abundance, increasing to 3.67 ± 0.47% in hydrogen peroxide and 4.27 ± 1.32% in mixed mesocosms on the last day. Hydrogen peroxide and mixed mesocosms were highly effective at reducing cyanobacterial relative abundance, representing less than 1% of phytoplankton community composition by the end of the experiment. Dominance by one genus, however, did influence Shannon and Simpson diversity indices, with Shannon Diversity indices found to be significantly different from

controls (H: $p < 0.05$; M: $p < 0.05$) and L-lysine (H: $p < 0.05$; M: $p < 0.05$). Phytoplankton composition was highly similar in these two mesocosms by the end of the experiment (Bray-Curtis dissimilarity index: 0.02 $\pm$ 0.00, $n = 9$) (Fig. 4.6).

L-lysine mesocosms exhibited a slower divergence from control mesocosms, however, by day 3 reached a Bray-Curtis dissimilarity index of 0.48 $\pm$ 0.08 ($n = 9$), becoming more dissimilar from all treatment mesocosms as visualized by NMDS plot (Fig. 4.5), and reaching the highest Shannon diversity index of the entire experiment (2.67 $\pm$ 0.11, $n = 3$). This was driven by a 35.6 $\pm$ 5.48% decline in

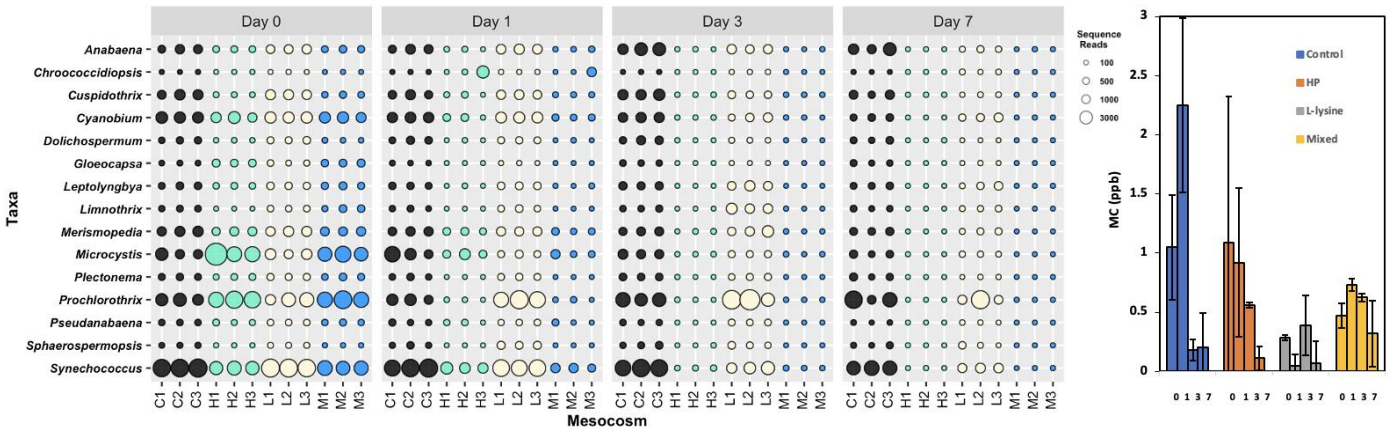

Figure 4.4. Cyanobacterial sequence read abundance, normalized 10,000 reads, showing major taxa (> 0.5%) (Left). Cyanobacteria taxa unidentified to the genus level were removed, however still represented in phyla relative abundance analyses. Microcystin (MC) toxin concentration on samplings days (0, 1, 3, 7) for control, hydrogen peroxide, L-lysine and mixed mesocosms (right). Cyanobacteria sequence read abundance declined rapidly 24 hours after treatment application in hydrogen peroxide and mixed mesocosms, while L-lysine notable shifts did not occur until day 3 and were found to maintain higher picocyanobacterial abundances. *Microcystis* abundance was found to increase in control mesocosms 24 hours after treatment application, correlating to peak in MC, while all other mesocosms were found to not increase throughout 7 day experiment.

cyanobacterial relative abundance, and relative abundance growth from Bacillariophyta (13.76 $\pm$ 6.6%) and Chlorophyta (18.53 $\pm$ 4.77%) likely contributing to the rise in chlorophyll seen on day 3 (Fig. 4.5). By this time *Microcystis* relative abundance had dropped by 83% (Fig. 4.4), and notable increases were seen from the chlorophyte *Chlorella* and bacillariophyte *Cyclotellla*. By day 7 cyanobacterial abundance had dropped to 30.1 $\pm$ 11.67% ($n = 3$), with most contributions coming from the picocyanobacterial genera *Synechococcus, Cyanobium* and *Prochlorothrix* (Fig. 4.4). Cyanobacterial dominance was succeeded by chlorophyte dominance (56.6 $\pm$ 13.1%), however, bacillariophyte relative abundance declined (Figure 4.4). L-lysine mesocosms exhibited the highest Simpson diversity index (0.90 $\pm$ 0.01, $n = 3$).

Bacterioplankton shifts induced by algaecide treatments

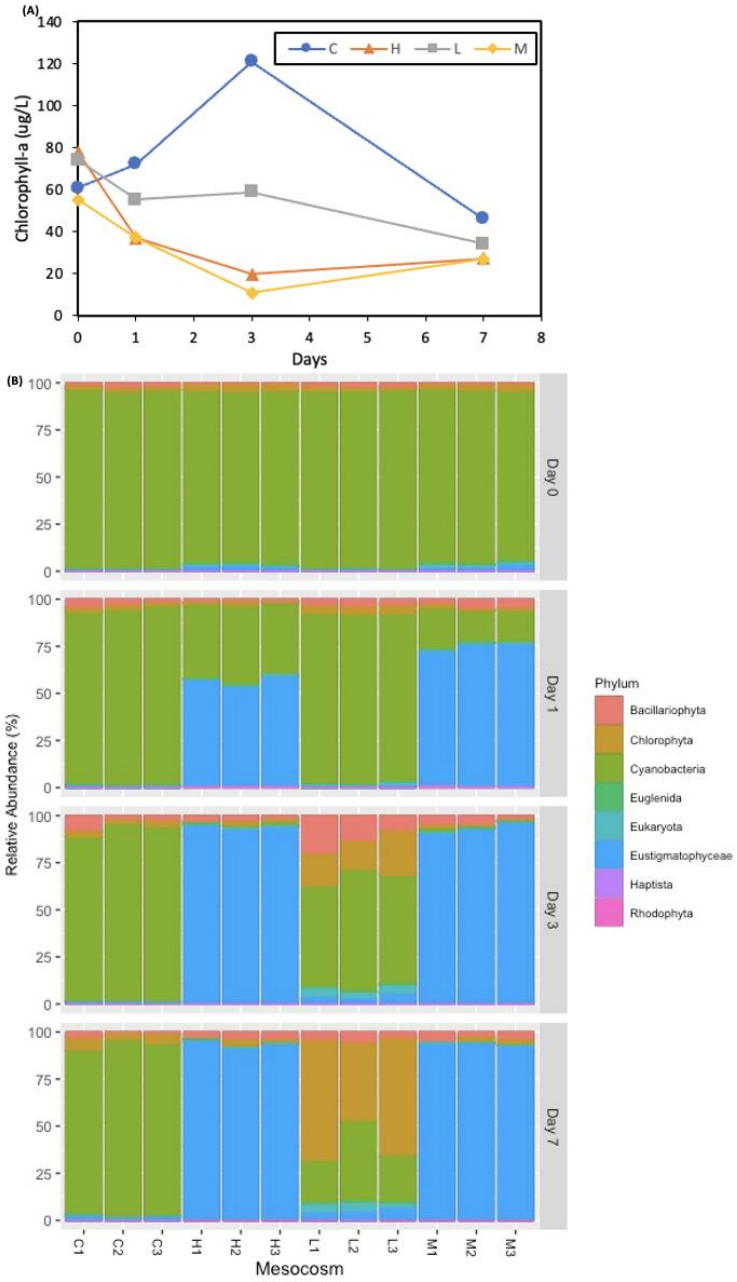

Figure 4.5. Chl-a measurements of treatment mesocosms (control (C), HP (H), L-lysine (L), mixed (M)), on sampling days (0, 1, 3, 7) (A). Sequence read relative abundance (%) of phytoplankton phyla from cyanobacteria/ eukaryotic algae specific primer, after removal of non-target bacterioplankton taxa, normalized 10,000 reads (B). Control mesocosms maintained cyanobacteria dominated phytoplankton communities throughout 7 day experiment, while cyanobacterial abundance was reduced in treatment mesocosms, correlating to reduction in chlorophyll-a, shifting toward phytoplankton communities with higher eukaryotic abundance.

After chemical application, bacterioplankton communities in treatment mesocosms displayed similar were found to be similar to controls (Bray-Curtis dissimilarity index: H: 0.17 $\pm$ 0.02, *n* = 9; L: 0.19 $\pm$ 0.06, *n* = 9; M: 0.18 $\pm$ 0.02, *n* = 9). Proteobacteria had the highest relative abundance in all mesocosms (32.0 $\pm$

2.18%, *n* = 12), followed by Bacteroidetes (20.2 ± 1.47%, *n* = 12), and Actinobacteria (19.6 ±2.10%, *n* = 12) (Fig. 4.7). Bacterial composition within control mesocosms was relatively stable throughout the experiment (Bray-Curtis dissimilarity index: 0.19 ± 0.07, *n* = 27), however, proteobacterial dominance was taken over by Verrucomicrobia, which contradicted trends in other treatment mesocosms (Fig. 4.7). Alphaproteobacteria saw the most significant growth in relative abundance across treatment mesocosms, becoming the dominant taxa and compromising an average of 29.13 ± 0.60% (*n* = 9) of bacterial communities by the end of the experiment. Hydrogen peroxide and mixed mesocosms were found to be the most different from control mesocosms on the last day, with mean Bray-Curtis dissimilarity indices of 0.81 ± 0.03 (*n* = 9) and 0.82 ± 0.34 (*n* = 9), respectively. Unlike algal communities, however, mixed and hydrogen peroxide mesocosms became more dissimilar by the final day (Bray-Curtis dissimilarity index: 0.48 ± 0.08, *n*=18) (Fig. 4.6). Hydrogen peroxide saw a 10% increase in betaproteobacteria relative abundance, while mixed remained stable, and both L-lysine and control mesocosms saw large reductions in relative abundances (Fig. 4.7). L-lysine bacterial communities were found to be more different from hydrogen peroxide and mixed mesocosms (Bray-Curtis dissimilarity index: HP: 0.73 ± 0.04; M: 0.78 ± 0.03) compared to controls (Bray-Curtis dissimilarity index: 0.61 ± 0.06) by the end of the experiment and differed from all three in the significant growth of Actinobacteria, which occupied 27.3 ± 7.73% of the bacterial community (Fig. 4.7).

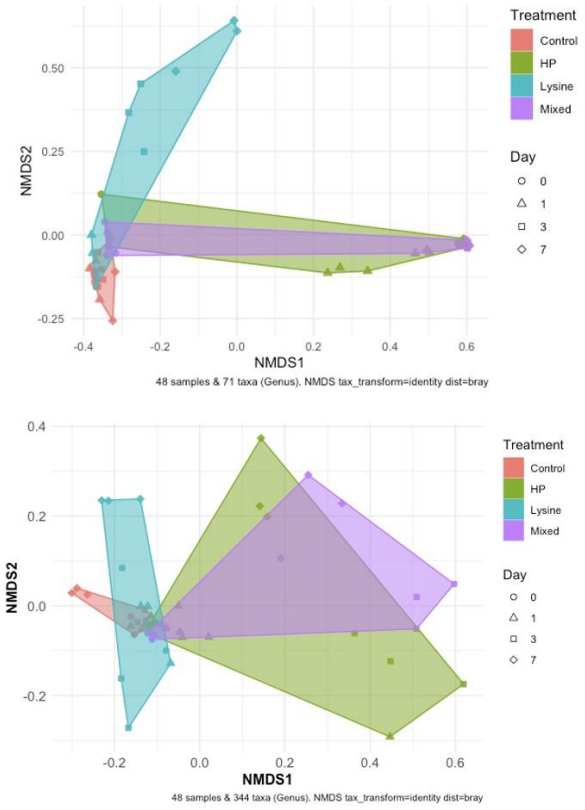

Figure 4.6. Non-metric multidimensional scaling (nMDS) plot in two dimensions of Bray-Curtis dissimilarity matrices, analyzed at the genus level, for phytoplankton communities (top) and bacterioplankton communities (bottom). Data points represent sampling days (0, 1, 3, 7) and are connected by a convex polygon for each treatment and associated replicate mesocosm (*n*=3). Microbial communities were found to differ from control mesocosms by day 3, with HP and mixed communities being more similar.

Transcriptome

Photosynthesis subsystems transcription was found to significantly decrease in relative abundance 24 hours after treatment application in hydrogen peroxide mesocosms with a 20% reduction in relative abundance, along with an 18% reduction in mixed mesocosms, while lysine was only slightly less than controls (Fig. 4.8). Mixed mesocosms saw a greater recovery in photosynthetic subsystem activity than hydrogen peroxide did on the last day. Oxidative stress subsystem sequence reads were also found to increase for hydrogen peroxide and mixed mesocosms 24 hours after application (Fig. 4.9), with pronounced catalase (CAT), superoxidase (SOD), and ferroxidoxins (Fds) increases seen relative to control and lysine mesocosms. Rubreythrin oxidative stress sequence reads were found to be more abundant in lysine mesocosms (Fig. 4.9).

DISCUSSION

Hydrogen peroxide influence on microbial communities and implications for water management

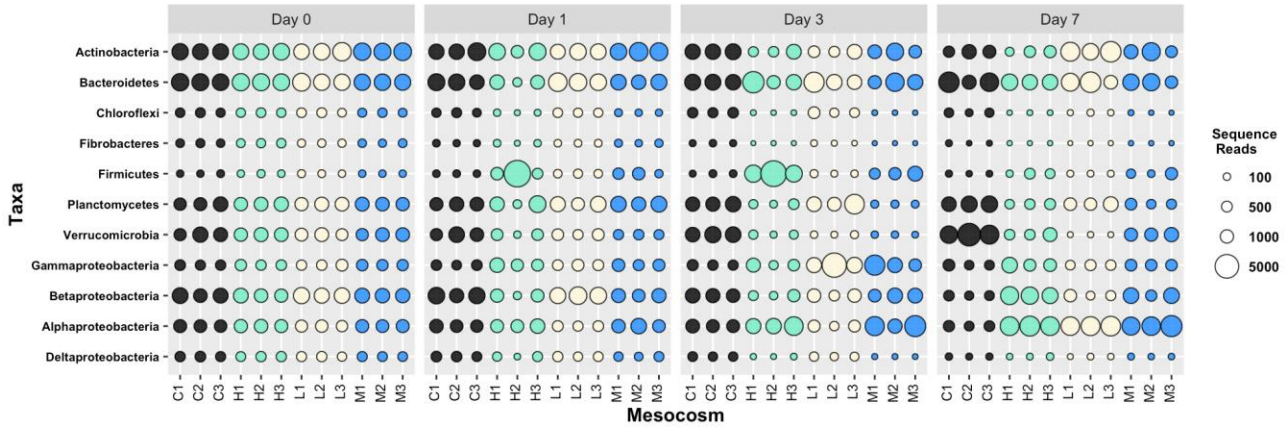

Figure 4.7. Bacterioplankton sequence read abundance, normalized to 10,000 reads of major taxa (>0.5%) after removal of non-target taxa. Proteobacterial classes (Gammaproteobacteria, Betaproteobacteria, Alphaproteobacteria) were found to be highly abundant in treatment mesocosms (Hydrogen peroxide, L-lysine, Mixed) compared to controls at the end of the experiment and were used for phyla-level bacterioplankton analysis due to large contributions to overall abundance.

Alphaproteobacteria became the dominant bacterial taxa by the end of the experiment, with notable increases in relative abundance from the *Rhodobacter*, which was 6.9% of hydrogen peroxide bacterial communities on the final day of the experiment. This agrees with findings from other hydrogen peroxide mesocosm and field experiments (Santos et al., 2021; Piel et al., 2021), and is most likely due to the taxa's ability to employ aerobic, anaerobic, and photoautotrophic growth mechanisms allowing for adaptability under changing conditions (Kiley and Kaplan, 1998). The relative abundance of Betaproteobacteria was

also found to increase after hydrogen peroxide treatment, while in all other mesocosms these taxa decreased or remained stable (Fig. 4.7). Interestingly, a majority of this growth came from the family Comamonadaceae, which grew from 2.18% relative abundance on day 0 to 16.79% of the bacterial composition by the end of the experiment. Santos et al. (2021) found that this bacterial group also positively correlated to hydrogen peroxide treatments after 120 hours. Gammaproteobacteria were also found to increase more under hydrogen peroxide treatments, which agrees with findings from other hydrogen peroxide mesocosms (Santos et al., 2021). The relative abundance of Planctomycetes and Actinobacteria was found to decline in hydrogen peroxide mesocosms; from 11.5% on day 0 to 4.33% by day 7 for Planctomycetes, and from 17.9% to relative abundances of 5.4% for Actionbacteria (Fig. 4.7).

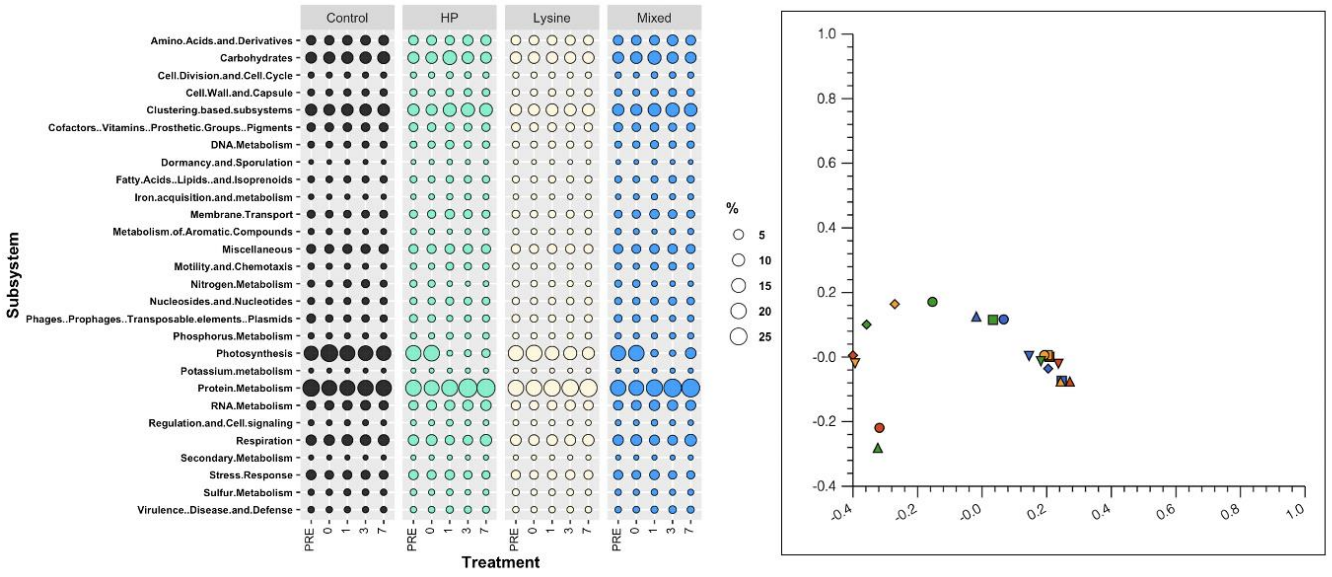

Figure 4.8. Bubble chart (left) and PCoA plot (right) of relative abundance of microbial metatranscriptome level one SEED subsystems on sampling days (Pre-treatment, 0, 1, 3, 7). PCoA plot used Bray-Curtis dissimilarity indices. Photosynthesis subsystem relative abundance transcription was found to decrease in HP and mixed mesocosms after 24-hours, correlating to collapse of cyanobacterial relative abundance. L-lysine had less significant declines in photosynthesis transcription.

The prominent advantage of cyanobacterial toxicity by hydrogen peroxide algaecidal treatments was demonstrated during our experiment using a 33.3 mg/L hydrogen peroxide solution. cyanobacterial populations crashed within a few days, reducing from a relative abundance of 92.2% on day 0 to 1.7% by day 3, and less than 1% representation of the phytoplankton community by day 7. A concern with freshwater management and overabundance of toxic cyanobacteria is the potential exposure to

cyanotoxins. *Microcystis* was found to have a high relative abundance in HP mesocosm phytoplankton communities at the start of the experiment (19%) (Fig. 4.4). Past studies have reported elevated levels of microcystin after hydrogen peroxide application resulting from *Microcystis* cell lysis and toxin release into the environment (Wang et al., 2019), however, this was not found in our study, microcystin levels in hydrogen peroxide mesocosms steadily declined throughout the experiment even while seeing a 99% reduction in *Microcystis* (Fig. 4.4). Although not analyzed in this study, past reports have shown hydrogen peroxide can be a strong detoxifier of microcystins leading to degradation (Wang et al., 2015), and with our hydrogen peroxide dosage may have been responsible for the measured decline.

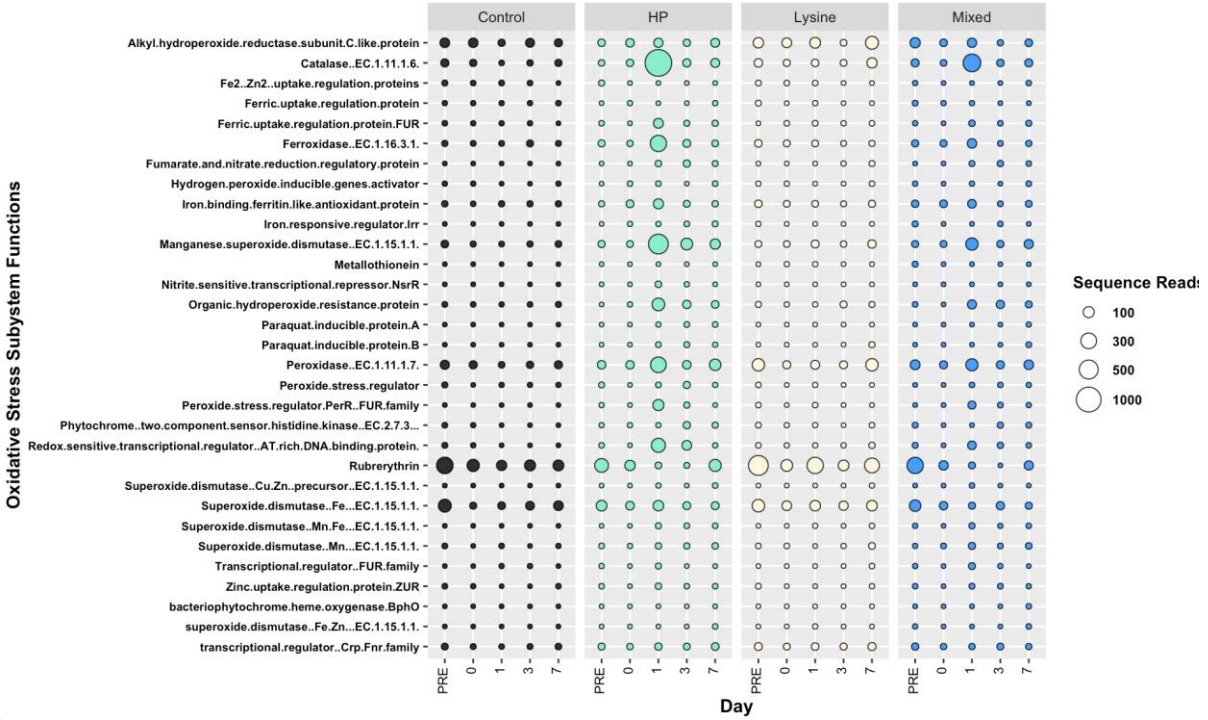

Figure 4.9. Metatranscriptome oxidative stress function SEED subsystem level sequence reads from 7-day experiment.

As mentioned, an advantageous dilemma found with hydrogen peroxide application is the fast decomposition rate, making it less harmful to the environment and other biota, however, shortened residence can also prevent complete eradication of cyanobacteria (Weenick et al., 2015). In selecting our experimental hydrogen peroxide dosage, a higher concentration of 33.3 mg/L was chosen due to high hydrogen peroxide concentrations found in surface waters of regional freshwater bodies (Ndungu et al., 2019), which may correspond to potential adaptive advantages this may pose for natural Cyanobacteria populations used in our study. Hydrogen peroxide was found to rapidly degrade during our experiment, returning to concentrations found in the control by day 3 (Fig. 4.1). Previous studies have suggested hydrogen peroxide dosages between 2.5 and 5 mg/L were less harmful for eukaryotic algae, allowing for

positive succession of these organisms in the phytoplankton community (Drabkova 2007; Weenick et al., 2015). Although our dosage of 33.3 mg/L was significantly higher, eukaryotic succession was observed, predominantly by the Eustigamatophyte phyla which became the dominant phytoplankton type just 24 hours after treatment (Fig. 4.5). This period coincided with a peak in orthophosphorus (OP), which dropped the next day and is when Bacillariophyte relative abundance began to increase along with the recovery of chlorophytes (Figs. 4.3 and 4.5). This may represent OP release by dead Cyanobacteria, and nutrient acquisition by these eukaryotic phyla (Zhang et al., 2018). Metatranscriptome data supports these finding with phosphorus metabolism relative abundance increasing from 0.62% on day 0 to 1.07% 24 hours later in HP mesocosms, which was the highest relative abundance for this subsystem recorded throughout the experiment (Fig. 4.8).

The Eustigmatophyta genus *Nannochloropsis,* was found to be solely responsible for the high relative abundance of this phyla in mixed and hydrogen peroxide phytoplankton mesocosm communities (Fig. 4.4), showing great resistance to stress caused by hydrogen peroxide treatment application. Oxidative stress subsystem sequence reads increased significantly in hydrogen peroxide and mixed mesocosms one day after treatment application (Supp. Oxidative), which also coincides with growth of this genus. Resistance to oxidative stress created by hydrogen peroxide application for this genus is likely due to the various antioxidant response systems found for this organism (Wei et al., 2020). Transcriptomic study by Wei et al. (2020) found that unlike many other algal taxa, catalase (CAT) was not regulated by varying light intensities suggesting this genus employs other systems to cope with ROS, and some of those mechanisms included Ferredoxins (Fds) which were found to increase in our study 24 hours after application (Fig. 4.9).

L-lysine Treatment Influence on Microbial Communities and Implications for Water Management

Amongst Alphaproteobacteria, *Methylosinus* was found to continually grow throughout the experiment, going from relative abundance of less than 1% on day 0 to occupying 18% of the bacterial community in lysine treatments by day 7, which was unique amongst all other mesocosms (Figure 4.7). Actinobacteria growth was also unique among lysine mesocosms, predominantly coming from the *Mycobacterium* with relative abundance of 15% on the last day of the experiment. Other notable changes came from a decline in Betaproteobacteria, similar to controls, and a stable Planctomycetes composition which was not seen in hydrogen peroxide and mixed mesocosms (Fig. 4.7).

Lysine was found to quickly degrade going from a concentration of 45.87 μg/L after application and returning to concentrations similar to controls by day 3 (Table 4.1). These findings highlight the advantages of high solubility and biological metabolism characteristics in using this amino acid treatment (Tian et al., 2018). L-lysine treatments were successful at inhibiting the growth of *Microcystis,* in 24 hours relative abundance in lysine mesocosms dropped to below 1%, this was followed by a slight increase in measured microcystin on day 3, however, values by the end of the experiment were lower than the start (Fig. 4.4). This agrees with previous findings that *Microcystis* is highly sensitive to lysine (Zimba et al., 2001; Hehmann et al., 2002; Takamura et al., 2004; Tian et al., 2018). Laboratory and field trials have reported that L-lysine did not inhibit the growth of *Dolichospermum, Anabaena,* or other nitrogen-fixing Cyanobacteria (Takamura et al., 1999), possibly caused by differential growth characteristics (Takamura et al., 2004), or nitrogen metabolism (Kaya et al., 2004). In our study, however, relative abundance of nitrogen-fixing cyanobacterial genera *Anabaena, Dolichospermum,* and *Cuspidothrix* were all found to decrease with a minor increase in *Sphaerospermopsis* (+0.16% relative abundance) (Fig. 4.4). A positive discovery was that all toxin-producing cyanobacteria from order Nostocales declined when compared to the control, however this could also be the result of increased competition from eukaryotic phytoplankton succession (Fig. 4.4).

As cyanobacterial dominance declined by day 3 in lysine mesocosms, Chlorophyta and Bacillariophyta relative abundance increased (Fig. 4.4), this period also coincided with degradation of L-lysine and a spike in available ammonia, followed by a decline on the final day (Fig. 4.3). By this time chlorophyte relative abundance had grown to 56.6%, becoming the dominant algal phyla, where ammonia acquisition, explained by the final day's decline (Fig. 4.3), may have aided this growth. Chlorophyta that strongly contributed to this shift were *Chlorella, Pectinodesmus, Choricystis, Mychonastes*, *Picochlorum*, and *Dicloster. Chlorella* was found to be the dominant taxa in this group, similar to findings by Yamamoto et al. (1998) that *Chlorella vulgaris* was not sensitive to lysine concentrations up to 1000 mg/L.

A concern brought with the use of L-lysine as a biological algaecide, is the introduction of bioavailable nitrogen into water bodies, potentially exacerbating eutrophication or leading to proceeding cyanobacterial blooms after decomposition (Shao et al., 2013). Contrary to this, our mesocosm experiment found that both lysine and mixed mesocosm total nitrogen (TN) concentrations were significantly less than those in hydrogen peroxide mesocosms on the last day, while still slightly higher than controls (Fig. 4.3). Potential succession by bloom-forming cyanobacteria was also not realized, as 27.4% of the 30% cyanobacterial relative abundance came from non-bloom forming picocyanobacterial

genera *Cyanobium*, *Synechococcus*, *and Prochlorothrix* (Fig. 4.6). Beneficial community shifts were seen on the last day of the experiment, where 70.0% of phytoplankton relative abundance was occupied by eukaryotic algae, compared to 91.4% cyanobacterial dominance in control mesocosms (Fig. 4.5). However, these findings are unique to a mesocosm experiment, as previous field studies by Takamura et al. (2004) found that after lysine application and the disappearance of a *Microcystis* bloom, the cyanobacterium *Phormidium* began to become dominant about 15 days later. Further investigation is needed to confirm long-term results of L-lysine application, taking into consideration current nutrient regimes and microbial community dynamics. The need for better molecular understanding of selective growth inhibition mechanisms caused by lysine application is also needed for improved application.

Mixed treatment

Alphaproteobacteria were found to grow continually in mixed mesocosms during the experiment, specifically *Gemmobacter, Sphingomonas* and *Rhodobacter* from the family Rhodobacteraceae. The abundances of Gammaproteobacteria and Betaproteobacteria were found to remain stable throughout the experiment, while Bacteroidetes and Planctomycetes abundances declined (Fig. 4.7). Bacterioplankton diversity remained high relative to control and lysine mesocosms throughout the experiment.

hydrogen peroxide and L-lysine concentrations in the mixed treatment were found to degrade at similar rates as their respective single treatment mesocosms, with both concentrations returning to levels found in controls by day 3 (Fig. 4.2; Table 4.1). Mixed mesocosms were found to be most effective at rapidly inhibiting the growth of cyanobacteria, with relative abundance having decreased from 92.2% to 18.9% after 24 hours was nearly absent afterwards (Fig. 4.4). Similar to hydrogen peroxide mesocosms, mixed treatment application had immediate effects on *Microcystis* relative abundance, dropping from 10.9% of the phytoplankton community on day 0 to less than 1% 24 hours later, which continued to decline and was no longer detectable on day 7. This resulted in a 0.26 μg/L increase in microcystin content. However, this was less than what was found in control mesocosms on this day, and microcystin concentrations were found to be lower on the last day of the experiment than the starting point (Fig. 4.7).

Immediate crash of cyanobacterial populations 24 hours after treatment application led to a more pronounced dominance by Eustigmatophytes than what was found in hydrogen peroxide mesocosms on day 1 (relative abundance of 75.1 %) (Fig. 4.5). Mixed mesocosms also saw the greatest growth in Bacillariophytes of all other mesocosms on this day and maintained the highest relative abundance on the

last day of the experiment (4.3%). Although nutrient fluxes of nitrogen and phosphorus in mixed mesocosms behaved more similarly to lysine mesocosms (Fig. 4.3), this did not have an apparent influence on phytoplankton community composition, which behaved similarly to hydrogen peroxide mesocosms for the remainder of the experiment (Bray-Curtis dissimilarity index: 0.02 ± 0.00, $n = 18$) (Fig. 4.6).

To our understanding the pairing of both L-lysine and hydrogen peroxide for algaecidal treatment application has never been examined before. Our results show this pairing was highly successful at reducing cyanobacterial abundance within just 24 hours and was sustained throughout the remainder of the 7-day experiment. This treatment pairing was used to explore potential solutions to hydrogen peroxide fast decomposition rates which can contribute to the need for costly re-application or potentially harmful situations for eukaryotic phytoplankton as well as zooplankton when the dosage is too high (Weenick et al., 2015). Although eukaryotic succession was observed, there were signs of harm caused to Chlorophyta phytoplankton. This is likely due to the high hydrogen peroxide dosage as previously discussed found to be harmful for some eukaryotic algae (Drabkova et al., 2007), future studies may look to lower hydrogen peroxide concentration when pairing with lysine or another biologically derived substance, which from our results, will still offer selective inhibition of toxic cyanobacterial genera, such as *Microcystis,* while allowing for positive phytoplankton succession such as seen in lysine mesocosms. Given the varying hydrogen peroxide sensitivity of *Microcystis* strains (Shuurmans et al., 2018), and the potential for adaptive succession of *Microcystis* strains that are less sensitive to hydrogen peroxide after continual application, paired treatments with selective lysine toxicity to the *Microcystis* may provide suitable treatment options for this ubiquitous cyanoHAB species.

Chapter 5: Field application of hydrogen peroxide #1

ABSTRACT

On April 12, 2021, we found a minor shoreline bloom of *Microcystis aeruginosa* at Franklin Lock and Dam in the Caloosahatchee River. As a response, we sprayed 3% hydrogen peroxide to control cyanobacterial blooms to 400 m^2 of the area (downstream side of the lock) on April 14, 2021. The hydrogen peroxide concentration used (16.7 mg/L, 0.0015%) was within the concentrations reported in literature (2 mg/L to 100 mg/L). This concentration was determined based on the laboratory experiments and was good to stop the growth of *Microcystis aeruginosa* in the laboratory condition. In the Netherlands, which is the most advanced country for this technology, dosing is restricted to a maximum of 5 mg/L. Therefore, we wanted to test a small area to minimize the potential damage to other aquatic life. After spraying hydrogen peroxide using a kayak, the hydrogen peroxide concentration in the surface water was monitored every 15 min in the first hour then on days 1, 3, 7, and 14 after the first treatment. The monitoring showed that the concentration of hydrogen peroxide decreased within the first hour and went back to the background level on the next day. No significant decrease in Chl-a concentration in the surface bloom was observed. However, we were able to detect the succession of the phytoplankton community after the treatment using high-throughput 16S rRNA gene amplicon sequencing. A reduction of the relative abundance was observed in the populations of *Dolichospermum* and our major target species, *M. aeruginosa*. Other phytoplankton populations took over the niche and their relative abundance increased. The major successor was picocyanobacteria. Our results indicated that hydrogen peroxide induced the succession of phytoplankton community from HAB to non-harmful groups and could be used for the selective suppression of harmful cyanobacteria. Overall, we demonstrated the effectiveness of the use of hydrogen peroxide for cyanobacterial bloom control.

INTRODUCTION

Recent harmful algal blooms (HAB) occurred in the Caloosahatchee River and Lake Okeechobee causing devastative damage to Florida water and watersheds (Kramer et al. 2018). However, few methods exist for the rapid suppression of HAB blooms. The development of the prediction and prevention method of HAB is a top priority issue in Florida.

The use of hydrogen peroxide for algal control was first time tested in Netherland water (Matthijs et al. 2012) and is a promising algal control approach because hydrogen peroxide does not last long in aquatic environments and is degraded into water and oxygen (no harmful byproducts are produced) within a few days. A Well managed hydrogen peroxide treatment does not harm aquatic life (e.g. zooplankton, insects, and fish) because cyanobacteria are more sensitive to hydrogen peroxide than eukaryotic phytoplankton and stimulate the rapid succession of phytoplankton populations from harmful bloom-forming species to non-harmful species, which are smoothly consumed in classic/microbial food chains.

The strength of our hydrogen peroxide-based approach is that we can predict and mitigate HAB using a cost-effective manner. Our approach is safe and scientifically backed up, however, the use of hydrogen peroxide is the first time attempt and required to be examined more before use in natural waters. We will also apply cutting-edge molecular techniques to monitor phytoplankton communities and identify key growth factors of phytoplankton communities. These gene expression screening methods are suitable for detecting hidden growth factors that are not nitrogen and phosphorus and help the prediction of blooms. Cyanobacteria treatments will center on the use of formulations of hydrogen peroxide, used here as a rapid response application, but also potentially useful as a “clean-up” method in confined areas such as boat slips and canals. As the method proposed does not remove nutrients, it is important that we determine the destination of the nutrients released by oxidized cyanobacteria, with the hypothesis that beneficial members of the phytoplankton community will take advantage of the released nutrients.

Since there was no past application, we decided to use a low and safe concentration. In this study, the hydrogen peroxide concentration used (16.7 mg/L, 0.0015%) was within the concentrations of literature data (2 mg/L to 100 mg/L). This concentration stopped the growth of *Microcystis aeruginosa* in the laboratory condition (see chapter 7). In the Netherlands, which is the most advanced country for this technology, dosing is restricted to a maximum of 5 mg/L. The reason is that some zooplankton are sensitive to hydrogen peroxide (Matthijs et al., 2012).

Our project will reveal how hydrogen peroxide can repress harmful algal growth and induce the succession of phytoplankton communities from harmful to non-harmful algal species. It must be determined in southwest Florida because the data from Europe is not applicable dues to the difference in the climate. Our project will also monitor the fate of cyanotoxins after treatments. Our data will help improve the State's ability to mitigate and clean up HAB. Manipulation of the phytoplankton community from harmful algae to non-harmful algae using selective community shifts is a relatively new approach. Our study and technology application may set an avenue for the next generation harmful algae mitigation and water quality management in Florida.

MATERIALS AND METHODS

Field site and hydrogen peroxide treatment

On April 12, 2021, we found a minor shoreline bloom of *Microcystis aeruginosa* at Franklin Lock and Dam in the Caloosahatchee River during our routine biweekly monitoring. Based on this finding, we sprayed 3% hydrogen peroxide in a 400 m^2 area (8 m x 50 m, brackish side of the Lock) on April 14, 2021 (Fig. 5.1). Before and after spraying, hydrogen peroxide level in surface water was monitored every 15 min in the first hour then on days 1, 3, 7, and 14. The final concentration was calculated based on the 1 cm of depth.

Water sampling

Water samples were collected by grab sampling using a kayak from 30 cm of the water depth in two new 1 L amber bottles. A part of water samples was filtered through a sterilized 0.45 µm disposable syringe filters immediately upon sampling. The water samples are transferred to the laboratory in the cooler on ice.

Water quality analysis

Physiochemical parameters of the river surface water were measured at a depth of 30 cm with an Aqua TROLL sonde (In-Situ, CO, USA). Analytical details are available in chapter 1.

Nutrient analyses

We used Benchmark EnviroAnalytical to analyze Total organic carbon (TOC), nutrients, and chlorophyll *a*. TOC was quantified using high temperature combustion with a Shimadzu TOC analyzer. Nutrients and Chl-a were quantified via autoanalyzer and spectrophotometer, respectively, using a NELAC-approved

laboratory and methods (Benchmark EnviroAnalytical Inc., FL, USA) within 48 hours. Analytical details are available in chapter 1.

Microcystin analysis

The concentration of microcystin was separately measured as intracellular and extracellular forms. For the separation, 0.2 µm syringe disk filters were used. Microcystin samples were handled and analyzed via USEPA method 546 and manufacturer directions using an enzyme-linked immunosorbent assay (ELISA) (Beacon Analytic Systems Inc., ME, USA). Analytical details are available in chapter 1.

Hydrogen peroxide measurements

Samples taken for hydrogen peroxide measurement were immediately filtered through 0.2 µm syringe disk filters on-site and stored at -80°C until analyzed. Hydrogen peroxide was measured using a fast response amperometric 250 µm diameter tip hydrogen peroxide microelectrode with a built-in reference electrode (HP-250, Innovative Instruments). Analytical details are available in chapter 1.

Total iron analysis

The concentration of total iron was separately measured as intracellular and extracellular forms. For the separation, 0.2 um syringe disk filters were used. Total iron was determined by USEPA FerroVer Hach method 8008 (FerroVer® Iron Reagent Powder Pillows). Analytical details are available in chapter 1.

Colored dissolved organic matter (CDOM)

Colored dissolved organic matter (CDOM) was measured at the laboratory using a Trilogy fluorometer with a CDOM/NH4 module (Model 7200-041). Analytical details are available in chapter 1.

Total bacterial and picocyanobacterial counts

Samples for cell enumeration were preserved with 2% formalin and stored at -80°C. Bacterial cells were enumerated on the 0.02 µm pore-size black polycarbonate filters by directly counting SYBR Green I stained cells via epifluorescence microscopy. Autofluorescent signals produced by chlorophyll pigments under a Texas Red filter were used to count picocyanobacteria. Analytical details are available in chapter 1.

Algal colony counts

Colony abundance was quantified by filtering 50 ml of water with a glass fiber filter (GF/F) and counting macroscopic algal colonies under a dissection microscope. Analytical details are available in chapter 1.

Amplicon sequencing of cyanobacteria and eukaryotes

Algal cells were collected by filtering 200 ml of water with a 0.22 µm cellulose nitrate filter. Genomic DNA was extracted from half cut filter samples using the DNeasy PowerSoil Pro Kit (Qiagen) following the manufacturer's instructions. High-throughput amplicon sequencing targeting cyanobacteria/eukaryotic algae was conducted via amplification of 16S rRNA gene using primer pair cya359Fmod and Dcya781R (Nübel et al., 1997) using the Illumina MiSeq system (MR DNA, Shallowater, TX, USA). For analysis, sequences are joined and those less than 150 bp were removed. Sequences with ambiguous base calls were also removed. The dereplicated or unique sequences were denoised; unique sequences identified with sequencing and/or PCR point errors and removed, followed by chimera removal, thereby providing a denoised sequence or Amplicon Single Variant (ASV). Final ASVs were taxonomically classified via representative ASVs through BLAST at NCBI.

Metatranscriptome

RNA Samples for transcriptome sequencing were collected by filtering 200 ml of water using 0.2 µm Sterivex filters on-site, which were promptly frozen in liquid nitrogen for transport to a -80°C freezer until further analysis. Total RNA was isolated from Sterivex filters using the RNeasy PowerMicrobiome Kit (Qiagen) following manufacturer's instructions. For each filter sample, three extractions were performed. RNA was eluted in 100 µL RNase-free water and pooled. DNA contamination was removed using Baseline-ZERO™ DNase (Epicentre) following the manufacturer's instructions followed by purification using the RNA Clean & Concentrator columns (Zymo Research). DNA-free RNA samples were used for rRNA removal by using Ribo-Zero Plus rRNA Depletion Kit (Illumina). rRNA depleted samples were used for library preparation via the KAPA mRNA HyperPrep Kits (Roche) by following the manufacturer's instructions. The average library size was determined using the Agilent 2100 Bioanalyzer (Agilent Technologies) and the samples were then pooled in equimolar ratios of 0.6 nM, and sequenced paired-end for 300 cycles using the NovaSeq 6000 system (Illumina). Resulting data were processed and analyzed via the MG-RAST pipeline (Meyer et al., 2008) using SEED subsystems (Overbeek et al., 2014).

RESULTS AND DISCUSSION

Table 5.1. Water quality data during the two weeks of monitoring period.

Parameter		Day 0 pre	Day 0 post	Day 1	Day 3	Day 7	Day 14
Temp.	(°C)	25.7	25.9	28.7	nd	27.0	28.0
DO	(%)	76	77.3	106.2	119.6	84.6	84.9
DO	(mg/L)	6.3	6.3	8.4	9.6	7.1	6.8
Cond.	(uS/cm)	433	461	643	571	425	463
pH		7.9	7.9	8.3	8.5	7.9	7.6
CDOM	(µg/L)	194.1	200.7	202.0	242.0	198.1	210.5
Chl-a (Benchmark)	(µg/L)	8.2	9.1	11.3	27.5	35.0	14.5
Chl-a (surface)	(µg/L)	41.5	23.0	40.4	70.0	86.3	44.4
Pheophytin (surface)	(µg/L)	7.3	16.1	2.3	8.0	10.1	7.5
Hydrogen peroxide	(µg/L)	87.5	146.1	64.4	48.5	15.3	5.1
Colony count	(per L)	2640	2416	1261	2784	1984	872
Microcystin	(µg/L)	0.1	0.1	0.8	0	0.1	0
Microcystin filtrate	(µg/L)	0	0	0	0	0	0
Total iron	(µg/L)	150	117	107	153	193	260
Total iron filtrate	(µg/L)	93	40	113	73	140	160
Total iron intracellular	(µg/L)	57	77	nd	80	53	100
PICO	(cells/mL)	2.29E+06	1.91E+06	1.85E+06	2.16E+06	1.74E+06	2.49E+06
BAC	(cells/mL)	1.05E+07	7.19E+06	6.17E+06	7.81E+06	5.32E+06	7.86E+06
TOC	(mg/L)	16.1	14.4	12.9	14.6	13.4	20.3
TKN	(µg-N/L)	1070	1050	1100	1290	1400	1080
TN	(µg-N/L)	1150	1121	1193	1296	1473	1154
TP	(µg-P/L)	91	51	100	92	135	114
NOx	(µg-N/L)	78	71	93	6	73	74
NH3	(µg-N/L)	75	105	8	84	141	8
OP	(µg-P/L)	64	51	62	42	79	51
TN/TP		12.6	22.0	11.9	14.1	10.9	10.1
TOC/TN		14.0	12.8	10.8	11.3	9.1	17.6
ION/OP		2.4	3.5	1.6	2.1	2.7	1.6

nd: No data.

Water and bloom condition

Physicochemical parameters and biological analytes during two weeks of monitoring period are listed in Table 1. *Microcystis aeruginosa* formed a minor surface bloom. The concentration of Chl-a was 8.2 µg/L at the depth of 30 cm, however the surface Chl-a concentration was 41.5 µg/L. Microcystin was detected but the concentration was low and ranged between 0 to 0.8 µg/L. Total iron concentration ranged

between 107 to 260 µg/L. Approximately 45% of iron existed within an intracellular pool. Based on the inorganic nitrogen and OP concentrations, nitrogen was identified as a limiting factor.

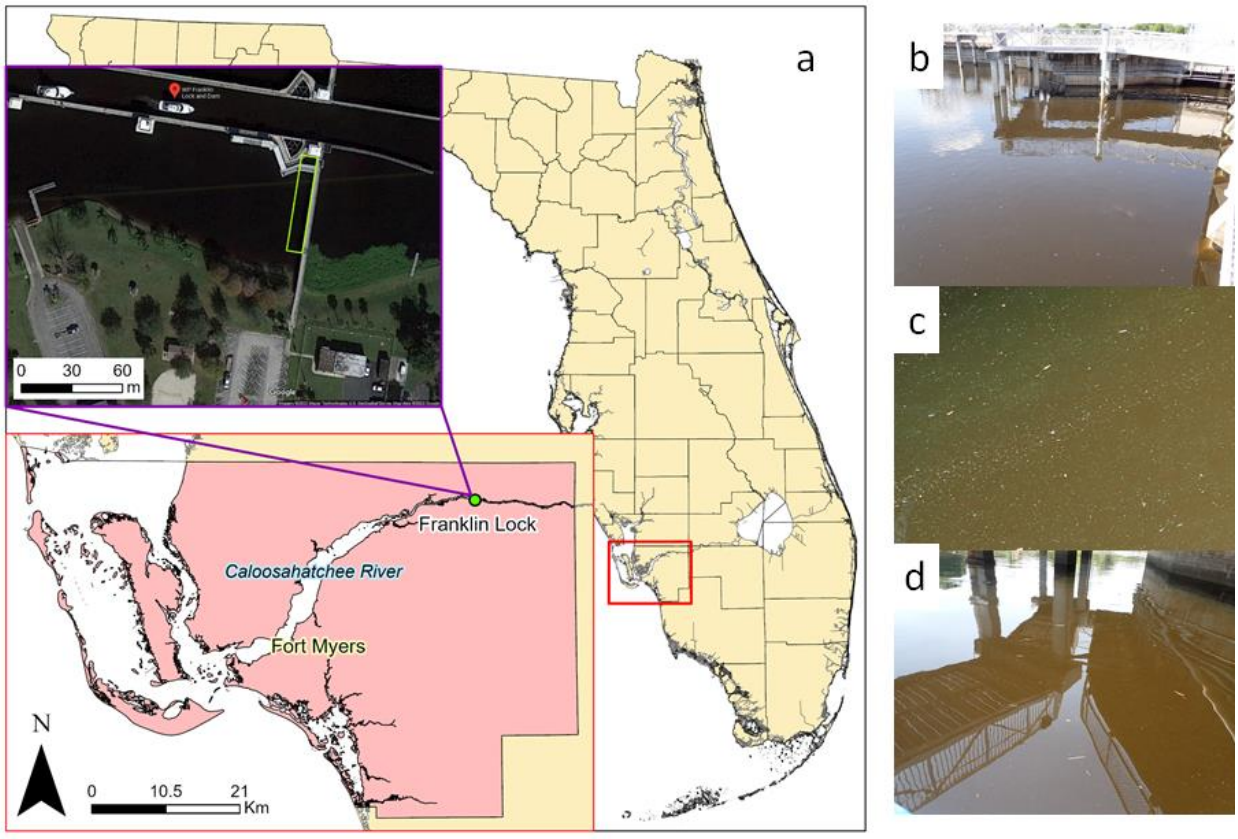

Figure 5.1. Hydrogen peroxide application at Franklin Lock and Dam in the Caloosahatchee River. (a) Location map. The location of hydrogen peroxide treatment is highlighted as yellow. (b) water condition before the treatment, (c) minor surface bloom observed, (d) water condition after the treatment.

Hydrogen peroxide dynamics

We sprayed hydrogen peroxide to be the concentration of 0.0015% (16.7 mg/L) within 30 cm of the surface water (Fig. 5.1). The concentration of hydrogen peroxide was examined every 15 min after the treatment (Fig. 5.2). Hydrogen peroxide concentration before the treatment was 2.58 µM. Approximately 10 µM of hydrogen peroxide was detected within the first hour, however, the concentration returned to the background level on the next day.

Influence on other aquatic life

We observed no death of wildlife during and after the field application. As fish, we observed Eastern Mosquitofish, Blue Tilapia, and armored catfish. As birds, we observed a Little Blue Heron and Boat-tailed Grackle during our monitoring. We also did not find any changes of aquatic vegetation within the two weeks of the monitoring period.

The succession of the phytoplankton community before and after the treatment

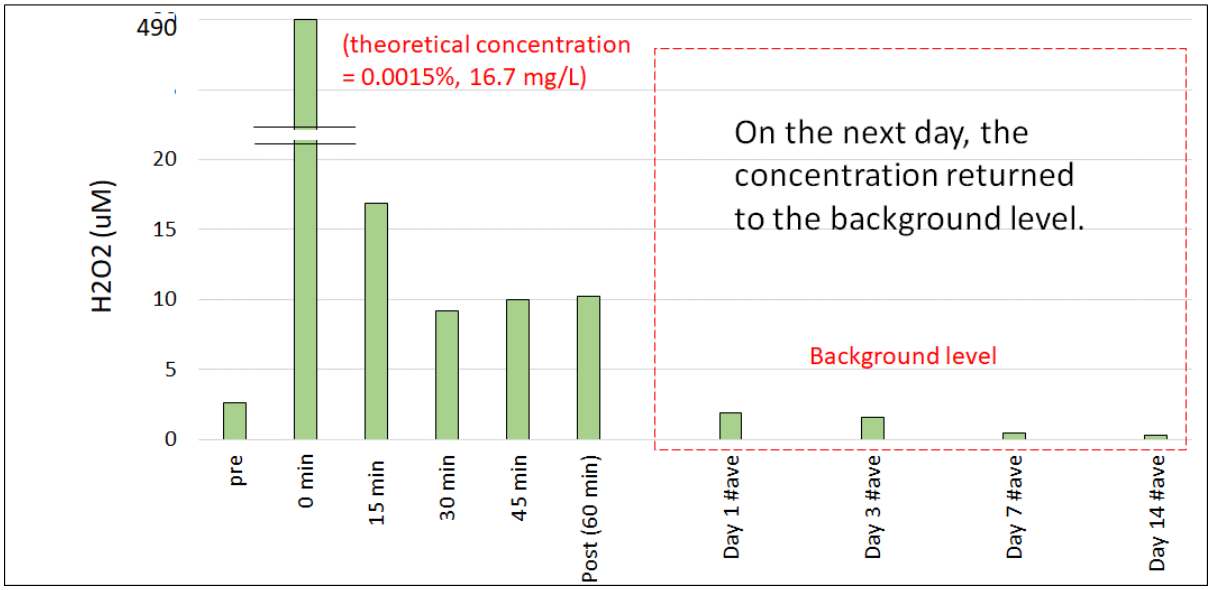

Figure 5.2. Succession of hydrogen peroxide concentrations after the surface application. The measurement at 0 min is a theoretical concentration and not a real measurement. It should be noted that the hydrogen peroxide concentration of pretreatment condition was higher than the normal condition because of the high activity of *Microcystis aeruginosa*.

The succession of the phytoplankton community before and after the treatment was monitored up to 14 days. In total, 41 cyanobacterial genera were found using high-throughput amplicon sequencing. Among 41 genera, 18 genera were found from a surface bloom sample. The surface bloom was mainly formed by cyanobacteria and dominated by *Microcystis aeruginosa* and composed 97.3% of the relative abundance (Fig. 5.3). After the treatment, *Microcystis* and *Dolichospermum* declined after Day 3 (Fig. 5.4). *Microcystis* declined from 12.0% to 1.3% and *Dolichospermum* declined from 7.4% to 2.1%. Picocyanobacteria increased. Cyanobacterium was the most abundant picocyanobacteria and their number increased after the treatment from 37.1% to 51.6%. The abundance of total eukaryotic algae increased from 7 to 9% after the treatment and cyanobacteria occupied over 90% of the relative abundance of phytoplankton communities even after the treatment (Fig. 5.3). Therefore, we found that in the Caloosahatchee River,

we did not see the typically documented population shift from HAB to eukaryotic algae. Instead of eukaryotic algae, the relative abundance of picocyanobacteria increased (Fig. 5.4). Eukaryotic phytoplankton community was minority in this study. *Cryptomonas*, motile green algae, was the most abundant eukaryotic algae (Fig. 5.5).

The dynamics of microcystin level

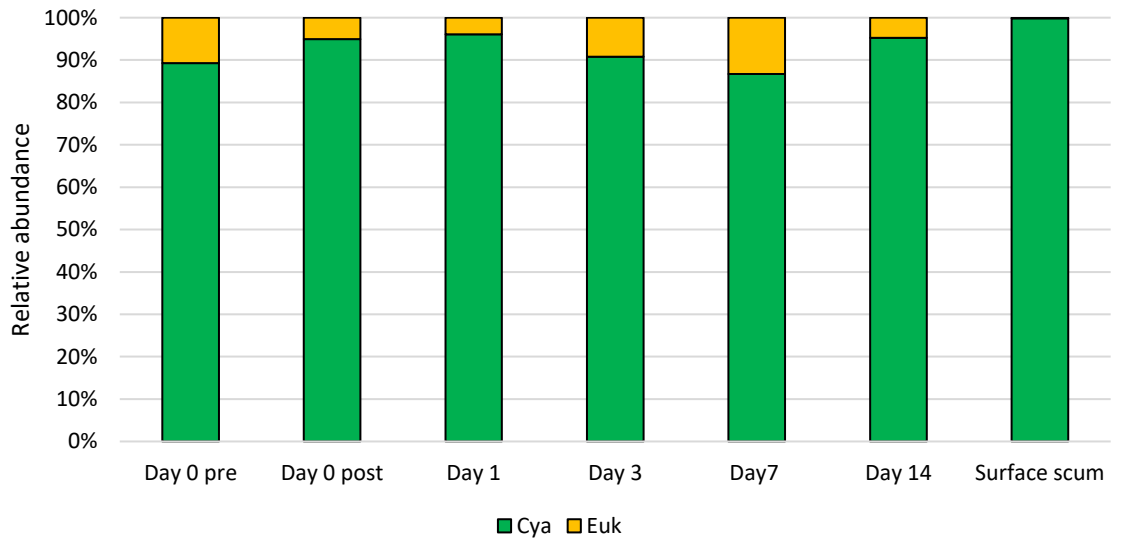

Figure 5.3. Relative abundance of phytoplankton community at the genus level during surface water hydrogen peroxide treatment. Cyanobacteria dominated the phytoplankton communities.

The examined *M. aeruginosa* bloom was a toxic bloom. Microcystin concentration followed the similar pattern with the relative abundance of *Microcystis* (Fig. 5.6). The concentration ranged between 0 to 0.8 µg/L and the highest concentration was detected on day 1. The comparison between intracellular and extracellular microcystin revealed that the majority of microcystin existed as intracellular form. It should be noted that we did not measure the microcystin concentration of surface scum but we assume the surface scum contained much higher microcystin concentration.

The surface algal scum was formed by sixteen *Microcystis* phylotypes

We found that the surface scum was formed by four *Microcystis* phylotypes (Fig. 5.7). Initially, these four phylotypes were also abundant in the water column and occupied approximately 70% of the relative abundance. The 30% of water column populations were formed by 12 phylotypes, which were not found

in the scum sample. On day 1, the proportion of surface scum forming *Microcystis* increased in the sample collected at the depth of 30 cm because a part of the surface scum *Microcystis* was damaged and sank down. This observation suggested our hypothesis (Fig. 5.8). Each phylotype had different sensitivity to hydrogen peroxide. For example, the relative abundance of Zotu4 decreased and Zotu141 (red) increased.

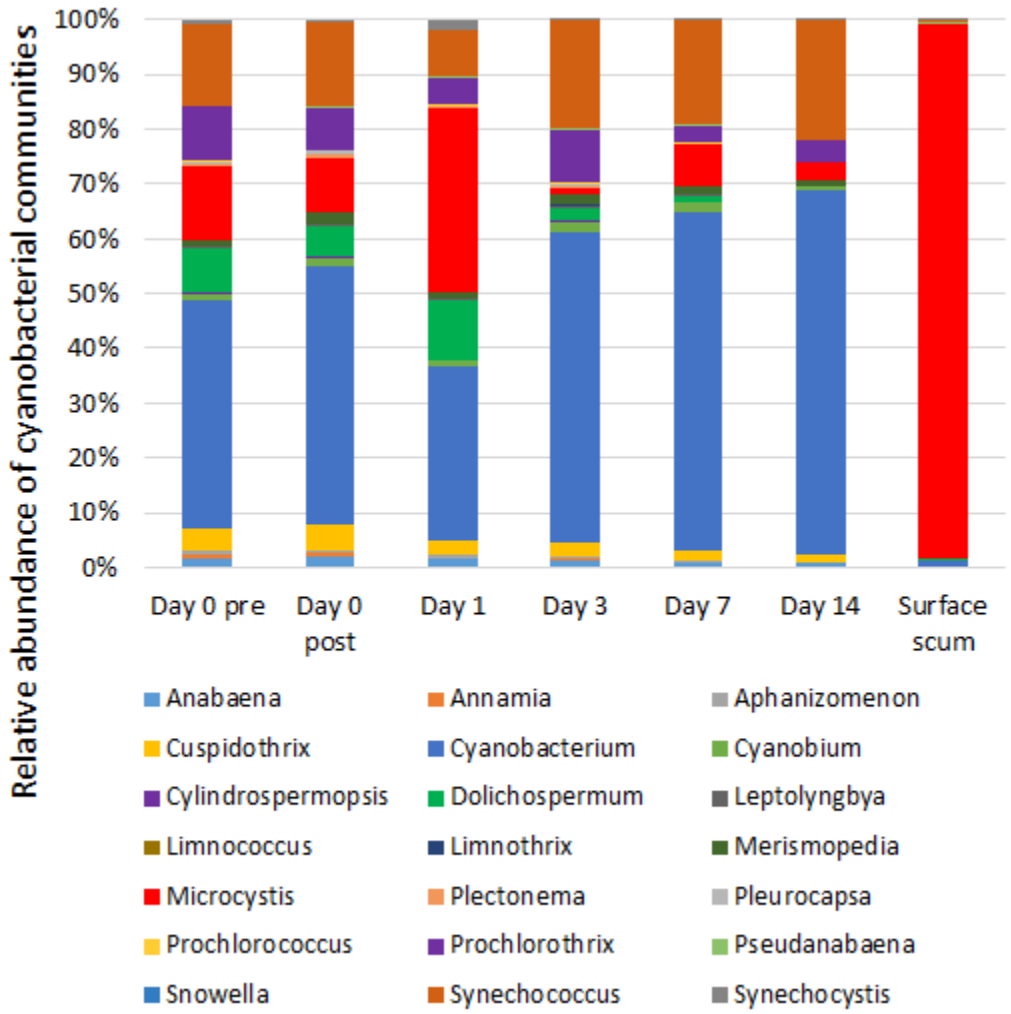

Figure 5.4. The relative abundance of cyanobacterial community at the genus level during surface water hydrogen peroxide treatment.

However, the relative abundance of Zotu173 (yellow) did not change. Overall, the scum forming phylotypes declined from 70% to 45%. Thus, the treatment induced the shift of *Microcystis* populations. It has been reported that the succession of the bloom changes the toxin level (Baker et al., 2002). It also supports our previous finding that non-toxic *M. aeruginosa* strain FD4 was isolated from toxic *M. aeruginosa* bloom occurred in the Caloosahatchee River in 2018 (Urakawa et al., 2020). Our data could

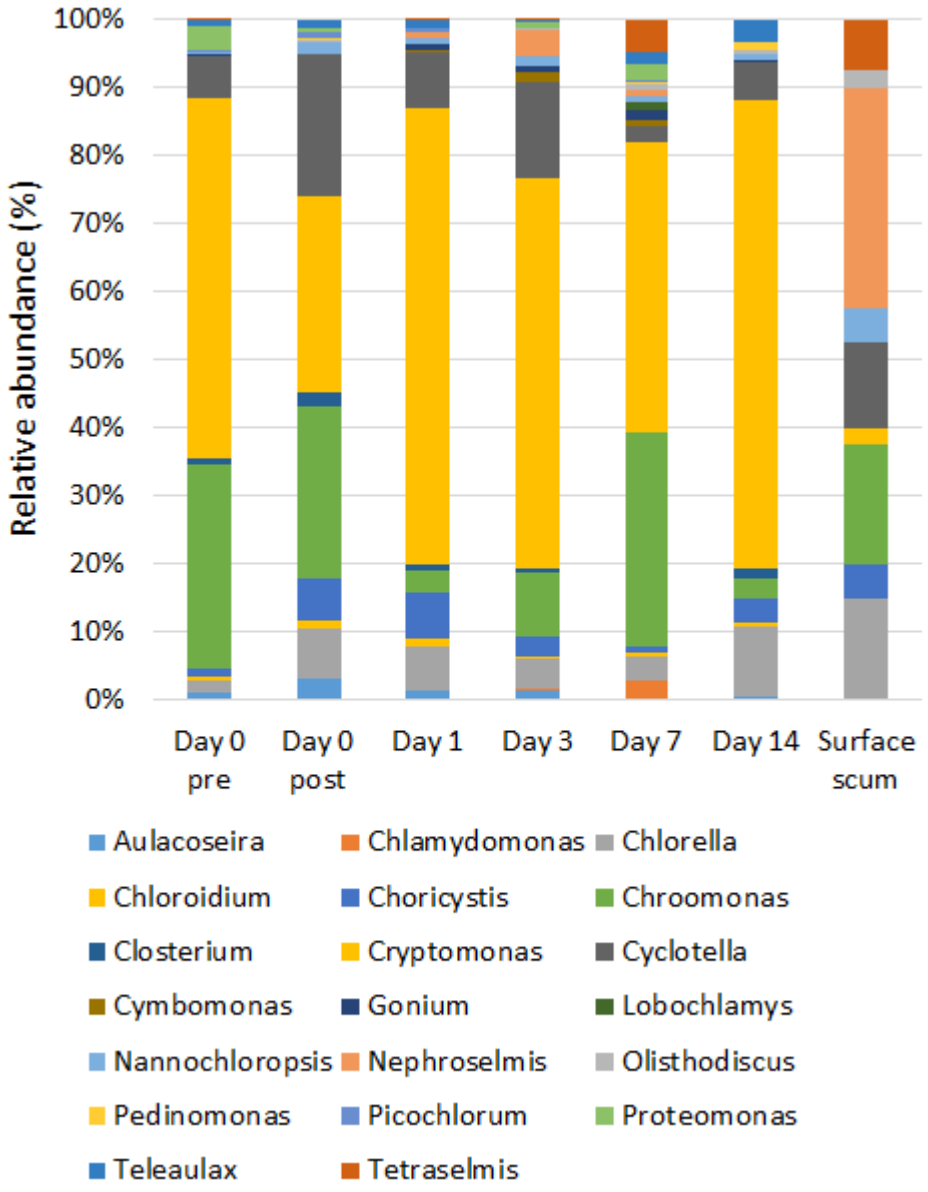

Figure 5.5. Relative abundance of eukaryote communities at the genus level during surface water hydrogen peroxide treatment.

partially explain it because we confirmed a single bloom was formed by multiple phylotypes, which have different sensitivity to hydr ogen peroxide. It is interesting that if we can find the interaction between oxidative responses caused by hydrogen peroxide and the production and cellular microcystin level of hydrogen peroxide resistant *M. aeruginosa* phylotypes in the future study.

Metatranscriptome

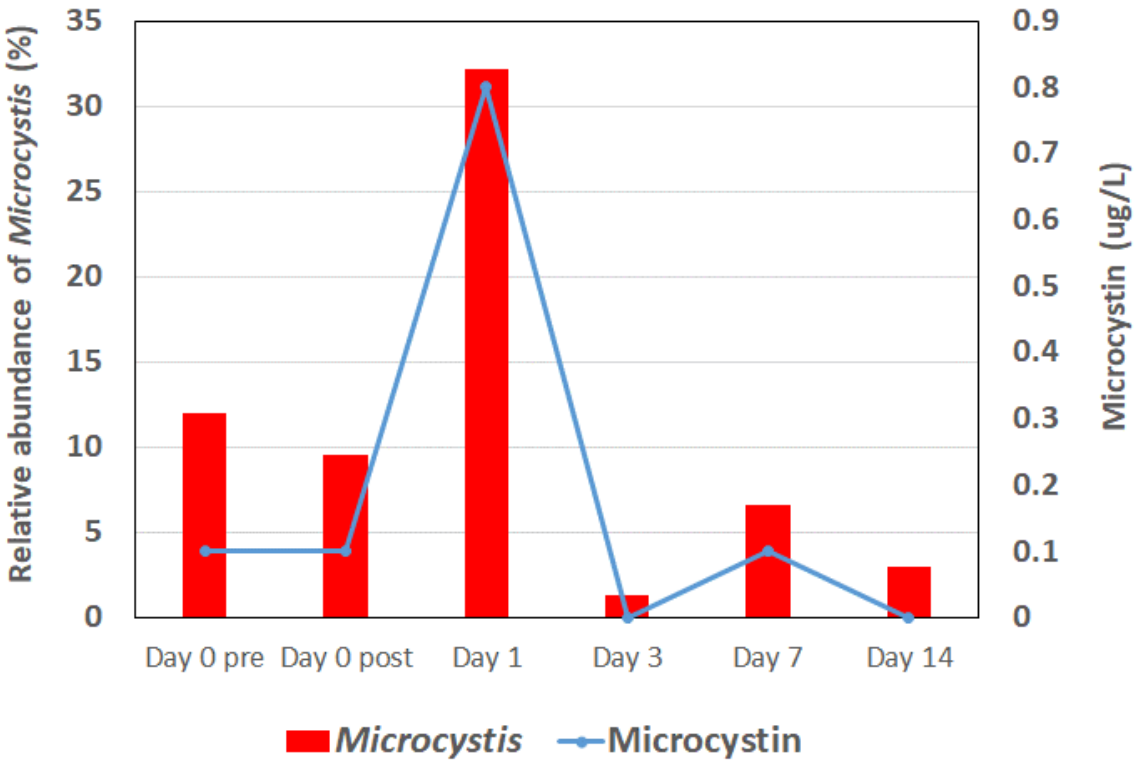

Figure 5.6. Relative abundance of *Microcystis* and microcystin concentration after hydrogen peroxide treatment

In total across seven samples, 7,070,607 sequences were determined. The mean number of cyanobacterial sequence reads was 287,950 ± 76,007 (± SE). As expected, photosynthesis, protein metabolism, carbohydrates, and respiration were the most abundant SEED subsystems for cyanobacteria, making up 72.4% of transcripts (Fig. 5.9). *Microcystis* sequence reads (38,047 ± 7,817) mostly followed the trend of cyanobacteria overall, although phages, specifically a r1t-like streptococcal phage, were more abundant. Throughout the experiment, both the *Microcystis* and overall cyanobacterial metatranscriptome were relatively stable, exhibiting no change in functionality. However, taxonomic representation of the cyanobacterial metatranscriptome shifted overtime with most of the dominant genera (*Microcystis, Nostoc, and Anabaena*) decreasing in relative abundance. At the same time, *Cyanobium* and the consistently dominant *Synechococcus* increased. However, this represented surface water collection up to 14 days after hydrogen peroxide treatment, whereas the surface scum sample

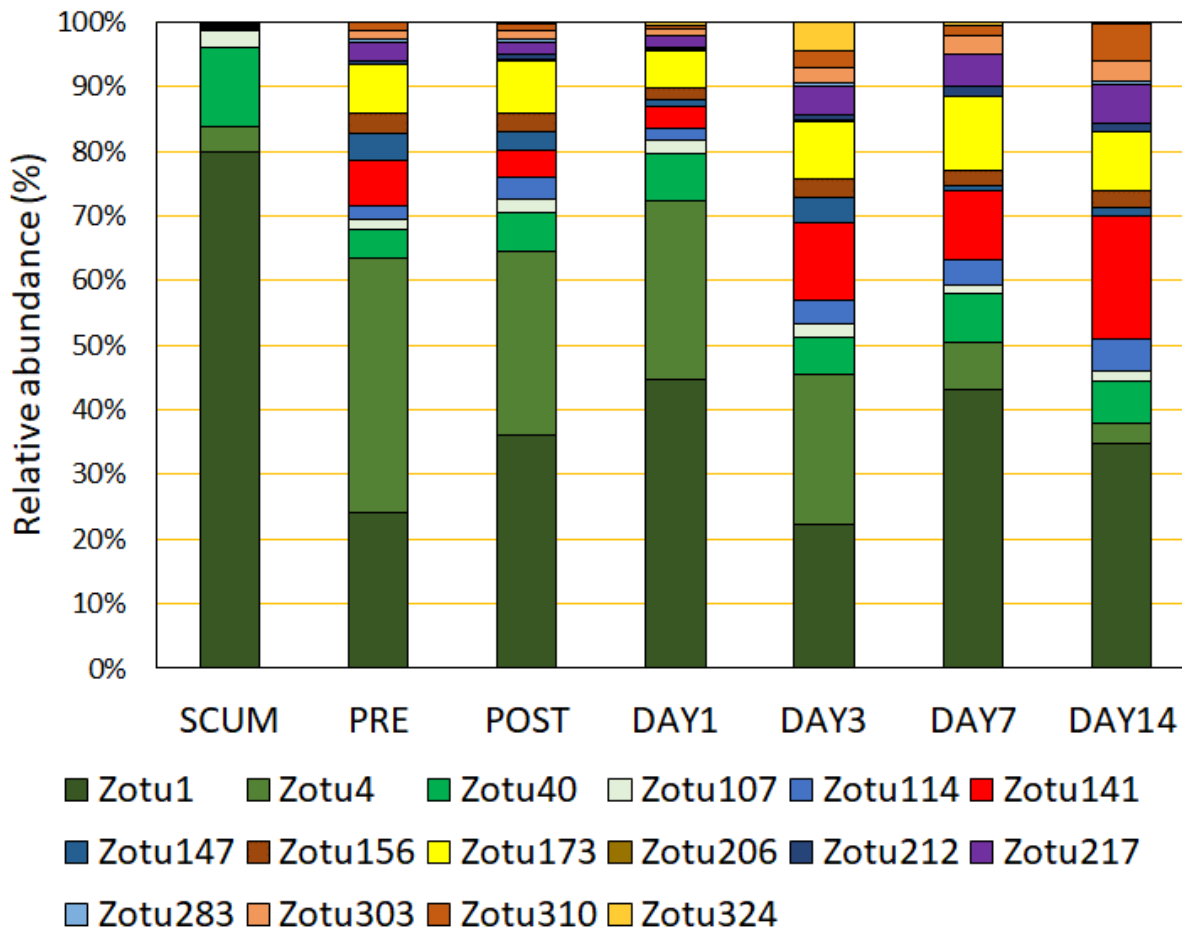

Figure 5.7. Succession of *Microcystis aeruginosa* phylotypes during a surface water hydrogen peroxide application.

exhibited a very different taxonomic distribution of expression with *Microcystis* as the dominant at 34.8%, followed by *Cyanothece* at 22.0%. In this scum sample, the *Synechococcus* and *Cyanobium*, which dominant in the surface water samples, had much lower relative abundance at 7.1% and 0.5%, respectively (Fig. 5.9).

Hydrogen peroxide application for freshwater harmful algal blooms

A hydrogen peroxide level goes back to a natural level within one day (Fig. 5.2). Based on our first mesocosm experiment and field application, we confirmed that the loss of hydrogen peroxide after treatment mainly occur because of the dilution of hydrogen peroxide with untreated water. Thus, the concentration of hydrogen peroxide may have to be increased when we apply it to high water bodies

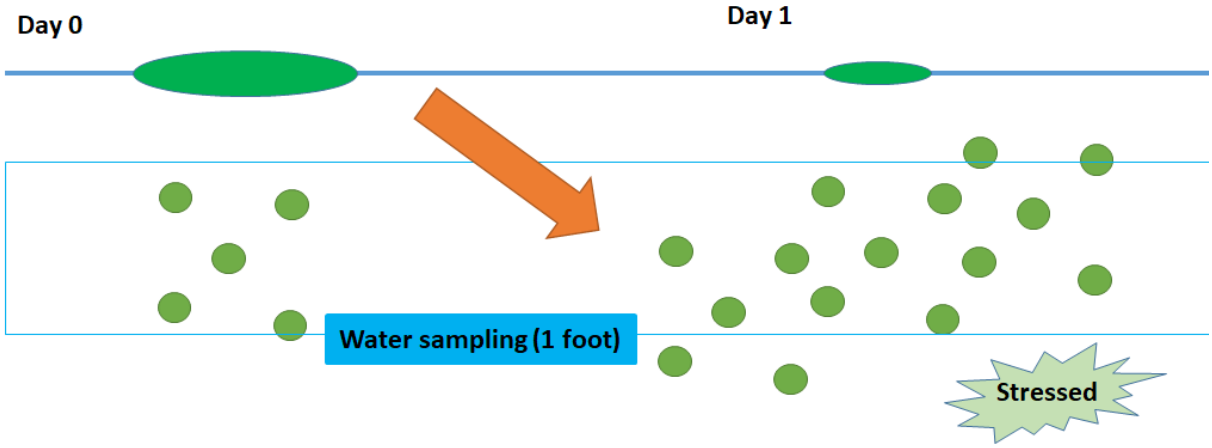

Figure 5.8. Hypothesis of surface *Microcystis aeruginosa* succession to explain why less cells were observed on the surface while more cells were detected at the depth of 30 cm. On the day 0, before the hydrogen peroxide treatment, the majority of *M. aeruginosa* cells were on the surface. On the day 1, after the treatment, damaged cells lost their buoyancy and sank down below the surface around the depth of 30 cm.

where have high water exchange or flow rates, such as river and canal systems. Our data and other literature demonstrated that hydrogen peroxide treatment is not the method that instantly kills HAB cyanobacteria (Matthijs et al. 2012). It induces a succession of algal communities from toxic cyanobacteria to non-harmful phytoplankton members. Our high-throughput amplicon sequencing showed that hydrogen peroxide induced the succession of algal communities. We found that the population shift from harmful cyanobacteria to picocyanobacteria. In previous studies, green algae were always successors, however, picocyanobacteria (*Synechococcus*/*Cyanobacterium*) were successors in the case of the Caloosahatchee River. It indicates the importance of the application of the technology in each region of interest because phytoplankton communities may locally show a different response. Surface treatment does not evenly hit *Microcystis* phylotype populations because every phylotype does not distribute in the same manner; even in a single bloom, some phylotypes form the surface scum but others prefer to stay in the water column. We found that surface hydrogen peroxide treatment could alter *Microcystis* phylotypes before and after the treatment, most likely based on the differential sensitivity to each phylotype.

We confirmed that hydrogen peroxide treatment is an effective method to remediate HAB. The total cost we spent for the preparation of hydrogen peroxide was $48 (1L bottle x 24 bottles). It took one hour for spraying the 400 m^2 of area size. Thus, we can say that hydrogen peroxide treatment is potentially

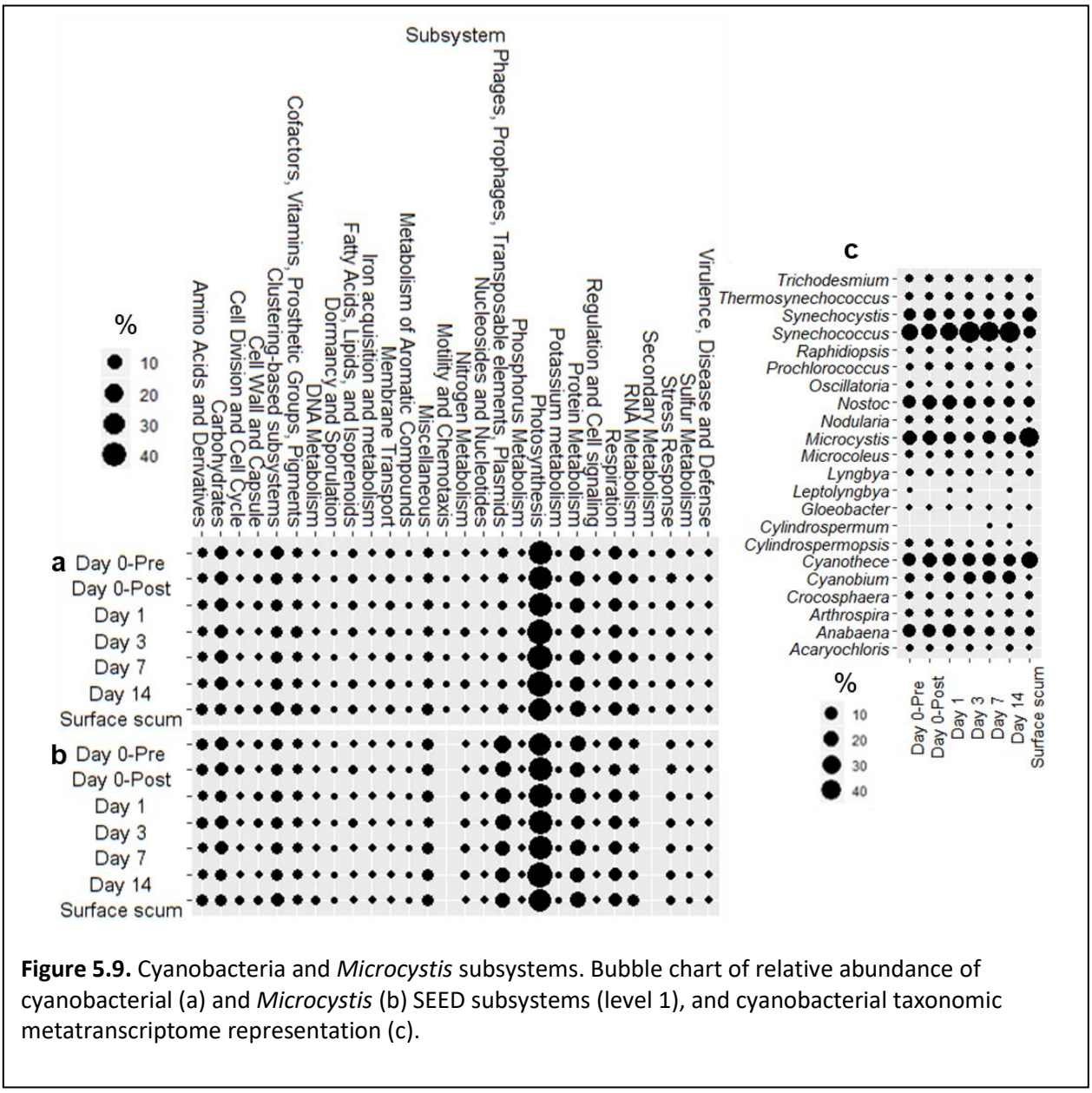

Figure 5.9. Cyanobacteria and *Microcystis* subsystems. Bubble chart of relative abundance of cyanobacterial (a) and *Microcystis* (b) SEED subsystems (level 1), and cyanobacterial taxonomic metatranscriptome representation (c).

very cost effective. The succession of phytoplankton community was detected after the treatment. In the case of the Caloosahatchee River, it is likely that HABs will be replaced by picocyanobacteria instead of green algae after the treatment. Although picocyanobacteria are not considered as a part of harmful bloom-forming cyanobacteria, some picocyanobacteria may cause harms. Therefore, in the future, we need to study these picocyanobacteria if they are suitable successor of hydrogen peroxide treatments.

Chapter 6: Field application of hydrogen peroxide #2

ABSTRACT

Hydrogen peroxide is considered as an effective chemical treatment method for harmful algal blooms, however, the effectiveness could be influenced by a variety of physiochemical and biological factors. For example, the types of water body and strategy of the chemical use may influence the treatment results. In a real application of hydrogen peroxide on an algal bloom, repetitive application may be required in respond to an algal community succession. In this application, we examined the application effect of repeated hydrogen peroxide dosing. This time, we were able to find the reduction of surface blooming biomass. Algal colony numbers declined from 4.8 x 10^4 cells to 4.2 x 10^3 colonies / L, suggesting 91.3% of algal biomass reduction. The surface hydrogen peroxide concentration dropped to the natural level on the next day. We confirmed that Lake Guard Oxy remained much longer time and higher concentration on the surface. The chemical was considered effective because it helped hydrogen peroxide concentration higher near the surface. In the period of monitoring, we did not observe any fish kill and the corruption of ecosystem. It suggests that our field application was correctly managed and no further harm for aquatic life was observed. We found healthy Smalltooth Sawfish, alligators, West Indian manatees, and a variety of birds and fish after the treatment. In total across seven samples, 784,282 metatranscriptome sequences were determined. Metatranscriptome approach was conducted to examine algal gene expression patters to find the effect of hydrogen peroxide on algae with molecular level. Photosynthesis and protein metabolism were the most abundant functions (SEED subsystems) expressed in cyanobacteria, making up 54.73% of transcripts. *Microcystis* sequence reads mostly followed the trend of cyanobacteria overall, although phages, specifically a r1t-like streptococcal phage, were more abundant. Throughout the experiment, both the *Microcystis* and other cyanobacterial metatranscriptomes were relatively stable, exhibiting no change in functionality. However, taxonomic representation of the cyanobacterial metatranscriptome shifted overtime with *Synechococcus* (30.9%) as most abundant followed by *Microcystis* (14.6%). One hour after the initial hydrogen peroxide application treatment, *Microcystis* decreased to 8.9% before rising to most abundant on day 1 (29.9%) and day 2 (31.9%). Between day 2 and day 3, the second application of hydrogen peroxide by BlueGreen Water Technologies occurred, which saw a decrease in *Microcystis* to 20.3% and a doubling of *Synechococcus* representation from 9.1% to 20.5%. Between our day 3 and subsequent day 7 sampling, more hydrogen peroxide was applied by BlueGreen Water Technologies and *Microcystis* representation greatly declined to 2.9%, replaced by

Synechococcus (23.1%), *Anabaena* (20.0%), and *Nostoc*, (15.9%) as most abundant. However, on our next sampling on day 14, cyanobacterial metatranscriptome representation had further changed with a peak of *Microcystis* relative abundance of 29.0%, similar to days 1 and 2, followed by *Cyanothece* (15.6%), *Synechocystis* (15.5%), and *Synechococcus* (13.5%). These data suggest that overall hydrogen peroxide treatment is effective to induce the succession of phytoplankton communities, however, in a real application of hydrogen peroxide on an algal bloom, repetitive application may be required in respond to an algal community succession.

INTRODUCTION

Harmful blooms of Cyanobacteria are an expanding concern for human and environmental health worldwide. Although various methodologies have been developed to control harmful algal blooms (HAB), hydrogen peroxide has a great potential to control HAB. Hydrogen peroxide is a strong oxidant that occurs naturally in aquatic systems, and quickly decomposes into water and gaseous oxygen (Drábkováet al., 2007a). Hydrogen peroxide releases hydroxyl radicals as it decomposes, which are strong reactive oxygen species (ROS) that can be detrimental to the growth of cyanobacteria, and are capable of significantly reducing HAB species (Barrington et al., 2011 ; Matthijs et al., 2012).

Hydrogen peroxide treatment is recognized as a selective algaecide because cyanobacteria are more sensitive to hydrogen peroxide than other eukaryotic algae such as green algae and diatoms (Drábková et al., 2007). Mechanistically, a lack of membrane bound photosystems and the incompleteness of ROS scavenging enzymes leave cyanobacteria more vulnerable to hydrogen peroxide than eukaryotic phytoplankton (Barrington et al., 2013; Barrington and Ghadouani, 2008). *Microcystis*, for example, is an order of magnitude more sensitive than multiple species of green algae and diatoms (Drábková et al., 2007).

The increment of the successful application reports of hydrogen peroxide treatments support the effectiveness of this approach, however, effectiveness could be influenced by a variety of factors. For example, the types of water body and strategy of the chemical use may strongly influence the treatment results. In our previous application, we did not observed a short algal community response. We also did not notice any fish kill and the corruption of ecosystem. Therefore, in this opportunity, we increased the concentration of hydrogen peroxide (0.018% [5.8 mM] as a final concentration) than the first application and the treratment was repeated three times: once by FGCU clues and twice by BlueGreen Water Technologies.

Our project will reveal how hydrogen peroxide can repress harmful algal growth and induce the succession of phytoplankton communities from harmful to non-harmful algal species. Our project will also monitor the fate of cyanotoxins after treatments. We will also conduct transcriptomic approach to examine algal gene expressions after hydrogen peroxide treatments. In a real application of hydrogen peroxide on an algal bloom, repetitive application may be required in respond to an algal community succession. Therefore, in this application, we also examined the application effect of repeated hydrogen peroxide dosing. Our data will help improve the State's ability to mitigate and clean up HAB. Manipulation

of the phytoplankton community from harmful algae to non-harmful algae using selective community shifts is a relatively new approach in the US. In this application, we examined the application effect of repeated hydrogen peroxide dosing.

MATERIALS AND METHODS

Field site and hydrogen peroxide treatment by Florida Gulf Coast University

The second field application of hydrogen peroxide was conducted from May 17 to June 8, 2021. We treated the same area (8 m x 50 m = 400 m^2) at Franklin Lock and Dam with 12 times more hydrogen peroxide (200.4 mg/L, 0.018%, 5.8 mM as a final concentration) than the first field experiment (Fig. 6.1). We aimed hydrogen peroxide directly contacts to blooming algal biomass. Before and after spraying, hydrogen peroxide level in surface water was monitored every 15 min in the first hour then on days 1, 2, 3, 7, and 14. The final concentration was calculated based on the 1 cm of the depth.

Coincidently, our field application period and working schedule of BlueGreen Water Technologies to treat C-43 canal overlapped each other. The second and third algaecide treatments were conducted at Franklin Lock and Dam by BlueGreen Water Technologies on May 27 and June 1, 2021, respectively (Fig. 6.2). In the second application, the company applied 65 kg of "Lake Guard Oxy" to the downstream side of Franklin Lock and Dam. Multiple local media appeared, and the demonstration was released as the collaboration effort of SFWMD and FDEP (Fig. 6.3).

Lake Guard Oxy treatment of C-43 canal and following monitoring by BlueGreen Water Technologies

BlueGreen Water Technologies, together with the South Florida Water Management District ("SFWMD") and Florida Department of Environmental Protection ("FDEP") have established a treatment regime for the environmental remediation of the Caloosahatchee River (C-43 Canal) in order to mitigate cyanobacterial blooms in specific heavily contaminated sections of the canal, using Lake Guard Oxy, hydrogen peroxide-based algaecide developed by BlueGreen Water Technologies. The product is a granular form composed of 98% (w/w) sodium percarbonate that releases hydrogen peroxide and 2% (w/w) of an inert, which is a biodegradable encapsulating agent that floats and time-releases the active ingredient on the water surface. Monitoring, inspection, and treatment application initiated on May 27 and continued daily through the Memorial Day weekend until June 10, 2021. The average dosage rate

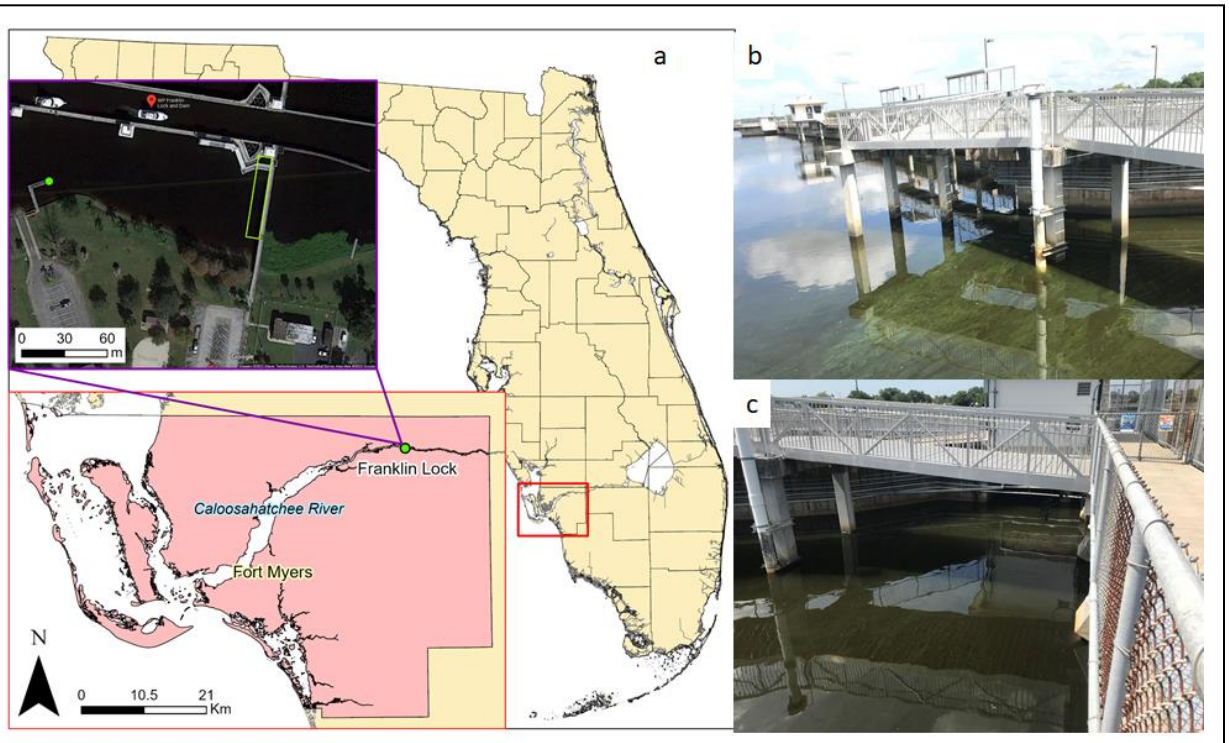

Figure 6.1. Hydrogen peroxide application at Franklin Lock and Dam in the Caloosahatchee River. (a) the treatment area (rectangle zone), a green spot indicates the downstream control site where the surface bloom is not severe. (b) before the FGCU's first treatment, (c) after the first treatment. Both were taken on June 26, 2021.

over the 15-day project was about 40 lb/acre with a range between 0.8 and 181.8 lb/acre. Due to heavy boating activity on weekends, the US Army Corps of Engineers only permit the treatment applications between 6:30-8:30 am and between 5-8 pm during the weekend. The total amount of the Lake Guard Oxy product used in this remediation project reached 10,260 lb (5.1 tons). It was used for over 112 treatments and retreatments at 56 different areas. The amount of product required for maintaining bloom free conditions in the residential canals declined substantially after the initial interventional treatments. All the information provided here was abstracted from Trainic et al. (2020).

Most of the monitoring consisted of visual inspection of the residential canals. Additional extensive monitoring was conducted in selected areas, which included the following parameters: in-situ field water measurements with a YSI ProDSS multiparameter, sampling of water temperature, pH, dissolved oxygen (DO), chlorophyll-b (Chl-b; proxy to the total biomass of green algae), phycocyanin (PC, proxy to the total biomass of cyanobacteria), and conductivity; field microscopy of samples obtained from the water surface, for detection of the variety of cyanobacterial species present in the water. Laboratory work included taxa analysis and presence of toxins (microcystins/nodularins and saxitoxins) and

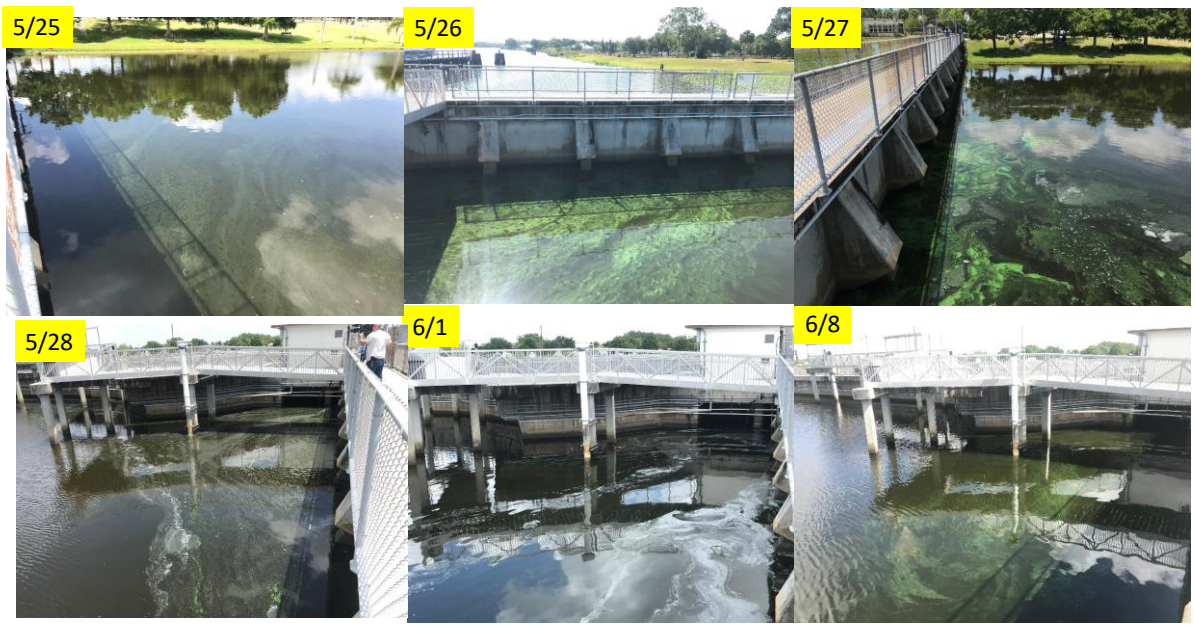

Figure 6.2. Change of the surface bloom condition during two weeks of the treatment. Day 0 (5/25) the day FGCU conducted hydrogen peroxide treatment, day 1 (5/26), day 2 (5/27) the day BlueGreen Water Technologies applied Lake Guard Oxy, day 3 (5/28), day 7 (6/1) the day BlueGreen Water Technologies applied Lake Guard Oxy, and day 14 (6/8).

conducted at GreenWater Laboratories (Palatka, FL). BlueGreen Water Technologies set four sampling sites (Spot A, 2, 3, and 4) within the southern end of the Franklin Lock and Dam and our monitoring site was marked as Spot A in their report (Trainic et al. 2020).

Water sampling

Water samples were collected by grab sampling using a kayak from 30 cm of the water depth in two new 1 L amber bottles. A part of water samples was passed through a sterilized 0.45 µm disposable syringe filters immediately upon sampling. The water samples are transferred to the laboratory in the cooler on ice (one hour of travel time). Analytical details are available in chapter 2.

Water quality analysis

Physiochemical parameters of the river surface water were measured at a depth of 30 cm with an Aqua TROLL sonde (In-Situ, CO, USA). Analytical details are available in chapter 2.

Nutrient analyses

We used Benchmark EnviroAnalytical Inc. to analyze TOC, nutrients, and Chl-a. Total organic carbon (TOC) was quantified using high temperature combustion with a Shimadzu TOC analyzer. Nutrients and Chl-a were quantified via autoanalyzer and spectrophotometer, respectively, using a NELAC-approved laboratory and methods (Benchmark EnviroAnalytical Inc., FL, USA) within 48 hours. Analytical details are available in chapter 2. Chl-a concentrations of surface water samples were determined as described previously (Ndungu et al., 2019).

Microcystin analysis

Microcystin toxin samples were handled and analyzed via USEPA method 546 and manufacturer directions using an enzyme-linked immunosorbent assay (ELISA) (Beacon Analytic Systems Inc., ME, USA). Analytical details are available in chapter 2.

Hydrogen peroxide measurements

Samples taken for hydrogen peroxide measurement were immediately filtered through 0.2 µm syringe disk filters on-site and stored at -80°C until analyzed. Hydrogen peroxide was measured using a fast response amperometric 250 µm diameter tip hydrogen peroxide microelectrode with a built-in reference electrode (HP-250, Innovative Instruments). Analytical details are available in chapter 2.

Figure 6.3. Hydrogen peroxide treatments. (a) The first treatment conducted by Blue Green Water Technologies on May 27, 2021. (b) Monitoring of hydrogen peroxide by FGCU after the BlueGreen Water Technology treatment. (c) Surface water condition after a day from the treatment. Lake Guard Oxy is still visible on the surface of water.

Total iron analysis

Total iron was determined by USEPA FerroVer Method Hach method 8008 (FerroVer® Iron Reagent Powder Pillows).

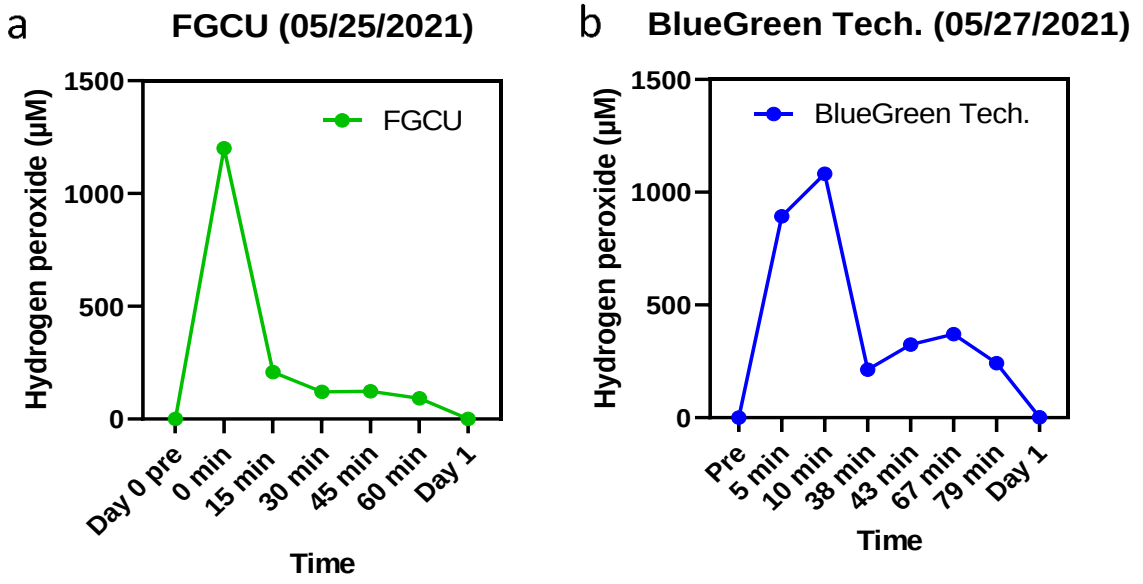

Figure 6.4. Succession of hydrogen peroxide concentrations after the surface application. (a) The first application of regular hydrogen peroxide (3% liquid) treated by FGCU and (b) the second dose application of Lake Guard Oxy (sodium carbonate peroxyhydrate Na2CO3·1.5 H2O2, 27% H2O2) treated by BlueGreen Water Technologies. The data at 0 min in the first dose was theoretical concentration based on the concentration and area.

Colored dissolved organic matter (CDOM)

Colored dissolved organic matter (CDOM) was measured in the laboratory using a Trilogy fluorometer with a CDOM/NH4 module (Model 7200-041).

Total bacterial and picocyanobacterial counts

Samples for cell enumeration were preserved with 2% formalin and stored at -80°C. Bacterial cells were enumerated on the 0.02 µm pore-size black polycarbonate filters by directly counting SYBR Green I stained cells via epifluorescence microscopy. Autofluorescent signals produced by chlorophyll pigments under a Texas Red filter were used to count picocyanobacteria. Analytical details are available in chapter 2.

Algal colony counts

Colony abundance was quantified by filtering 50 ml of water with a glass fiber filter (GF/F) filter and counting macroscopic algal colonies under a dissection microscope. Analytical details are available in chapter 1.

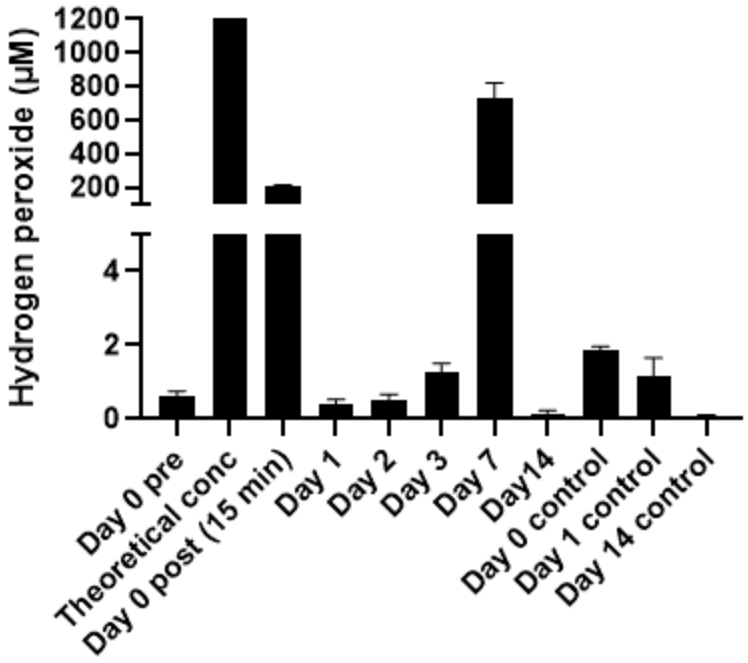

Figure 6.5. Two weeks of the monitoring of hydrogen peroxide concentrations after the first surface application. The second dose application of Lake Guard Oxy (sodium carbonate peroxyhydrate $Na_2CO_3 \cdot 1.5\ H_2O_2$, 27% H_2O_2) was conducted right after the sampling of day 2 and right before the sampling of day 7. Controls are from hydrogen peroxide treatment free areas.

High-throughput sequencing

Microbial cells were collected by filtering 200 ml of water with a 0.22 µm cellulose nitrate filter. Genomic DNA was extracted from half cut filter samples using the DNeasy PowerSoil Pro Kit (Qiagen) following the manufacturer's instructions. High-throughput amplicon sequencing targeting cyanobacteria/eukaryotic algae was conducted via amplification of 16S rRNA gene using primer pair cya359Fmod and Dcya781R (Nübel et al., 1997) using the Illumina MiSeq system (MR DNA, Shallowater, TX, USA). For analysis, sequences are joined and those less than 150 bp were removed. Sequences with ambiguous base calls were also removed. The dereplicated or unique sequences were denoised; unique sequences identified

with sequencing and/or PCR point errors and removed, followed by chimera removal, thereby providing a denoised sequence or Amplicon Single Variant (ASV). Final ASVs were taxonomically classified via representative ASVs through BLAST at NCBI.

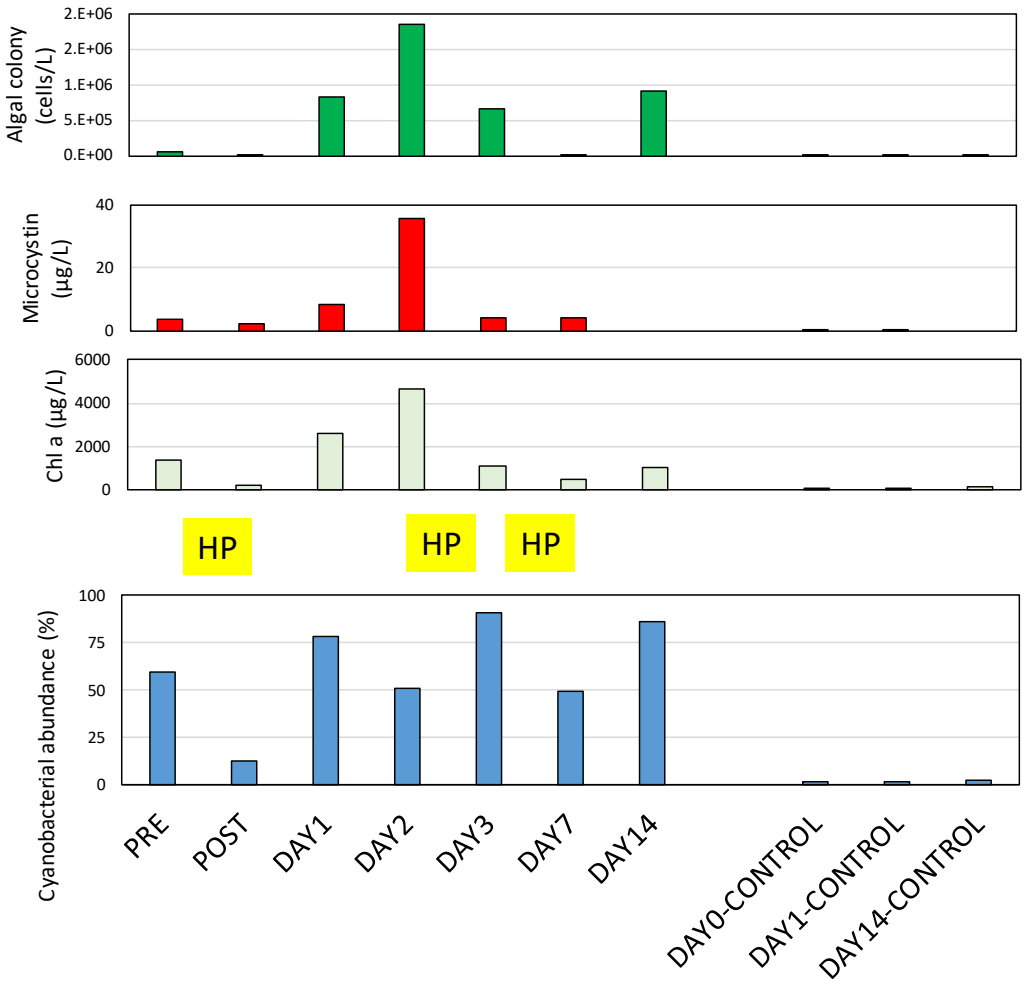

Figure 6.6. Impact of hydrogen peroxide dosing on biological parameters. The succession of algal colony counts (a), microcystin-LR concentration (b), Chl-a (c), and the relative cyanobacterial abundance determined by amplicon sequencing (d) during three surface water hydrogen peroxide applications. The data from the downstream control site (non-algal bloom site) are shown on the right. Date: PRE, POST (05/25/2021), DAY1 (05/26/2021), DAY2 (05/27/2021), DAY3 (06/28/2021), DAY7 (06/01/2021), DAY14 (06/08/2021). HP indicates the timing that hydrogen peroxide treatment was used. BlueGreen Technology applied Oxy Clean right after our sampling on day 2, and right before on day 7 (Less than 1 hour).

Metatranscriptome

RNA Samples for transcriptome sequencing were collected by filtering 200 ml of water using 0.2 µm Sterivex filters on-site, which were promptly frozen in liquid nitrogen for transport to a -80°C freezer until further analysis. Total RNA was isolated from Sterivex filters using the RNeasy PowerMicrobiome Kit (Qiagen) following manufacturer's instructions. For each filter sample, three extractions were performed. RNA was eluted in 100 µL RNase-free water and pooled. DNA contamination was removed using Baseline-ZERO™ DNase (Epicentre) following the manufacturer's instructions followed by purification using the RNA Clean & Concentrator columns (Zymo Research). DNA-free RNA samples were used for rRNA removal by using Ribo-Zero Plus rRNA Depletion Kit (Illumina). rRNA depleted samples were used for library preparation via the KAPA mRNA HyperPrep Kits (Roche) by following the manufacturer's instructions. The average library size was determined using the Agilent 2100 Bioanalyzer (Agilent Technologies) and the samples were then pooled in equimolar ratios of 0.6 nM, and sequenced paired-end for 300 cycles using the NovaSeq 6000 system (Illumina). Resulting data were processed and analyzed via the MG-RAST pipeline (Meyer et al., 2008) using SEED subsystems (Overbeek et al., 2014).

RESULTS AND DISCUSSION

Decay patterns of hydrogen peroxide

Surface water dynamics of hydrogen peroxide were compared between the first application of regular hydrogen peroxide (3% liquid) treated by FGCU (top right) and the second and third dose applications of Lake Guard Oxy (sodium carbonate peroxyhydrate $Na_2CO_3 \cdot 1.5\ H_2O_2$, 27% H_2O_2) treated by BlueGreen Water Technologies (Fig. 6.4). The major difference was found after 10 to 15 min. In the case of regular hydrogen peroxide, the concentration hydrogen peroxide greatly decreased. On the other hand, in the case of Lake Guard Oxy, the concentration of hydrogen peroxide increased after 10 min. We infer that it was caused by the gradual release of hydrogen peroxide from sodium carbonate peroxyhydrate. The concentration of hydrogen peroxide did not change between 38 to 79 min. In both cases, the concentration of hydrogen peroxide went back to the pretreatment condition on the next day (Fig. 6.4). Hydrogen peroxide concentration was monitored for two weeks (Fig. 6.5). On day 7, a large peak of hydrogen peroxide was found because the water sampling was made right after (within 30 min) the Lake Guard Oxy treatment conducted by BlueGreen Water Technologies.

Microcystin concentrations

Microcystin concentrations were monitored during three surface water hydrogen peroxide applications. Microcystin concentration followed the similar pattern with algal colony counts and Chl-a concentrations (Fig. 6.6). We did not observe the increment of microcystin concentration after treatments.

Algal response to hydrogen peroxide treatment

Algal response to hydrogen peroxide treatment was conducted through algal colony counting and Chl-a monitoring. The reduction of surface blooming biomass was observed after the first treatment. Algal colony numbers declined from 4.8×10^4 cells to 4.2×10^3 colonies / L, suggesting 91.3% of algal biomass reduction (Fig. 6.6). This result was also supported by the decline of Chl-a, microcystin concentrations, and the relative abundance of cyanobacteria. The surface hydrogen peroxide concentration dropped to the natural level on the next day (Fig. 6.5). The concentration of algal colonies, microcystin, and Chl-a increased on day 1. It seems the bloom peaked on this day (Fig. 6.2) and the first hydrogen peroxide application was only able to give partial remediation to the algal community. The second application was conducted on day 2 and the reduction of algal colony numbers, microcystin, and Chl-a concentrations were detected (Fig. 6.6). The third application, which is seen as a change between day 3 and day 7, was more effective. Lake Guard Oxy significantly reduced the number of algal colonies along with Chl-a and microcystin concentrations, suggesting the effectiveness as algaecide. This treatment drastically altered phytoplankton composition (Fig. 6.7). Despite the short time effectiveness of the hydrogen peroxide treatments, *Microcystis* was not eliminated from the phytoplankton communities.

The succession of phytoplankton community before and after the treatment

The succession of phytoplankton community before and after the treatment was monitored up to 14 days (Fig. 6.7). The studied phytoplankton community was mainly formed by cyanobacteria and the contribution of eukaryotic algae was minor (Fig. 6.8). The surface bloom was dominated by *Microcystis aeruginosa* (right end column, red color). After the treatment *Dolichospermum* declined but the relative abundance of *Microcystis* increased in all the time (Fig. 6.7). Eukaryotic algae increased after hydrogen peroxide treatments, however, they did not replace cyanobacteria (Fig. 6.8). Therefore, we found that in the Caloosahatchee River, we did not see the typically documented population shift from HAB to eukaryotic algae (Fig. 6.8).

Metatranscriptome

In total across seven samples, 784,282 metatranscriptome sequences were determined. The mean number of cyanobacterial sequence reads was 25,541 ± 13,119 (± SE). As expected, photosynthesis and

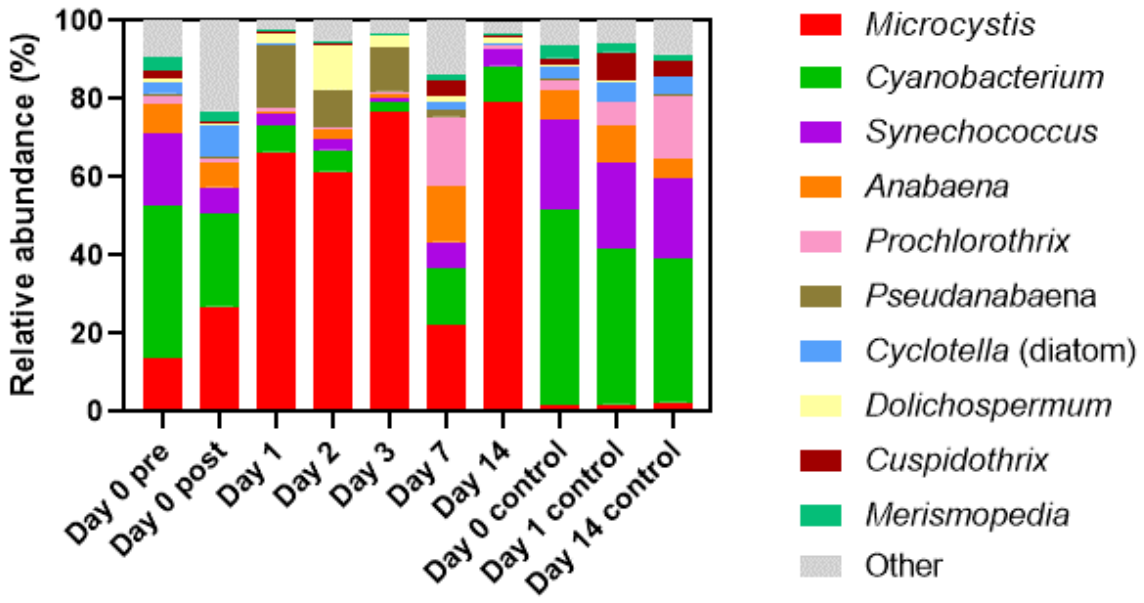

Figure 6.7. Relative abundance of top 10 phytoplankton genera during hydrogen peroxide treatment. The data from the downstream control site (non-algal bloom site) are shown on the right.

protein metabolism were the most abundant SEED subsystems for cyanobacteria, making up 54.7% of transcripts (Fig. 6.9). *Microcystis* sequence reads (3,613 ± 1,311) mostly followed the trend of cyanobacteria overall, although phages, specifically a r1t-like streptococcal phage, were more abundant. Cyanophages may ecologically play important roles in HAB (Stough et al., 2017). Throughout the experiment, both the *Microcystis* and overall cyanobacterial metatranscriptome were relatively stable, exhibiting no change in functionality. However, taxonomic representation of the cyanobacterial metatranscriptome shifted overtime with *Synechococcus* (30.9%) as most abundant followed by *Microcystis* (14.6%). One hour after the initial hydrogen peroxide application treatment, *Microcystis* decreased to 8.9% before rising to most abundant on day 1 (29.9%) and day 2 (31.9%). Between day 2 and day 3, the second application of hydrogen peroxide by BlueGreen Water Technologies occurred, which saw a decrease in *Microcystis* to 20.3% and a doubling of *Synechococcus* representation from 9.1% to 20.5%. Between our day 3 and subsequent day 7 sampling, more hydrogen peroxide was applied by BlueGreen Water Technologies and *Microcystis* representation greatly declined to 2.9%, replaced by *Synechococcus* (23.1%), *Anabaena* (20.0%), and *Nostoc*, (15.9%) as most abundant. However, on our next

sampling on day 14, cyanobacterial metatranscriptome representation had further changed with a peak of *Microcystis* relative abundance of 29.0%, similar to days 1 and 2, followed by *Cyanothece* (15.6%), *Synechocystis* (15.5%), and *Synechococcus* (13.5%). Our transcriptome data clearly demonstrated that *Microcystis* was susceptible to hydrogen peroxide treatments and their gene expression pattern was influenced by oxidative stress, however, each treatment suppressed algal bloom only short time and *Microcystis* population did not collapse by the treatment applied.

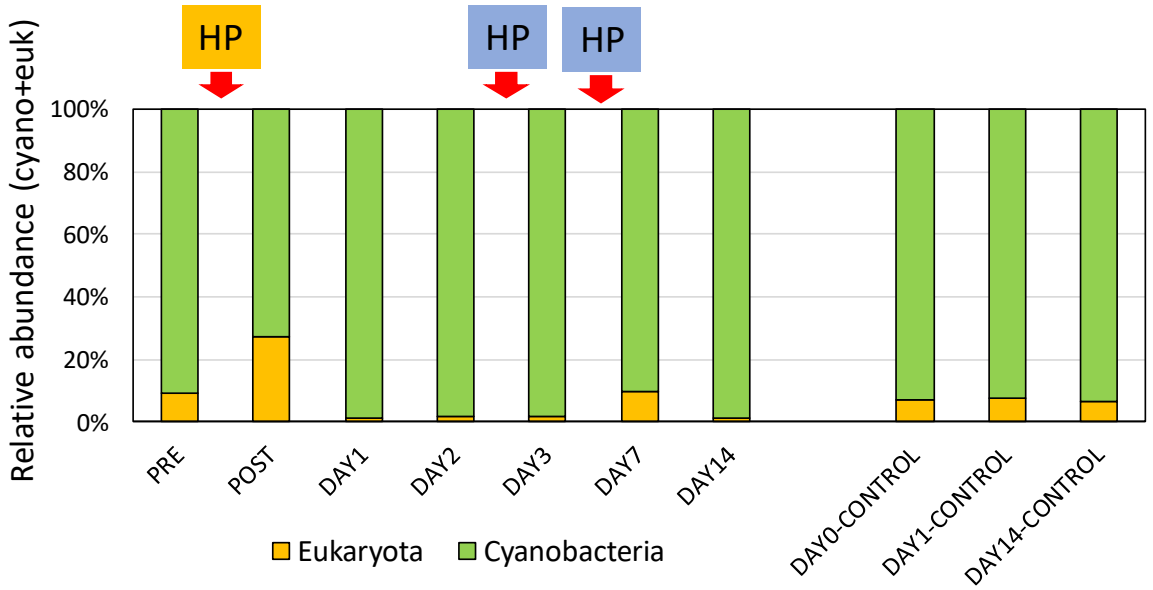

Figure 6.8. Relative abundance of eukaryotic algae and cyanobacteria during three surface water hydrogen peroxide applications. The data from the downstream control site (non-algal bloom site) are shown on the right.

Death of aquatic life

In the period of monitoring, we did not notice any fish kill and the corruption of ecosystem. It suggests that our field application was correctly managed and no further harm for aquatic life was observed. We found healthy smalltooth sawfish, alligators, West Indian manatees, and a variety of birds and fish after the treatment. We also did not find any death of aquatic vegetation after the treatment.

Hydrogen peroxide application for freshwater harmful algal blooms

Throughout our project, we confirmed that hydrogen peroxide treatment is an effective method to remediate HAB. Hydrogen peroxide induced the succession of algal communities. We observed no death of wildlife during and after our two field applications. We confirmed that Lake Guard Oxy remained much

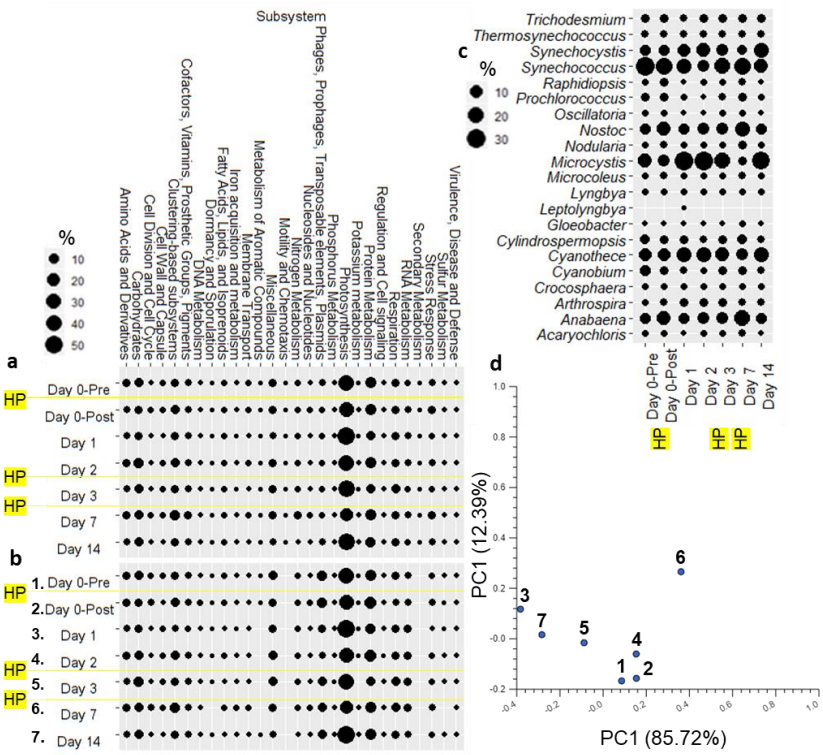

Figure 6.9. Cyano and *Microcystis* subsystems. Bubble chart of relative abundance of cyanobacterial SEED subsystems (level 1) (a) and taxonomic metatranscriptome representation (c), and bubble chart (b) and PCoA (d) of *Microcystis* SEED subsystems. PCoA of *Microcystis* transcripts in two dimensions explained 98.11% of variation of samples (n = 7).

longer time and higher concentration on the surface. The chemical was considered effective because it helped hydrogen peroxide concentration higher near the surface. Even chemical and algae directly contacted, no major cell rupture was observed (Fig. 6.2). White powder remained on the surface water for a few days, however, the hydrogen peroxide level decreased to the natural level on the next day. BlueGreen Water Technologies kept spraying the algaecide every day for a few days to completely remove the bloom until the arrival of the Florida Governor. It suggested that a one-time dosing was not sufficient to manage the surface bloom. Miss understanding of the nature of the method by citizen could be a major concern. Lake Guard Oxy treatment is not an instant cyanobacteria killing technology. Based on this field application, we concluded that a higher concentration of hydrogen peroxide is needed to immediately

remove a surface HAB, which is expected by Floridians. We will need an additional study that can determine appropriate concentration of hydrogen peroxide to effectively control HAB.

Chapter 7: Laboratory evaluation of hydrogen peroxide and L-lysine treatments

ABSTRACT

Harmful cyanobacteria blooms of the toxin-producing cyanobacterium *Microcystis* have become a growing problem for southwest Florida freshwater bodies. Recently a 2016 bloom in Lake Okeechobee and a 2018 bloom in the Caloosahatchee River both led to the declaration of a state of emergency for the state of Florida. Current long-term mitigation efforts such as nutrient reduction do not protect against the immediate risk these blooms pose for residents and wildlife. Additionally, many short-term chemical spray methods can cause harm through biomagnification of toxic substances and increased cyanotoxin release upon application. Hydrogen peroxide and L-lysine have shown promising results in selectively inhibiting the growth of *Microcystis aeruginosa* and are more ecologically friendly due to fast degradation in water or biological enhancement of non-target organisms, respectively. We further explored the use of hydrogen peroxide, L-lysine and combined treatments of both chemicals, which have never been tested before, for rapid suppression of *Microcystis.* We assessed seven *Microcystis aeruginosa* strains with varying culture conditions and morphological characteristics, four of which were locally isolated. We found axenic strains were generally more sensitive to hydrogen peroxide (13.3 mg/L) and southwest Florida strains were generally more sensitive to L-lysine (8 mg/L). All tested strains were highly sensitive to mixed treatments of Lysine (8 mg/L) and hydrogen peroxide (13.3 mg/L), with median growth inhibition of 94% on the last day of the experiment, showing this novel treatment combination can be an effective mitigation method. We also examined susceptibility of six other phytoplankton commonly found in the southwest Florida region to assess potential community succession if sensitivity to treatments were diverse.

INTRODUCTION

Microcystis is one of the most common and widely distributed toxic bloom-forming Cyanobacteria in freshwater and brackish ecosystems (Falconer et al., 1999), these organisms can produce microcystin (MC) cyanotoxins, which threaten human health and wildlife in aquatic systems where they are overly abundant (Guedes et al., 2014). In recent years Cyanobacteria harmful algal blooms (cyanoHABs) have become a growing problem for southwest Florida (SWFL) inland and coastal water bodies, where noxious blooms of *Microcystis* have become seasonally abundant and threaten residents, wildlife, and the economy (Havens et al., 2016; Kinley-Baird et al., 2021). Lake Okeechobee, the largest lake in the southern United States, and its connecting waterways the Caloosahatchee and St. Lucie River, frequently experience *Microcystis* cyanoHABs (Havens et al., 2016; Kramer et al., 2018). Recent cyanoHABs in Lake Okeechobee led to the declaration of a state of emergency for counties along the St. Lucie River in 2016, and again in 2018 in Lake Okeechobee and along both connecting waterways, where *Microcystis* was highly abundant and concern over toxin-exposure drove these decisions (Kramer et al., 2018; Kinley Baird et al., 2021). Nutrient reduction is currently considered the best strategy to reduce cyanoHAB events, however, these strategies can take many years to show positive results (Kinley-Baird et al., 2021). The characteristically shallow nature of these subtropical freshwater systems and reduced stratification periods also leaves them more vulnerable to nutrient loading, making nutrient reduction strategies more difficult (Lee et al., 2015; Havens et al., 2019). Many short-term reduction methods have focused on chemical spraying methods, such as copper sulfate and aluminum, however, these chemicals can become concentrated in the environment, and often are non-selective in targeting Cyanobacteria (Hanson and Stefan, 1984). Rapid bloom-suppression methods are desperately needed to address these regional cyanoHABs issues to reduce risk for human health and wildlife.

Hydrogen peroxide has gained popularity as an environmentally safe algaecide that targets Cyanobacteria over other eukaryotic algae due to differential coping mechanisms when dealing with oxidative stress (Matthijs et al., 2012; Weenink et al., 2015). This algaecide is considered environmentally safe due to fast degradation rates in water and ecologically friendly due to positive succession by non-toxic eukaryotic algae (Weenink et al., 2015). L-lysine, an amino acid, has been found to selectively inhibit the growth of *Microcystis* over other eukaryotic algae and Cyanobacteria (Hehmann et al., 2002). Mechanisms targeting *Microcystis* specifically are still not well understood (Takamura et al., 2004; Tian et al., 2018). Pond experiments have had success in removal of *Microcystis* cyanoHABs leading to positive succession by eukaryotic phytoplankton (Kaya and Sano et al., 2004; Takamura et al., 2004). This

Table 7.1. *Microcystis aeruginosa* strains used in this study

Strain	MC-Toxin production	Axenic	Isolation location
NIES-88	X		Lake Kawaguchi, Japan
NIES-102	X	X	Lake Kasumigaura, Japan
NIES-843	X	X	Lake Kasumigaura, Japan
NIES-4325		X	Lake Abashiri, Japan
FD4*			Caloosahatchee River, Fort Denaud, FL
HC1*	X		Hickey Creek, Alva, FL
AL2*	X		Caloosahatchee River, Alva, FL

* *Microcystis aeruginosa* strains isolated in southwest Florida

biologically derived substance is also considered environmentally friendly, as an essential amino acid for many fish and aquatic organisms it can be easily metabolized in these systems and is also freely soluble (Takamura et al., 2004).

In this study we assessed the use of L-lysine, hydrogen peroxide, and the novel use of both together for inhibiting the growth of *Microcystis.* The novel use using both L-lysine and hydrogen peroxide for treatment of *Microcystis* has never been examined to our knowledge, and we hypothesized synergetic effects of both algaecides acting on different growth inhibition mechanisms toward *Microcystis* will be highly effective in their removal. For this study we assessed both axenic and bacterial containing *Microcystis* strains, with different morphological characteristics to gain an overall understanding of treatment sensitivity. We also used three *Microcystis* strains isolated from the Caloosahatchee River to

Table 7.2. Chlorophyte and cyanobacteria taxa examined in this study

Strain	Species	Phylum	Isolation location
FGCU-122	*Dolichospermum planctonica*	Cyanophyta	Lake Okeechobee, FL
FGCU-52	*Synechococcus* sp.	Cyanophyta	Caloosahatchee River, Moore Haven, FL
FGCU-3	*Cyanobium* sp.	Cyanophyta	Hickey Creek, Alva, FL
FGCU-54	*Cyanobium* sp.	Cyanophyta	Caloosahatchee River, Fort Denaud, FL
FGCU-15	*Mychonastes homeosphaera*	Chlorophyta	Lake Okeechobee, FL
FGCU-59	*Chromochloris zofingiensis*	Chlorophyta	Lake Okeechobee, FL

better understand suitable treatment options for regional water bodies, as well as six other commonly found phytoplankton taxa isolated in local areas to gain insight into potential phytoplankton community succession patterns that may occur after treatment.

MATERIALS AND METHODS

Organisms and cultural conditions

M. aeruginosa strains used in this study are listed in Table 7.1 along with isolation location, ecological characteristics as well as axenic or non-axenic conditions. NIES-90, 88, 102, 843 and 4325 were obtained from the Microbial Culture Collection, National Institute for Environmental Studies (NIES), Tsukuba, Japan. Other phytoplankton species assessed in this study are listed in Table 7.2. *M. aeruginosa* and other phytoplankton strains isolated by Florida Gulf Coast University were identified through use of both 23S rRNA and 16S rRNA genes with Sanger sequencing.

Prior to treatment experiments, phytoplankton were cultured to exponential phase, collected, and then transferred to fresh BG-11 diluted to 1X strength. For initial examination using *M. aeruginosa* strain FD4 and *Cyanobium* sp. strain FGCU-54, 3 ml of culture was transferred to 27 ml of diluted BG-11, for the proceeding treatment experiments 1 ml of culture was transferred to 9 ml of diluted BG-11. Cultures were incubated at 25°C in a Precision Plant Growth Chamber at an irradiance of 27.8 µmol/m^2 *s and a light/dark cycle of 12/12 hours. All tests were done in triplicate, where same exponential phase batch culture was used for each strain's examination.

M. aeruginosa strain FD4 and *Cyanobium* sp. FGCU-54 were initially used to find optimal concentrations of each treatment for further testing of other *Microcystis* and phytoplankton strains. L-lysine was added to a final concentration of 3 mg/L and 8 mg/L and compared to a control. Hydrogen peroxide was added to a final concentration of 16.7 mg/L and 33.3 mg/L and compared to a control. The initial low and high-dose concentrations of L-lysine and hydrogen peroxide treatments were then combined for assessment of mixed treatments of both chemicals (low dose 3 mg/L L-lysine: 16.7 mg/L hydrogen peroxide; high dose 8 mg/L L-lysine: 33.3 mg/L hydrogen peroxide). Treatment experiments ran for an 8-day period. After initial examination it was found that high-dose treatments of single application hydrogen peroxide greatly suppressed the growth of *Cyanobium* sp. FGCU-54, leading to the decision to use low-dose concentrations (16.7 mg/L)of hydrogen peroxide for further testing. Minimal impact of high dose L-lysine concentration (8 mg/L) on *Cyanobium* sp. FGCU-54 led to the decision to move forward with

testing this concentration, and final mixed treatment concentrations of 16.7 mg/L hydrogen peroxide: 8 mg/L L-lysine. The proceeding treatment experiments examining other *M. aeruginosa* strains and phytoplankton ran for a period of 7 days, with OD measurements taken at the start of the experiment and on days 3 and 7.

Measurement of growth of phytoplankton

Phytoplankton growth was examined spectrophotometrically at an optical density (OD) of 750 nm using a HACH DR/2400 Spectrophotometer. Growth was examined over a 7-to-8-day period. Prior to absorbance measurements cultures were vortexed to disperse colonies and attain a homogeneous mixture. Three replicate readings were used for each treatment culture to average optical density readings for each recording day. Relative growth inhibition (GI) ratios were calculated using the formula:

$$(GI)= [(ODc-ODt)/ODc] \times 100$$

where ODc and ODt are the OD growth at 750 nm of the control and treated samples, respectively. ODc for control samples were averaged (n = 3) for comparison to treatment replicates, which are displayed as ± standard deviation. To confirm spectrophotometer readings correlated to phytoplankton growth Chl-a was measured during initial FD4 testing. Chl-a was measured using US EPA Method 445.0, where 0.5 ml of water sample were passed through a GF/F (0.7 µm pore size, 25 mm diameter, Whatman) with Swinnex filter holder (MiliporeSigma) to collect phytoplankton biomass, extracted with 90% acetone, and quantified using a Trilogy Laboratory Fluorometer (Turner Designs, Sane Jose, CA, USA). Linear regression of Chl-a and OD growth measurements confirmed that OD was representative of algal growth (R^2 = 0.92, p-value = 0.45) (Fig. 7.1).

RESULTS AND DISCUSSION

Initial Toxicity Trials

M. aeruginosa strain FD4 and *Cyanobium* sp. FGCU-54 were initially used to find optimal concentrations of each treatment for further testing of the susceptibility of other *M. aeruginosa* and phytoplankton strains to hydrogen peroxide, L-lysine (lysine), and mixed treatments of both chemicals. When compared to controls, all treatment application concentrations were found to have an inhibitory effect on the growth of *M. aeruginosa* strain FD4 after two days, this was not found for *Cyanobium* sp. FGCU-54 (Fig.

7.2). The inhibitory effect on *Microcystis* varied after this period by treatment application and concentration. Low dose lysine (3 mg/L) and hydrogen peroxide (16.7 mg/L) treatments showed signs of recovery on the last day of the experiment, while mixed low dose treatments of both chemicals (3 mg/L lysine: 16.7 mg/L hydrogen peroxide) showed synergetic effects in deterring recovery, with a growth inhibition ratio of 81.57 ± 0.69% (*n* = 3) on the last day (Fig. 7.2). *M. aeruginosa* strain FD4 was found to be highly sensitive to 8 mg/L lysine treatment applications, with growth inhibition reaching 90% just 48-hours after treatment application, while *Cyanobium* sp. FGCU-54 did not show signs of sensitivity to any of the lysine treatment concentrations, however, was found to be more sensitive to hydrogen peroxide high dose (33.3 mg/L) (Fig. 7.2). High dose mixed treatments of both chemicals were most effective at inhibiting the growth of *M. aeruginosa* (Fig. 7.2).

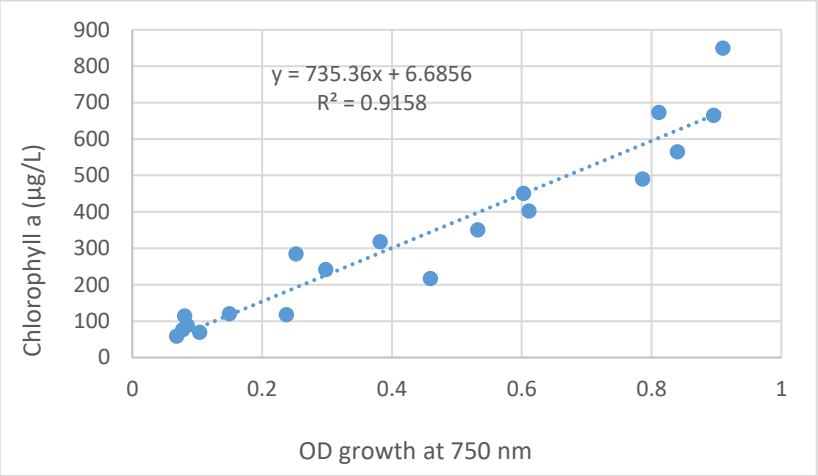

Figure 7.1. Linear regression of *Microcystis* FD4 spectrophotometer growth at OD 750 nm and Chl-a measurements during initial L-lysine toxicity trials with control, and L-lysine treatments (3 mg/L, 8 mg/L) measurements over 8-day period confirming OD measures are representative of growth (R2 = 0.92). These data were not used report.

Although *M. aeruginosa* strain FD4 was found to be less sensitive to high dose hydrogen peroxide (33.3 mg/L), previous findings have shown other *Microcystis* sensitivity at less than 1 mg/L, with other eukaryotic phytoplankton also being sensitive at ranges higher than 5 mg/L (Drabkova et al., 2007), *Cyanobium* sp. FGCU-54 sensitivity was also apparent at this concentration (Fig. 7.2). To better understand strain sensitivity and safe application for the natural environment, it was decided to proceed with the low dose hydrogen peroxide (16.7 mg/L) for single application and mixed treatments, and high dose lysine (8mg/L).

Differences in sensitivity of *M. aeruginosa* strains to hydrogen peroxide, L-lysine, and mixed treatments

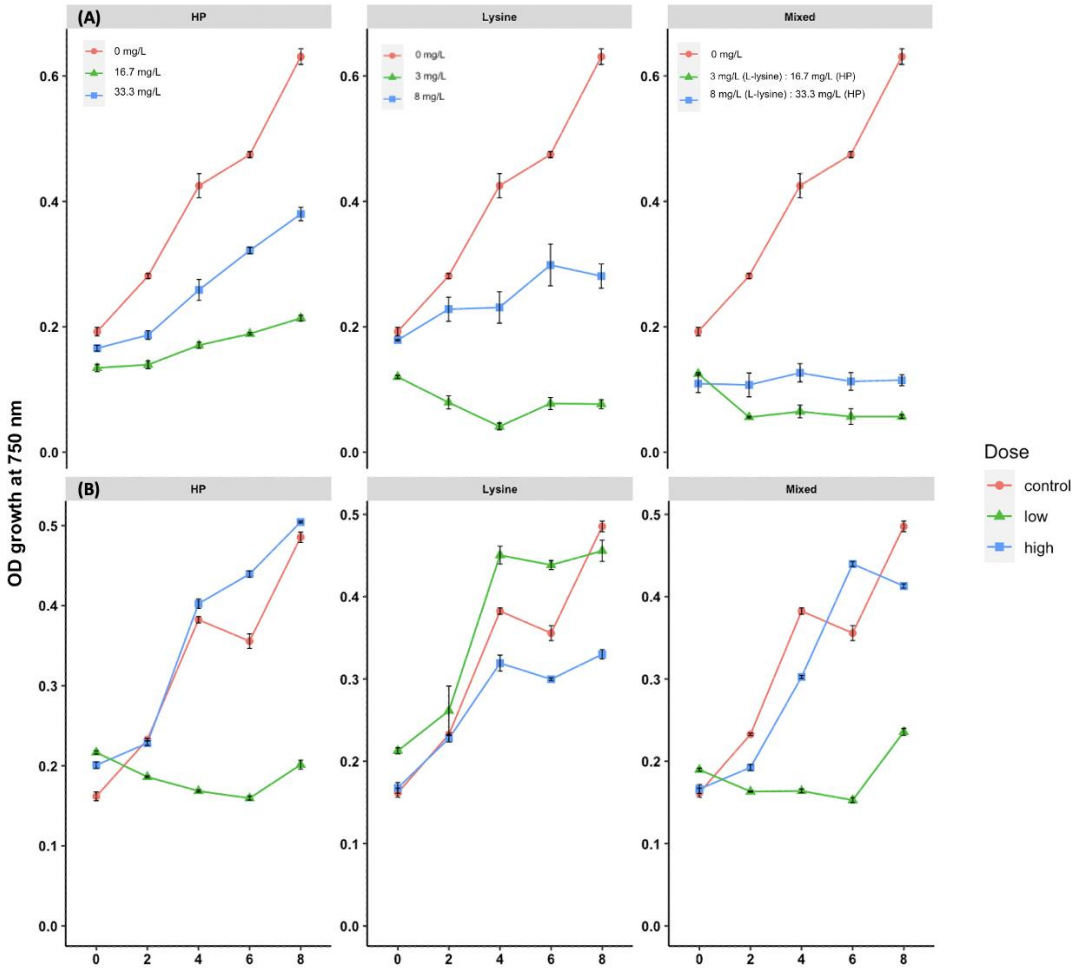

Figure 7.2. Susceptibility of *Microcystis aeruginosa* strain FD4 (A) and *Cyanobium* sp. strain FGCU-54(B) to low and high dose hydrogen peroxide (16.7 mg/L, 33.3 mg/L), L-lysine (3 mg/L, 8 mg/L), and mixed treatments (3 mg/L L-lysine: 16.7 mg/L hydrogen peroxide, 8 mg/L L-lysine: 33.3 mg/L hydrogen peroxide) compared with controls. Growth was measured at optical density (OD) 750 nm.

To examine variable susceptibility of *M. aeruginosa* strains to hydrogen peroxide, lysine, and mixed treatments three axenic strains (NIES-843, NIES-4325, and NIES-102) and three non-axenic strains (NIES-88, HC1, AL2) were assessed in a 7-day treatment experiment (Table 7.1). *Microcystis* strains were found to differ in sensitivity to treatments. Mixed treatments of 16.7 mg/L hydrogen peroxide: 8 mg/L lysine were found to be most effective at inhibiting the growth of *Microcystis*, by day 3 of the experiment growth

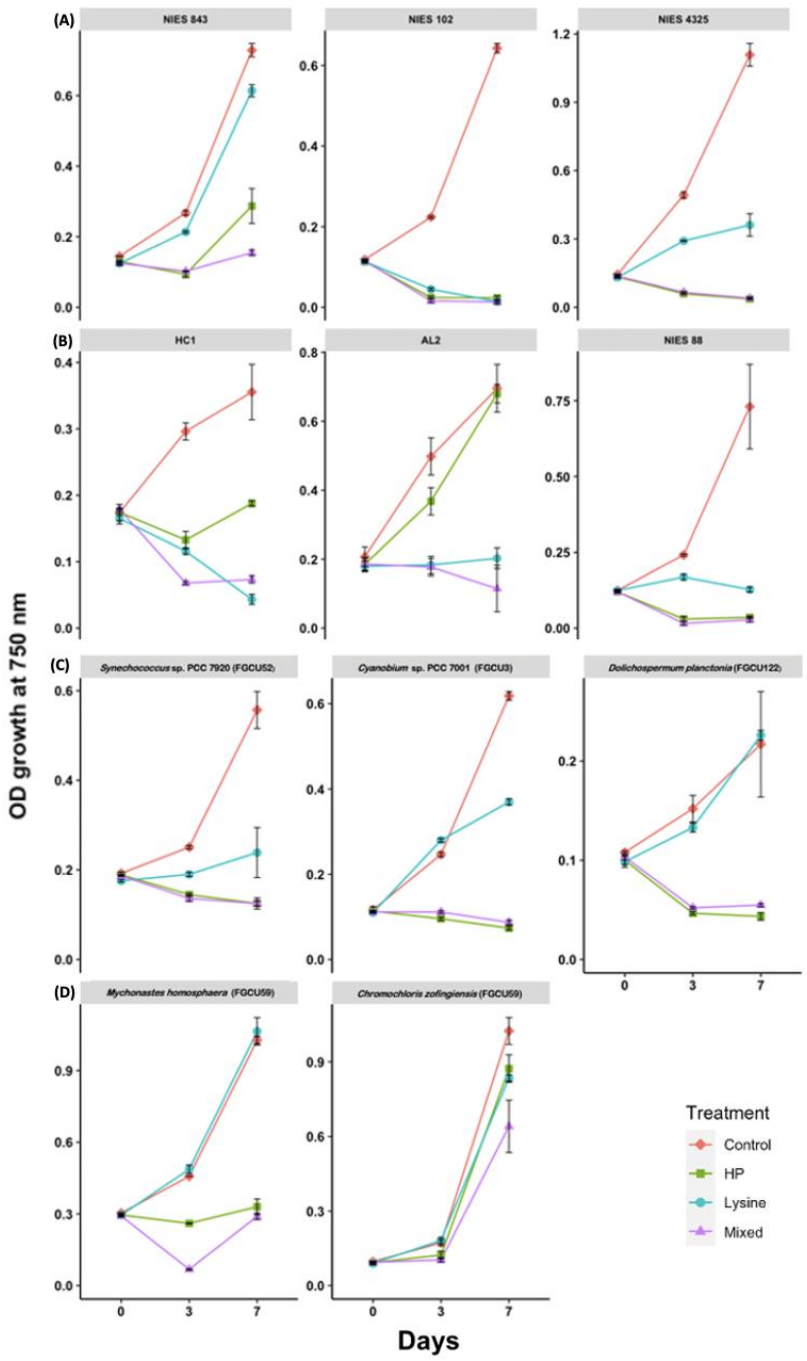

Figure 7.3. Susceptibility of axenic *Microcystis aeruginosa* strains: NIES 843, NIES 102, NIES 4325 (A), non-axenic *Microcystis* strains: HC1, AL2, NIES 88 (B), southwest Florida isolated cyanobacteria strains: *Synechococcus* sp. PCC 7920 (FGCU52), *Cyanobium* sp. 7001 (FGCU3), *Dolichospermum planctonica* (FGCU122) (C), and chlorophyte strains: *Mychonastes homosphaera* (FGCU15), *Chromochloris zofingiensis* (FGCU59) (D), to hydrogen peroxide (13.3 mg/L), lysine (8 mg/L) and mixed treatments of both chemicals (13.3 mg/L hydrogen peroxide: 8 mg/L lysine).

at OD 750 nm of all mixed treatment samples had dropped to below 50% of measured OD 750 nm growth for control samples. Mixed treatments resulted in near complete growth inhibition of tested *Microcystis* strains by day 7, with median relative growth inhibition of 94.2% (IQR: 79.4-96.3%, *n* = 18). *Microcystis* strains had variable sensitivity to hydrogen peroxide (16.7 mg/L) treatments, displaying near total growth inhibition on *Microcystis* strains NIES-102, NIES-4325 and NIES-88 which had growth inhibition ratios ranging from 95-97% on day 7 (Fig. 7.4), while *Microcystis* AL2 grew significantly under hydrogen peroxide treatments (Fig. 7.3). Hydrogen peroxide treatment application was found to have faster growth inhibitory effects on

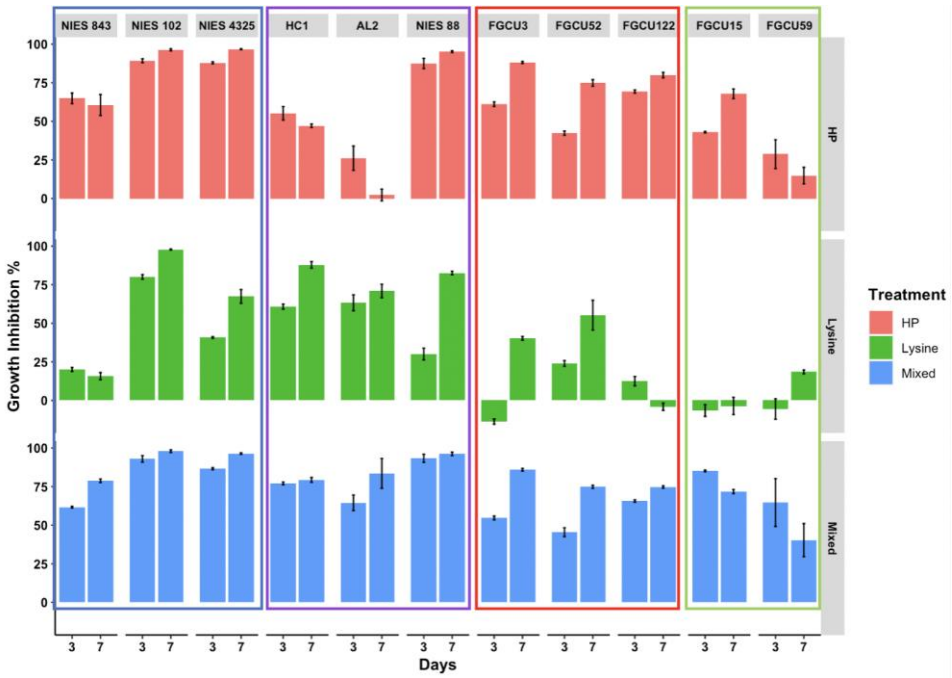

Figure 7.4. Relative growth inhibition (%) for axenic *Microcystis* strains: NIES-843, NIES-102, NIES-4325 (blue box), non-axenic *Microcystis* strains: HC1, AL2, NIES 88 (purple box), FGCU cyanobacteria strains: *Cyanobium* sp. FGCU-3, *Synechococcus* sp. FGCU-52, *Dolichospermum planctonica* FGCU-122 (red box), and FGCU chlorophyte strains: *Mychonastes homosphaera* FGCU15, *Chromochloris zofingiensis* FGCU59 (green box) under hydrogen peroxide, L-lysine and mixed treatments.

Microcystis than lysine, with median growth inhibition of 76.4% (IQR: 57.6 - 88.6%) on day 3 of the experiment compared to 47.6% for lysine (IQR: 33.2 - 64.8%). SWFL *Microcystis* strains (AL2 and HC1) were found to be more sensitive to lysine, along with NIES 102 which had growth inhibition of 98% on the last day of the experiment (Fig. 7.3).

As was found with SWFL *Microcystis* strain FD4, the other two SWFL strains (AL2 and HC1) were found to be more resilient to hydrogen peroxide treatment applications (Figs. 7.2-4). This may be the result of colony formation and bacterial presence in these non-axenic strains. *Microcystis* lacks the genes for catalase which is used for ROS scavenging under high hydrogen peroxide conditions (Hishinuma et al., 2006). Kim et al. (2019) found that *Microcystis* co-cultured with *Rhizobium* bacteria containing catalase genes had significantly higher growth rates than axenic *Microcystis* cultures under 500 μM hydrogen peroxide treatments. Kim et al. (2021) further confirmed this bacterial ROS remediation activity using additional high light stress along with hydrogen peroxide treatments, where *Microcystis* co-cultured with high catalase functioning bacterial groups were less sensitive to both ROS conditions compared to co-

cultured *Microcystis* with low catalase functioning bacterial groups, hydrogen peroxide also degraded significantly faster in high catalase bacterial communities (Kim et al., 2021). This may have been demonstrated in our results, where axenic *Microcystis* strains (NIES-843, NIES-102, NIES-4325) were more sensitive to hydrogen peroxide than non-axenic SWFL strains (FD4, HC1, AL2) (Fig. 7.4). Another difference that may have lessened SWFL strain hydrogen peroxide sensitivity compared with unicellular axenic *Microcystis,* is these strains phenotypic characteristic of colony formation, which may be an adaptive advantage for *Microcystis* species found in this subtropical region. Subtropical regions experience greater solar ultraviolet (UV) radiation, where algal cells are at enhanced risk of UV damage and photoinhibition at the water surface (Lee and Shiu, 2009). *Microcystis* colonies have been found to be better adapted to these high light conditions compared with unicells due to self-shading mechanisms and increased extracellular polysaccharide content which can facilitate the attachment of UV-B screening compounds (Reynolds, 2006; Beardall et al., 2009). Colony formation may also be favored due to environmental chemical stressors (Xiao et al., 2018), Ndungu et al. (2019) found that along the Caloosahatchee River, where SWFL *Microcystis* strains were isolated (Table 7.1), hydrogen peroxide surface water concentrations were measured as high as 5.07 μM, and during bloom and rain events surface concentrations were significantly elevated, suggesting phytoplankton from this region may be exposed to high levels of environmental oxidative stress. Colonies may be better protected from these conditions due to reduced surface area interaction of inner cells with chemical stressors (Xiao et al., 2018), as well as increased antioxidative enzyme activity, such as superoxide dismutase (SOD), which has been reported in observations of colonies and unicellular cells under oxidative stress (Wu et al., 2007). These unique conditions may promote the survival of *Microcystis* morphospecies with phenotypic plasticity toward colony formation, allowing better protection from these localized environmental stressors, as well as heterotrophic bacterial communities capable of remediating this environmental ROS stress, together making them less sensitive to hydrogen peroxide algicidal treatments (Wu et al., 2007; Kim et al., 2019). This hypothesis is supported by the dense colony morphology and high bacterial presence found in the mucilage of SWFL strain AL2 (Fig. 7.5), which was least sensitive to hydrogen peroxide of tested *Microcystis* strains (Fig. 7.3, Fig. 7.4), however bacteria were present in cultures were not assessed for this study. These findings may hold important insight for water management of *Microcystis* cyanoHABs, where increased concentrations of hydrogen peroxide may be necessary to effectively remove bloom.

As demonstrated, *Microcystis* strains, and specifically SWFL strains were highly sensitive to lysine treatment application compared with other examined phytoplankton (Fig. 7.3). Lysine toxicity

mechanisms on *Microcystis,* over other phytoplankton and cyanobacterial genera, are still not well understood (Hehmann et al., 2002). Takamura et al. (2004) suggested meso-diaminopimelic acid may be replaced by lysine in cell wall peptidoglycan, and differentiation in cyanobacterial sensitivity may be the result of carbon sources used for growth or varied metabolization rates of amino acids. Zimba et al. (2001) examined *Microcystis* sensitivity to L-arginine and L-leucine which had more and fewer nitrogen groups than L-lysine, respectively, and found these basic amino acids were not inhibitory to growth, postulating L-lysine may increase enzyme active sites causing feedback inhibition relating to Chl-a accumulation. Tian et al. (2018) found that *Microcystis* cells treated with lysine had significant increases in malondialdehyde (MDA) content likely causing lipid peroxidation cell membrane damage, and SOD oxidative stress relief mechanisms were induced. These mechanisms inhibiting *Microcystis* growth warrant further study as lysine could act as an environmentally safe *Microcystis* specific cyanoHABs mitigation method, where the essential amino acids can be easily metabolized and degraded in freshwater ecosystems (Takamura et al., 2004; Tian et al., 2018). This research using both axenic and bacterial containing strains with different morphological characteristics provides expanded insight into *Microcystis* response to lysine addition, Takamura et al. (2004) noted in her study that axenic laboratory tested *Microcystis* appeared to be less sensitive than pond experiment *Microcystis* communities, which also correlates to our findings of reduced sensitivity for tested axenic strains (Fig. 7.4). Mechanisms causing this should be further explored.

The novel use of combining both hydrogen peroxide and lysine chemicals for cyanoHABs treatment, to our knowledge has never been examined before, and was found to be highly successful at inhibiting the growth of examined *Microcystis* strains (Figs. 7.3 and 7.4). Mixed treatments resulted in near total growth inhibition of all tested *Microcystis* strains, showing no variation in toxicity based on presence of bacteria, or unicellular and colony morphological characteristics (Fig. 7.3). Past algaecide combination treatments have largely focused on combinations of chemical and coagulant algaecides; however, coagulants are not suitable for shallow lakes where resuspension is prevalent and have been noted to cause potential ecological harm through non-selective targeting of phytoplankton (Jancula and Marsalek, 2012), growth reductions of aquatic plants (Gensmer and Playle, 1999), acute toxicity to fish and benthic invertebrates (Smeltzer, 1990), and accumulation of coagulant in sediments (Reitzel et al., 2013). Given the efficacy of fast degradation rates found for both lysine and hydrogen peroxide, while also providing more selective targeting of Cyanobacteria over eukaryotic algae (Weenink et al., 2015; Takamura et al., 2004), we suggest this chemical and biological combination warrants further exploration for water management of *Microcystis* cyanoHABs where synergetic effects are achieved, similar to other

algaecidal combinations, without causing enhanced ecological harm. Although hydrogen peroxide is recognized as being a safe and effective cyanoHABs mitigation method due to fast degradation rates, and reduced sensitivity of beneficial eukaryotic plankton, low-dose application to achieve these benefits may not be sufficient to eliminate dense *Microcystis* blooms with environmental and physiological characteristics discussed previously (Weenink et al., 2015; Wang et al., 2019; Kim et al., 2021). This can lead to the need for costly reapplication of chemicals, where residents and wildlife have prolonged risk to exposure of cyanotoxins. Our results demonstrate that mixed treatments of hydrogen peroxide and lysine chemicals were highly effective at inhibiting the growth of *Microcystis* in just 3 days. However, further laboratory and field studies are needed to understand how these chemicals interact in the natural environment as well as other impacts to microbial communities.

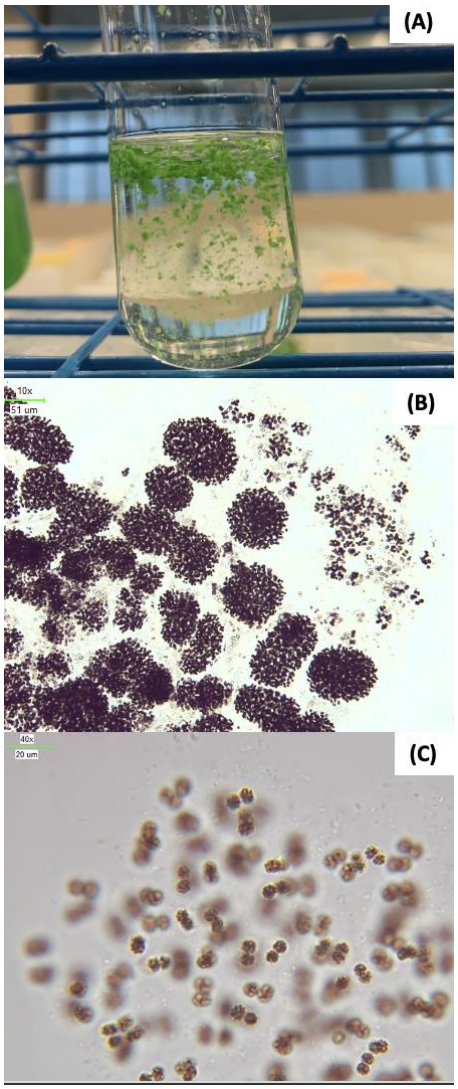

Figure 7.5. *Microcystis aeruginosa* strain AL2. (A) Surface scum (B) colony (C) Phycosphere bacteria.

Differences in sensitivity of other phytoplankton to hydrogen peroxide, L-lysine, and mixed treatments

Other Cyanobacteria and chlorophyte strains isolated from SWFL water bodies were used to assess sensitivity and potential succession that may occur if hydrogen peroxide, lysine, and mixed treatments were applied to treat local *Microcystis* cyanoHABs. Similar to *Cyanobium* sp. FGCU-54 (Fig. 7.3), the two other picocyanobacterial strains (FGCU-3 and FGCU-52) were found to be less sensitive to lysine than examined *Microcystis* strains (Fig. 7.4). These strains were found, however, to be sensitive to hydrogen peroxide, with average growth inhibition ratios on the last day of the experiment being 74.9% for *Cyanoboium* sp. FGCU-3 and 88.1% for *Synechococcus* sp. FGCU-52 (Fig. 7.4). The growth of cyanobacterium *Dolichospermum planctonica* strain FGCU-122 was also not susceptible to lysine addition (Fig. 7.4). This finding agrees with past studies showing *Anabaena,* also a member of the

Nostocales order, was not sensitive to lysine concentrations up to 10 mg/L (Hehmann et al., 2002). *Dolichospermum* was highly sensitive, however, with growth never recovering after the initial crash on day 3 (Fig. 7.3). *Dolichospermum* is another genus of toxin-producing cyanobacteria known to frequently form nuisance blooms in SWFL (Van Dam et al., 2018), and this result highlights the diverse application of hydrogen peroxide for treatment of diverse cyanoHABs (Lusty and Gobler, 2020). All forementioned cyanobacteria strains (FGCU-3, FGCU-52, FGCU-122) were found to be highly sensitive to mixed treatments, with growth inhibition ranging from 73.2-87.5% (n = 9) on the last day of the experiment (Fig. 7.4). Examined SWFL chlorophytes had variable sensitivity to hydrogen peroxide, lysine, and mixed treatments (Fig. 7.3). Both *Chromochloris zofingiensis* strain FGCU-59 and *Mychonastes homosphaera* strain FGCU15 chlorophyte strains were not sensitive to lysine (Fig. 7.4), which is supported by previous findings indicating eukaryotes are less susceptible to lysine, where the chlorophyte *Chlorella* was found to not be affected by lysine concentrations up to 1000 mg/L (Yamamoto et al., 1998), minimal growth inhibition has also been seen for the bacillariophyte *Cyclotella meneghiniana* up to concentrations of 250 mg/L (Zimba et al., 2001). *Chromochloris zofingiensis* growth was not found to be significantly inhibited by hydrogen peroxide and was the least susceptible of tested phytoplankton to mixed treatment applications (Figs. 7.3 and 7.4). *Mychonastes homosphaera,* a small picoplankton, was susceptible to these treatments, however it showed signs of recovery on the last day (Fig. 7.3).

The specificity of lysine toxicity to *Microcystis* was clearly demonstrated in this study, other tested cyanobacteria and chlorophytes were not nearly as inhibited by its application, with a median growth inhibition ratio of 18.7% (IQR: -14.1 - 39.1%, n= 15) on the last day of the experiment, compared with median inhibition ratio of 78.5% (IQR: 62.7 - 86.0%, n =18) for tested *Microcystis* strains (Fig. 7.4). These results demonstrate lysine may be a viable option for targeting *Microcystis* cyanoHABs specifically, leading potentially to positive succession by eukaryotic algae. Takamura et al. (2004) found in a pond experiment, lysine application of 50 μM was able to completely remove *Microcystis* colonies after 3 days, where the eukaryote *Euglena* then became dominant and *Microcystis* remained absent for the proceeding 11 days of the experiment. Kaya et al. (2004) had different findings in pond experiments where after application, *Microcystis* dominance was succeeded by diatoms but only lasted 7 days before *Microcystis* returned. Our laboratory results therefore are cautionary findings, and further investigation of lysine mechanisms acting on *Microcystis* growth suppression should be investigated to further improve application in field studies. Given the high nitrogen content in lysine, nutrient regimes and potential for further eutrophication should also be considered when potentially using this algaecide. For example, our concentration of 8 mg/L would

be equivalent to 1.5 mg/L as nitrogen when applied, which if continually treated could have potentially harmful effects (Takamura et al., 2004; Shao et al., 2013). To our understanding picocyanobacterial sensitivity to lysine application has never been examined before, and our finding that tested strains (FGCU54, FGCU52, FGCU3) were less sensitive than most examined *M. aeruginosa* strains is beneficial as these organisms are found to have high annual abundance in this subtropical region (Murrell and Lores, 2004), where they contribute significantly to carbon fixation and biogeochemical cycling (Jardillier et al., 2010).

Hydrogen peroxide algaecides, although highlighted for specific toxicity toward cyanobacteria, at high concentrations can be harmful toward non-target eukaryotic phytoplankton (Matthijs et al., 2012; Weenink et al., 2015). Growth inhibition toward the chlorophyte *Mychonastes homosphaera* strain FGCU-15 was observed under hydrogen peroxide (13.3 mg/L) treatments. However, the small size of this strain (1.5-4.5 μm) may be why it was found to be more sensitive than chlorophyte *Chromochloris zofingiensis.* Similar results were also found for chlorophyte sensitivity under mixed treatments; a notable discovery was that both chlorophytes and other tested SWFL cyanobacterial strains (FGCU-122, FGCU-52, FGCU-54) were overall much less sensitive to mixed treatments (median: 74.1%; IQR: 70 - 76.2%) than examined *Microcystis* strains (median: 94.2%; IQR 79.4 - 96.3%) on the last day of the experiment. These results suggest this novel combination of hydrogen peroxide and biological lysine may be a viable option for targeting *Microcystis* cyanoHABs, where potential for positive succession by eukaryotic phytoplankton may be achieved. Residence time and resulting water body reductive power on hydrogen peroxide could greatly influence degradation and therefore toxicity to phytoplankton in comparison to our laboratory culture conditions. Further examination through field studies is needed to assess safe hydrogen peroxide dosage that can should be used, along with appropriate lysine concentrations as to not oversaturate available nitrogen (Wang et al., 2016; Shao et al., 2013). With our result of *M. aeruginosa* strain FD4 as sensitive to mixed combinations of low dose hydrogen peroxide (16.7 mg/L) and lysine (3 mg/L), it suggests that lowered concentrations to achieve ecologically beneficial results may still be effective for removal of *Microcystis* cyanoHABs.

Chapter 8: Transcriptome analysis of the effect of hydrogen peroxide and L-lysine on *Microcystis aeruginosa*

ABSTRACT

Microcystis is a ubiquitous Cyanobacteria found throughout freshwater and brackish ecosystems, where increased occurrences of bloom formation and potential toxin exposure threaten human health and wildlife. In this study, we assessed two algaecidal mitigation methods for the treatment of *Microcystis.* Hydrogen peroxide and L-lysine are both highlighted as safe alternatives for environmental application due to fast degradation rates and non-lethal toxicity toward other aquatic organisms and therefore were the targets of this study. Transcriptome RNA-seq methods were used to assess the modes of action these algaecides take in inhibiting the growth of *Microcystis,* where two axenic and two non-axenic strains were used to assess biological differences between these groups that may improve mitigation efforts and understanding of these microorganisms. Expression of photosynthetic genes were found to be diversely regulated between hydrogen peroxide and L-lysine treatments, however overall abundance of these genes was also found to be downregulated. Differential antioxidant coping mechanisms were also discovered between toxic and non-toxic strains. We found that both hydrogen peroxide and L-lysine led to downregulation of microcystin-toxin genes, further highlighting their use for safe application. To our knowledge the expression of microcystin synthetase genes after exposure to L-lysine has never examined before, seeing as this a safe biological algaecide specifically targeting *Microcystis* this was another beneficial finding.

INTRODUCTION

Microcystis is one of the most common and widely distributed toxic bloom-forming Cyanobacteria in freshwater and brackish ecosystems (Falconer et al., 1999), these organisms can produce microcystin (MC) cyanotoxins, which threaten human health and wildlife in aquatic systems where they are overly abundant (Guedes et al., 2014). Due to this, mitigation of these Cyanobacteria harmful algal blooms (cyanoHABs) are a top concern for water managers. During instances where growth and potential risk of toxin-exposure cannot be maintained, fast suppressive methods should be considered (Kinley-Braird et al., 2021).

Hydrogen peroxide has gained popularity as a safe chemical algaecidal treatment due to fast degradation rates into water and selective control of Cyanobacteria through reactive oxygen species (ROS) induced oxidative stress (Matthijs et al., 2012). L-lysine is an amino acid biological algaecide that has been found to selectively target the *Microcystis* genera in lab and field application studies, where when applied in the environment it is easily soluble or metabolized (Takamura et al., 2004; Tian et al. 2019).

Transcriptomic analysis and RNA-sequencing (RNA-seq) methods have become important tools for improved understanding of the mechanisms involved in photosynthetic metabolic processes and toxin production in cyanoHAB organisms (Qian et al., 2010; Shin et al., 2015). Understanding the role gene expression and regulation play in mediating oxidative stress has important implications for chemical and biological mitigation efforts as many of these mechanisms target the photosynthetic capabilities of cyanobacterial genera by increasing oxidative stress. qPCR analysis by Tian et al. (2018) showed that L-lysine influenced two polysaccharide synthesis genes, which have a strong scavenging ability toward various ROS including superoxide (Gao et al., 2014). Another study by Qian et al. (2010) reported the down regulation of the transcription of photosynthetic genes *rbcl, psb*D1 and *psa*B under oxidative stress created by exposure to hydrogen peroxide. Improved understanding of how chemical and biological treatments affect transcriptional levels of *mcy* toxin genes is also imperative for improved mitigation efforts that do not cause their upregulation. The two previous studies mentioned have employed qPCR methods, which can only detect a few target gene. To overcome this methodological limitation, here we propose the use of RNA-seq methods, which can allow for detection of both known and novel transcripts, leaving more room for discovery through unbiased assumptions of target genes that will be affected (Fassbinder-Orth, 2014).

MATERIALS AND METHODS

Organisms and cultural conditions

Axenic *M. aeruginosa* strains used in this study were obtained from the Microbial Culture Collection of National Institute for Environmental Studies (MCC-NIES). NIES-102 and NIES-843 are both toxin-producing strains. NIES-4325 and NIES-4285 are non-toxin producing strains. Cyanobacteria were first cultivated in 50 ml test tubes containing 27 ml of BG11 medium diluted to 1X strength. Medium was inoculated with 3 ml of seed culture and allowed to grow until obtaining optical density (OD) of 0.3 at 750 nm, measured spectrophotometrically (HACH DR/2400 Spectrophotometer). Cultures (n = 12) were incubated at 25°C in a Precision Plant Growth Chamber at an irradiance of 27.8 μmol/m2*sec and a light/dark cycle of 12/12 hours. Cultures were then combined to make a batch culture (360 mL), vortexed to create homogeneous mixture, and then 30 ml of batch culture was re-suspended in 170 ml of fresh diluted BG11 medium using a 250 ml flask. For each strain of *M. aeruginosa*, flasks were prepared in triplicate for hydrogen peroxide and L-lysine treatments, and control groups (n = 12). *M. aeruginosa* was cultured to exponential phase to test effects of each treatment: hydrogen peroxide, (final concentration of 33.3 mg/L) L-lysine (a final concentration of 8 mg/L) for their respective treatment groups.

Measurement of photosynthetic activity

Photosynthetic efficiency was measured in terms of quantum yield (QY) using an AquaPen (AquaPen-C AP 110-C; Photon System Instruments, The Czech Republic) to monitor treatment effects on photosystem II (PSII) QY. All measurements were dark-adapted for 15 min prior to reading, where dark-adapted Aquapen QY values are equivalent Fv/Fm. Aliquotes (2 ml) were taken prior to treatment for baseline measurements of all samples. A 50% reduction in QY value of treatment cultures, indicating high stress, was chosen for the termination of treatment experiments. Measurement periods were decided on from previous *M. aeruginosa* treatment experiments of both chemicals. Hydrogen peroxide and paired controls were measured every two hours, L-lysine and paired controls were measured twice daily based on decreasing QY values of treated *Microcystis* cells until they reached <50% of starting QY values.

Total cell counting

For total cell counting, after each treatment experiment flasks were shaken to attain a homogenous mixture from which 1.5 ml was taken and fixed with glutaraldehyde. For counting later that day, 400 μl was filtered onto 0.2 μm pore-size black polycarbonate filters (Millipore, MA, USA) and transferred to a slide glass for quantification using epifluorescence microscope (Olympus BX51) under 400Xmagnification.

For each slide, enumeration was done using 15 random subsample fields from a grid system to attain cells/ml.

Chlorophyll-a

To measure chlorophyll-*a* (Chl-a) concentrations, after treatment experiments 5 mL of each sample was filtered using GF/F filter (0.7 μm pore size, 25 mm diameter, Whatman), extracted with 90% acetone and quantified using Trilogy Laboratory Fluorometer (Turner Designs, San Jose, CA, USA).

RNA filtering and analysis

At the termination of treatment experiments, samples were rapidly prepared for RNA filtering. Samples were filtered using 0.22 μm Sterivex filters (Millipore, MA, USA), depending on available biomass, 50-150 ml of each sample was filtered and then stored at -80°C until analysis.

Total RNA was isolated from Sterivex filters using the RNeasy PowerMicrobiome Kit (Qiagen) following manufacturer's instructions. RNA was eluted in 100 μl of RNase-free water. Control and Treatment triplicate samples were pooled and used to remove the DNA contamination using Baseline-ZERO Dnase (Epicentre), followed by purification using the RNA Clean & Concentrator-^{5} columns (Zymo Research). The total RNA concentration was determined using Quibit RNA assay Kit (Life Technologies), where then 200-800 ng of RNA sample was used for rRNA removal by using Ribo-Zero Plus rRNA depletion Kit (Illumina). The rRNA depleted samples were then used

Table. 8.1. Aquapen photosynthetic efficiency quantum yield (QY) values measured after application of hydrogen peroxide and L-lysine treatment application.

Treatment		Control		Hydrogen Peroxide	
Strain	Hour	QY	±SD	QY	±SD
NIES-843	0	0.40	0.05	0.42	0.04
	1	0.38	0.01	0.28	0.07
	2	0.39	0.01	0.03	0.05
NIES-102					
	0	0.49	0.13	0.50	0.11
	1	0.46	0.13	0.52	0.02
	2	0.49	0.13	0.14	0.04
NIES-4285					
	0	0.43	0.05	0.41	0.01
	1	0.45	0.07	0.38	0.03
	2	0.47	0.03	0.27	0.05
	3	0.45	0.08	0.03	0.05
NIES-4325	0	0.33	0.03	0.36	0.03
	1	0.27	0.01	0.40	0.03
	2	0.26	0.06	0.15	0.03
		Control		L-lysine	
	Hour	QY	±SD	QY	±SD
NIES-843	0	0.39	0.00	0.36	0.05
	8	0.37	0.03	0.37	0.06
	24	0.40	0.01	0.36	0.09
	28	0.37	0.02	0.33	0.06
	32	0.38	0.01	0.36	0.06
	48	0.41	0.02	0.35	0.09
	52	0.39	0.03	0.34	0.07
	56	0.41	0.02	0.31	0.11
	70	0.40	0.01	0.29	0.08
	76	0.34	0.02	0.19	0.07
NIES-102	0	0.52	0.10	0.48	0.10
	9	0.53	0.04	0.47	0.01
	24	0.53	0.09	0.21	0.08
	27	0.53	0.15	0.18	0.05
NIES-4285	0	0.42	0.03	0.50	0.06
	8	0.49	0.02	0.53	0.05
	24	0.47	0.01	0.34	0.16
	28	0.50	0.02	0.13	0.10
NIES-4325	0	0.35	0.03	0.37	0.02
	8	0.27	0.03	0.31	0.04
	24	0.27	0.02	0.45	0.01
	28	0.30	0.02	0.37	0.05
	33	0.31	0.04	0.14	0.06

for library preparation using the KAPA mRNA HyperPrep Kits (Roche) by following manufacturer's instructions. The final concentrations of all libraries were then measure using the Qubit dsDNA HS Assay Kit (Life Technologies), and the average library size was determined using the Agilent 2100 Bioanalyzer (Agilent Technologies). The libraries were then pooled in equimolar ratios of 0.6 nM, and sequenced paired end for 300 cycles using the NovaSeq 6000 system (Illumina). Paired end reads for replicates treatment conditions were pooled together for RNA-seq and mapped to reference NIES genomes (NIES-843, NIES-102, NIES-4325, NIES-4285) using TopHat v.2.10, and assembled using StringTie v.2.15 (Trapnell et al., 2009). Differential expression between the treatment and reference condition was computed using Cuffdiff v2.2.1 packages for comparisons among samples, comparing fragments per Kilobase of exon per Million fragments mapped (FPKM) (Trapnell et al., 2009). Two logarithmic fold changes (Log2FC) $\geq$ 2 and a p-value $\leq$ 0.05 were set for criteria identifying significant changes in gene expression levels.

Table 8.2. Chlorophyll-a and total cell count measurements taken at termination of treatment experiment prior to filtering for RNA-seq analysis.

Measurement	Treatment		NIES-843	NIES-8432	NIES-4285	NIES-4325
Chl-a (µg/L)	Control		111.277	104.310	162.900	82.653
		±SD	23.113	10.613	21.618	22.460
	Hydrogen peroxide		89.080	89.950	85.213	88.913
		±SD	8.154	23.798	24.467	22.460
TCC (cells/ml)	Control		9E+05	2E+05	4E+05	3E+05
		±SD	4E+04	1E+05	3E+04	6E+04
	Hydrogen peroxide		9E+05	3E+05	4E+05	2E+05
		±SD	6E+04	2E+04	3E+04	1E+04
Chl-a (µg/L)	Control		220.260	108.557	182.047	153.307
		±SD	20.496	23.157	28.476	11.821
	Lysine		101.367	118.003	107.420	108.727
		±SD	20.433	4.714	86.263	45.568
TCC (cells/ml)	Control		1E+06	4E+05	5E+05	3E+05
		±SD	5E+04	3E+04	1E+04	1E+04
	L-lysine		1E+06	4E+05	4E+05	3E+05
		±SD	7E+04	3E+04	3E+05	2E+04

RESULTS AND DISCUSSION

The growth of *Microcystis*

Hydrogen peroxide and L-lysine effects on *Microcystis* photosynthetic efficiency (PSII) were measured using Aquapen QY values which are equivalent to Fv/Fm (Table 8.1). When QY values of treated *Microcystis* cultures reached below <50% of starting value the experiment was terminated for RNA-seq filtering. Hydrogen peroxide algaecidal mechanisms acted quickly on measured PSII photosynthetic efficiency of *Microcystis* with replicates

reaching below <50% starting values in 2-3 hours (Table 8.1). Chl-a was already found to be slightly lower at this period of the experiment for some *Microcystis* (NIES-843, NIES-102, NIES-4285), however, severe

Table 8.3. Analysis of *Microcystis aeruginosa* genes encoding antioxidant enzymes that were differently expressed from controls under hydrogen peroxide (HP) and L-lysine treatment application after reaching Fv/Fm (QY) values <50% from starting values. Toxic NIES-843 and NIES-102 were found to have similar antioxidant genes, and Non-toxic NIES-4325 and NIES-4285 were found to have more similar genes and are grouped together for comparison.

	NIES-4325			**NIES-4285**		
Gene	HP Log_2 Fold Change	Lysine Log_2 Fold Change	Locus Tag	HP Log_2 Fold Change	Lysine Log_2 Fold Change	Locus Tag
sodB1	0.52	-1.42	MiAbW_00184	-2.7	-2.8	MiAbB_01772
sodB2	-3.07	-0.41	MiAbW_01740	0.4	-2.0	MiAbB_04878
hPrx5	4.36	5.01	MiAbW_02916	5.8	6.3	MiAbB_01146
bcp2	2.02	0.33	MiAbW_02054	0.3	-0.6	MiAbB_00487
bcp3	0.08	0.41	MiAbW_00142	-0.3	-1.4	MiAbB_01655
bcp4	0.90	-0.22	MiAbW_02183	0.5	-2.3	MiAbB_04480
prxU	2.56	4.42	MiAbW_01346	1.3	2.0	MiAbB_04122
aphC	-3.88	-2.63	MiAbW_01868	-2.5	-2.9	MiAbB_02924
trxA	-1.60	3.89	MiAbW_00038	0.3	2.8	MiAbB_00022
trxA	-0.16	-2.11	MiAbW_00095	-1.2	-2.3	MiAbB_01181
trxA	1.21	0.53	MiAbW_01268	0.7	0.3	MiAbB_01291
trxB	4.53	3.11	MiAbW_02330	3.6	1.5	MiAbB_00153
	NIES-102			**NIES-843**		
sodB1	-0.10	-0.65	myaer102_26600	0.4	0.2	MAE_53390
sodB2	0.52	0.97	myaer102_50430	18.9	20.0	MAE_16920
prx5	3.66	4.75	myaer102_34790	4.8	7.5	MAE_62780
prx BCP-A	-0.88	-0.71	myaer102_18960	-5.5	-1.7	MAE_44920
prx BCP-A	-0.16	-0.91	myaer102_33040	0.2	-2.0	MAE_60930
prx BCP-B	-0.46	1.90	myaer102_49060	-1.3	3.2	MAE_15330
prx 2-Cys	1.18	0.80	myaer102_10960	2.2	4.0	MAE_35830
prx 1-Cys	-0.53	-0.34	myaer102_11490	-1.7	-1.7	MAE_36510
prx1	-0.57	-0.55	myaer102_31920	-0.7	0.0	MAE_59730
trxA	-0.42	-0.54	myaer102_3780	-1.2	-1.1	MAE_02790
trxA	-0.49	-0.50	myaer102_19780	-1.3	1.2	MAE_06830
trxA	-0.54	0.85	myaer102_19780	0.7	3.6	MAE_46030
trxB	2.81	1.59	myaer102_25580	4.1	5.0	MAE_52800

cell bleaching total cell counts did not reflect major loss of viable cells (Table 8.2). L-lysine PSII inhibition on *Microcystis* was slower and response varied by culture (Table 8.1). NIES-102, NIES-4325, and NIES-4285 showed PSII inhibition 27-33 hours after treatment application, while NIES-843 was found to be much

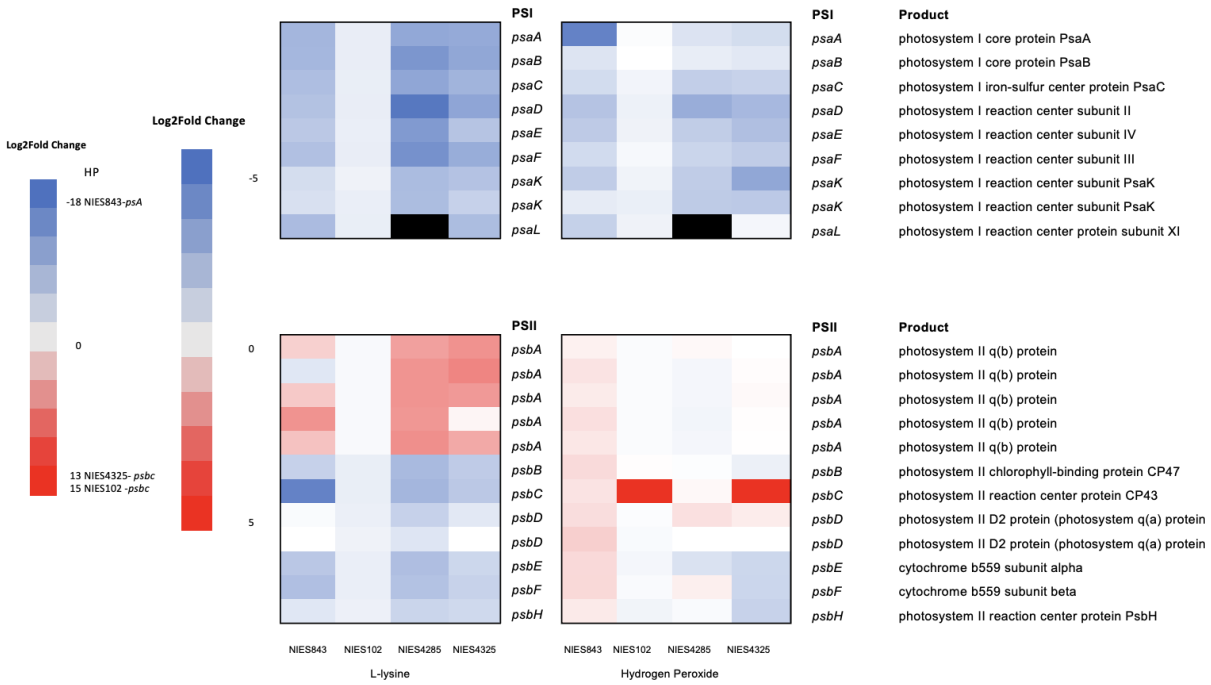

Figure 8.1. Heatmap of differential gene expression for L-lysine (left) and hydrogen peroxide (right) treated *Microcystis* photosynthesis genes when compared with controls. Blue represents a decrease in transcriptional abundance, red mean increases in abundance, and white represents no change when compared with controls. Log2 fold change scale bar for photosynthetic genes is next to heatmap, a conditional scale bar was made for hydrogen peroxide treated NIES-843 (*psbA)*, NIES-4325 and NIES-102 (*psbC)* which had significant expression changes relative to other genes.

more resilient, taking 76 hours for photosynthetic efficiency to drop below <50% (Table 8.1). Again Chl-a was found to be slightly lower in L-lysine treated *Microcystis* at the point of terminating the experiment for RNA filtering, however, this reduction was not reflected in total cell counts (Table 8.2).

Oxidative stress response

Oxidative stress caused by ROS, such as hydrogen peroxide, is mediated by antioxidant enzymes such as catalases, peroxidases and peroxiredoxins (Kim et al., 2021). Examined *Microcystis* transcriptomes reveal these strains did not contain catalase enzymes, a commonly used antioxidant enzyme, which is in agreeance with past genome sequencing of *Microcystis* species (Sandrini et al., 2007; Harke and Gobler,

2013; Schuurmans et al., 2018). Non-toxic *Microcystis* strains (NIES-4325, NIES-4285) were found to express similar antioxidant genes under oxidative stress (Table 3.3), while toxic strains (NIES-102, NIES-843) were found also to be behave more similarly (Table 8.3). *Microcystis* have commonly been found to upregulate peroxiredoxin (*prx*) genes after exposure to hydrogen peroxide, reducing hydrogen peroxide to water, and diverse expression characteristics were found for this gene in our experimental hydrogen peroxide exposure (Table 8.3). NIES-843 was found to upregulate the *prx-2-cys* peroxiredoxin encoding gene (2.18-Log2FC), and less significantly in NIES-102 (1.18-Log2FC), which is agreeance with the

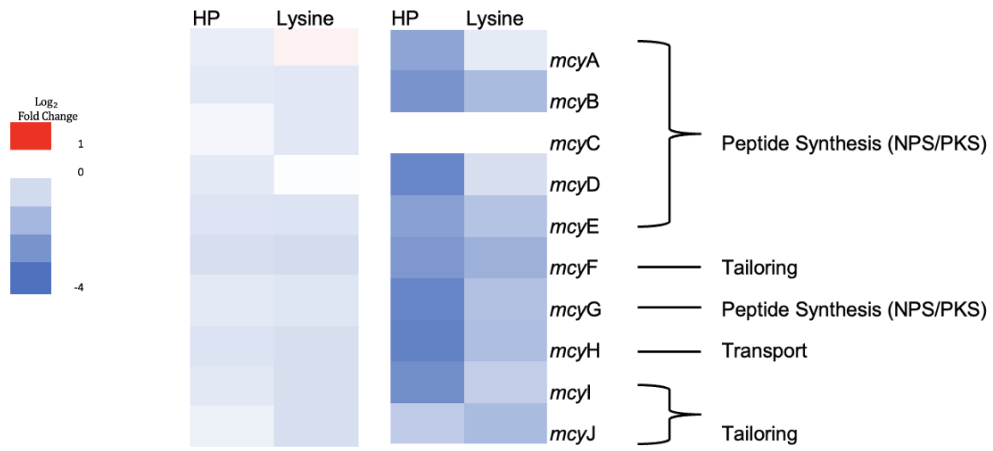

Figure 8.2. Heatmap of microcystin synthetase gene expression for toxic *Microcystis aeruginosa* strains NIES-102 (left) and NIES-843 (right) compared with controls after exposure to hydrogen peroxide (HP) and L-lysine chemicals. Blue represents a decrease in in transcriptional abundance, red represents an increase in transcriptional abundance, and white represents no change relative to controls.

upregulation response of this gene in past studies of *Microcystis* PCC 7806 after exposure to hydrogen peroxide (Schuurmans et al., 2018; Sandrini et al., 2020). Non-toxic *Microcystis* (NIES-4325 and NIES-4285) were found to upregulate the selenocysteine-containing peroxiredoxin gene (*prxU*), NIES-4325 had significantly higher transcriptional abundance of this gene (2.5-Log2FC) as well as the putative peroxiredoxin gene *bcp2* (2.1-Log2FC). Thioredoxin (*trx*) is used to regenerate the catalytic activity of peroxiredoxins by acting as an electron donor, where past examinations of *Microcystis* exposed to hydrogen peroxide resulted in congruent transcriptional increases of this gene along with *trxA* (Schuurmans et al., 2018; Sandrini et al., 2020). The thioredoxin-disulfate reductase gene (*trxB*) functions to reduce *trxA* when it becomes oxidized during catalytic activity with peroxiredoxins, such as reducing

Table 8.4. Transport genes that were significantly upregulated relative to controls under hydrogen peroxide treatments.

Transport	Strain	Symbol	Log2 Fold Change	Function	Locus tag
Nitrogen					
	NIES-843	*ntrB*	2.06	nitrate ABC transporter permease	MAE_20000
	NIES-4325	*ntrB*	3.08	nitrate ABC transporter permease	MiAbB_03130
	NIES-4325	*nrtS*	3.39	nitrate/nitrite transporter	MiAbW_02817
	NIES-102		6.66	ammonium transporter	myaer102_14780,
Sulfate					
	NIES-4325	*sbpA_2*	5.07	sulfate ABC transporter substrate-binding protein	MiAbB_03202,
	NIES-4325	*tauA*	2.87	aliphatic sulfonate ABC transporter substrate-binding protein	MiAbB_04598
Phosphate					
	NIES-4325	*pstS_4*	3.19	PstS family phosphate ABC transporter substrate-binding protein	MiAbB_03201,
	NIES-4325	*kdpA*	2.72	potassium-transporting ATPase subunit A	MiAbB_02469
	NIES-4325	*arsA_1*	2.98	TRC40/GET3/ArsA family transport-energizing ATPase	MiAbB_01701
Amino Acids					
	NIES-843		4.65	amino acid ABC transporter ATP-binding protein (L-amino acid)	MAE_36170
Metals					
	NIES-843		2.99	metal ABC transporter permease (Zinc transporter)	MAE_52810
	NIES-4325	*corA*	2.83	magnesium/cobalt transporter CorA	MiAbW_01115
	NIES-4325		5.77	cadmium resistance transporter	MiAbB_03203
Other					
	NIES-843		12.82	ABC transporter permease subunit (Gliding motility associated transporter)	MAE_20480,
	NIES-843		2.72	molybdate ABC transporter permease subunit	MAE_55530
	NIES-4325	*mdtA*	4.26	efflux RND transporter periplasmic adaptor subunit (multidrug resistance)	MiAbW_00143,
	NIES-4325		3.02	folate/biopterin family MFS transporter	MiAbW_03423,
	NIES-4325	*cmpB*	3.59	ABC transporter permease	MiAbB_04726
	NIES-102		15.28	ABC transporter permease subunit	myaer102_53590,
	NIES-102		10.93	ABC transporter ATP-binding protein	myaer102_53600
	NIES-102		2.04	ABC transporter ATP-binding protein	myaer102_26050
	NIES-4325		3.29	ABC transporter substrate-binding protein	MiAbB_04727

ROS stress, and was found in our experiment to be significantly upregulated in all *Microcystis* exposed to hydrogen peroxide (Log2FC $\geq$2) (Table 8.3) (Zeller and Klug, 2006). The transcript abundance of the gene glutathione peroxidase (*gpx*) was also found to be significantly higher in hydrogen peroxide treated

Table 8.5. Transport genes that were significantly upregulated relative to controls under L-lysine treatments peroxide treatments.

Transport Nitrogen	Strain	Symbol	Log2 Fold Change	Function	Locus tag
	NIES-4285	ntrB	6.45	nitrate ABC transporter permease	MiAbB_03130
Sulfate					
	NIES-843	cysT	5.35	sulfate ABC transporter permease subunit CysT	MAE_31530
	NIES-4325	cysT	3.65	sulfate ABC transporter permease subunit CysT	MiAbW_00647
	NIES-4325	cysT	3.82	sulfate ABC transporter permease subunit CysT	MiAbB_00673
	NIES-4325		5.30	sulfate ABC transporter substrate-binding protein	MiAbW_00645
	NIES-4325	sbpA_2	2.68	sulfate ABC transporter substrate-binding protein	MiAbW_02771
	NIES-4285		5.81	sulfate ABC transporter substrate-binding protein	MiAbB_00671
	NIES-4285	sbpA_1	5.29	sulfate ABC transporter substrate-binding protein	MiAbB_03202
	NIES-4285	sbpA_3	3.31	sulfate ABC transporter substrate-binding protein	MiAbB_03783
	NIES-4285	tauA	3.86	aliphatic sulfonate ABC transporter substrate-binding protein	MiAbB_04598
	NIES-4285		2.69	sulfate ABC transporter substrate-binding protein	myaer102_06970
	NIES-4325	cysA	3.14	sulfate/molybdate ABC transporter ATP-binding protein	MiAbW_01444
Phosphate					
	NIES-4325	pstS	3.45	PstS family phosphate ABC transporter substrate-binding protein	MiAbW_03155,
Amino Acids					
	NIES-4325		3.81	amino acid ABC transporter substrate-binding protein	MiAbW_01314
	NIES-4285		4.36	ABC transporter permease	MiAbB_04067
	NIES-102		3.28	ABC transporter permease subunit (amino acid)	myaer102_07390
	NIES-4325	glnM	3.27	ABC transporter permease subunit (putative glutamine)	MiAbW_03521
	NIES-4285	yecS	3.51	ABC transporter permease subunit (L-cystine)	MiAbB_00301
Cations					
	NIES-4325	znuA	2.45	zinc ABC transporter substrate-binding protein	MiAbW_02062
	NIES-4285	corA	3.54	magnesium/cobalt transporter CorA	MiAbB_04049
	NIES-4285		3.20	zinc ABC transporter substrate-binding protein	MiAbB_01111
	NIES-4285		4.00	cadmium resistance transporter	MiAbB_01914
	NIES-4285		6.06	cadmium resistance transporter	MiAbB_03203
	NIES-4325	modB	2.46	molybdate ABC transporter permease subunit	MiAbW_01337
	NIES-4285	modB	2.84	molybdate ABC transporter permease subunit	MiAbB_02108
	NIES-4285	modA	2.68	molybdate ABC transporter substrate-binding protein	MiAbB_02107
	NIES-843		4.52	efflux RND transporter permease subunit (cation or drug efflux)	MAE_07150
	NIES-4325	fieF	2.39	cation transporter (ferrous-iron efflux pump)	MiAbW_01148
Bicarbonate					
	NIES-4285	cmpB	3.84	ABC transporter permease (bicarbonate)	MiAbB_04726
	NIES-4325	cmpA	2.50	ABC transporter substrate-binding protein	MiAbW_00669
	NIES-4285	cmpC	5.07	ABC transporter substrate-binding protein	MiAbB_03131
Other					
	NIES-102		16.01	ABC transporter ATP-binding protein	myaer102_26050
	NIES-4285		2.41	ABC transporter ATP-binding protein	myaer102_53610
	NIES-843		4.13	ABC transporter substrate-binding protein	MAE_53310
	NIES-843		4.63	ABC transporter permease	MAE_53300
	NIES-843		3.72	AI-2E family transporter	MAE_26360
	NIES-4285		3.51	ABC transporter substrate-binding protein	MiAbB_04727
	NIES-843		4.26	phosphoribosylglycinamide formyltransferase	MAE_62490

Microcystis relative to controls ($p \leq 0.05$, Log2FC ≥ 3) (Table 8.3). Glutathione peroxidases, like peroxiredoxins, are another important family of peroxidase-degrading enzymes found in cyanobacteria

that use reduced glutathione as an electron donor to catalyze the reduction of hydrogen peroxide into water (Bernroitner et al., 2009), and as demonstrated in this experiment this may be an effective antioxidant method employed by *Microcystis* to mediate hydrogen peroxide stress. Superoxide dismutase (*sodB2*) was found to be highly expressed in NIES-843 (18.9-Log2FD), and functions as another oxidative stress antioxidant enzyme in cyanobacteria, however, was not highly expressed in the other examined *Microcystis* strains.

L-lysine was also found to induce oxidative stress responses in examined *Microcystis* (Table 8.3). A previous study by Tian et al. (2018) found that SOD activity in *M. aeruginosa* NaRes975 increased after exposure to L-lysine, in our study NIES-843 was again found to significantly upregulate sodB2 activity ($p \leq 0.05$; Log2FC ≥ 19), supporting this finding (Table 8.3). In the forementioned study, SOD activity did not significantly increase however until after 48-hours, given NIES-843's described resilience to lysine treatments and prolonged exposure time, may have been why these changes were not significant for other examined strains. Transcription abundance of *gpx* peroxidase enzymes again were found to be significantly higher in when compared to controls for L-lysine treatment application as well ($p \leq 0.05$; Log2FC ≥ 4.5), with NIES-843 having a 7.5 Log2FC when compared to controls (Table 8.3). The *prxU* peroxiredoxin gene was also found to be upregulated under L-lysine treated non-toxic *Microcystis* strains (NIES-4325 and NIES-4284), with NIES-4325 transcriptions being 4.4 Log2FC higher than controls (Table 8.3). The hybrid peroxiredoxin *hprx5* was also highly upregulated in non-toxic *Microcystis* (NIES-4325, NIES-4285) (Log2FC ≥ 5). NIES-843 was again found to have increase transcriptional abundance of *prx-2-cys* peroxiredoxin gene (2.18-Log2FC), both NIES-102 and NIES-843 were found to upregulate the *prx BCP-B*. As previously mentioned, thioredoxin genes assist in catalytic activity of peroxiredoxins and some of these *trxA* genes were found to be significantly expressed under L-lysine treatments for *Microcystis* strains NIES-4285, NIES-4325 and NIES-843 ($p \leq 0.05$). Unlike for hydrogen peroxide treatment exposure, significant transcription activity of the *trxB* gene was only observed for NIES-843 and NIES-4325 (Table 8.3). Sulfate ABC transport proteins, such as *cysT,* were found to be highly upregulated in L-lysine treated *Microcystis* when compared to controls (Table 8.5). Cysteine and sulfate are essential components of peroxiredoxins and thioredoxins, where significant upregulation of this transmembrane transporters could have been to support the activities of these enzymes (Bernroitner et al., 2009).

Photosynthesis response

Cyanobacterial physiology and metabolic activities are directly linked to their photosynthetic activities (Wang et al., 2012), in this study we found that *Microcystis* photosynthetic genes were differently expressed under both hydrogen peroxide and L-lysine treatment application for NIES-843, NIES-4285, and NIES-4325, while NIES-102 differential expression was not found to be significant (Figure 8.1). *Microcystis* photosystem I (PSI) genes were generally downregulated under both hydrogen peroxide and L-lysine treatments, with more significant log2 fold changes seen in PSI genes under L-lysine treatments, however, NIES-843 saw an 18 log2 fold change in the *psA* PSI core protein gene (Fig. 8.1). Similar findings were seen by Qian et al. (2010) and colleagues where PSI core protein gene *psaB* was severely downregulated after hydrogen peroxide exposure.

Microcystis transcriptional responses to hydrogen peroxide and L-lysine addition for photosystem II (PSII) genes varied by strain and by treatment (Fig.8.1). PSII *psbC* transcription abundance was significantly downregulated in L-lysine exposed *Microcystis* strains NIES-843, NIES-4285 and NIES-4325 (Log2FC $\geq$ 3), this response was highly represented in NIES-843 which saw a 19-Log2FC decrease when compared with controls (Figure 8.1). *Microcystis* response was highly different for hydrogen peroxide exposed strains NIES-102 and NIES-4325, which expressed a 13 and 15 Log2FC increase (Figure 8.1). All other PSII *Microcystis* genes treated with hydrogen peroxide were not found to be significantly different from controls, however, L-lysine treated *Microcystis* strains NIES-4285, NIES-4325 and NIES-843 showed significant decreases in transcriptional abundances of PSII cytochrome subunit genes *psbE* and *psbF* (Log2FC $\geq$2). The general downregulation of photosynthetic-related genes for L-lysine and hydrogen peroxide exposed *Microcystis* cells likely influenced photosynthetic efficiency seen in QY values (Table. 8.1), inhibiting the growth and metabolic functioning of these organisms (Harke and Gobler, 2015). As shown by the upregulation of many oxidative stress removal genes (Table. 8.3), excess electrons as a result of ROS stress may have inhibited activity of the photosynthetic electron transport chain, *psbC* catalyze the oxide production from water and may have been why this gene was severely downregulated in some *Microcystis* strains, where prolonged exposure could likely inhibit carbon assimilation necessary for survival (Qian et al., 2009).

Microcystin

Genes involved in microcystin synthesis were severely reduced for toxin producing *Microcystis* strains NIES-843 and NIES-102 under both L-lysine and hydrogen peroxide treatments (Fig. 8.2). Transcription abundance of all microcystin related genes decreased under hydrogen peroxide treatments for NIES-843,

with significant reductions for *mcy*(*BDFGHI*) genes ($p \leq 0.05$; Log2FC ≥ 2.5). NIES-102 transcription of microcystin genes under hydrogen peroxide treatments were not found to be significantly different from controls, however, all were downregulated in comparison (Fig. 8.2). This agrees with findings reported by Sandrini et al. (2020) that microcystin synthetase genes (*mcyBE)* were all downregulated after addition of 2-10 mg/L hydrogen peroxide. Qian et al. (2010) also found that high-dose hydrogen peroxide treatments reduced microcystin gene expression relative to controls, the expression of both *mcyD* and *mcyH* microcystin synthetase genes were reduced 48-hours after application and became significantly lower than controls 96-hours later. Schuurmans et al. (2018) suggested that microcystin may bind to the thiol groups of peroxiredoxins, reducing oxidative stress removal functionality of these peroxidase genes, leading to the downregulation of microcystin genes and upregulation of peroxiredoxin and thioredoxin genes. *Prx-2-cys* and *trxB* were all significantly upregulated in NIES-843, corresponding to the significant downregulation in microcystin synthetase genes found in our experiment (Table 8.3; Fig. 8.1), supporting this hypothesis and demonstrating that toxin-producing *Microcystis* may downregulate microcystin synthetase genes as coping mechanisms to deal with oxidative stress created by high levels of hydrogen peroxide (Schruurmans et al., 2018; Sandrini et al., 2020). This has important impactions for the mitigation of toxin-producing *Microcystis* blooms possibly suggesting high-dose hydrogen peroxide lowers microcystin synthetase gene expression therefore likely lowering microcystin intracellular content which may be released upon cell lysis after application of hydrogen peroxide (Qian et al., 2010). Given exposure to microcystin is a top concern for water management of cyanoHABs, this finding highlights the great potential for hydrogen peroxide as a safe algaecide.

Microcystis NIES-843 and NIES-102 were also found largely to reduce transcription of microcystin synthetase genes after L-lysine treatment application (Figure 8.3). NIES-102 was found to have higher transcriptional abundance of the *mcyA* peptide synthesis gene, however it was very minimal and non-significant when compared with controls (Log2FC= 0.052). Transcription levels of all NIES-843 microcystin synthetase genes were found to be downregulated, and transcription of the tailoring *mcyF* gene was found to be significantly different ($p < 0.05$; log2 fold change > 2). Given the longer exposure time of NIES-843 to L-lysine and reduced transcription of microcystin genes, this also may demonstrate likelihood of reduced intracellular toxin-release upon cell lysis. To our knowledge the expression of microcystin synthetase genes after exposure to L-lysine has never examined before, seeing as this a safe biological algaecide specifically targeting *Microcystis* this was another beneficial finding.

Conclusion

In summary, hydrogen peroxide and L-lysine were found to cause significant oxidative stress in *Microcystis* cells as seen by increased transcriptional abundance of antioxidant genes. Non-toxic and toxic *Microcystis* strains were found to display different oxidative stress regulatory genes to reduce oxidative stress levels. Both hydrogen peroxide and L-lysine were found largely to inhibit photosynthetic gene activities in PSI, which likely is related oxidative stress, where reduced activities suppress necessary metabolic functions for energy transport. L-lysine and hydrogen peroxide were also found largely to lower microcystin synthetase gene activities, providing evidence that treatment application could reduce the potential amount of microcystin intracellular content release by these cells after cell-lysis. Varied transport systems that were upregulated under each treatment revealed what systems these algaecides target and may improve application use to treat cyanoHABs. To our knowledge, L-lysine RNA-seq has never been done and may provide insight into specific targeting of *Microcystis.*

Chapter 9: Early molecular detection of toxin genes using Biomeme qPCR

ABSTRACT

Cyanobacteria, common called blue-green algae, are small single-cell organism that have in recent years become an important topic of discussion and research in worldwide. Cyanobacteria can multiply quickly in surface waters and form blooms when favorable conditions prevail. Uncontrolled growth of these cyanobacteria colonies can cause harmful algal blooms (HABs) and certain HAB forming cyanobacteria are particularly concerning, largely due to their ability to produce a class of toxins called cyanotoxins which include potent neurotoxins, hepatotoxins, cytotoxins, and endotoxins. To characterize the threat to human health we worked on two aspects of understanding and characterizing the nature of freshwater cyanobacteria blooms and we believe that early detection of toxin genes could be used in conjunction with control methods before a bloom becomes too difficult to treat. The aim of this study was to identify the gene complexes responsible for producing specific cyanotoxins and develop a field molecular detection method to test for the specific gene presence in a waterbody and determine the potential toxin production, even though the bloom may not have been producing the toxin at time of collection. This is due to toxins being released during cell lysis. Measuring the toxin itself would require the presence of the toxins in high enough quantities to be detectible though alternative testing methods and it wouldn't allow us to be proactive in controlling it. In this study, we developed and tested four separate quantitative Polymerase Chain Reaction (qPCR) assays to implement in the field. The assays developed were used to test for of the target gene responsible for four different cyanotoxins; microsystin (*mcyE* gene) saxitoxin (*sxtA* gene), anatoxin (*anaC* gene), cylindrospermopsin (*cyrA* gene).

INTRODUCTION

During the last few decades, cyanobacterial bloom occurrence has been constantly increasing worldwide (Paerl et al., 2011). These blooms can affect oxygen levels in the water body causing an ecosystem imbalance but can also cause adverse effects on human health. Human health risks from cyanobacterial blooms are primarily related to cyanotoxins that some cyanobacteria produce. Toxic potential associated with cyanobacterial blooms has become a growing concern (Sabart et al., 2015). Not all species of cyanobacteria can produce toxins and those that do often do not produce toxins at levels harmful to human health. However, the presence of these toxins in drinking water or recreational waterways could pose a threat to human health. Monitoring programs that are currently in use can overestimate risk and lead to unnecessary health advisories because toxic and non-toxic strains of the same cyanobacterial species often coexist in the environment (Chiu et al., 2017). Normally samples would be collected in the field, sent to the laboratory, where the sample DNA could be extracted in a sterile environment then the samples could be tested on a standard bench top qPCR device. Using this method, results can be achieved in approximately 24 hours but there are other factors that affect that time frame such as transportation delays or workload management in the laboratory. When results are delayed it can impact the ability to make decisions regarding potential HABs or health advisories. Due to these factors, we believe there is need for a field methodology that would allow us to achieve results in approximately 2 hours with the goal of determining the potential toxin production in a waterbody while visiting. Biomeme is a Philadelphia-based technology company that produces commercially available handheld, portable qPCR platforms that can be used for a more efficient method of rapid molecular testing of cyanobacteria. We developed four custom assays for the Biomeme Franklin by adapting previously established protocols from the literature and laboratory testing. To characterize the true threat to human health we focused on two aspects of understanding and characterizing the nature of freshwater cyanobacteria blooms and we believe that early molecular detection of toxin genes could be used in conjunction with control methods before a bloom becomes too difficult to treat.

MATERIALS AND METHODS

The methods for testing were optimized in the laboratory environment before field testing began. With the understanding that field testing doesn't offer the same access to certain equipment or a sterile environment we adapted the laboratory protocol to best fit the field application. When procedural testing began, we started with three rounds of the freeze-thaw process using the -80°C freezer and a 65°C heating block for the lysis of cyanobacterial cells but this process was determined to be unsustainable for a field

extraction and was eventually phased out due to the freeze-thaw method requiring additional equipment in the field such as a cooler with dry ice and an isotemp block which would require a power source. Due to these factors the field extraction method was developed.

Figure 9.1. 12V cordless SoniBeast

Testing samples using the Franklin™ by Biomeme

For this DNA extraction, water samples were collected and 0.5-1ml of the sample was transferred into our premade bead tubes consisting of zirconia/silica beads (0.1mm diameter). The bead tube is then placed into our handheld bead beater, which was run for approximately 5 min at a time in order to lyse the cells (Fig. 9.1). The resulting sample was tested using qPCR (Franklin™ by Biomeme) to test for the presence of the gene complexes responsible for four different cyanotoxins. The Franklin Biomeme can be seen in Fig. 9.2 along with the mobile app used to control all of the qPCR settings. In order to maintain as much sterile procedure as possible, the Biomeme Go-Strips were prepared with the master mix, primers/probes, and non-nuclease water ahead of time under sterile conditions (Fig. 9.3). Each of the developed qPCR systems was performed individually and separately with the qPCR device. For the *Microcystis* system, a primer set MicrF (AGCCACACTGGGACTGAGACA)/MicrR (TCGCCCATTGCGGAAA) was used to target

Figure 9.2. Franklin by Biomeme and mobile app

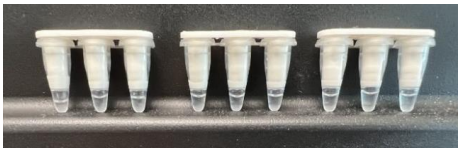

Figure 9.3. Biomeme Go-Strips, wells prepared for qPCR

Table 9.1. Primer and probe sequences, cycling conditions and amplicon length (bp) for Biomeme field-based qPCR assays

Target gene	Primer/Probe sequence (5'-3')	Cycling protocol	Amplicon length	Reference
mcyE	mcyF – AAT TCT AAA GCC CAA AGA CG mcyR – GAA ATT TGT GTA GAA GGT GC	1 cycle 50°C 2 min, 1 cycle 95°C 2 min, 45 cycles 95°C 30 sec, 72°C 2 min	128	Al-Tebrineh *et al*., 2012
sxtA	SxtF – GGA GTG GAT TTC AAC ACC AGA A SxtR – GTT TCC CAG ACT CGT TTC AGG SxtP – AGA AGA AAG TAT CCT CTC AG	1 cycle 95°C 3 min, 50 cycles 95°C 15 sec, 62.5°C 60 sec	148	Al-Tebrineh *et al*., 2012
cyrA	CyrF – GTC TGC CCA CGT GAT GTT ATG AT CyrR – CGT GAC CGC CGT GAC A CyrP – ACG AAA TTC TCG AAG CAA CT	1 cycle 95°C 3 min, 50 cycles 95°C 15 sec, 62.5°C 60 sec	71	Al-Tebrineh *et al*., 2012
anaC	anaF – CAC TCT TAG AAG CAT TTG TTT GCA anaR – ATA GAG GTT GTA ATA GCA AGC ATG G anaP – TCC CAA CAA ATA TTT GCG CCA	1 cycle 95°C 10 min, 50 cycles 95°C 15 sec, 62.5°C 60 sec	100	E. Karwacki et al. (unpublished)

the 16S rRNA region unique to *Microcystis* cells, while mcyF/mcyR were used to specifically target the microcystin synthetase (*mcyE*) region unique to potentially toxic *Microcystis* cells. Samples were also tested individually and separately for saxitoxin (*sxtA* gene), anatoxin (*anaC* gene), and cylindrospermopsin (*cyrA* gene). All primers and TaqMan probes used in this study were purchased from Integrated DNA Technologies. The qPCR cycling protocol for each primer pair was applied by adapting previously established protocols from the literature and laboratory testing (Table 1).

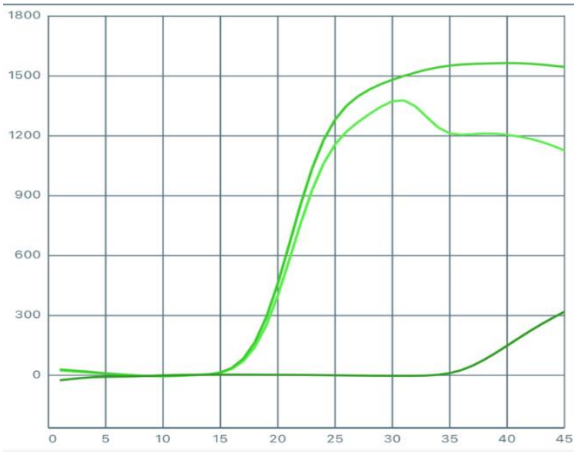

Figure 9.4. Successful amplification of the target gene *mcyE*.

RESULTS

The field qPCR systems were successfully optimized and developed for quantifying commonly observed harmful cyanobacteria in this study. The Biomeme assays exhibited a high success rate of amplifying genetic material in two hours without the need of standard DNA extraction and purification methods, but some samples required a more rigorous extraction with purified DNA. When run on an agarose gel we can visually see that microcystin amplified a 128 bp region in the *mcyE* gene, saxitoxin reagents amplified a 148 bp region of the *sxtA* gene, cylindrospermopsin amplified a 71 bp region of the *cyrA* gene, and anatoxin-A reagents amplified a 100 bp region of the *anaC* gene. In Figs. 9.4 and 9.5, we showed that the Biomeme has successfully amplified the target gene *mcyE* in two hours using a positive control, sample, and negative control. The image in Fig. 9.5 shows the melt curve for the 3 wells, this is used as a quality check when our negative control shows minor amplification. We can see two distinct melt regions that tells us that the minor amplification is due to primer dimers.

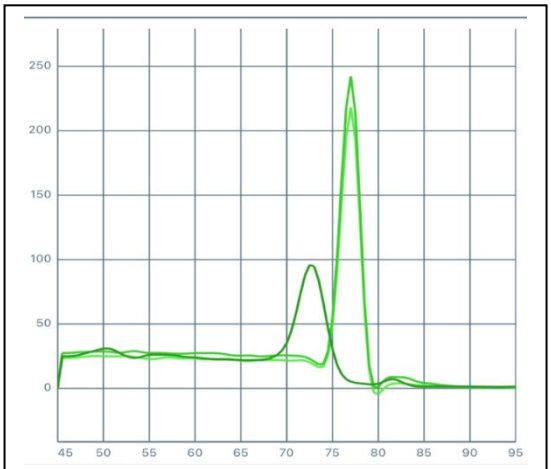

Figure 9.5. Image of the melting curve.

DISCUSSION

The qPCR systems were successfully optimized and developed for quantifying commonly observed harmful cyanobacteria in this study; both the MICR and *mcyE* primers and protocols established in the literature (Al-Tebrineh et al., 2012) proved successful. For the *sxtA* primers it was difficult to find a positive control that we already knew was producing the saxitoxins, once the positive control was found we still had trouble getting specific binding of the primers, so we switched to using the primers and probe (*sxtP*) which proved to be much more successful. A lot of time was also spent trying to establish a positive control for anatoxin and optimize the protocols using the *anaC* primer, we also used a primer and probe method for anatoxin-a (Karwacki et al. unpublished). While this information is important to understanding and characterizing the nature of freshwater cyanobacteria blooms, it only focuses on the molecular presence of toxin genes and potential toxin production, the research needs to be continued specifically with the toxin analysis testing to see if the samples that were positive for the gene complex are currently producing the toxins at time of collection. Testing for known toxin producers in combination with toxin analysis testing can improve our understanding of the effect they have as well as our response to HABs.

Chapter 10: Conclusions and recommendations

Hydrogen peroxide application for freshwater harmful algal blooms

In this project, the use of hydrogen peroxide was proposed as an innovative technology for early detection and rapid response to HAB in southwest Florida, with the anticipated large-scale application if blooms occur. To complete this mission, we combined the use of field monitoring and the development of a new rapid toxin gene detection technology for early detection of HAB, and mesocosm experiments for optimizing and evaluation of HAB control using hydrogen peroxide. We also conducted field experiments to evaluate the effectiveness of the hydrogen peroxide treatment of natural HAB. If the use of hydrogen peroxide for HAB control in both mesocosm and field experiments can be proven effective, it will provide valuable scientific data for cost-effective water management purposes.

Field monitoring

We recently published two manuscripts entitled "Hydrogen peroxide measurements in subtropical aquatic systems and their implications for cyanobacterial blooms." in Ecological Engineering 138:444-453 (2019) and "Subtropical freshwater cyanobacterial blooms as hydrogen peroxide hot spots" in Environmental Science & Technology Letters (2021) 8(10):911-917. We found that natural hydrogen peroxide levels were associated with cyanobacterial bloom conditions in Florida. Through this research, we hypothesized that hydrogen peroxide plays a key role in the biology and ecology of *Microcystis aeruginosa*. The unique physiology of *M. aeruginosa* such as toxin production and scum formation may couple with hydrogen peroxide dynamics in and outside of cells. An interaction of satellite heterotrophic bacteria and cyanobacteria can be also partially explained by the mutualistic interaction through hydrogen peroxide detoxification (Kim et al., 2021). Understanding the cell-to-cell communications between cyanobacteria and heterotrophs, and the mechanisms of microcolony and scum formations of *M. aeruginosa* were partially focused on this project. Understanding the natural hydrogen peroxide level in Florida's water and their association with cyanobacterial blooms must be understood to make hydrogen peroxide treatments more effective and safer.

We monitored a single site at the downstream end of the non-tidally influenced portion of the Caloosahatchee River known to experience isolated cyanobacterial HAB for a full year at twice monthly intervals from February 2021 through January 2022. This focused water monitoring program allowed us

to perform in-depth analyses of the cyanobacterial community and witness two distinct HAB events during the second and last quarters of the year.

Our data exhibit that environmental hydrogen peroxide in the subtropical waters of the Caloosahatchee River greatly increased before and during increases in bloom-forming *Microcystis* biomass. We observed the same phenomenon in our 2019 weekly monitoring at Franklin Lock and Dam. Cory and colleagues (2016) also documented a similar phenomenon from Lake Erie right before the massive *Microcystis* bloom was formed. We observed a correlation between algal colony numbers, which are mainly associated with *M. aeruginosa* abundance, and hydrogen peroxide concentrations. During our biweekly monitoring, two weeks before the spring bloom, hydrogen peroxide increased greatly and was maintained until the bloom dissipated. During the brief December bloom, there was a smaller but noticeable increase of hydrogen peroxide level along with the increase of *M. aeruginosa* abundance. The hydrogen peroxide concentration spanned greatly and ranged between 41 nM to 1582 nM. The baseline concentration was around 50 nM in this study. The average concentration was 390 nM and median was 273 nM. It should be noted that the baseline hydrogen peroxide concentration differ in every aquatic environment (Ndungu et al., 2019). Based on this one year monitoring, and two previous reports (Cory et al., 2016; Ndungu et al., 2019), we tentatively set a warning threshold value as 500 nM.

The molecular fingerprinting using high-throughput amplicon sequencing was proved as an effective tool to monitor the succession of cyanobacteria, eukaryotic algae, and bacteria. We also found that the accumulation phase of *Microcystis* HABs in the Caloosahatchee River appears to exhibit a distinct metatranscriptome profile and may be useful for HAB forecasting and understanding more detailed bloom formation mechanisms. There are many reasons why hydrogen peroxide levels could be extremely high in Florida (e.g., high dissolved organic matter, strong sunlight, seasonally heavy rain) (Urakawa et al., 2021). Hydrogen peroxide appears promising as an effective early warning system for HAB development given the cost efficiency and ease of measurement.

Optimizing and evaluation of HAB control using hydrogen peroxide

Hydrogen peroxide has recently gained popularity as an environmentally friendly treatment for cyanobacterial HAB when used at low concentrations. However, the general populace desires rapid removal of HAB. High concentration treatments can achieve this but may introduce an elevated risk to the aquatic environment. Most susceptible is the microbial community, with hydrogen peroxide noted to

have temporary but recoverable impacts at low concentrations. This is concerning as the importance of HAB-associated microorganisms shown to directly impact HAB succession and nutrient modulation.

It was possible to distract the algal bloom within 24 hours when we used 13 mM of hydrogen peroxide under the mesocosm condition. The high dose of hydrogen peroxide under the mesocosm experiment was not quickly degraded by microbial communities. The differential response of hydrogen peroxide between mesocosm studies and field applications revealed that the quick decline of hydrogen peroxide concentrations in the field application is mainly caused by the dispersion of hydrogen peroxide in the water column and not by biological and chemical degradations. Molecular fingerprinting approaches revealed the removal of cyanobacteria and some groups of bacteria and subsequent succession of the microbial community occurred. Our study identified hydrogen peroxide resilient microbial components of a South Florida *Microcystis* HAB, specifically Planctomycetes and Gammaproteobacteria which steadily increased in relative abundance post-treatment. These taxa are different from previously reported hydrogen peroxide resilient bacteria and even show opposite trends in studies from other geographic regions. This further highlights the importance of understanding local systems and populations with respect to water resources and HAB management.

One great advantage of hydrogen peroxide as an ideal algaecide is that it is quickly degraded into oxygen and water after use. However, it is hard to detect this chemical reaction in environmental monitoring. We used a higher concentration of hydrogen peroxide treatment in our first mesocosm study. The treatment mesocosms had higher dissolved oxygen (DO) levels throughout the experimental period with a range of 136 to 150% DO as opposed to 103 to 114% in the control. This was presumably from oxygenation by the hydrogen peroxide as it reacted in the mesocosm.

We found no evidence that human and animal pathogens increase after hydrogen peroxide treatment. However, further research is needed to examine the ecological responses of zooplankton and small fish species. It is also recognized that hydrogen peroxide can shut down nitrification, which is a pivotal step in the global nitrogen cycle. Therefore, we also have to monitor microbial biogeochemical cycles when we use hydrogen peroxide to mitigate algal blooms. In an open system, non-target microbial impacts should be minimized because replacement of microbial communities from the surrounding environment, which will quickly occur after treatment.

L-lysine application for freshwater harmful algal blooms

We confirmed the usefulness of the use of amino acid as a non-harm algaecide through our laboratory and mesocosm studies. We applied L-lysine to different algal species including cyanobacteria and green algae. We found that L-lysine is particularly toxic to *M. aeruginosa* but no other cyanobacteria (*Synechococcus*, *Cyanobium*, *and Dolichospermum*) and eukaryotic algae species (*Mychonastes* and *Chromochloris*). Therefore, L-lysine is a unique and selective algaecide for *M. aeruginosa*. We observed a synergetic effect when we combined hydrogen peroxide and L-lysine in the treatment of cyanobacteria. Our transcriptome research showed that *Microcystis aeruginosa* receives different types of stresses when the species was exposed to either hydrogen peroxide or L-lysine. The capability of treatments will be enhanced when combined the use of L-lysine along with hydrogen peroxide.

Transcriptome study to examine cellular response of *M. aeruginosa* to hydrogen peroxide and L-lysine treatments

Our transcriptome studies showed that gene expression of microcystin synthase genes were down regulated by hydrogen peroxide treatment while oxidative stress gene expressions were upregulated. We also found L-lysine treatment downregulates the transcription level of microcystin synthetase genes. This has important implications for the mitigation of toxin-producing *Microcystis* blooms, suggesting that high-dose of hydrogen peroxide lowers microcystin synthetase gene expression which should result in lower microcystin intracellular content which may be released upon cell lysis after application of hydrogen peroxide (Qian et al., 2010). Given exposure to microcystin is a top concern for water management of cyanoHAB, this finding highlights the great potential for hydrogen peroxide as a safe algaecide.

Field application of hydrogen peroxide

We conducted two field applications. On April 12, 2021, we found a minor shoreline bloom of *M. aeruginosa* at S-79 in the Caloosahatchee River. We sprayed 3% hydrogen peroxide to control cyanobacterial blooms to 400 m^2 of the area (downstream side of the lock) on April 14, 2021. The hydrogen peroxide concentration used (16.7 mg/L, 0.0015%) was within the concentrations reported in literature (2 mg/L to 100 mg/L). This concentration was determined based on the laboratory experiments where it was able to stop growth of *Microcystis aeruginosa*. The second field application of hydrogen peroxide was conducted from May 17 to June 8. We treated the same area (8 m x 50 m = 400 m^2) with 12 times more hydrogen peroxide (200.4 mg/L, 0.018%, 5.8 mM as a final concentration) than the first field experiment. We aimed hydrogen peroxide directly contacts to blooming algal biomass.

Both field applications showed that the hydrogen peroxide concentration returned to a background level on the next day. The first application showed that the concentration of hydrogen peroxide decreased within the first hour and went back to the background level on the next day. In the first application (16.7 mg/L, 0.0015%, 0.48 mM as a final concentration), no significant decrease was detected in Chl-a concentration in the surface bloom. In the second application (200.4 mg/L, 0.018%, 5.8 mM), we noticed the reduction of surface blooming biomass. Algal colony numbers declined from 4.8×10^4 cells to 4.2×10^3 colonies / L, suggesting 91.3% of algal biomass reduction. Hydrogen peroxide induced the succession of algal communities. HAB species were replaced by picocyanobacteria, which was different from literature documentations in which eukaryotic algae such as green algae replace cyanobacteria. To reduce the surface scum of *M. aeruginosa*, BlueGreen Water Technologies required multiple applications of Lake Guard Oxy. It was obvious that hydrogen peroxide treatment was not the method that instantly kills HAB cyanobacteria although it induced a succession of algal communities. Throughout our project, we confirmed that hydrogen peroxide treatment is an effective and practical method to remediate HAB. We observed no death of wildlife during and after our two field applications.

Recommendations

Monitoring of algal blooms: a key to the prevention of a large bloom

M. aeruginosa showed two bloom peaks in 2021. One was April-May and the other was November-December. The April-May activity was greater than the activity found in November-December. Both blooms produced microcystin. This year and data from 2019 and 2020 showed the importance of March and April to monitor the *Microcystis* population in the Caloosahatchee River. The activity of *Microcystis* population can be monitored by the counting of algal colonies, which is easily attained by dissecting microscopy. We confirmed a simple ecological rule of bloom formation. Before bloom formation, *Microcystis* always make colonies in the water column. It will take some time when these colonies begin to float on the surface and establish a bloom. The developed method had been adapted by Lee County's environmental laboratory for routine algal monitoring. We have received positive feedback from the County. This method is more reliable than visual observation (five-level ranking system at fields) and Chl-a data to predict the bloom condition of *Microcystis* in a target year. The spring activity of *Microcystis* always follows the spring activity of *Dolichospermum*. Microscopic examination of algal colony can easily differentiate *Dolichospermum* and *Microcystis*. We suggest the use of algal colony counting to predict the level of forthcoming blooming activity. The method must be standardized in future studies.

Through this project, we conceived two potentially important ecological questions to be addressed in the future. The first one is that we must understand where we find *Microcystis* population when this species is inactive. Our 16S rRNA gene amplicon sequence data suggest that this species annually exist in the water column in low relative abundance. The method was able to detect *Microcystis* even when cells were microscopically undetectable. We need to know the absolute numbers to use the information for future growth model construction. The second question is for a better understanding of the importance and the size of *Microcystis* seed pool in sediment. It has been reported that *Microcystis* can produce colonies that are temporarily inactive in the sediment (Ståhl-Delbanco et al., 2002) and these seeds can contribute to future bloom events (Kitchens et al., 2018; Wang et al., 2018).

Water discharge management of Franklin Lock and Dam

Our study revealed that the phytoplankton community at Franklin Lock and Dam in the Caloosahatchee River was controlled by the dynamics of inorganic nitrogen (nitrate + nitrite, ammonia) that is provided from both Lake Okeechobee and the watershed (Rumbold et al., 2020). The increase of inorganic nitrogen concentration will induce the increase of Chl-a with two weeks of lag time. This lag time could be shorter if the environmental condition is suitable for phytoplankton communities. TN in the river water was high (mean 1.36 mg-N/L) and stable (range 0.73 – 3.25 mg/L). This fluctuation was much smaller than the inorganic nitrogen pool. The organic nitrogen content percent in TN was 86% and this was much higher than the total organic phosphate pool (43%). In general, TN and TP are mainly used for water quality management because of their stability and methodological reliability. It is ideal if we can correctly identify the source of inorganic nitrogen species (e.g., water discharge, degradation of organic nitrogen, sediment, groundwater, microbial process, watershed, rainwater) and manage their quantity through the manipulation in which these nutrients are not consumed by harmful algae.

Our monitoring data suggested that a high flow rate induces the decrease of Chl-a and particularly the abundance of picocyanobacteria, which are the major phytoplankton group in the Caloosahatchee River water. In a closed lake and pond, it will take some time to be recharged once nutrients are depleted by phytoplankton. However, in the case of river and canal systems, nutrients are continuously supplied along the river flow. Thus, simply continuous low flow rate is an ideal condition for picocyanobacteria. Once water flows become high and some portion of phytoplankton is washed off, an ecological niche becomes available for other phytoplankton populations. Water discharge may provide the resuspension of sediment and release of phosphate in sediment. Based on the availability and the balance of nutrients,

some of these populations will occupy more ecological niche. When it happens in March to June, there are some chances in which harmful cyanobacterial groups can dominate in the community.

It should be noted that the increase of water flow will temporarily reduce the number of phytoplankton in Franklin Lock and Dam, however, once water flow becomes slow again, it will induce the succession of phytoplankton community. If it happens under the favorite condition for cyanobacteria, cyanobacterial bloom formation may be stimulated.

Our data strongly suggested that the major source of nitrogen and phosphorus at Franklin Lock and Dam was different. Phosphate concentration and total iron concentration was surprisingly highly correlated to each other. In general, phosphate concentration was low in spring and high in fall. Phosphate is low when algae are active and high when algae are inactive. We found that the surface DO concentration and OP concentration show an inverted relationship and negatively correlated significantly. This finding is relevant because it may imply that the major source of phosphorus is likely river sediment and it is released when DO level near the bottom water is low along with iron, which is an important trace element for phytoplankton communities. We also need to understand the influence of groundwater in which high OP, ammonia, and iron are contained.

Hydrogen peroxide treatment of HAB

If we can demonstrate the effectiveness of the use of hydrogen peroxide for HAB control, it will provide valuable scientific data for cost effective water management purposes. We combine a novel amino acid-based technology, which induce the selective death of specific cyanobacterial cells (i.e., *M. aeruginosa*), release of amino acids, and enhancement of the microbial loop, which can outcompete to algae for nutrient competition, particularly phosphorus. Our data will be an excellent asset for local water managers to select effective and safe HAB management tools. Since hydrogen peroxide can be a selective and non-invasive algal control method, it will provide a sustainable mitigation program nationwide. It has been used in Europe more often but not in the US. Algal responses after hydrogen peroxide treatment should be different between Europe and south Florida, thus, scientific assessment of phytoplankton dynamics and the impact of hydrogen peroxide on other aquatic fauna must be studied.

Apparently, the success of hydrogen peroxide application as an effective algaecide depends on appropriate concentration settings. It is recognized that hydrogen peroxide at the recommended maximal cyanocidal concentration of 5 mg/L is safe for macrofauna, fishes and aquatic plants (Matthijs et al., 2016).

Hydrogen peroxide could be used in different approaches. The information is based on this research and literature search.

1) **Closed lake or pond system:** The concentration of hydrogen peroxide must be kept low because the impact of hydrogen peroxide could reach entire lake or pond ecosystems. These cases have been tested by European countries (Matthijs et al., 2012) and recently in the US (Lusty and Gobler, 2020). In these two cases, 2mg/L and 4 mg/L of hydrogen peroxide were used, respectively. If the surface bloom is severe, the concentration of hydrogen peroxide could be increased but, in this case, a surface application should be used. It should be noted that although algal scums are heavily accumulated on the shore, shoreline spraying should be avoided because shoreline vegetation and numerous small aquatic organisms may be exposed to an extremely high level of undiluted hydrogen peroxide. The use of large volume of low concentration hydrogen peroxide is safer than the use of small volume of high concentration hydrogen peroxide because in the latter case water managers may accidentally create an extremely high concentration area due to misapplication.

2) **A part of a large water body:** This is a case of the Caloosahatchee River, Lake Okeechobee, and associated canal systems: All our hydrogen peroxide application resulted in the background concentration on the next day. The applied hydrogen peroxide in the surface water was quickly diluted by mixing with non-treated water and disappeared within the water column. The higher concentration of hydrogen peroxide is required to ensure the suppression of harmful algae. High concentration of hydrogen peroxide has a potential to induce the death of aquatic life (Matthijs et al., 2012; Matthijs et al., 2016). However, aquatic life that has a capability to swim can easily avoid the turmoil of hydrogen peroxide treatments. Zooplankton and bacterioplankton cannot swim away from the treatment and they could be exposed by strong hydrogen peroxide. However, the ecologically negative impact from a treatment of a small area in a large water body is negligible because these microscopic organisms are more evenly distribute in the water column and damaged individuals can be easily replaced by non-exposed individuals. Therefore, understanding of the susceptibility of zooplankton to hydrogen peroxide is crucial. However, the lethal concentration for zooplankton does not always correspond to ecologically relevant damages to the system tested. We still do not know the optimum and save concentration of hydrogen peroxide to treat a massive cyanobacterial bloom (Lusty and Gobler, 2020). It seems that surface treatment is safer than the entire water column treatment however, this approach needs repetitive applications of algaecide.

Acknowledgments

First, we thank the Office of Water Policy and Ecosystems Restoration, Florida Department of Environmental Protection for selecting our project as one of the innovative technologies for algal mitigation. We are deeply indebted to Tammy Cleveland and Robert Hill in the US Army Corps of Engineers Jacksonville District for their great support to permit and use the property of W.P. Franklin South Recreation Area for our fieldwork and mesocosm deployments. We also thank Jessica Spencer in the Invasive Species Management Branch, Jacksonville District, USACE, for including us in the USACE permit for to use of hydrogen peroxide. We would like to extend our sincere thanks to Rick Armstrong in the Lee County Environmental Laboratory for sharing Lee County's data and for helpful discussion. We thank Rory Feeney and Anna Wachnicka at South Florida Water Management District for the arrangement and the support of our research. It was our great pleasure to work with BlueGreen Water Technologies scientists, Moshe Harel, Waleed Nasser, Oori Weisshaus, Gad Weiss, and Professor Aaron Kaplan. We are also grateful to Jose Lopez and Lauren Krausfeldt for your support and helpful discussion to conduct our project. We thank Greg Tolley, Director of The Water School, Florida Gulf Coast University for many financial supports. We thank our laboratory students, Julia Davis, Coleen McMullen, and Diana Diaz for your great support of sampling and laboratory work. We could not make this project without your great contribution. Lastly, we thank Haruka Urakawa at the Department of Marine and Earth Sciences at FGCU for encouraging us to apply for the FDEP's funding opportunity and for her dedicated work on many aspects of this project.

References

Al-Tebrineh, J., Pearson, L.A., Yasar, S.A. and Neilan, B.A., 2012. A multiplex qPCR targeting hepato-and neurotoxigenic cyanobacteria of global significance. Harmful Algae, 15, pp.19-25.

Alvarez, S., Lupi, F., Solís, D. and Thomas, M., 2019. Valuing provision scenarios of coastal ecosystem services: the case of boat ramp closures due to harmful algae blooms in Florida. Water, 11(6), p.1250.

Baker, J.A., Entsch, B., Neilan, B.A. and McKay, D.B., 2002. Monitoring changing toxigenicity of a cyanobacterial bloom by molecular methods. Applied and Environmental Microbiology, 68(12), pp.6070-6076.

Barnett, J.P., Millard, A., Ksibe, A.Z., Scanlan, D.J., Schmid, R. and Blindauer, C.A. 2012. Mining genomes of marine cyanobacteria for elements of zinc homeostasis, Frontiers in Microbiology, 3(APR).

Beardall, J., Allen, D., Bragg, J., Finkel, Z.V., Flynn, K.J., Quigg, A., Rees, T.A.V., Richardson, A.J. and Raven, J.A., 2009. Allometry and stoichiometry of unicellular, colonial and multicellular phytoplankton. New Phytologist, 181, pp.295-309.

Bernroitner, M., Zamocky, M., Furtmüller, P.G., Peschek, G.A. and Obinger, C., 2009. Occurrence, phylogeny, structure, and function of catalases and peroxidases in cyanobacteria. Journal of Experimental Botany, 60(2), pp.423-440.

Burns, J., Lake, F., Society, M. and Street, E. 2008. Chapter 5 : Toxic cyanobacteria in Florida waters, in cyanobacterial harmful algal blooms: State of the science and research needs. Palatka, FL: Springer Science & Business Media, pp. 117–126.

Buzzelli, C., Doering, P., Wan, Y. and Sun, D. 2014. Modeling ecosystem processes with variable freshwater inflow to the Caloosahatchee River Estuary, southwest Florida. II. Nutrient loading, submarine light, and seagrasses, Estuarine, Coastal and Shelf Science, 151, pp. 272–284.

Cai, H.Y., Yan, Z. sheng, Wang, A.J., Krumholz, L.R. and Jiang, H.L. 2013. Analysis of the attached microbial community on mucilaginous cyanobacterial aggregates in the eutrophic Lake Taihu reveals the importance of Planctomycetes, Microbial Ecology, 66(1), pp. 73–83.

Charette, M.A., Henderson, P.B., Breier, C.F. and Liu, Q. 2013. Submarine groundwater discharge in a river-dominated Florida estuary, Marine Chemistry, 156, pp. 3–17.

Chiu, Y.T., Chen, Y.H., Wang, T.S., Yen, H.K. and Lin, T.F., 2017. A qPCR-based tool to diagnose the presence of harmful cyanobacteria and cyanotoxins in drinking water sources. International Journal of Environmental Research and Public Health, 14(5), p.547.

Chorus, I. and Welker, M., 2021. Toxic cyanobacteria in water: a guide to their public health consequences, monitoring and management (p. 858). Taylor & Francis.

Cory, R.M., Davis, T.W., Dick, G.J., Johengen, T., Denef, V.J., Berry, M.A., Page, S.E., Watson, S.B., Yuhas, K. and Kling, G.W. 2016. Seasonal dynamics in dissolved organic matter, hydrogen peroxide, and cyanobacterial blooms in Lake Erie, Frontiers in Marine Science, 3(APR), pp. 1–17.

Delmont, T.O., Quince, C., Shaiber, A., Esen, Ö.C., Lee, S.T., Rappé, M.S., MacLellan, S.L., Lücker, S. and Eren, A.M. 2018. Nitrogen-fixing populations of Planctomycetes and Proteobacteria are abundant in surface ocean metagenomes, Nature Microbiology, 3(7), pp. 804–813.

Drábková, M., Admiraal, W. and Maršálek, B. 2007. Combined exposure to hydrogen peroxide and light-selective effects on cyanobacteria, green algae, and diatoms, Environmental Science and Technology, 41(1), pp. 309–314.

Falconer, I., Bartram, J., Chorus, I., Kuiper-Goodman, T., Utkilen, H., Burch, M. and Codd, G.A., 1999. Safe levels and safe practices. Toxic cyanobacteria in water, pp.155-178.

Fassbinder-Orth, C.A., 2014. Methods for quantifying gene expression in ecoimmunology: from qPCR to RNA-Seq. Integrative and Comparative Biology, 54(3), pp.396-406.

Gensemer, R.W. and Playle, R.C., 1999. The bioavailability and toxicity of aluminum in aquatic environments. Critical reviews in Environmental Science and Technology, 29(4), pp.315-450.

Giannuzzi, L., Lombardo, T., Juárez, I., Aguilera, A. and Blanco, G. 2021. A stochastic characterization of hydrogen peroxide-induced regulated cell death in *Microcystis aeruginosa*, Frontiers in Microbiology, 12(July), pp. 1–15.

Guedes, I.A., da Costa Leite, D.M., Manhães, L.A., Bisch, P.M., Azevedo, S.M. and Pacheco, A.B.F., 2014. Fluctuations in microcystin concentrations, potentially toxic *Microcystis* and genotype diversity in a cyanobacterial community from a tropical reservoir. Harmful Algae, 39, pp.303-309.

Harke, M.J. and Gobler, C.J., 2015. Daily transcriptome changes reveal the role of nitrogen in controlling microcystin synthesis and nutrient transport in the toxic cyanobacterium, *Microcystis aeruginosa*. BMC Genomics, 16(1), pp.1-18.

Harke, M.J. and Gobler, C.J., 2013. Global transcriptional responses of the toxic cyanobacterium, *Microcystis aeruginosa*, to nitrogen stress, phosphorus stress, and growth on organic matter. PLoS One, 8(7), p.e69834.

Havens, K.E., Ji, G., Beaver, J.R., Fulton, R.S. and Teacher, C.E., 2019. Dynamics of cyanobacteria blooms are linked to the hydrology of shallow Florida lakes and provide insight into possible impacts of climate change. Hydrobiologia, 829(1), pp.43-59.

Havens, Karl E., Rolland S. Fulton III, John R. Beaver, Erin E. Samples, and James Colee. "Effects of climate variability on cladoceran zooplankton and cyanobacteria in a shallow subtropical lake." Journal of Plankton Research 38, no. 3 (2016): 418-430.

Hanson, M.J. and Stefan, H.G., 1984. Side effects of 58 years of copper sulfate treatment of the Fairmont lakes, Minnesota 1. JAWRA Journal of the American Water Resources Association, 20(6), pp.889-900.

Hehmann, A., Watanabe, M.M. and Kaya, K., 2002. Killing of *Microcystis* by an amino acid: Results of laboratory and enclosure experiments. Internationale Vereinigung für theoretische und angewandte Limnologie: Verhandlungen, 28(2), pp.1147-1150.

Hong, Y., Hu, H.Y., Xie, X., Sakoda, A., Sagehashi, M. and Li, F.M., 2009. Gramine-induced growth inhibition, oxidative damage and antioxidant responses in freshwater cyanobacterium *Microcystis aeruginosa*. Aquatic Toxicology, 91(3), pp.262-269.

Hu, C., Muller-Karger, F.E. and Swarzenski, P.W. 2006. Hurricanes, submarine groundwater discharge, and Florida's red tides, Geophysical Research Letters, 33(11), pp. 1–5.

Hu, Z., Xiao, Q., Yang, J., Xiao, W., Wang, W., Liu, S. and Lee, X., 2015. Temporal dynamics and drivers of ecosystem metabolism in a large subtropical shallow lake (lake Taihu). International Journal of Environmental Research and Public Health, 12(4), pp.3691-3706.

Huisman, J. and Hulot, F.D., 2005. Population dynamics of harmful cyanobacteria. In Harmful cyanobacteria (pp. 143-176). Springer, Dordrecht.

Huisman, J., Codd, G.A., Paerl, H.W., Ibelings, B.W., Verspagen, J.M. and Visser, P.M., 2018. Cyanobacterial blooms. Nature Reviews Microbiology, 16(8), pp.471-483.

Jančula, Daniel, and Blahoslav Maršálek. "Critical review of actually available chemical compounds for prevention and management of cyanobacterial blooms." Chemosphere 85, no. 9 (2011): 1415-1422.

Jardillier, Ludwig, Mikhail V. Zubkov, John Pearman, and David J. Scanlan. "Significant CO2 fixation by small prymnesiophytes in the subtropical and tropical northeast Atlantic Ocean." The ISME journal 4, no. 9 (2010): 1180-1192.

Jeppesen, E., Søndergaard, M., Meerhoff, M., Lauridsen, T.L. and Jensen, J.P., 2007. Shallow lake restoration by nutrient loading reduction—some recent findings and challenges ahead. Shallow Lakes in a Changing World, pp.239-252.

Kaya, K., Liu, Y.D., Shen, Y.W., Xiao, B.D. and Sano, T., 2005. Selective control of toxic *Microcystis* water blooms using lysine and malonic acid: An enclosure experiment. Environmental Toxicology: An International Journal, 20(2), pp.170-178.

Kiley, P.J. and Kaplan, S., 1988. Molecular genetics of photosynthetic membrane biosynthesis in *Rhodobacter sphaeroides*. Microbiological Reviews, 52(1), pp.50-69.

Kinley-Baird, C., Calomeni, A., Berthold, D.E., Lefler, F.W., Barbosa, M., Rodgers, J.H. and Laughinghouse IV, H.D., 2021. Laboratory-scale evaluation of algaecide effectiveness for control of microcystin-producing cyanobacteria from Lake Okeechobee, Florida (USA). Ecotoxicology and Environmental Safety, 207, p.111233.

Kitchens, C.M., Johengen, T.H. and Davis, T.W., 2018. Establishing spatial and temporal patterns in Microcystis sediment seed stock viability and their relationship to subsequent bloom development in Western Lake Erie. PloS One, 13(11), p.e0206821.

Kim, M., Kim, W., Lee, Y. and Park, W., 2021. Linkage between bacterial community-mediated hydrogen peroxide detoxification and the growth of *Microcystis aeruginosa*. Water Research, 207, p.117784.

Kim, Minkyung, Bora Shin, Jaebok Lee, Hye Yoon Park, and Woojun Park. Culture-independent and culture-dependent analyses of the bacterial community in the phycosphere of cyanobloom-forming *Microcystis aeruginosa*. Scientific Reports 9, no. 1 (2019): 1-13.

Kramer, B.J., Davis, T.W., Meyer, K.A., Rosen, B.H., Goleski, J.A., Dick, G.J., Oh, G. and Gobler, C.J., 2018. Nitrogen limitation, toxin synthesis potential, and toxicity of cyanobacterial populations in Lake Okeechobee and the St. Lucie River Estuary, Florida, during the 2016 state of emergency event. PLoS One, 13(5), p.e0196278.

Kardinaal WEA, Tonk L, Janse I, Hol S, Slot P, Huisman J, Visser PM. 2007. Competition for light between toxic and nontoxic strains of the harmful cyanobacterium *Microcystis*. Applied and Environmental Microbiology 73:2939–2946.

Li, H., Xing, P., Chen, M., Bian, Y. and Wu, Q.L. 2011. Short-term bacterial community composition dynamics in response to accumulation and breakdown of *Microcystis blooms*, Water Research, 45(4), pp. 1702–1710.

Lindsay, M.R., Webb, R.I., Strous, M., Jetten, M.S.M., Butler, M.K., Forde, R.J. and Fuerst, J.A. 2001. Cell compartmentalisation in Planctomycetes: Novel types of structural organisation for the bacterial cell, Archives of Microbiology, 175(6), pp. 413–429.

Liu, M., Shi, X., Chen, C., Yu, L. and Sun, C. 2017. Responses of *Microcystis* colonies of different sizes to hydrogen peroxide stress, Toxins, 9(10).

Lusty, M.W. and Gobler, C.J. 2020. The Efficacy of Hydrogen Peroxide in Mitigating Communities across Four Lakes in NY, USA, Toxins, 12, p. 428.

Matthijs, H.C., Jančula, D., Visser, P.M. and Maršálek, B., 2016. Existing and emerging cyanocidal compounds: new perspectives for cyanobacterial bloom mitigation. Aquatic Ecology, 50(3), pp.443-460.

Matthijs, H.C., Visser, P.M., Reeze, B., Meeuse, J., Slot, P.C., Wijn, G., Talens, R. and Huisman, J., 2012. Selective suppression of harmful cyanobacteria in an entire lake with hydrogen peroxide. Water Research, 46(5), pp.1460-1472.

Meyer, F., Paarmann, D., D'Souza, M., Olson, R., Glass, E.M., Kubal, M., Paczian, T., Rodriguez, A., Stevens, R., Wilke, A., Wilkening, J. and Edwards, R.A. 2008. The metagenomics RAST server - A public resource for the automatic phylogenetic and functional analysis of metagenomes, BMC Bioinformatics, 9, pp. 1–8.

Ndungu, L.K., Steele, J.H., Hancock, T.L., Bartleson, R.D., Milbrandt, E.C., Parsons, M.L. and Urakawa, H. 2019. Hydrogen peroxide measurements in subtropical aquatic systems and their implications for cyanobacterial blooms, Ecological Engineering, 138(June), pp. 444–453.

Nübel, U., Garcia-Pichel, F. and Muyzer, G., 1997. PCR primers to amplify 16S rRNA genes from cyanobacteria. Applied and Environmental Microbiology, 63(8), pp.3327-3332.

Overbeek, R., Olson, R., Pusch, G.D., Olsen, G.J., Davis, J.J., Disz, T., Edwards, R.A., Gerdes, S., Parrello, B., Shukla, M., Vonstein, V., Wattam, A.R., Xia, F. and Stevens, R. 2014. The SEED and the Rapid Annotation of microbial genomes using Subsystems Technology (RAST), Nucleic Acids Research, 42(D1), pp. 206–214.

Paerl, H.W., Fulton, R.S., Moisander, P.H. and Dyble, J. 2001. Harmful freshwater algal blooms, with an emphasis on cyanobacteria., The Scientific World Journal, 1, pp. 76–113.

Paerl, H.W., Hall, N.S. and Calandrino, E.S., 2011. Controlling harmful cyanobacterial blooms in a world experiencing anthropogenic and climatic-induced change. Science of the Total Environment, 409(10), pp.1739-1745.

Paerl, H.W. and Huisman, J., 2009. Climate change: a catalyst for global expansion of harmful cyanobacterial blooms. Environmental Microbiology Reports, 1(1), pp.27-37.

Palma, M., DeLuca, D., Worgall, S. and Quadri, L.E.N. 2004. Transcriptome analysis of the response of *Pseudomonas aeruginosa* to hydrogen peroxide, Journal of Bacteriology, 186(1), pp. 248–252.

Pang, C.M., Hong, P., Guo, H. and Liu, W.T. 2005. Biofilm formation characteristics of bacterial isolates retrieved from a reverse osmosis membrane, Environmental Science and Technology, 39(19), pp. 7541–7550.

Parra, M., Stahl, S. and Hellmann, H. 2018. Vitamin B6 and its role in cell metabolism and physiology, Cells, 7(7).

Peng, G., Lin, S., Fan, Z. and Wang, X., 2017. Transcriptional and physiological responses to nutrient loading on toxin formation and photosynthesis in *Microcystis aeruginosa* FACHB-905. Toxins, 9(5), p.168.

Piel, T., Sandrini, G., Muyzer, G., Brussaard, C.P., Slot, P.C., van Herk, M.J., Huisman, J. and Visser, P.M., 2021. Resilience of microbial communities after hydrogen peroxide treatment of a eutrophic lake to suppress harmful cyanobacterial blooms. Microorganisms, 9(7), p.1495.

Qian, H., Chen, W., Li, J., Wang, J., Zhou, Z., Liu, W. and Fu, Z., 2009. The effect of exogenous nitric oxide on alleviating herbicide damage in *Chlorella vulgaris*. Aquatic Toxicology, 92(4), pp.250-257.

Qian, H., Yu, S., Sun, Z., Xie, X., Liu, W. and Fu, Z., 2010. Effects of copper sulfate, hydrogen peroxide and N-phenyl-2-naphthylamine on oxidative stress and the expression of genes involved photosynthesis and microcystin disposition in *Microcystis aeruginosa*. Aquatic Toxicology, 99(3), pp.405-412.

Rach, J.J., Schreier, T.M., Howe, G.E. and Redman, S.D. 1997. Effect of species, life stage, and water temperature on the toxicity of hydrogen peroxide to fish, Progressive Fish-Culturist, 59(1), pp. 41–46.

Reichwaldt, E.S., Zheng, L., Barrington, D.J. and Ghadouani, A. 2012. Acute toxicological response of *Daphnia* and *Moina* to hydrogen peroxide, Journal of Environmental Engineering, 138(5), pp. 607–611.

Reitzel, K., Balslev, K.A. and Jensen, H.S., 2017. The influence of lake water alkalinity and humic substances on particle dispersion and lanthanum desorption from a lanthanum modified bentonite. Water Research, 125, pp.191-200.

Reynolds, C.S., 2006. The ecology of phytoplankton. Cambridge University Press.

Riboldi, G.P., Bierhals, C.G., de Mattos, E.P., Frazzon, A.P.G., d'Azevedo, P.A. and Frazzon, J. 2014. Oxidative stress enhances the expression of sulfur assimilation genes: Preliminary insights on the *Enterococcus faecalis* iron-sulfur cluster machinery regulation, Memorias do Instituto Oswaldo Cruz, 109(4), pp. 408–413.

Rumbold, D.G. and Doering, P.H., 2020. Water quality and source of freshwater discharge to the Caloosahatchee Estuary, Florida. Florida Scientist, 83(1), pp.1-20.

Sabart, M., Crenn, K., Perrière, F., Abila, A., Leremboure, M., Colombet, J., Jousse, C. and Latour, D., 2015. Co-occurrence of microcystin and anatoxin-a in the freshwater lake Aydat (France): Analytical and molecular approaches during a three-year survey. Harmful Algae, 48, pp.12-20.

Sandrini, G., Matthijs, H.C., Verspagen, J.M., Muyzer, G. and Huisman, J., 2014. Genetic diversity of inorganic carbon uptake systems causes variation in CO_2 response of the cyanobacterium *Microcystis*. The ISME journal, 8(3), pp.589-600.

Sandrini, G., Piel, T., Xu, T., White, E., Qin, H., Slot, P.C., Huisman, J. and Visser, P.M., 2020. Sensitivity to hydrogen peroxide of the bloom-forming cyanobacterium *Microcystis* PCC 7806 depends on nutrient availability. Harmful Algae, 99, p.101916.

Santos, A.A., Guedes, D.O., Barros, M.U., Oliveira, S., Pacheco, A.B., Azevedo, S.M., Magalhães, V.F., Pestana, C.J., Edwards, C., Lawton, L.A. and Capelo-Neto, J., 2021. Effect of hydrogen peroxide on natural phytoplankton and bacterioplankton in a drinking water reservoir: Mesocosm-scale study. Water Research, 197, p.117069.

Schuurmans, J.M., Brinkmann, B.W., Makower, A.K., Dittmann, E., Huisman, J. and Matthijs, H.C., 2018. Microcystin interferes with defense against high oxidative stress in harmful cyanobacteria. Harmful Algae, 78, pp.47-55.

Seo, S.W., Kim, D., Szubin, R. and Palsson, B.O. 2015. Genome-wide reconstruction of OxyR and SoxRS transcriptional regulatory networks under oxidative stress in *Escherichia coli* K-12 MG1655, Cell Reports, 12(8), pp. 1289–1299.

Shao, J., Li, R., Lepo, J.E. and Gu, J.D., 2013. Potential for control of harmful cyanobacterial blooms using biologically derived substances: Problems and prospects. Journal of Environmental Management, 125, pp.149-155.

Sharma, P., Bano, A., Singh, S.P., Dubey, N.K., Chandra, R. and Iqbal, H.M.N. 2022. Microbial fingerprinting techniques and their role in the remediation of environmental pollution, Cleaner Chemical Engineering, 2(March), p. 100026.

Shin, HyeonSeok, Seong-Joo Hong, Hyojin Kim, Chan Yoo, Hookeun Lee, Hyung-Kyoon Choi, Choul-Gyun Lee, and Byung-Kwan Cho. "Elucidation of the growth delimitation of *Dunaliella tertiolecta* under

nitrogen stress by integrating transcriptome and peptidome analysis." Bioresource Technology 194 (2015): 57-66.

Small, D.A., Chang, W., Toghrol, F. and Bentley, W.E. 2007. Comparative global transcription analysis of sodium hypochlorite, peracetic acid, and hydrogen peroxide on *Pseudomonas aeruginosa*, Applied Microbiology and Biotechnology, 76(5), pp. 1093–1105.

Sommaruga, R., Chen, Y. and Liu, Z. 2009. Multiple strategies of bloom-forming *Microcystis* to minimize damage by solar ultraviolet radiation in surface waters, Microbial Ecology, 57(4), pp. 667–674.

Ståhl-Delbanco, A. and Hansson, L.A., 2002. Effects of bioturbation on recruitment of algal cells from the "seed bank" of lake sediments. Limnology and Oceanography, 47(6), pp.1836-1843.

Stevenson, J. 2014. Ecological assessments with algae: a review and synthesis, Journal of Phycology, 50(3), pp. 437–461.

Sukenik, A. and Kaplan, A. 2021. Cyanobacterial harmful algal blooms in aquatic ecosystems: A comprehensive outlook on current and emerging mitigation and control approaches, Microorganisms, 9(7).

Takamura, Y., Chino, M., Osada, A., Nishihara, H. and Yagi, O., 1999. Growth responses of *Microcystis* and *Oscillatoria* cyanobacteria to various organic compounds and growth inhibition by L-lysine and L-histidine. Environmental Science (Japan), Volume 12(3) pp. 329-337.

Tian, L., Chen, M., Ren, C., Wang, Y. and Li, L., 2018. Anticyanobacterial effect of L-lysine on *Microcystis aeruginosa*. RSC advances, 8(38), pp.21606-21612.

Trainic, M., Weiss, G., Nasser, W., Harel, M., Weisshaus, O., Kaplan, A., 2021. Harmful cyanobacterial bloom mitigation in the C-43 canal/ Caloosahatchee River using BlueGreen Water Technologies ("BlueGreen") Lake Guard® Oxy solution. Technical report submitted to St. Johns River Water Management District and South Florida Water Management District.

Trapnell, C., Hendrickson, D.G., Sauvageau, M., Goff, L., Rinn, J.L. and Pachter, L., 2013. Differential analysis of gene regulation at transcript resolution with RNA-seq. Nature biotechnology, 31(1), pp.46-53.

Urakawa, H. and Bernhard, A.E. 2017. Wetland management using microbial indicators, Ecological Engineering, 108(July), pp. 456–476.

Urakawa, H., Hancock, T.L., Steele, J.H., Dahedl, E.K., Urakawa, H.E., Ndungu, L.K., Krausfeldt, L.E., Rosen, B.H. and Lopez, J.V., 2020. Complete genome sequence of *Microcystis aeruginosa* FD4, isolated from a subtropical river in southwest Florida. Microbiology Resource Announcements, 9(38), pp.e00813-20.

Urakawa, H., Ndungu, L.K., Hancock, T.L., Steele, J.H. and Bartleson, R.D., 2021. Subtropical freshwater cyanobacterial blooms as hydrogen peroxide hot spots. Environmental Science & Technology Letters, 8(10), pp.911-917.

Van Dam, B.R., Tobias, C., Holbach, A., Paerl, H.W. and Zhu, G., 2018. CO_2 limited conditions favor cyanobacteria in a hypereutrophic lake: an empirical and theoretical stable isotope study. Limnology and Oceanography, 63(4), pp.1643-1659.

Van Teeseling, M.C.F., Mesman, R.J., Kuru, E., Espaillat, A., Cava, F., Brun, Y. V., Vannieuwenhze, M.S., Kartal, B. and Van Niftrik, L. 2015. Anammox Planctomycetes have a peptidoglycan cell wall, Nature Communications, 6(May), pp. 1–6.

Wan, L., Chen, X., Deng, Q., Yang, L., Li, X., Zhang, J., Song, C., Zhou, Y. and Cao, X. 2019. Phosphorus strategy in bloom-forming cyanobacteria (*Dolichospermum* and *Microcystis*) and its role in their succession, Harmful Algae, 84(August), pp. 46–55.

Wang, B., Song, Q., Long, J., Song, G., Mi, W. and Bi, Y., 2019. Optimization method for *Microcystis* bloom mitigation by hydrogen peroxide and its stimulative effects on growth of chlorophytes. Chemosphere, 228, pp.503-512.

Wang, C., Feng, B., Tian, C., Tian, Y., Chen, D., Wu, X., Li, G. and Xiao, B., 2018. Quantitative study on the survivability of *Microcystis* colonies in lake sediments. Journal of Applied Phycology, 30(1), pp.495-506.

Wang, X., Ma, B., Bai, Y., Lan, H., Liu, H. and Qu, J. 2018. The effects of hydrogen peroxide pre-oxidation on ultrafiltration membrane biofouling alleviation in drinking water treatment, Journal of Environmental Sciences (China), 73, pp. 117–126.

Wang, K., Mou, X., Cao, H., Struewing, I., Allen, J. and Lu, J. 2021. Co-occurring microorganisms regulate the succession of cyanobacterial harmful algal blooms, Environmental Pollution, 288(January), p. 117682.

Weenink, E.F., Luimstra, V.M., Schuurmans, J.M., Van Herk, M.J., Visser, P.M. and Matthijs, H.C., 2015. Combatting cyanobacteria with hydrogen peroxide: a laboratory study on the consequences for phytoplankton community and diversity. Frontiers in Microbiology, 6, p.714.

Wei, L., You, W., Gong, Y., El Hajjami, M., Liang, W., Xu, J. and Poetsch, A., 2020. Transcriptomic and proteomic choreography in response to light quality variation reveals key adaption mechanisms in marine *Nannochloropsis oceanica*. Science of the Total Environment, 720, p.137667.

Wiegand, S., Jogler, M. and Jogler, C. 2018. On the maverick Planctomycetes, FEMS Microbiology Reviews, 42(6), pp. 739–760.

Wilson, A.E., Sarnelle, O. and Tillmanns, A.R., 2006. Effects of cyanobacterial toxicity and morphology on the population growth of freshwater zooplankton: Meta-analyses of laboratory experiments. Limnology and Oceanography, 51(4), pp.1915-1924.

Wu, Z.X., Gan, N.Q., Huang, Q. and Song, L.R., 2007. Response of *Microcystis* to copper stress–do phenotypes of *Microcystis* make a difference in stress tolerance? Environmental Pollution, 147(2), pp.324-330.

Wu, Y., Li, L., Zheng, L., Dai, G., Ma, H., Shan, K., Wu, H., Zhou, Q. and Song, L. 2016. Patterns of succession between bloom-forming cyanobacteria *Aphanizomenon flos-aquae* and *Microcystis* and related environmental factors in large, shallow Dianchi Lake, China, Hydrobiologia, 765(1), pp. 1–13.

Xiao, M., Li, M. and Reynolds, C.S., 2018. Colony formation in the cyanobacterium *Microcystis*. Biological Reviews, 93(3), pp.1399-1420.

Yamamoto, Y., Kouchiwa, T., Hodoki, Y., Hotta, K., Uchida, H. and Harada, K.I., 1998. Distribution and identification of actinomycetes lysing cyanobacteria in a eutrophic lake. Journal of Applied Phycology, 10(4), pp.391-397.

Yoon, H., Kim, H.C. and Kim, S. 2021. Long-term seasonal and temporal changes of hydrogen peroxide from cyanobacterial blooms in fresh waters, Journal of Environmental Management, 298(June), p. 113515.

Zeller, T. and Klug, G., 2006. Thioredoxins in bacteria: functions in oxidative stress response and regulation of thioredoxin genes. Naturwissenschaften, 93(6), pp.259-266.

Zhang, S., Wang, W., Zhang, K., Xu, P. and Lu, Y., 2018. Phosphorus release from cyanobacterial blooms during their decline period in eutrophic Dianchi Lake, China. Environmental Science and Pollution Research, 25(14), pp.13579-13588.

Zhang, J. et al. 2021. Diversity, seasonal succession and host specificity of bacteria associated with cyanobacterial aggregates in a freshwater lake, Environmental Technology & Innovation, 24, p. 101988.

Zimba, P.V., Dionigi, C.P. and Brashear, S.S., 2001. Selective toxicity of exogenous l-lysine to cyanobacteria, relative to a chlorophyte and a diatom. Phycologia, 40(5), pp.483-486.

Appendix

Appendix A Photo documentation of bimonthly water samplings at Franklin Lock and Dam

Appendix B Water quality parameters of bimonthly water samplings at Franklin Lock and Dam

Appendix C Photo documentation of the time series of first mesocosm experiment

Appendix D Photo documentation of first mesocosm experiment

Appendix E The first mesocosm water quality parameters

Appendix F Photo documentation of second mesocosm

Appendix G The second mesocosm water quality parameters

Appendix H Water quality parameters of the second mesocosm

Appendix I Photo documentation of first field application: time series of field experiment

Appendix J Water quality parameters of the first field application of hydrogen peroxide

Appendix K Photo documentation of second field application: time series of field experiment

Appendix L Water quality parameters of the second field application of hydrogen peroxide

Appendix A. Photo documentation of bimonthly water samplings at Franklin Lock and Dam

Month	Date	Water	Shoreline	Date	Water	Shoreline
February	2/1/2021			2/15/2021		
March	3/1/2021			3/15/2021		
April	4/12/2021	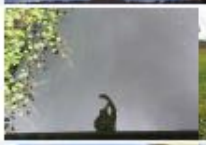		4/26/2021		
May	5/1/2021			5/24/2021		
June	6/7/2021			6/21/2021	nd	nd
July	7/8/2021	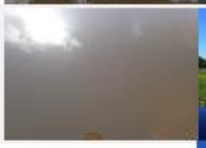		7/19/2021		
August	8/2/2021	nd		8/17/2021		
September	9/13/2021			9/27/2021		
October	10/11/2021			10/25/2021	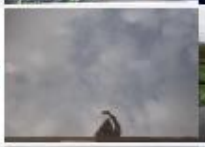	
November	11/8/2021			11/22/2021		
December	12/6/2021			12/20/2021		
January	1/3/2022			1/17/2022	nd	

Appendix B. Water quality parameters of bimonthly water samplings at Franklin Lock and Dam

Date	Temp.	Sal.	DO	DO	Cond.	TDS	pH	Colony count	Chl-a	HP*	MC**	Total iron	TOC	TKN	TN	TP	NOx	NH3	OP	CDOM	Water discharge	PICO†	BAC‡
	°C	ppt	%	mg/L	µS/cm	mg/L		per L	µg/L	nM	µg/L	µg/L	mg/L	µg/L	µg/L	µg/L	µg/L	µg/L	µg/L	µg/L	cfs	cells/ml	cells/ml
2/1/2021	20.2	0.20	82.32	7.50	416.00	0.27	7.83	70	7.61	73.83	**0.01***	123	14.8	1050	1210	92	158	8	47	204.4	987	1520825	6984529
2/15/2021	23.9	0.19	93.75	8.06	392.62	0.26	7.90	108	20	407.90	**0.00**	114	16.4	910	961	108	51	10	29	205.0	1974	1620961	5995680
3/15/2021	23.3	0.10	90.41	7.85	226.15	0.14	7.87	228	46.1	138.77	**0.01**	140	16.3	1220	1280	169	57	8	67	202.0	2059	2052801	6909426
3/29/2021	27.4	0.19	100.92	8.42	402.11	0.26	8.18	312	18.6	359.44	**0.01**	57	15.7	1320	1320	82	6	37	29	181.7	1577	2209264	6734187
4/12/2021	25.1	0.19	80.70	6.73	398.44	0.26	8.02	1424	49.4	1287.11	**0.03**	170	15.0	1440	1460	144	20	108	42	191.2	1958	3880294	21103792
4/26/2021	27.1	0.21	68.27	5.51	427.54	0.28	7.61	1672	11.3	797.20	**0.02**	220	12.9	1100	1190	100	93	8	62	186.6	1835	4118118	15996824
5/10/2021	29.3	0.20	64.08	5.04	416.23	0.27	7.58	1828	23	1582.10	**0.04**	193	13.9	716	733	244	17	110	41	177.2	3021	3479747	27712808
5/24/2021	27.6	0.20	104.97	8.44	422.56	0.27	8.29	35080	77.7	1402.20	3.77	267	13.1	1100	1250	107	155	108	43	172.6	1121	4881660	12166599
6/7/2021	29.7	0.20	98.56	7.70	410.84	0.27	8.22	1084	79.3	385.16	0.37	143	42.6	1510	1510	116	8	21	73	164.4	944	4118118	23657275
6/21/2021	30.5	0.13	92.07	7.00	265.77	0.17	8.18	1313	50.6	277.20	**0.12**	123	13.7	1460	1470	129	8	54	32	163.8	1503	5651460	24633607
7/8/2021	28.8	0.24	47.26	3.74	494.71	0.32	7.42	1233	13.3	328.23	**0.06**	197	15.0	1220	1350	103	134	138	77	194.7	1675	3342060	17686630
7/19/2021	27.8	0.29	53.14	4.09	589.14	0.38	7.39	2678	22.2	60.08	**0.00**	287	17.3	1340	1540	142	200	113	117	288.7	2186	4881660	12016394
8/2/2021	30.4	0.27	59.16	4.57	555.23	0.36	7.44	93	37.1	505.11	**0.00**	387	19.4	3210	3250	138	38	28	119	284.2	2134	1595927	6884392
8/17/2021	29	0.27	40.71	3.19	549.01	0.36	7.35	150	7.66	405.10	**0.00**	470	20.1	1220	1370	133	151	13	135	306.1	2430	1251708	6158402
9/13/2021	29.9	0.26	47.54	3.70	530.34	0.35	7.19	116	11	45.49	**0.03**	426	20.3	723	882	133	159	96	116	298.4	2263	1068124	4906694
9/27/2021	27.9	0.16	40.53	3.25	330.86	0.21	7.09	44	16.8	48.39	**0.00**	513	20.7	1470	1580	166	108	132	119	261.2	6613	1783683	6421260
10/11/2021	27.6	0.18	36.29	2.90	368.79	0.24	7.22	1620	27.4	55.16	**0.04**	502	20.2	1590	1750	153	159	19.1	131	274.5	2913	1764908	5726563
10/25/2021	26.7	0.17	38.52	3.13	343.45	0.22	7.32	160	1.03	40.93	**0.00**	543	20.9	1130	1340	163	211	8	122	219.5	1678	1322638	6008197
11/8/2021	23.3	0.22	60.83	5.27	452.50	0.29	7.53	80	2.43	212.56	**0.00**	427	19.6	981	1300	180	320	64	117	300.9	3665	1164088	6220987
11/22/2021	23.2	0.26	61.29	5.29	538.74	0.35	7.94	1747	4.32	42.30	0.17	263	21.9	1080	1350	129	272	43	83	337.0	2303	1967684	11903740
12/6/2021	21.9	0.21	74.30	6.71	437.20	0.28	8.04	3347	3.63	486.41	1.04	223	19.6	1030	1050	122	22	8	48	212.7	1808	1817480	10026179
12/20/2021	23.9	0.18	52.30	4.49	372.06	0.24	7.81	1293	4.11	55.28	**0.00**	267	23.5	1080	1260	115	177	298	74	330.8	2304	1764908	10026179
1/3/2022	22.8	0.19	70.69	6.20	390.97	0.25	7.94	987	8.3	103.30	**0.00**	110	22.8	946	1050	73	103	8	30	225.1	1911	2515932	13781302
1/17/2022	20.13	0.19	70.07	6.41	392.31	0.25	7.95	300	5.7	269.00	**0.01**	117	18.6	1210	1330	90	124	8	35	213.6	2004	1890079	5182070

*HP: Hydrogen peroxide

**MC: Microcystin values in bold are below manufacturer determined detection limit.

†PICO: Picocyanobacterial cells.

‡BAC: Bacterial cells.

Appendix C. Photo documentation of the time series of first mesocosm experiment

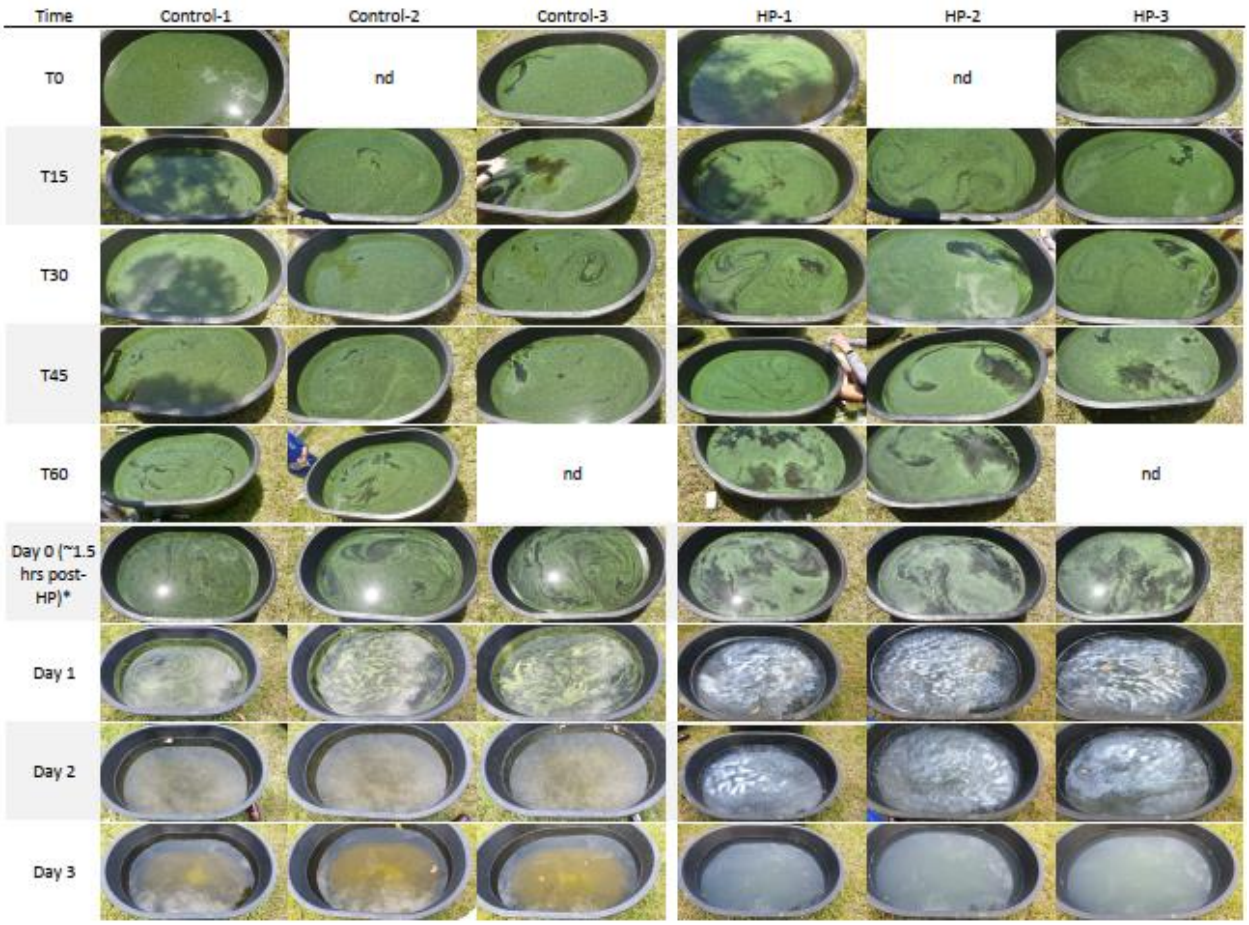

*Does not correspond to data collection.
nd: No data

Appendix D. Photo documentation of the first mesocosm experiment: mesocosm arrangement (a); collected Lake Okeechobee *Microcystis* biomass used (b); surface spray application of hydrogen peroxide away from control mesocosms (c); spray effectively mixed the mesocosm (d).

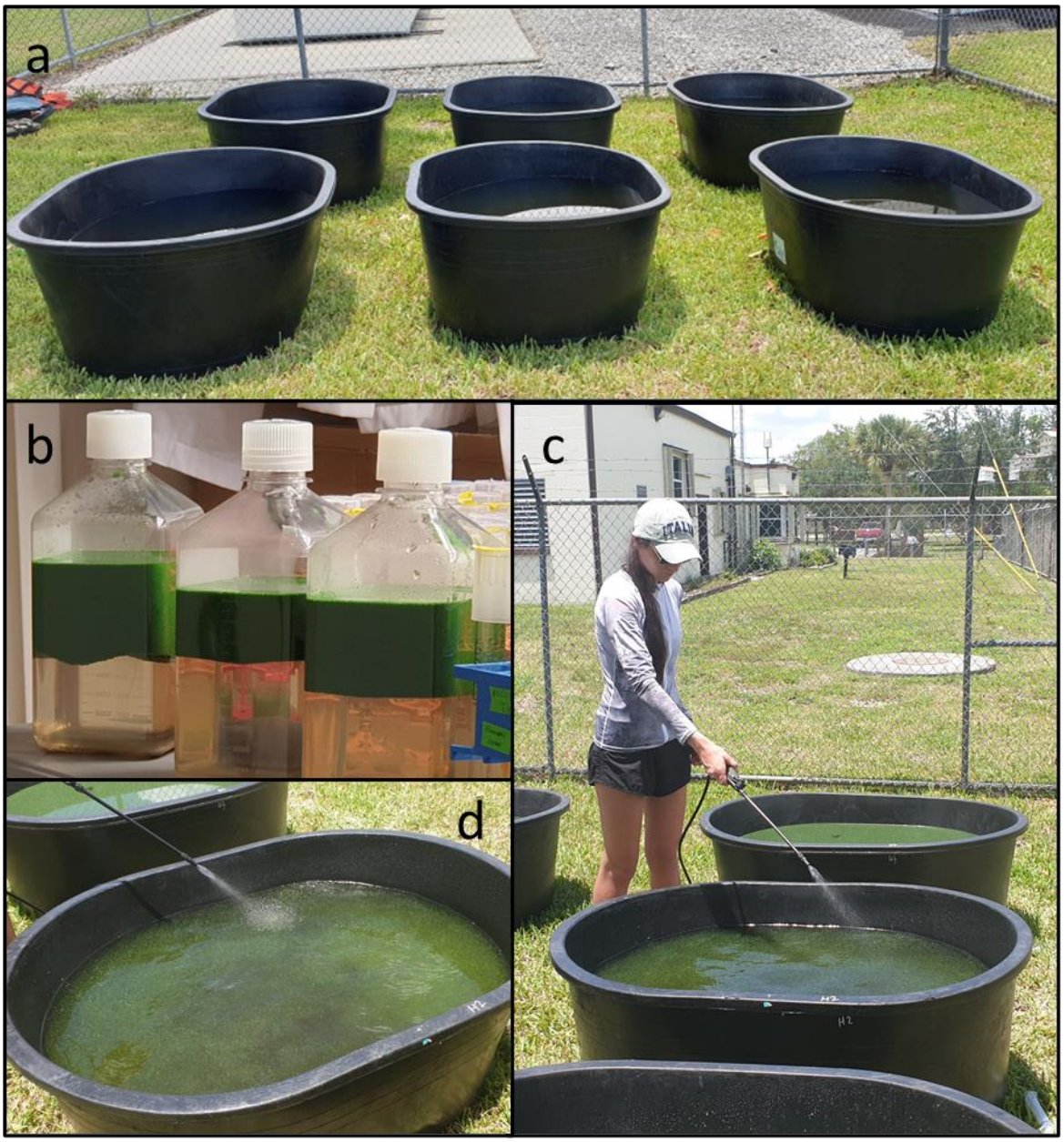

Appendix E. The first mesocosm water quality parameters

Day	Treatment	Temp.	Sal.	DO	DO	Cond.	TDS	pH	Chl-a	HP**	MC***	MC filtrate	TOC	TKN	TN	TP	NOx	NH3	OP	CDOM	PICO†	BAC‡
		°C	ppt	%	mg/L	µS/cm	mg/L		µg/L	µM	µg/L	µg/L	mg/L	µg/L	µg/L	µg/L	µg/L	µg/L	µg/L	µg/L	cells/ml	cells/ml
Day 0-PRE	Control	26.0*	0.20	98.70	8.20	409.81	0.27	8.47	478.0	0.26	5.86	2.09	26.9	11400	11426	981	26	75	22	191.3	726191	4759493
Day 0-POST	Control	31.5	0.18	113.90	8.80	363.73	0.27	8.87	1536.0	0.11	4.20	2.12	54.6	14000	14034	1020	34	69	27	233.0	2680282	4279046
Day 1	Control	26.6	0.19	104.90	8.50	389.92	0.25	8.96	513.0	0.77	10.79	2.56	18.3	9210	9216	780	6	104	28	215.7	1033253	4303580
Day 2	Control	26.5	0.20	106.60	9.00	418.23	0.27	9.07	58.3	1.34	4.33	0.61	24.5	2470	2477	122	7	56	15	178.6	813693	6992039
Day 3	Control	22.6	0.19	102.90	9.00	393.77	0.26	9.13	15.9	2.43	0.85	0.04	15.0	1060	1066	69	6	20	20	181.2	2160990	6930705
Day 0-PRE	HP	25.4*	0.20	99.00	8.30	413.92	0.27	8.50	878.0	0.09	6.66	0.93	22.2	15800	15831	1150	31	85	33	189.7	685404	7110618
Day 0-POST	HP	31.7	0.18	135.90	10.50	368.55	0.27	8.30	967.0	12520.77	7.50	4.95	43.4	16500	16520	1930	20	1250	2	174.5	799382	7920222
Day 1	HP	26.6	0.19	147.00	12.10	388.40	0.25	7.94	6.1	13936.76	9.74	9.13	41.1	6770	6776	951	6	1270	27	139.6	1125984	615790
Day 2	HP	26.5	0.21	137.60	11.60	424.99	0.28	8.20	0.8	10129.64	2.96	2.96	24.1	4450	4930	819	478	1260	6	109.1	1106732	5640654
Day 3	HP	22.6	0.20	149.60	11.00	405.62	0.26	8.16	0.3	11918.56	5.18	5.18	20.8	2490	2940	224	448	1180	14	154.6	238384	8153290

*Temperature readings taken approximately one hour prior to other data sampled.
**HP: Hydrogen peroxide
***MC: Microcystin
†PICO: Picocyanobacterial cells.
‡BAC: Bacterial cells.

Appendix F. Photo documentation of second mesocosm: Mesocosm arrangement (A), mesocosm replicate arrangement graphical (B), *Microcystis* surface colonies pre-treatment day 0 (C), algal cell bleaching 24 hours after treatment in hydrogen peroxide mesocosm (D), mesocosm arrangement (E), *Microcystis* bloom on freshwater side of Franklin Lock and Dam (S-79) during experiment, where added *Microcystis* biomass was taken from (F), *Microcystis* bloom on brackish side of Franklin Lock and Dam (S-79) on day 3 of the experiment (G).

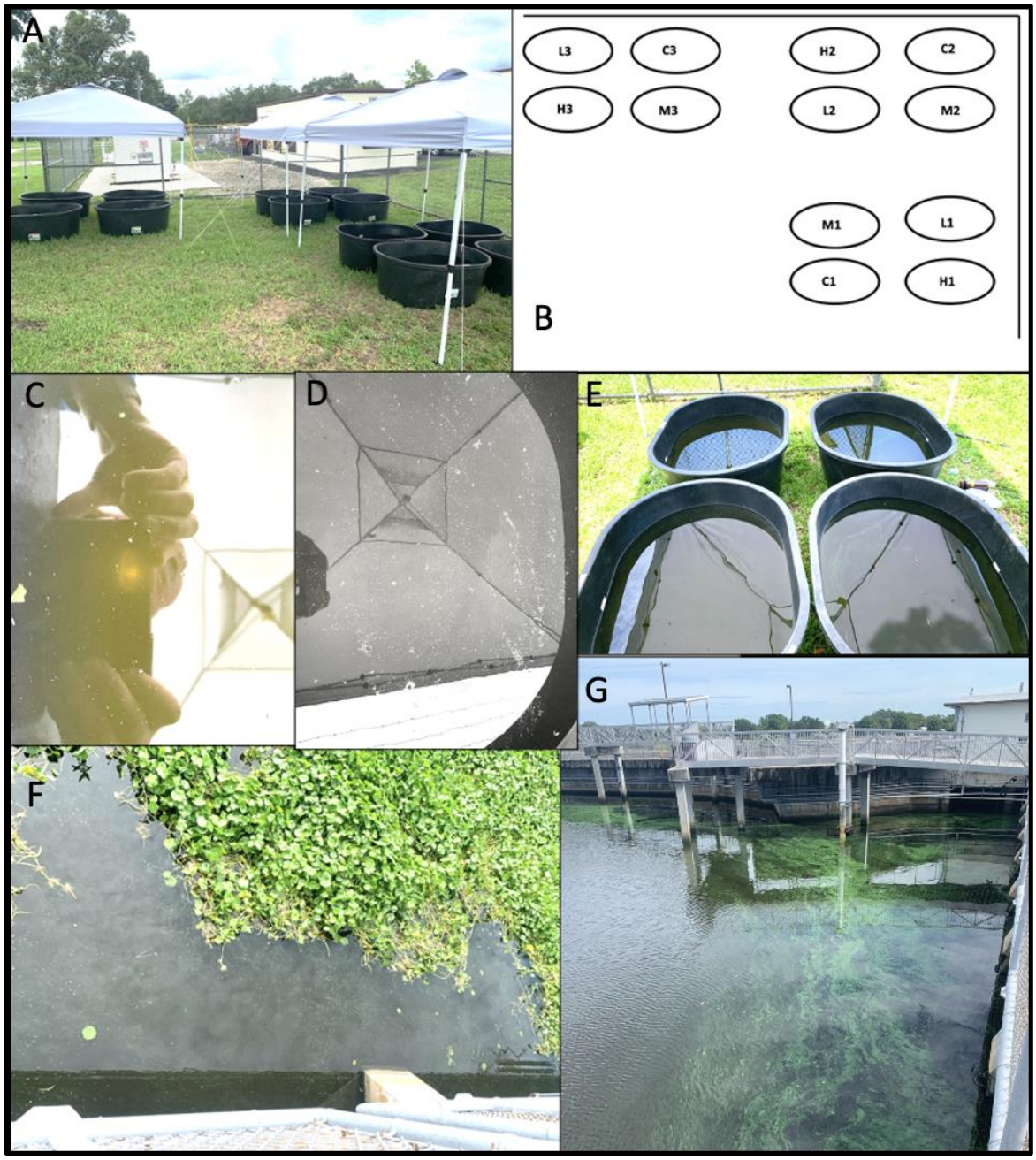

Appendix G. The second mesocosm water quality parameters

Treatment	Day	Chlorophyll-a (µg/L)	TOC (mg/L)	TKN (µg-N/L)	TP (µg-P/L)	TN (µg-N/L)	OP (µg-P/L)	NOx (µg-N/L)	NH3 (µg-N/L)	TN / TP	HP (nM)	MC (µg/L)	L-lysine (µg-N/L)	MC-filtered (µg/L)	CDOM (µg/L)
Control	0	60.7	16.0	1950	189	2086	53	136	13	11.0	0.07	1.05	0.54	0.02	181.94
	1	72.1	18.9	1380	173	1405	81	6	25	8.1	0.32	2.25	0.17	0.00	188.94
	3	121.0	17.9	1670	184	1676	67	6	25	9.1	0.59	0.18	0.99	0.07	178.44
	7	46.0	17.2	1430	164	1436	71	6	12	8.8	0.41	0.20	0.99	1.36	208.86
HP	0	78.0	15.3	1690	197	1758	54	68	55	8.9	309.2	1.09		0.15	187.31
	1	36.9	20.7	1180	513	1298	446	118	53	2.5	204.3	0.92		1.03	195.18
	3	19.6	16.6	1520	242	1639	139	119	151	6.8	0.36	0.56		0.76	193.50
	7	27.2	17.8	3050	249	3164	144	114	143	12.7	0.06	0.11		0.19	213.08
L-lysine	0	74.1	17.1	2750	95	2872	66	122	40	30.2		0.28	45.88	0.03	185.46
	1	55.2	18.3	2350	170	2358	98	8	53	13.9		0.05	67.97	0.01	189.39
	3	58.7	15.8	2440	156	2446	142	6	741	15.7		0.39	0.41	0.60	188.54
	7	34.0	17.0	1670	154	1721	55	51	376	11.2		0.07	0.06	0.19	255.24
Mixed	0	55.1	17.5	2890	201	2954	57	64	56	14.7	246.0	0.47		0.09	187.99
	1	37.1	21	2370	151	2473	136	103	70	16.4	212.6	0.73	55.53	0.71	199.02
	3	10.8	16.9	2620	249	2739	93	119	953	11	0.02	0.62	0.73	0.49	193.71
	7	26.9	17.0	2020		2152		132	641	2.7	0.16	0.32		0.34	219.52

Appendix H. Water quality parameters of the second mesocosm. Data are shown as mean and standard deviation (SD).

Mesocosm	Day	Temp. (°C)	Sal. (ppt)	DO (%)	DO (mg/L)	Cond. (uS/cm)	TDS (mg/L)	pH
Control	0	28.77	0.22	118.6	9.43	452.17	0.29	8.80
	SD	0.25	0.00	3.07	0.25	1.05	0.00	0.06
	1	26.21	0.22	106.0	8.84	452.06	0.29	8.76
	SD	0.16	0.00	4.07	0.34	0.70	0.00	0.08
	3	24.68	0.22	97.2	8.32	448.00	0.29	8.87
	SD	0.11	0.00	1.3	0.05	1.77	0.00	0.06
	7	25.66	0.23	79.2	6.64	473.43	0.31	8.46
	SD	0.14	0.00	6.2	0.52	3.06	0.00	0.07
HP	0	28.72	0.22	117.3	9.32	451.73	0.29	8.78
	SD	0.16	0.00	6.1	0.42	1.14	0.00	0.11
	1	26.25	0.22	129.5	10.80	452.13	0.29	8.73
	SD	0.16	0.00	10.2	0.84	0.63	0.00	0.09
	3	24.70	0.22	84.3	7.22	460.65	0.30	8.27
	SD	0.17	0.00	1.7	0.20	0.68	0.00	0.03
	7	25.75	0.23	82.2	6.90	474.30	0.31	8.35
	SD	0.23	0.00	5.0	0.39	1.14	0.00	0.13
L-lysine	0	29.05	0.22	117.0	9.28	452.68	0.29	8.79
	SD	0.44	0.00	3.7	0.35	1.79	0.00	0.06
	1	26.16	0.22	97.8	8.19	455.53	0.30	8.68
	SD	0.06	0.00	2.0	0.17	1.07	0.00	0.04
	3	24.61	0.23	53.8	4.62	465.28	0.30	8.13
	SD	0.19	0.00	5.3	0.45	1.90	0.00	0.06
	7	25.70	0.23	77.8	6.55	474.72	0.31	8.31
	SD	0.21	0.23	2.8	0.22	1.75	0.00	0.10
Mixed	0	28.68	0.22	119.1	9.49	450.43	0.29	8.83
	SD	0.35	0.00	3.0	0.23	1.41	0.00	0.06
	1	26.24	0.22	125.6	10.49	456.03	0.30	8.75
	SD	0.19	0.00	8.2	0.64	1.31	0.00	0.04
	3	24.55	0.23	44.5	3.83	468.98	0.31	7.81
	SD	0.09	0.00	1.8	0.15	0.82	0.00	0.02
	7	25.64	0.23	82.7	6.97	479.40	0.31	8.30
	SD	0.03	0.00	4.4	0.39	1.69	0.00	0.09

Appendix I. Photo documentation of first field application: time series of field experiment (a); field site at Franklin Lock and Dam (b); surface spray application of hydrogen peroxide (c); surface water bubbling from hydrogen peroxide application one hour after application (d).

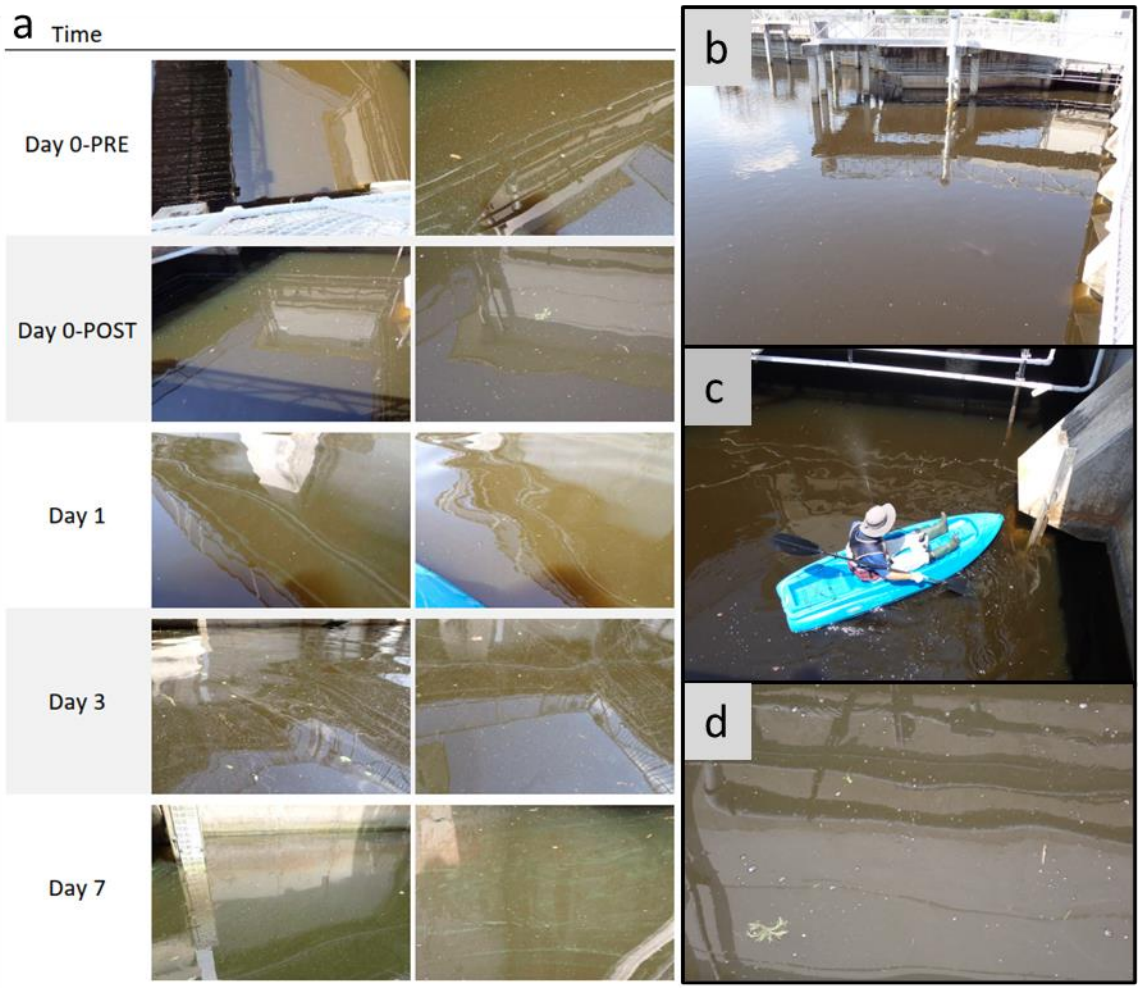

Appendix J. Water quality parameters of the first field application of hydrogen peroxide.

Day	Temp.	DO	DO	Cond.	pH	Chl-a	HP*	MC**	Total Iron	TOC	TKN	TN	TP	NOx	NH3	OP	CDOM	PICO†	BAC‡
	°C	%	mg/L	µS/cm		µg/L	µM	µg/L	µg/L	mg/L	µg/L	µg/L	µg/L	µg/L	µg/L	µg/L	µg/L	cells/ml	cells/ml
Day 0-PRE	37.0	76.0	6.3	433	7.9	8.2	2.58	**0.10**	150	16.1	1070	1150	91	78	75	64	194.1	5726563	26285861
Day 0-POST	32.3	77.3	6.3	461	7.9	9.1	4.30	**0.10**	117	14.4	1050	1121	51	71	105	51	200.7	4769006	17987039
Day 1	35.1	106.2	8.4	643	8.3	11.3	1.90	0.80	107	12.9	1100	1193	100	93	8	62	202.0	4618801	15433556
Day 3	38.0	119.6	9.6	571	8.5	27.5	1.43	**0.00**	153	14.6	1290	1296	92	6	84	42	242.0	5388602	19526640
Day 7	31.3	84.6	7.1	425	7.9	35.0	0.45	**0.10**	193	13.4	1400	1473	135	73	141	79	198.1	4355943	13293136
Day 14	35.8	84.9	6.8	463	7.6	14.5	0.20	**0.00**	260	20.3	1080	1154	114	74	8	51	210.5	6233504	19639294

*HP: Hydrogen peroxide

**Microcystin values in bold are below manufacturer determined detection limit.

†PICO = Picocyanobacterial cells.

‡BAC = Bacterial cells.

Appendix K. Photo documentation of second field application: time series of field experiment (a); Second BlueGreen Water Technologies overlapping dry treatment on Day 7 (b); alligator present during the bloom on day 2 before and after BlueGreen Water Technologies treatment on Day 2, not visibly impacted by either their dry or our liquid treatments (c). A family of ducks on the shoreline of our study area on day 7, not visibly impacted by either treatment.

Appendix L. Water quality parameters of the second field application of hydrogen peroxide.

Day	Colony Count	Chl-a	HP**	MC	TOC	TKN	TN	TP	NOx	NH3	OP	CDOM	PICO‡	BAC°
	per L	µg/L	µM	µg/L	mg/L	µg/L	µg/L	µg/L	µg/L	µg/L	µg/L	µg/L	cells/ml	cells/ml
Day 0- Control	9050	50.2	1.84	**0.11†**	13.5	1580	1586	133	6	24	66	205.8	5407377	22493187
Day 0-PRE	48467	196.0	1.49	3.71	13.1	2350	2356	187	6	16	67	208.3	5914319	21629509
Day 0-POST	4200	38.9	110.6	2.40	12.8	1430	1436	123	6	25	56	237.1	4806558	14494775
Day 1-Control	4683	37.2	1.14	**0.07**	24.9	1240	1407	124	167	32	51	201.4	5651460	16560093
Day 1	830000	477.0	0.41	8.28	11.8	5570	5617	131	47	30	50	343.1	8111066	10026179
Day 2	1863333	2076.0	0.54	35.61	11.5	34100	34100	1890	27	64	46	416.0	2641103	17573976
Day 3	656667	1094.0	1.26	3.99	46.9	6250	6264	1060	14	35	20	229.3	7848207	13480892
Day 7	18067	111.0	733.4	4.23	19.7	1560	1566	26	6	57	3	206.0	3736347	11190267
Day 14	906000	447.0	0.15	4.44	11.5	5970	6020	124	52	15	102	nd	2328176	4299616
Day 14-Control	5427	114.8*	0.05	nd	nd	nd	nd	nd	nd	nd	nd	nd	nd	nd

*Data measured by FGCU, not Benchmark EnviroAnalytical.
**HP = Hydrogen peroxide
†MC: Microcystin values in bold are below manufacturer determined detection limit.
‡PICO = Picocyanobacterial cells.
°BAC = Bacterial cells.